

# Frontier Areas in Chemical Technologies

*Editors*

*Dr. G. PARUTHIMAL KALAIANAN*

*Dr. M. SUNDRARAJAN*

*Dr. T. STALIN*



**ALAGAPPA UNIVERSITY**

{A State University Graded Category-I by MHRD-UGC & A+ Grade by NAAC (CGPA: 3.64)}

Karaikudi - 630 003

First Impression: 2018

© Alagappa University, Tamil Nadu

## **Frontier Areas in Chemical Technologies**

**A Compendium of Research Papers presented in the International Conference FACTs  
2018, March 22.03.2018**

**Conference Organised by:  
Department of Industrial Chemistry  
Alagappa University, Karaikudi-6300 003.**

**ISBN: 978-8192-8760-2-4**

Price : ₹ 1,000/- \$ 30

No part this publication may be reproduced or transmitted in any form by any means, electronic or mechanical, including photocopy, recording, or any information storage and retrieval system, without permission in writing from the copyright owners.

### **DISCLAIMER**

The authors are solely responsible for the contents of the papers compiled in this volume. The publishers or editors do not take any responsibility for the same in any manner. Errors, if any, are purely unintentional and readers are requested to communicate such errors to the editors or publishers to avoid discrepancies in future.

*Published by*  
Alagappa University  
Karaikudi-630 002.

*Printed by:*  
Poocharam Printers,  
Karaikudi – 630 002.



Prof. S. SUBBIAH  
Vice - Chancellor

## ALAGAPPA UNIVERSITY

(State University, Government of Tamil Nadu and recognised by UGC  
Accredited with 'A+' Grade by NAAC (CGPA : 3.64) in the Third Cycle)  
& Graded as Category-I University by MHRD-UGC)



### MESSAGE

It gives me great pleasure to learn that the Department of Industrial chemistry, Alagappa University is organizing a National Seminar on "Frontier Areas in Chemical Technologies" (FACTs-2018) on 22<sup>nd</sup> and 23<sup>rd</sup> of March 2018.

Of the different disciplines in sciences Chemistry has a unique position. Currently application of Chemical Technology has become more widespread because of its diverse benefits in almost all areas of science. With the advent of a new technology driven global economy, revolutionary advances have been made in almost all sectors. It is an urgent need to apply Chemical Technology to solve environmental problems, and to encourage the replacement of existing products with new products that are more environmental friendly throughout their life cycles.

I am sure that this seminar will enlighten the participants to deliberate and exchange ideas on diversified topics on recent developments in Chemical Technology. My Compliments are due to the Faculty, Research Scholars and students of the Department of Industrial Chemistry, for their enthusiasm in organizing this seminar with an objective to undertake studies and research in the frontier areas of Chemical Technology.

I congratulate the organizers for bringing national experts to the campus for inter-disciplinary communication and intensify collaborations between scientists, teachers and students to bring innovations in Chemical Technology.

I wish the seminar all success.

Date: 14.03.2018

  
(S.SUBBIAH)





# ALAGAPPA UNIVERSITY

(Established by an Act of the Govt. of Tamil Nadu and recognized by UGC)  
Accredited with A+ Grade by NAAC (CGPA : 3.64) in the Third Cycle



**Prof. H. Gurumallesh Prabu**  
Registrar

Date: 08.03.2018



## MESSAGE

I am happy to note that the Department of Industrial Chemistry, School of Chemical Sciences is organizing a National Seminar on Frontier Areas in Chemical Technologies -2018 (FACTs - 2018) during 22-23 March 2018.

The aim of the seminar is to provide a platform for the young researchers to develop and bring forth the latest advances in all areas of chemical science including the interfaces with related disciplines such as biology, medicine and material science. In this regard, it is appropriate that the Department of Industrial Chemistry, School of Chemical Sciences has taken efforts to arrange this National Seminar with invited lectures from eminent personalities in India and paper presentation by academicians, scientists, scholars and industrialists.

I am sure that all the delegates would be greatly benefited by the deliberations of this Seminar with many innovative ideas.

I wish the Seminar a grand success.

*H. Gurumallesh Prabu*  
8/3/18

(Prof. H. Gurumallesh Prabu)

Alagappapuram  
Karaikudi - 630 003.  
Sivagangai District  
Tamilnadu, India.

Tele : 04565 - 223 100,  
Fax : 04565 - 225 525, 04565 - 225 202  
Web : [www.alagappauniversity.ac.in](http://www.alagappauniversity.ac.in)  
Email : [registraralagappauniv@gmail.com](mailto:registraralagappauniv@gmail.com)





**ALAGAPPA UNIVERSITY**  
[Accredited with A+ Grade by NAAC (CGPA : 3.64) in the Third Cycle]  
**DEPARTMENT OF INDUSTRIAL CHEMISTRY**  
(DST-FIST, DST-PURSE and UGC-SAP ASSISTED Department)  
**SCHOOL OF CHEMICAL SCIENCES**  
KARAIKUDI-630 003, Tamilnadu, INDIA.



**Dr. G. PARUTHIMAL KALAIANAN** M.Sc., Ph.D., D.Sc.,  
Professor and Head  
Dean - Faculty of Science

Convener



WELCOME TO THE DELEGATES

On behalf of the Staff and students of the Department of Industrial Chemistry, Alagappa University, Karaikudi, I am pleased to extend a hearty welcome to all the delegates of the National Seminar on Frontier Areas in Chemical Technologies (FACTs - 2018) during 22- 23 March 2018.

Though the conference announcement was at short notice, there was an overwhelming response. About 150 technical papers and 6 invited lectures were received during this short notice of time. These cover a wide range of topics and are programmed to be deliberated in 6 sessions.

I am delighted to the response received from Academicians, Scientists from R & D Institutions and Chemists from Industries. The seminar would also provide a common platform to share their ideas/achievements of research into industrial applications to reach the common man and also help to establish a strong academic-research-industrial relationship. I hope that the conference will provide the unique opportunity for participants to interact and share the knowledge and experience.

I wish the delegates for enjoyable and memorable stay at Karaikudi.

  
Dr.G.Paruthimal Kalaignan

Phone No : +91 4565-228836  
Fax No : +91 4565-225202

Mobile No : +91 9443135307  
E-mail : gpkalaignan@gmail.com

# Preface

---

Advancements in research activities on Chemical Technologies attain greater momentum and reached hallmark in the era of scientific developments. Chemical technologies are a challenging as well as fascinating branch of chemistry and finding applications in almost all areas of science and technology. It is important for the researchers, educators and developers from academic institution and industries to know the research and recent developments that have been made on various aspects of Chemical Sciences and Technologies. For the effective discussions and interactions the Department of Industrial Chemistry, Alagappa University, Karaikudi is organizing a National Level Seminar on Frontier Areas in Chemical Technologies (FACTs - 2018) to bring together National Experts from academic, research Institutions and industries on a common platform. The technical sessions of the seminar consists of Invited Lectures by Eminent Speakers from CSIR-CECRI , IIT, NIT, Universities and papers for both Oral and Poster presentations during the seminar on various advanced aspects in chemical Technology, Nano Technology, Green Technology, Polymer Technology, Textile Technology, Sensor Technology, Solar Energy Technology, Water Technology, Photochemical Technology and allied areas.

It is indeed a matter of great pleasure and satisfaction to the editors to present this volume containing abstracts of the Invited Lectures and Research Scholars Presentations to be discussed in the seminar to be held in Alagappa University, Karaikudi during 22 – 23<sup>rd</sup> March 2018. In the present's seminar, there are about 6 Invited Lectures, 31 Oral and 79 Poster presentations. In addition, the programme would include open forum discussions. About 250 delegates from various research institutes, Universities, Colleges and Industries in India would participate in the seminar.

The editors are thankful to **Prof. S. Subbiah, Patron**, Vice-Chancellor, Alagappa University, Karaikudi for supporting all the activities of this National Seminar and advising in promoting the growth of the Department of Industrial Chemistry. Our sincere thanks are to all the Syndicate Members, **Prof. H. Gurumallesh Prabu, Co-patron**, Registrar and authorities of Alagappa University, Karaikudi for their constant support and encouragement. Sincere thanks are due to the Organizing Committee Members of the seminar, Faculty Members, Research Scholar and students of the Department of Industrial Chemistry. We take this opportunity to wish all the delegates a pleasant stay in Karaikudi and stimulating discussions during the National Seminar on Frontier Areas in Chemical Technologies.

Edited By

**Dr. G. PARUTHIMAL KALAI GNAN**

**Dr. M. SUNDRARAJAN**

**Dr. T. STALIN**



# Organising Committee

---

Patron	:	<b>Prof. Dr. S.Subbiah,</b> Vice-Chancellor
Co-patron	:	<b>Prof. H. Gurumallesh Prabu,</b> Registrar
Convener	:	<b>Prof. G. Paruthimal Kalaigan,</b> Prof. & Head
Organizing Secretary	:	<b>Dr. M. Sundrarajan,</b> Assistant Professor Cell No.: 94444 96151 E- mail:sundrarajan@yahoo.com
Joint Secretary	:	<b>Dr. T. Stalin,</b> Assistant Professor Cell No.: 63810 44538 E- mail:drstalin76@gmail.com

## **ORGANIZING COMMITTEE MEMBERS**

Dr. S. Thambidurai, Associate Professor  
Dr. G.Gopu, Assistant Professor  
Dr. S. Viswanathan, Assistant Professor  
Dr. S. Umadevi, UGC-Assistant Professor  
Dr. P. Muthu Mareeswaran, DST - INSPIRE Faculty  
Dr. N. Sengottuvelan, Assistant Professor (DDE)

# Advisory Committee

---

**Prof. H. Surya Prakash Rao**

Pondicherry University, Puducherry

**Prof. S. Baskaran**

IIT Madras, Chennai.

**Dr. Vijayamohanan K. Pillai**

Director, CSIR-CECRI, Karaikudi

**Dr. D. Velayutham**

Chief Scientist, CSIR-CECRI, Karaikudi

**Prof. S. Natarajan**

Indian Institute of Science, Bangalore.

**Prof. K. Palanivelu**

Anna University, Chennai

**Prof. E. Murugan**

University of Madras, Chennai

**Prof. A. Ramu**

Madurai Kamaraj University, Madurai

**Prof. V. Raj**

Periyar University, Salem

**Dr.M. Anbu Kulanthainathan**

Principal Scientist, CSIR-CECRI, Karaikudi

**Dr. L. Ammayappan**

Principal Scientist, NIRJAFT, Kolkata.

**Dr. K. Krishnamoorthy**

Scientist, NCL, Pune.

**Prof. A. Ilangovan**

Bharathidasan University, Trichy.

**Prof. P.S. Mohan**

Bharathiar University, Coimbatore.

**Prof. S. Kabilan**

Annamalai University, Chidambaram

**Prof. S. Syed Shafi**

Thiruvalluvar University, Vellore.

# PROGRAMME

---

<b>DAY - I: 22<sup>nd</sup> March 2018, Thursday</b>	
<b>8.30 am – 10.00 am</b>	<b>Registration</b>
<b>10.00 am – 11.15 am</b>	<b>INAGURATION</b>
<i>Welcome Address</i>	<b>Prof. G. PARUTHIMAL KALAI GNAN</b> Dean Faculty of Science Senior Professor & Head, Department of Industrial Chemistry Alagappa University, Karaikudi – 630 003
<i>Thematic Address</i>	<b>Dr. M. SUNDRARAJAN</b> Assistant Professor, Department of Industrial Chemistry Alagappa University, Karaikudi – 630 003
<i>Presidential Address</i>	<b>Prof. S. Subbiah</b> Vice - Chancellor Alagappa University, Karaikudi – 630 003
<i>Inaugural Address</i>	<b>Prof. H. Surya Prakash Rao</b> Senior Professor, Department of Chemistry, Pondicherry University, Puducherry – 605 014
<i>Felicitations</i>	<b>Prof. K. Gurunathan,</b> Member of the Syndicate Professor & Head, Department of Nanoscience and Technology Alagappa University, Karaikudi – 630 003
<i>Vote of Thanks</i>	<b>Dr. T. Stalin</b> Joint Secretary Assistant Professor, Department of Industrial Chemistry Alagappa University, Karaikudi – 630 003
<b>11.15 am – 11.30 am</b>	<b>Tea Break</b>

<b>TECHNICAL SESSION - I</b>	
<b>11.30 am – 12.15 pm</b>	<b>Dr. K. Palanivelu</b> Professor Centre for climate and Adaptation Research Anna University, Chennai – 600 025
<b>Topic:</b>	<i>Water management in the context of Climate Change</i>
<b>12.15 pm – 1.00 pm</b>	<b>Dr. H. Surya Prakash Rao</b> Senior Professor, Department of Chemistry Pondicherry University, Puducherry – 605 014
<b>Topic:</b>	<i>The story of camphor</i>
<b>1.00 pm – 2.00 pm</b>	<b>Lunch Break</b>
<b>TECHNICAL SESSION – II</b>	
<b>2.00 pm – 2.45 pm</b>	<b>Dr. S. Baskaran</b> Professor Department of Chemistry Indian Institute of Technology Madras, Chennai – 600 036
<b>Topic :</b>	<i>SET oxidative cyclization: Stereoselective synthesis of heterocyclic ring systems</i>
<b>2.45 pm – 4.15 pm</b>	<b>ORAL PRESENTATION</b>
<b>TECHNICAL SESSION –III</b>	
<b>4.15 pm – 5.15 pm</b>	<b>POSTER PRESENTATION &amp; Tea Break</b>
<b>DAY - II : 23<sup>rd</sup> March 2018, Friday</b>	
<b>TECHNICAL SESSION – IV</b>	
<b>10.00 am – 10.45 am</b>	<b>Dr. G. Sozhan</b> Chief Scientist, CSIR-CECRI, Karaikudi – 630 003
<b>Topic :</b>	<i>PEM - based electrolyser for the production of hydrogen</i>
<b>10.45 am – 11.30 am</b>	<b>Dr. P. Murugan</b> Senior Scientist Functional Materials Division, CSIR – CECRI, Karaikudi – 630 003
<b>Topic :</b>	<i>Carbon based nanocomposites for anode of rechargeable Li-ion battery</i>
<b>11.30 am – 11.45 am</b>	<b>Tea Break</b>
<b>11.45 am – 1.15 pm</b>	<b>ORAL PRESENTATION</b>
<b>1.15 pm – 2.00 pm</b>	<b>Lunch</b>
<b>TECHNICAL SESSION – V</b>	
<b>2.00 pm – 2.45 pm</b>	<b>Dr. S. Anandan</b> Professor and Head, Department of Chemistry National Institute of Technology, Tiruchirappalli – 620 015
<b>Topic :</b>	<i>Nanosized semiconductor materials: Diverse structures with tailored properties</i>
<b>2.45 pm – 3.45 pm</b>	<b>ORAL PRESENTATION</b>
<b>3.45 pm – 4.30 pm</b>	<b>TECHNICAL SESSION – VI</b> <b>POSTER PRESENTATION &amp; Tea Break</b>
<b>4.30 pm – 5.00 pm</b>	<b>VALIDICTORY SESSION &amp;</b> <b>CERTIFICATE DISTRIBUTION</b> <b>NATIONAL ANTHEM</b>

# CONTENTS

## Invited Lecturs

<b>IL 1</b>	Water management in the context of Climate Change <i>Dr. K. Palanivelu</i>	2
<b>IL 2</b>	The story of camphor <i>Dr. H. Surya Prakash Rao</i>	3
<b>IL 3</b>	SET oxidative cyclization: Stereoselective synthesis of heterocyclic ring systems <i>Dr. S. Baskaran</i>	4
<b>IL 4</b>	PEM - based electrolyser for the production of hydrogen <i>Dr. G. Sozhan</i>	5
<b>IL 5</b>	Carbon based nanocomposites for anode of rechargeable Li-ion battery <i>Dr. P. Murugan</i>	6
<b>IL 6</b>	Nanosized semiconductor materials: Diverse structures with tailored properties <i>Dr. S. Anandan</i>	6

## Oral Presentation (OP)

<b>OP 1</b>	Copper (I) - Catalyzed highly efficient homo coupling of terminal alkynes to 1,3-diyne <i>P. Tamilselvan*</i>	9
<b>OP 2</b>	Manganese dioxide nanospheres: A novel hydrophilic modifier for ultrafiltration water treatment membranes <b>M. Sri Abirami, Saraswathi, K. Divya, N. Kanimozhi and A. Nagendran*</b>	10
<b>OP 3</b>	Custom-made sulfonated poly (ether sulfone) /poly(vinyl alcohol) nanocomposite membranes containing tungsten disulfide nanosheets for DMFC applications <b>K. Divya, M. Sri Abirami Saraswathi, M. Rahumath Ayisha and A. Nagendran*</b>	13
<b>OP 4</b>	Novel approach for substituting hazardous Additives in Zinc Electrode for Alkaline Silver Oxide-Zinc Battery <b>K. Rathinakumar*, G.A. Pathanjali and R.Karvembu</b>	16
<b>OP 5</b>	Antimicrobial activity of cerium oxide nanoparticle synthesized by green approach <b>S. Induja, G.V. Geetha, M. Periyanyaki and R. Sivakumar*</b>	19
<b>OP 6</b>	Physical and Electrochemical Characterization of Direct Current Electrodeposited Ni - Tin Nanocomposite Coatings <b>S. Kasturibai and G. Paruthimal Kalaignan*</b>	22
<b>OP 7</b>	C- Dot/CuS Nanocomposite for Energy Storage Devices <b>P. Naveenkumar, and G. Paruthimal Kalaignan*</b>	24

<b>OP 8</b>	<i>Dodonaeaviscosa</i> Leaf Extract Mediated Synthesis of Silver Nanoparticles and its Characterization <b>M. Anandan and H. Gurumallesh Prabu*</b>	26
<b>OP 9</b>	Multifunctional Application of Iron Oxide – Chitosan Composite <b>AL. Kavitha and H.GurumalleshPrabu*</b>	28
<b>OP 10</b>	Synthesis and Characterization of Seaweed Biopolymer Based ZnO Composite <b>S. Rajaboopathi and S. Thambidurai*</b>	31
<b>OP 11</b>	Study on the Corrosion Behaviour of Mild Steel Using an Aqueous Leaf Extract <i>CissusQuadrangularis</i> <b>K Anuradha*, V Maasilamani and K Velmanirajan</b>	32
<b>OP 12</b>	Chromium Removal From Aqueous Solution Using <i>Prosopisjuliflora</i> Biochar and its Disposal Study in MFC <b>D. Krishnaveni and A.N. Senthilkumar*</b>	34
<b>OP 13</b>	Room Temperature Fiber Optic Gas Sensor Technology Based on $\text{Co}_2\text{VO}_4$ Nanoplatelets <b>M. Subramanian, V. Violet Dhayabaran and M. Shanmugavadivel</b>	36
<b>OP 14</b>	Photoluminescence Studies on Oxide and Borate Phosphors: Surface Modified $\text{Y}_2\text{O}_3:\text{Eu}^{3+}$ and $\text{Ba}_2\text{Mg}(\text{BO}_3)_2:\text{Bi}^{3+}$ <b>N. Radha * and K. Prabhavathi</b>	39
<b>OP 15</b>	Environmental pollutants simultaneous determination: Polyaniline composite $\alpha\text{-Fe}_2\text{O}_3$ on $\text{MoS}_2$ binder free hybrid nanostructures <b>P. Thivya and J. Wilson*</b>	40
<b>OP 16</b>	Synthesis, Characterization and inhibitive evaluation of 2-(4,5-diphenyl-1H-imidazol-2-yl)phenol on mild steel in 1.0 M Hydrochloric acid <b>KT. Loganathan * and R. Natarajan</b>	41
<b>OP 17</b>	Biomimetic and Cell-Mediated Mineralization of graphene by Ionic liquid Assisted Nitrogen, phosphate, fluorine tri doped ternary nanocomposite <b>M. Balaji, S. Jegatheeswaran, S. Selvam, and M. Sundrarajan*</b>	42
<b>OP 18</b>	Ionic liquid Mediated Green Synthesis of Strontium Cerium Core Nanoparticles and its Antibacterial Activity <b>P. Nithya, M. Balaji, S. Jegatheeswaran, A. Surya, V. Muthulakshmi, A. Keerthana, A. Herculin Arun Baby, A. Mayakrishnan, S. Selvam and M. Sundrarajan*</b>	44
<b>OP 19</b>	Effect of mixed halide ions induced the inorganic cesium lead iodide light harvester photo-anode for perovskite solar cell application <b>K. Sakthivelu, B. Suganya Bharathi, G. Vignesh Kumar and T. Stalin*</b>	46
<b>OP 20</b>	Comparative Studies on Dissociation Constant Values of 4-Ethylbenzoic Acid Derivatives with DFT/HF Theories -Computational Approach <b>M. Nalini, C. Shanthi, S. Karthick and G. Gopu*</b>	47

<b>OP 21</b>	Voltammetric simultaneous determination of vitamin B <sub>2</sub> and B <sub>6</sub> using Gd-ZnO:f-MWCNT nanocomposite modified electrode <b>N. Dhanalakshmi, T. Priya, S. Thennarasu and N. Thinakaran*</b>	48
<b>OP 22</b>	Steric group in tripodal molecules enforces cyclic aromatic trimer Conformer <b>Deval Sathiyashivan Shankar, Chakkakirankumar, M. Sathiyendiran* and Dhanraj T. Masram<sup>a</sup></b>	49
<b>OP 23</b>	Synthesis and Antimicrobial screening of thiadiazolylcoumarins <b>Ganesh N Alawandi<sup>1</sup> Kiran K Pujar<sup>2</sup> and Manohar V Kulkarni<sup>2</sup></b>	51
<b>OP 24</b>	synthesis and characterization of novel acrylamide copolymers <b>S. Bharathi<sup>1*</sup> and P. Pazhanisamy<sup>2</sup></b>	52
<b>OP 25</b>	Analysis of inorganic toxic ions in environmental pollutants caused by the dyes used in korai mat weaving cottage industries in Ayyanaruthu, Kayatharu Taluk, Tuticorin District, Tamil Nadu: A case study <b>Subbiah Thangadurai* and Karuppasamy Gurusamy<sup>#</sup></b>	53
<b>OP 26</b>	Analysis of chlorate, perchlorate and nitrate by TLC, FTIR, Powder XRD and IC in Irrigation water, soil debris and sewage sludge samples from Fireworks and Safety Matches manufacturing areas in Sivakasi, Virudhunagar District, Tamil Nadu, India <b>Subbiah Thangadurai* and Bose Karthik prabu</b>	54
<b>OP 27</b>	Enzyme-Free Glucose Sensor Based on Copper Based Metal-Organic Framework/ rGO Composite <b>T. Ponmuthuselvi and S. Viswanathan*</b>	55
<b>OP 28</b>	Microwave Assisted Synthesis of Gold Microcubes: Greener Approach <b>M. Kiruba, R. Mangaiyarkarasi and S. Umadevi*</b>	57
<b>OP 29</b>	Interaction Study of Palladium(ii) ion with Coumarin 460 : an NMR Approach <b>B. M. Ashwin, M. Vinothini, M. Suganthi and P. Muthu Mareeswaran*</b>	59
<b>OP 30</b>	Copper(ii) l-tryptophan Schiff base Complexes: Synthesis, Spectral Studies and its Biological Evaluation <b>N. Kavitha, Fidali Stanley Edwin, P. Rajeshwari, FathimaFarhana N. Pavithra, K. Suganya and N. Sengottuvelan*</b>	61
<b>OP 31</b>	Biological screening studies of DNA relate metal complexes from Benzalidene-4-imino-2,3-dimethyl-1-phenyl-3-pyrazolin-5-one and 2-aminothiazole <b>A. Palanimurugan and A. Kulandaisamy*</b>	62

## Poster Presentation

PP1	Microwave assisted pyrazole derivative synthesis <i>Dr. N. Radha* and V. Suganya</i>	65
PP 2	Corrosion inhibition by leaves extract of vitexdoniana for mild steel in HCl solution <i>K. Akila and S. Kasturibai*</i>	65
PP 3	Enhanced Electrochemical performances of Al-doped $\text{LiNi}_{1/3}\text{Mn}_{1/3}\text{Co}_{1/3}\text{O}_2$ cathode materials for Lithium-ion batteries <i>V. Abinaya, K. Kalaiselvi and G. Paruthimal Kalaignan*</i>	68
PP 4	Improved high Rate Electrochemical performances of Zr-doped $\text{LiNi}_{1/3}\text{Mn}_{1/3}\text{Co}_{1/3}\text{O}_2$ cathode materials for Rechargeable Lithium-ion batteries <i>P. Gokila, K. Kalaiselvi and G. Paruthimal Kalaignan*</i>	70
PP 5	Dodonaeviscosasaas a corrosion inhibitor for mild steel in HCl solution <i>S. Nirosha and S. Kasturibai*</i>	72
PP 6	Synthesis and electrochemical characterization of $\text{CuCo}_{2-x}\text{Ni}_x\text{S}_4$ for supercapacitors <i>S. Gausalya, P. Naveenkumar and G. Paruthimal Kalaignan*</i>	75
PP 7	Structure and Electrochemical performances of Ru-doped $\text{LiNi}_{1/3}\text{Mn}_{1/3}\text{Co}_{1/3}\text{O}_2$ cathode materials for Rechargeable Lithium-ion batteries <i>K. Kalaiselvi and G. Paruthimal Kalaignan*</i>	77
PP 8	Corrosion behaviour of mild steel using an aqueous leaf extract of cynodondactylon <i>C. Sathya, K. Anuradha*, S. Keerthanapriya and K. Velmanirajan</i>	79
PP 9	Synthesis and characterization of rGO/MnS for supercapacitors <i>S. Manoj, P. Naveenkumar and G. Paruthimal Kalaignan*</i>	80
PP 10	Synthesis and Electrochemical Characterization of $\text{CuC}_2\text{S}_4 @ \text{NiCo}(\text{OH})_2$ for Supercapacitors <i>B. Priyadarshini, P. Naveenkumar and G. Paruthimal Kalaignan*</i>	82
PP 11	A study on the corrosion behaviour of mild steel using an aqueous leaf extract of lagenariasiceraria <i>K. Anuradha*, S. Keerthanapriya, C. Sathya and K. Velmanirajan</i>	83
PP 12	Bio synthesis of silver nanoparticles using <i>musaparadisiaca</i> flower extract and its antibacterial activity <i>P. Aiswarya and H. Gurumallesh Prabu*</i>	85
PP 13	Synthesis and characterisation of silver nanoparticles using <i>tectonagrands</i> leaf extract and its antibacterial activity <i>S. Manjuladevi and H. Gurumallesh Prabu*</i>	88
PP 14	Bio-power from chromium sorbed helianthus annuus biochar <i>A. Muthu and A.N. Senthilkumar*</i>	90
PP 15	Bio synthesis of silver nanoparticles using <i>azadirachta indica</i> leaf extract and its antibacterial activity <i>S. Manojkumar and H. Gurumallesh Prabu*</i>	92
PP 16	Synthesis and characterisation of silver nanoparticle using <i>ocimum basilicum</i> leaf extract and its antibacterial activity <i>N. Ramamani and H. Gurumallesh Prabu *</i>	95



PP 17	Characterization and water holding potential of peanut shell biochar <b>K. Rajeshwari and A.N. Senthilkumar*</b>	97
PP 18	synthesis and characterization of silver nanoparticle using <i>solanum trilobatum</i> leaf extract and its antibacterial activity <b>S. Gomathi and H. Gurumallesh Prabu*</b>	100
PP 19	Total synthesis of pyrazole pyrimidine and thienopyridines derivatives as inhibitor for KSP and its anticancer agents <b>P. Muthuraja, A. Susaimanickam, S. Prakash and P. Manisankar*</b>	103
PP 20	Adsorption of phosphate by biochar derived from acacia nilotica leaf <b>K. Shanthi and A.N. Senthilkumar*</b>	104
PP 21	Copper-based metal-organic framework for electrochemical detection of Tryptophan <b>S. Yogesh, S. Prakash, P. Muthuraja and P. Manisankar*</b>	106
PP 22	Synthesis and characterization of seaweed-PVA/ZnO composite for better thermal stability and antibacterial activity <b>R. Aiswarya, S. Rajaboopathi and S. Thambidurai*</b>	107
PP 23	Understanding the antibacterial activities of Terpenoids against Gram Positive & Negative bacteria through Biofilms <b>P. Venmathy, J. Jeyasundari and V. S. Vasantha*</b>	108
PP 24	Preparation and characterization of chitin-CdO composite for better antibacterial activity <b>S. Ilamathi., T. Revathi and S. Thambidurai*</b>	110
PP 25	Synthesis and characterization of chitin-ZnO composite for better antibacterial activity <b>S. Kanimozhi, T. Revathi and S. Thambidurai*</b>	112
PP 26	Electron beam-irradiated Polypyrrole decorated with Bovine serum albumin pores: Simultaneous determination of Epinephrine and L-Tyrosine <b>R. Ramya and J. Wilson*</b>	114
PP 27	Synthesis and characterization of bi doped ZnO-rGO/PANI hybrid composite for supercapacitor applications <b>R. Karthik and S. Thambidurai *</b>	115
PP 28	Synthesis and characterization of chitosan-bi <sub>2</sub> O <sub>3</sub> -sodium alginate hybrid composite for photo catalytic applications <b>K.Mariyappan, R.Karthik and S. Thambidurai*</b>	118
PP 29	Fibrous Silicon nanosphere tethered N-Heterocyclic carbene complexes: Synthesis and its Catalytic application <b>S. Saravanakumar*</b>	120
PP 30	Preparation and characterization of chitin-bi <sub>2</sub> O <sub>3</sub> composite for higher antibacterial activity <b>M. Pragathambal, T. Revathi and S. Thambidurai.*</b>	121
PP 31	layer structured chitosan-copper oxide nanocomposites for better thermal and antibacterial activity <b>T. Revathi and S. Thambidurai*</b>	123
PP 32	Synthesis and characterization of chitin-ZnO composite for excellent antibacterial activity <b>Roshni, T. Revathi and S. Thambidura*</b>	125

PP 33	An ionic liquid mediated synthesis of silver/zinc oxide nanoparticles intercalated into bentonite and their biological activities <b>K. Bama and M. Sundrarajan*</b>	127
PP 34	Green synthesis of silver nanoparticles using <i>morindacitrifolia</i> leaves extract and their Antifungal activity <b>P. Suganya, K. Bama, M. Bhavani, K. Bharathi and M. Sundrarajan*</b>	129
PP 35	Analysis of toxic inorganic ions by FTIR, AAS, ICP-AES and IC in drinking water of Pullalakkottai village, Virudhunagar District, Tamil Nadu: A case Study <b>S. Thangadurai*, G. Saravanakumar and S. Marimuthu</b>	131
PP 36	A novel synthesis of zinc oxide incorporated into $\beta$ -cyclodextrin nanocomposite by using hydrothermal method: biological activities <b>L.R. Sangavi, K. Bama and M. Sundrarajan*</b>	132
PP 37	Ionic liquid assisted green synthesis of rare earth lanthanum oxide nanoparticles: antibacterial and morphology properties <b>V. Muthulakshmi, M. Balaji, P. Nithya, A. Surya and M. Sundrarajan*</b>	134
PP 38	Separation and Detection of Melamine in Milk-based products and Beverage products by TLC and HPTLC methods <b>S. Thangadurai*, K. Isabella Elavarasi, G. Sivakavi, C. Prabhakar, A. Shankar and M. Kaleeswari</b>	136
PP 39	Green synthesis of yttrium oxide nanoparticles and its antibacterial activity <b>M. Alagumeenal, P. Nithya, M. Balaji, S. Jegatheeswaran, A. Surya, S. Selvam, K. Bharathi and M. Sundrarajan*</b>	137
PP 40	Ionic liquid assisted green synthesis of magnesium oxide nanoparticles and its antibacterial activity <b>S. Sathya, P. Nithya, M. Balaji, K. Bama, K. Ramanujam, S. Ambika, K. Elangovan and M. Sundrarajan*</b>	139
PP 41	Electrodeposition of Cu-Zn-Sn alloy using sulphate based electrolyte <b>N. Radha and V. Indragandhi</b>	141
PP 42	Ionic liquid – Assisted tri doping of nitrogen, phosphorus, and fluorine into graphene instantaneously enhanced the morphology of ternary composite <b>A. Mayakrishnan, M. Balaji, S. Jegatheeswaran, P. Nithya, V. Muththulakshmi, S. Selvam, M. Rajan and M. Sundrarajan*</b>	141
PP 43	Green synthesis of RuO <sub>2</sub> nanoparticles using gloriosa superba leaves extract and its antibacterial activity <b>R. Jegatheeswari, P. Nithya, M. Balaji, S. Jegatheeswaran, K. Ramanujam, S. Selvam, S. Ambika, M. Abdul Kadir, S. Gowri, G. Selvanathan and M. Sundrarajan*</b>	143
PP 44	Electrodeposition of Cu-Sn alloy using potentiostatic and galvanostatic method <b>M. Kavitha and C. Rani*</b>	145

PP 45	Characterization and in vitro bioactivity of strontium substituted hydroxyapatite /graphene oxide/ polyacrylic acid nanocomposite <i>A. Keerthana, M. Balaji, S. Jegatheewaran, M. Sundrarajan*, A. Rukmani and V. Mahesh Kumar</i>	146
PP 46	Study the <i>in-vitro</i> Antioxidant Activity of Alumina/PEO Electrospun nanofibrous Mats <i>G. Archana and T. Stalin*</i>	148
PP 47	A Facile and Efficient Synthesis of Carbocycle-Fused Bis-1,2,3-Selenadiazoles Derivatives and their Antimycobacterial Activities <i>C. Nanthini, S. Siyamasundhari, A. Saranya and S. Chitra*</i>	149
PP 48	Design and performance of a bromelain-alginate hydrogel membrane and their antibacterial studies <i>M. Jeyalakshmi and T. Stalin*</i>	150
PP 49	Preparation and characterizations of ferrocene coated PVA/HEC nanofibrous webs for anti tumour studies <i>P. Muthuselvi and T. Stalin*</i>	152
PP 50	A facile and efficient synthesis of carbocycle-fused mono-1,2,3-selenadiazoles derivatives and their antimycobacterial activities <i>S. Siyamasundhari, A. Saranya, C. Nanthini and S.Chitra*</i>	153
PP 51	Preparation of Chemically Crosslinked Chitosan-Curcumin Hydrogel and their Swelling behavior, Pore structure stability and biological activity <i>P. Vasanthi and T. Stalin*</i>	154
PP 52	Improve the stability and their performance of cesium lead bromide-iodide based photo-sensitizer for inorganic perovskite solar cell <i>M. Manoj Kumar, K. Sakthivelu, B. Suganya Bharathi, G. Vignesh Kumar and T. Stalin*</i>	155
PP 53	A facile domino protocol for the regioselective synthesis of 1,3-diphenyl-3-(4,5,6,7-tetrahydrobenzo[c]thiophen-4-yl)propan-1-one derivatives <i>A. Saranya, C. Nanthini, S. Siyamasundhari, P. Muthuraja and S.Chitra*</i>	156
PP 54	Polyethylene glycol assisted synthesis of inorganic cesium lead iodide polycrystalline photo-sensitizer for planar perovskite solar cell <i>P. Sathappan, K. Sakthivelu, B. Suganya Bharathi, G. Vignesh Kumar and T. Stalin*</i>	157
PP 55	Synthesis and characterizations of core-shell Ag@SiO <sub>2</sub> nanoparticles for enhanced antibacterial and cytotoxicity studies <i>B. Suganyabharathi and T. Stalin*</i>	158
PP 56	Development of PANI-based coating to suppress copper corrosion <i>M. Kowsalya, M. Priyanga, S. Sathiyarayanan and Aiswarya Bhaskar</i>	159
PP 57	Studies on chemical and radiation stability of some ionic liquids- theoretical approach <i>R. Josephine Punitha, S. Karthick and G. Gopu*</i>	160

PP 58	An efficient synthesis of dihydropyrimidine derivatives using biginelli multicomponent reaction as key step <i>P. Siva, M. Krishnan, A. Meenal, R. Eswar and G. Gopu*</i>	161
PP 59	Fe-containing oxides as conversion anode model systems for lithium-ion battery <i>M. Priyanga, M. Kowsalya and B. Aiswarya</i>	162
PP 60	Electrochemical detection of phenol on copper based metal-organic framework <i>S. Vijayabose, T. Ponmuthuselvi and S. Viswanathan*</i>	163
PP 61	Synthesis of new ionic liquid crystal bearing biphenyl core and investigation of mesophase behaviour <i>M. Parimala, R. Mangaiyarkarasi and S. Umadevi*</i>	165
PP 62	Phytochemical and biochemical screening of some solvent extracts of gracillariaedulis (family: gracilariaceae) collected from thondi coast, indiatamilnadu, india 3 <i>G. Chandralega and V. Ramadas</i>	168
PP 63	Facile synthesis of reduced graphene oxide using micorwave reaction <i>N. Sowndharya, R. Mangaiyarkarasi, S. Umadevi*</i>	171
PP 64	Lyotropic liquid crystal mediated synthesis of copper nanoparticles <i>N. Santhiya, PR. Meyyathal and S. Umadevi*</i>	174
PP 65	Synthesis and charcterization of spinal layered cathode materials for lithium ion batteries <i>N.Vimalasruthi, P. Periasamy and S. Umadevi*</i>	176
PP 66	Photoswitchable monolayer on indium tin oxide substrate for alignment of liquid crystal <i>S. Esakkimuthu, K. Mohana, B. Sivaranjini and S. Umadevi*</i>	178
PP 67	Synthesis and characterization of n-rich imine functionalized covalent organic polymers towards carbon dioxide capture <i>C. Saravanan, P. Kousalya, A. Pavithra and P. Muthu Mareeswaran*</i>	180
PP 68	Synthesis of schiff-base network (sbn) polymer membrane on silica support <i>M. Senthilkumaran, L. Eswaran and P. Muthu Mareeswaran*</i>	182
PP 69	Symmetric oxamidato –bridged binuclear cobalt (ii) complexes: synthesis, spectral, electrochemical and its DNA binding studies <i>M. Sethupathi, R. Indumathi, T. Valarmathi, V. Vinoth Kumar, A. R. Maheswari and N. Sengottuvelan*</i>	184
PP 70	Diplocyclos palmatus source for red luminescent carbon quantum dots to intercellular bioimaging in Artemiasalina: A Green approach <i>A. Hercularunbaby, P. Nithya, V. Muththulakshmi, A. Keerthana, C. Pragathiswaran H. Gurumallesh Prabu and M. Sundrarajan*</i>	185
PP 71	Imidazolium Based Ionic Liquid Template for Structurally Upgraded Cerium Oxide Nanorods <i>A. Surya<sup>a</sup>, M. Balaji<sup>a</sup>, M. Rajan<sup>b</sup> and M. Sundrarajan<sup>a*</sup></i>	187

PP 72	Development of Low Cost Carbon based material as counter electrode for dye-sensitized solar cells <b>M. R. Samantaray<sup>a</sup>, K. Ramachandran<sup>a</sup>, G. Murugadoss<sup>b</sup>, R. Thangamuthu<sup>b</sup> and S. Karuppuchamy<sup>a*</sup></b>	189
PP 73	Fabrication of Efficient Perovskite Solar Cell <b>K. Ramachandran<sup>a</sup>, G. Murugadoss<sup>b</sup>, VibhaSaxena<sup>c</sup>, R. Thangamuthu<sup>b</sup> and S. Karuppuchamy<sup>a*</sup></b>	189
PP 74	Synthesis and Characterization of Nickel Manganese Oxide Composite materials for Supercapacitor Application <b>K. Uma Maheswari, I. Karuppusamy, A. Senthamarai Selvam and S. Karuppuchamy*</b>	190
PP 75	Synthesis of Sn anchored $\text{Co}_3(\text{PO}_4)_2$ for the reduction of formaldehyde <b>R. Banupriya, R. Karkuzhali and G. Gopu*</b>	191
PP 76	Robust method of synthesis of metal chalcogenides doped GCN <b>R. Vennila, R. Karkuzhali and G. Gopu*</b>	192
PP 77	Electrochemical determination of guanine: using a boron doped Carbon quantum Dot/Mn <sub>3</sub> O <sub>4</sub> composite modified screen-printed carbon electrode <b>G. Muthusankar, Shen-Ming Chen* and G. Gopu</b>	194
PP 78	An efficient and eco-friendly synthesis of <i>N,N'</i> -disubstitutedthiourea derivatives <b>P. Shanmugavelan*, A. Ponnuswamy and S. Dhinakaran</b>	195
PP 79	Synthesis of Pd nanoparticles by bio-reduction process using natural plant of Aervalanata extract <b>R. Jayamani and M. Sundrarajan*</b>	197
PP 80	Highly potential membranes based on poly (aryl hexafluoro sulfone benzimidazole) for high-temperature PEM fuel cell <b>A. Susaimanickam, P. Muthuraja, S. Prakash, P. Manisankara*</b>	198
PP 81	A Facile Green Synthesis of Zinc oxide Nanoparticles Using Justicia gendarussa leaves extract for its enhanced antibacterial activities <b>R. Rajeswari, and H. GurumallesPrabhu</b>	198

# Abstracts

**INVITED LECTURES**

## **IL 1** WATER MANAGEMENT IN THE CONTEXT OF CLIMATE CHANGE

**K. Palanivelu**

*Centre for Climate Change and Adaptation Research, Anna University, Chennai – 600025*

*E-Mail: kpvelu@annauniv.edu*

Climate change is likely to intensify the current challenges of water scarcity and water competition within and between communities and nations particularly global south. The sectoral demand for water is more than the potential availability and it is likely to worsen in the future. Climate change, by increasing the frequency of extreme events such as droughts and torrential rains, risks having a negative effect on villages by reducing the supply of agricultural products and by causing a rural migration that the cities will be unable to manage. Extreme climate events may also aggravate urban-rural conflicts by reducing the amount of water available in reservoirs and bore holes. Over exploitation of ground water has led to the decline in ground water table in most of the areas. Due to erratic rainfall and inflation of agricultural inputs many agricultural lands were kept fallow or converted for other uses and agricultural labourers migrated to urban areas for searching jobs to sustain their life. Contamination of water bodies by pollutants also add more worry in the use of water for various purposes especially for drinking.

Some major impacts of CC on water resources are

- Increase in precipitation projected, hence Cyclones, Drainage and flood problems
- Ground Water likely to become more saline with sea water ingress due to sea level rise & increase in cyclone intensities
- Decrease in monsoon is projected leading to increase in demand for irrigation water
- Increase in Ground Water demand.
- Marginal increase in crop evapotranspiration leading to increase in water demand by crops

Strategies to mitigate the impacts are rainwater harvesting (RWH), constructing check dams/ mini-reservoirs, interlinking of rivers, desilting/ widening of channels and drains, removing weeds from channels, strengthening embankments & infrastructure to manage disasters, increase reservoir storage potential, artificial recharge of over exploited ground water and limit extraction, improve water-use efficiency in agriculture, renovate/ create small reservoirs, restoring and renovation existing tanks and traditional water bodies, construct and rehabilitate tail-end regulators to prevent intrusion of saline water into channels, installation of desalination water plants to ensure fresh water availability, strengthening infrastructure to manage disaster ,etc.

It is important to conserve water under the climate change context because the two extreme events namely excess rain fall (heavy rain short duration) and drought will make it

difficult its availability for various uses including agriculture. This problem is compounded with environmental pollution of water bodies by untreated sewage and industrial effluents. Water conservation like RWH avoids depletion of Ground Water and improves its quality. Similarly pond and lake are also to be protected and its storage capacity to be improved by innovative restoration effort and empowerment of community. Even grey Water has to be recycled wherever possible with simple treatment of nature based solution to avoid water shortage.

## **IL 2** THE STORY OF CAMPHOR

**H. Surya Prakash Rao**

*Department of Chemistry, Pondicherry University, Puducherry – 605 014*

*E-Mail: [hspr.che@pondiuni.edu.in](mailto:hspr.che@pondiuni.edu.in), [hspr@yahoo.com](mailto:hspr@yahoo.com)*

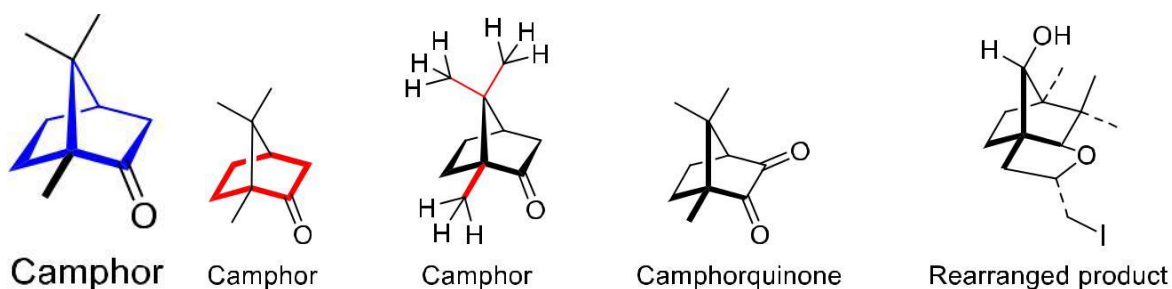
Camphor (Arabic: kafur; Sanskrit: korpur) is a quint essential natural product. It is a part of folklore and is an integral part of religious activities. It finds a unique place in traditional and to some extent modern medicine. Physically, it is a waxy white solid and sublimes when heated. It has characteristic aroma through which it can be recognized even from distance.

Camphor belongs to terpene family; a family that has a large group of secondary metabolites derived from mevalonyl coenzyme A. Within terpene family, it belongs to the sub-set of monoterpenes ( $C_{10}H_{16}O$ ) that it is assembled notionally from two units of isoprene. Structurally it has [2.2.1]bicyclic heptane skeleton which embeds cyclohexane ring in unfavorable boat form. It has one carbonyl functional group (ketone) that can be readily differentiated into exo- and endo-faces. Constrained [2.2.1]bicyclic frame work with a hybridized carbonyl carbon makes camphor a reactive organic compound.

The structure of camphor intrigued traditional organic chemists for a long time. Its structure elucidation took over four decades. Indeed the efforts of organic chemists to unravel the structure of this intricately designed natural product makes an engaging story. Extensive data accumulated through dedicated hard work that spanned over several decades lead to its structure which was confirmed by its synthesis from smaller well defined molecular entities.

Synthetic organic chemists found camphor to be an attractive starting material for the synthesis a variety of more complex optically active products. In recent years we have been engaged in the studies on the rearrangement of the carbon skeleton of camphor. Besides delivering a lecture on the story of camphor, we will disclose our results on rearrangement reactions of camphor derivatives.





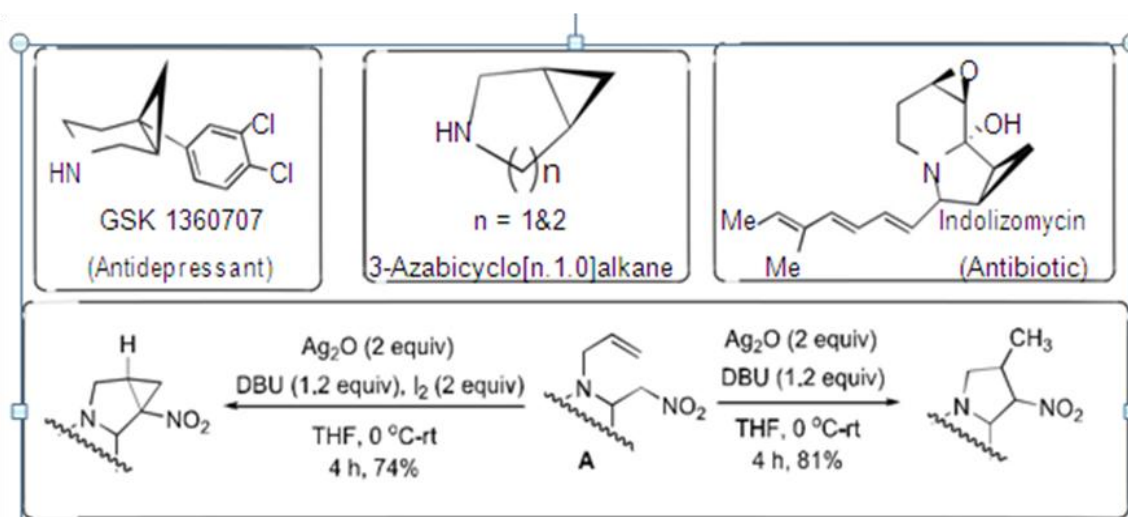
### IL3 SET OXIDATIVE CYCLIZATION: STEREOSELECTIVE SYNTHESIS OF HETEROCYCLIC RING SYSTEMS

**Sundarababu Baskaran**

*Department of Chemistry, Indian Institute of Technology Madras, Chennai - 600 036*

*E-Mail: sbhaskar@iitm.ac.in*

Stereoselective synthesis of biologically active molecules is a desired goal in organic synthesis.<sup>1</sup> The heterocyclic ring systems bearing cyclopropane are ubiquitous in many biologically active natural products and in particular 3-azabicyclo[n.1.0]alkane framework is very common in many pharmaceutically important lead molecules. As a result of their medicinal applications, several tedious multistep synthetic approaches have been reported for the construction of 3-azabicyclo[n.1.0]alkane derivatives. One way that molecular complexity can be expeditiously constructed is by combining two or more distinct reactions into a single transformation. Moreover, single electron transfer (SET) oxidation of carbanion is one of the best ways of generating carbon-centered radicals, however the synthetic potential of the oxidative cyclization of carbanion strategy has not been fully explored in the stereoselective synthesis of biologically important molecules. In this presentation, our cascade-based strategies towards the synthesis of some of the molecules will be discussed.<sup>2,3</sup>



## **IL 4** PEM - BASED ELECTROLYSER FOR THE PRODUCTION OF HYDROGEN

*Electro Inorganic Division  
CSIR Central Electrochemical Research Institute  
Karaikudi – 630 003, Tamil Nadu, India  
E-Mail: sozhan@cerci.res.in*

The growing demand for energy throughout the world has caused great importance to be attached to the exploration of new source of energy among them solar energy now holds much promise as we are approaching the end of the fossil fuel era, it has become clear that we shall have to manufacture our future fuel since there are no natural energy sources or fuels having the convenience of utilization of the fossil fuel especially that of the best fluid fossil fuels. This in fact provides humankind great opportunity to decide on the best fossil fuel to manufacture. In this context hydrogen is the best fuel with many unique and unmatched qualities; it is the best transportation fuel, environmentally the most compatible fuel, the safest fuel and most effective fuel to society.

Hydrogen is not freely available in nature, it exists as compound like hydrocarbons, water etc. Hydrogen can be produced from the renewable energy resources, water and biomass, extract from variety of processes by photolysis, electrolysis, thermo chemical, and biochemical methods etc. All large-scale hydrogen production facilities currently in operation use processes such as steam–methane reforming or partial oxidation of heavy hydrocarbons, which emit large amount of carbon dioxide.

Electrolysis of water is the simplest technology for producing hydrogen. The electrolytic production of hydrogen is currently the only way to produce large quantities of hydrogen without emitting the traditional byproducts associated with fossil fuels. High pure hydrogen can be produced by electrolysis of water; alkaline water electrolyser commercially available is having certain disadvantages (alkaline fumes, more space occupation, low current density and high energy consumption).

PEM (Polymer Electrolyte Membrane), water electrolyser consists of MEA (Membrane Electrode Assembly), current lead plates, fluid distributor, gaskets and end plates. PEM water Electrolyser is advanced version of the water electrolyzers. The hydrogen can be produced by availability of off peak power or surplus power from hydroelectric power stations. Likewise the excess power or low power from the wind source and solar power can be used for production of hydrogen by water electrolysis.

## **IL 5** CARBON BASED NANOCOMPOSITES FOR ANODE OF RECHARGEABLE LI-ION BATTERY

**P. Murugan**

*Functional Materials Division, CSIR Central Electrochemical Research Institute*

*Karaikudi – 630 003, Tamil Nadu, India*

*E-Mail: murugan@cerci.res.in*

In the present context, rechargeable Lithium Ion Battery (LIB) emerged as an irrefutable power source for portable electronic and electrical devices. Due to its various salient features, such as, high capacity, better operational voltage and compact size, the LIB outperforms conventional energy storage devices. Even though LIB is well commercialized long back, further modifications of its components are still considered as a very important task to achieve the fast growing demands in large scale electrical applications. Especially for anode, the well-commercialized material is graphite, for which the theoretical specific capacity is limited to 372 mAh/g as a result of the structural restriction of graphite which leads to form  $\text{LiC}_6$  compound. In this perspective, other elements from carbon family, known as intermetallics such as Si, Ge, and Sn are well attracted among the researchers since these materials possess higher theoretical capacity than that of graphite. In this work, we have explored the structural, electronic and electrochemical properties of Si/Ge/Sn-Li-CNT (or graphene) composites by employing first principles density functional theory (DFT) calculations. Our results show that the charge transfer between lithiated nano-clusters and CNT facilitates the adsorption cluster inside CNT, hence plays a crucial role for providing the higher structural stability for these composite anode materials. The calculated AIV of the composite manifest that they are suitable for LIB anode applications.

## **IL 6** NANOSIZED SEMICONDUCTOR MATERIALS: DIVERSE STRUCTURES WITH TAILORED PROPERTIES

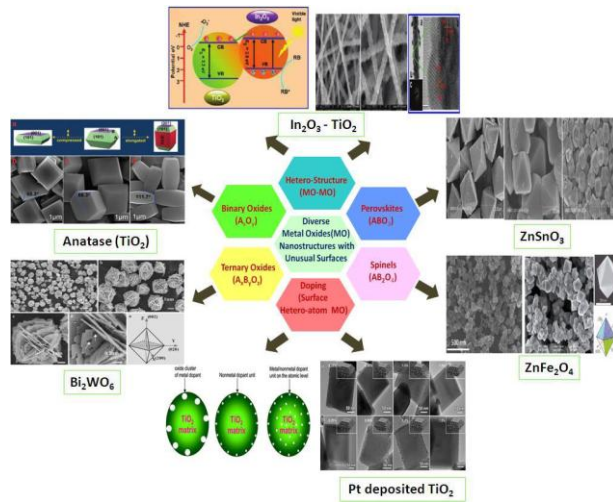
**Sambandam Anandan**

*Nanomaterials & Solar Energy Conversion Lab, Department of Chemistry,*

*National Institute of Technology, Trichy - 620 015, India*

The synthesis of nanoparticles with unique properties has been intensively investigated through the process of acoustic cavitation in addition to various synthetic approaches. However acoustic cavitation-induced “sonochemistry” provides a unique interaction between energy and matter. Extraordinary conditions, namely, hot spots of 5000 K, pressures of ~1000 bar, heating and cooling rates of  $>10^{10} \text{ K s}^{-1}$ , generated during acoustic cavitation permit access to a range of chemical reaction conditions. In this lecture, the sonochemical synthesis of nanosized semiconductor particles for energy and environmental applications were discussed.

**Keywords:** Sonochemistry, Noble metals, Nanomaterials

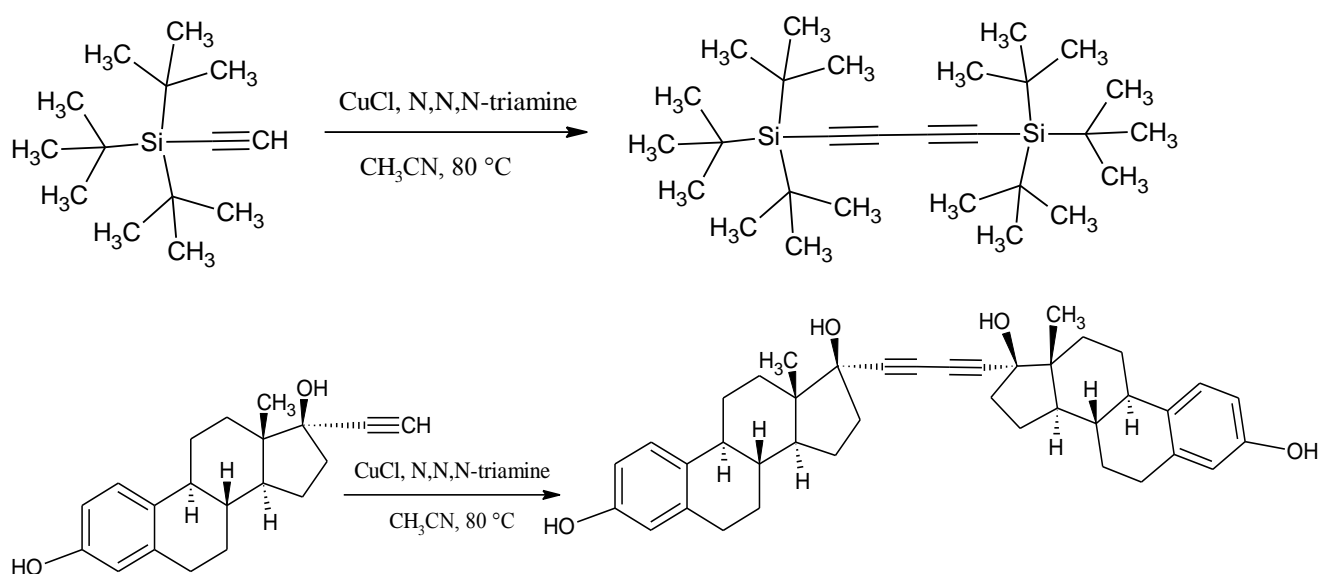


# Abstracts

**ORAL PRESENTATION**

**OP 1**    **Copper(I)-Catalyzed Highly Efficient Homo coupling of Terminal Alkynes to 1,3-Diynes****P. Tamilselvan***Associate Professor of Chemistry, Regional Institute of Education (NCERT, New Delhi), Mysuru-570006.*

Compounds containing 1,3-diyne linkage are known to have a variety of medicinal properties such as antifungal, antibacterial, anti-inflammatory, and antitumor activities. The diynes are also found to have their applications in the production of a variety of polymers and supramolecular materials. The synthesis of 1,3-diynes is better achieved by the classic homocoupling of terminal alkynes catalyzed by Cu(I) salts. Literature survey reveals the availability of numerous Cu(I) catalyzed homocoupling of terminal alkynes in the presence of various bases. Recently, palladium complexes in combination with Cu salts, Au, Ag, and Ni salts were also employed as catalysts. However the results are not as satisfying as the procedures involving Cu(I) salts. In an attempt to find versatile base free protocol involving Cu(I) salt, our group screened various combinations of CuI and CuCl and a variety of amine based ligands in various solvents such as nitromethane, acetonitrile, etc. The screening and the optimization conditions revealed that both CuI or CuCl could be used as the catalyst in combination with N,N,N-triamine in acetonitrile. In this procedure, a mixture of triamine, CuI or CuCl, alkyne, and acetonitrile was taken to a schlenk tube and immersed in a preheated oil bath and stirred typically for 30 to 45 minutes. The long chain alkynes such as nonyne are converted to corresponding 1,3-diynes in less than 2 hours. The progress of the reaction was monitored using fluorescent coated TLC plate. The solvent was removed under vacuum and column chromatographed using a short path column.



## **OP 2** Manganese dioxide nanospheres: A novel hydrophilic modifier for ultrafiltration water treatment membranes

**M. Sri Abirami Saraswathi, K. Divya, N. Kanimozhi and A. Nagendran\***  
*Polymeric Materials Research Lab, PG & Research Department of Chemistry,  
Alagappa Government Arts College, Karaikudi - 630 003, India*

In this study, MnO<sub>2</sub> nanospheres were prepared by hydrothermal technique, and their influence on the permeation and antifouling properties of poly (ether imide) (PEI) ultrafiltration (UF) membranes was investigated by the addition of three different concentrations such as 0.5, 1.0 and 2.0 wt.% (designated as PEI-0.5, PEI-1 and PEI-2 respectively). The hydrophilicity properties of PEI/MnO<sub>2</sub> membranes were investigated using contact angle and pure water flux measurements. The results revealed that the addition of MnO<sub>2</sub> nanospheres enhances the permeation and antifouling properties of the membranes due to the increased surface hydrophilicity and is also clearly implies the effect of added MnO<sub>2</sub> nanospheres. The morphological characterization such as SEM and AFM revealed that the modified membranes showed a noticeable change in the macrovoid formation, porosity and roughness parameters. During the fouling experiments using BSA and HA as model foulants, the modified membranes exhibited better antifouling capacity and enhanced flux recovery ratio (FRR) due to the improved hydrophilicity and water layer formation on the membrane surface. The membrane hydraulic resistance and tensile strength results suggested that, the PEI/MnO<sub>2</sub> membranes exhibited improved resistance to pressure and mechanical stress compared to standard PEI, due to the changes occurred in their morphologies. However, the additive loading limited at 2 wt.%, in order to avoid the barrier effects of MnO<sub>2</sub> nanospheres at higher concentrations.

**Key words:** Ultrafiltration membrane, Polyetherimide, MnO<sub>2</sub> nanospheres, Hydrophilicity, Anti-fouling

### **Introduction**

As an efficient separation technology, ultrafiltration (UF) process with polymers as base has been widely used in chemical, pharmaceutical and food industries [1]. However, the inherent hydrophobicity of the polymer materials often causes fouling due to the interactions between membrane surface and macromolecular foulants present in the feed water. In order to overcome this problem, blending of fillers with commercial polymers in fabrication has been employed by the researchers worldwide. In this study, PEI a commercially available polymer was employed as base material and the MnO<sub>2</sub> nanospheres, synthesized by hydrothermal method were employed as hydrophilic nanofiller. The performance hydrophilic and antifouling properties of the membranes were investigated and reported in detail.

## Experimental section

### Synthesis and characterization of MnO<sub>2</sub> nanospheres

The synthesis of MnO<sub>2</sub> nanospheres was carried out in a hydrothermal synthesis using MnCl<sub>2</sub>·4H<sub>2</sub>O, KMnO<sub>4</sub> and 2-propanol [2]. Briefly, to 100 ml of 2-propanol, the pre-determined amount of MnCl<sub>2</sub>·4H<sub>2</sub>O was added and kept on reflux at 80°C for 1h and few drops of KMnO<sub>4</sub> solution is added to the refluxed solution. Once a deep brownish colour MnO<sub>2</sub> nanospheres were got precipitated, it was further filtered and dried. The as synthesized MnO<sub>2</sub> nanospheres were characterized by Raman spectroscopy (ReinshawInvia Raman Microscope) and Field Emission Scanning Electron Microscope (FESEM) (Carl Zeiss, Germany) for the functional group and morphological analysis.

### Fabrication and characterization of PEI/MnO<sub>2</sub> nanocomposite membranes

#### Functional group and morphological characterizations

Phase inversion method was adopted to fabricate the novel PEI/MnO<sub>2</sub> nanocomposite membranes [3] by employing PEI as the base polymer material, NMP as solvent and the as synthesized MnO<sub>2</sub> nanospheres as nanoadditive. The prepared membrane samples were characterized by Energy Dispersive X-ray (EDX) analysis in order to detect their elemental composition using Bruker nano, German by keeping the accelerating voltage at 10keV.

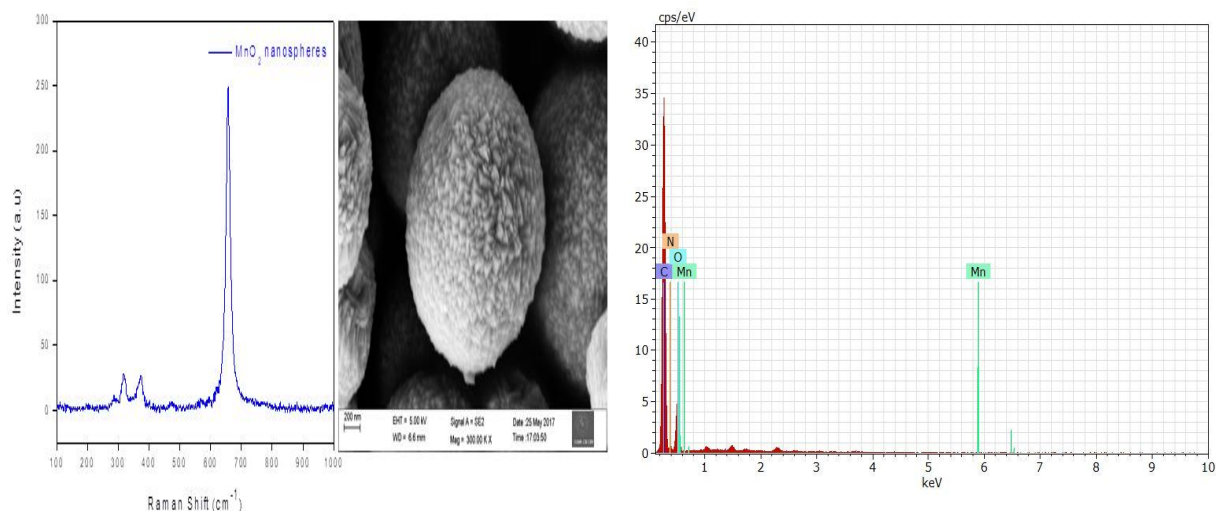
#### Hydrophilicity and Antifouling characterizations

The hydrophilicity characterizations were done using pure water flux, percent water content, contact angle and percentage porosity measurements. Further, the antifouling capacity and solute rejection properties of the membranes were analyzed by reversible and irreversible fouling, flux recovery ratio (FRR) and percent solute rejection.

## Results and Discussion

The Raman and FESEM showed the successful formation of MnO<sub>2</sub> nanospheres through hydrothermal method [4]. The EDX of nanocomposite membranes showed the elemental peaks of C, H, O, N and Mn, which confirms the existence of MnO<sub>2</sub> nanospheres in the membrane matrix [5]. With the increasing concentration of MnO<sub>2</sub> nanospheres, the PWF, percent WC, percent porosity increases and contact angle decreases. This is attributed to the intrinsic hydrophilic character of MnO<sub>2</sub> nanospheres. Also, the enhanced hydrophilicity leads to the formation of water molecule layer on to the membrane surface which makes the adhesion of foulants difficult. By this way, the antifouling and rejection properties of the nanocomposite membranes also enhanced [6, 7].





## Conclusion

MnO<sub>2</sub> nanospheres were successfully prepared by hydrothermal method and incorporated into PEI membrane matrix with increasing amounts of 0.5, 1.0 and 2.0 wt.% via phase inversion method and incorporated into the PEI membrane matrix. The improved hydrophilicity, enhanced BSA and HA rejection and improved mechanical and antifouling properties of the MnO<sub>2</sub> nanospheres incorporated membranes were confirmed by highly enhanced PWF, percent water content, percent solute rejection, tensile strength measurement, antifouling capacities. Hence, the results from this study showed that, the synthesized MnO<sub>2</sub> nanospheres is an excellent nanoadditive to be incorporated in appropriate amount can perform as a promising agent for new applications for this type of membranes.

## Reference

- L. Yan, Y.S. Li, C.B. Xiang, S. Xianda, J. Membr. Sci. Vol. 276 [1-2] 2006, 162–167.  
 R. Ramprasath, G. Kalpana, T. Pandiselvi, IJIR, Vol. 2 [6] 2016, 1409-1413.  
 M. Sri AbiramiSaraswathi, D. Rana, P. Vijayakumar, S. Alwarappan and A. Nagendran, Mater. Sci. Eng. C. Vol. 83 [23] 2018, 108-114.  
 Subhra Jana, SurojitPande, Arun Kumar Sinha, Sougata Sarkar, Mukul Pradhan, MrinmoyeeBasu, SandipSaha, and Tarasankar Pal, J. Phys. Chem. C, Vol. 113 [4] 2009, 1386–1392.  
 C. Zhao, X. Xu, J. Chen, F. Yang, J. Environ. Chem. Eng. Vol. 1 [3] 2013, 349-354.  
 S. Vetrivel, M. Sri AbiramiSaraswathi, D.Rana, A.Nagendran, J.Bio.Macro. Mol. 107, 2018, 1607-1612  
 M. Padaki, D. Emadzadeh, T. Maturra, A. F. Ismail, Desalination 362, 2015, 141–150

**Table 1. Polymer blend composition and hydrophilicity performance of Standard PEI and PEI/MnO<sub>2</sub> nanocomposite membranes**

Membrane	Blend composition		Solvent NMP	PWF (Lm <sup>-2</sup> h <sup>-1</sup> )	% WC	Contact angle (°)
	PEI	MnO <sub>2</sub>				
Standard PEI	17.5	0	82.5	39.5±1.2	45.2±0.5	79.4±0.5
PEI -0.5	17.0	0.5	82.5	79.4±1.8	56.1±0.8	71.2±0.8
PEI -1	16.5	1.0	82.5	98.5±1.0	66.4±1.2	64.2±1.2
PEI -2	15.5	2.0	82.5	106.5±1.2	74.5±0.8	58.6±1.2

**Table 2. Solute rejection and roughness parameters of Standard PEI and PEI/MnO<sub>2</sub> nanocomposite membranes**

Membrane code	Solute rejection (%)		Surface roughness (nm)		
	BSA	HA	R <sub>a</sub>	R <sub>q</sub>	R <sub>z</sub>
Standard PEI	84.5±0.2	83.4±0.2	20.6	26.2	46.8
PEI -0.5	87.2± 0.1	86.8±0.3	33.2	36.6	69.8
PEI -1	92.6± 0.5	91.6±0.2	32.6	43.2	75.8
PEI -2	96.5± 0.2	96.0±0.5	40.4	49.1	89.5

### **OP 3 Custom-made sulfonated poly (ether sulfone)/poly(vinyl alcohol) nanocomposite membranes containing tungsten disulfide nanosheets for DMFC applications**

**K. Divya, M. Sri Abirami Saraswathi, M. Rahumath Ayisha and A. Nagendran\***  
*Polymeric Materials Research Lab, PG & Research Department of Chemistry, Alagappa  
 Government Arts College, Karaikudi - 630 003, India*

Nanocomposite proton exchange membranes comprising of sulfonated poly (ether sulfone), poly (vinyl alcohol) and tungsten disulfide were fabricated successfully by solution casting method. Reinforcement owing to the existence WS<sub>2</sub> on SPES/PVA afforded good mechanical and thermal stabilities to the nanocomposite membrane, which was confirmed by the tensile strength and thermogravimetric analysis. The surface morphology of the membranes in terms of roughness were scrutinized using AFM, showed the intercalation of WS<sub>2</sub> nanosheets in polymer matrix. The intermolecular bond stretching, structural reorganization of membranes were analyzed using FT-IR and XRD. When PVA content was increased it was found that increase in water uptake and tensile strength of SPES membrane however decrease in proton conductivity upto 20 wt.% and increases from 30 wt.%. Further, incorporation of WS<sub>2</sub> nanosheets into SPES/PVA matrix, the mechanical stability, proton conductivity and methanol barrier properties

of membrane were enhanced. These results showed that SPES/PVA/WS<sub>2</sub> blend membranes were promising for possible use as a PEM in DMFCs.

**Keywords:** PEM, DMFC, SPES, nanocomposite membrane, WS<sub>2</sub>

## Introduction

In recent years Direct methanol fuel cells (DMFCs) are attracted huge attention for portable uses. Proton exchange membrane (PEM) plays an important role which should allow only proton transport and no methanol crossover from anode to cathode, since methanol leads to reduce the performance of fuel cell. Mostly perfluorinated membranes such as Nafion used due to their high proton conductivity, flexibility, and good chemical stability. Beside some disadvantages such as high methanol crossover, low proton conductivity at temperature above 80°C, and high cost to cause to focus alternative PEM. Sulfonated hydrocarbon polymers are mostly used because sulfonating group enhance the conductivity and good methanol barrier but the mechanical property deteriorate due to the plasticizing nature of sulfonic acid groups. Further, PVA crosslinking agent added to improve the mechanical property as well as to restrict the methanol cross over. However to improve the conductivity of SPES/PVA further, inorganic fillers such as WS<sub>2</sub> nanosheets are used and utilized to interact with hydroxyl group of SPES/PVA to enhance the overall performance [1].

## Experimental Section

PES sulfonated by using sulfonating agent such as sulfuric acid and chlorosulfonic acid under nitrogen atmosphere [2]. E-WS<sub>2</sub> nanosheets are synthesized by liquid exfoliation method [3]. SPES, SPES/PVA and SPES/PVA/WS<sub>2</sub> membranes were prepared and named as SPES, SP<sub>x</sub> and SPW<sub>y</sub>, where x and y were represented the weight percent of PVA and E-WS<sub>2</sub> respectively. The composite membranes with 10 wt% concentration of SPES/PVA (consisting of 10-30wt.% of PVA and 1, 3, 5 wt.% of WS<sub>2</sub>) were prepared via solution casting method and the characterized in terms of FT-IR, XRD, water uptake, IEC, AFM, mechanical stability, proton conductivity and methanol permeability.

## Results and Discussion

### Structural Characterisation

The sulfonation of PES is confirmed by FT-IR analysis of SPES as shown in Figure 1(a). The peak at 1024 cm<sup>-1</sup> is attributed to aromatic SO<sub>3</sub>H group whereas peaks at 1236 cm<sup>-1</sup> and 1074 cm<sup>-1</sup> is due to the asymmetric and symmetric stretching vibration of O=S=O respectively. Figure 1(b) shows a characteristic broad band at 3400 cm<sup>-1</sup> for -OH stretching and at 2924 cm<sup>-1</sup> for symmetric -CH<sub>2</sub>- stretching of nanocomposite membranes. The double peak observed around 1319 cm<sup>-1</sup> assigned to C-O stretching. These observations proved that the PVA participated in the SPES network and the absence of WS<sub>2</sub> peak in SPES/PVA matrix due to their fine distribution of

the membrane matrix. Figure 3 shows the XRD result of E-WS<sub>2</sub> sheets, and exhibited (002) peak intensity, arising from successive S-W-S sandwiches, tends to be quite sharp [3]. AFM image shows increase in surface roughness of membrane by the addition of WS<sub>2</sub> nanoparticle in SPES/PVA matrix,.

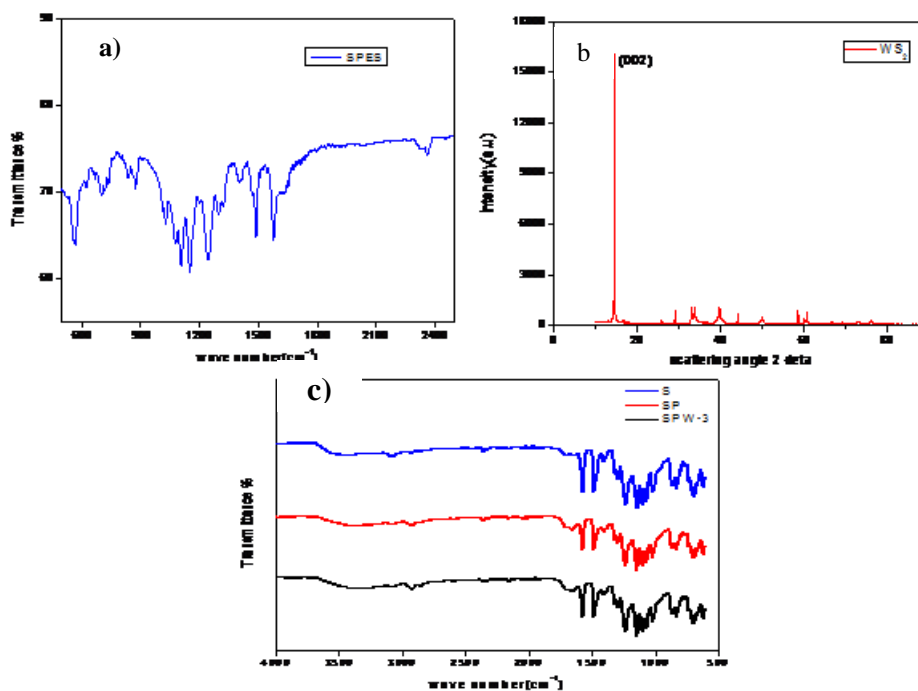


**Figure 1:** (a) FT-IR spectrum of SPES (b) FTIR spectrum of SPES, SP-30 and SPW-3 membranes (c) XRD spectrum of WS<sub>2</sub>

**Table 1.** Physicochemical properties of membranes

Membrane	Water uptake (%)	Swelling ratio (%)	IEC (meq. g <sup>-1</sup> )	Proton Conductivity (Scm <sup>-1</sup> )	Mechanical strength (Mpa)
SPES	16.2	9.7	1.65	$3.32 \times 10^{-2}$	50
SP-10	19.3	11.1	1.24	$3.94 \times 10^{-3}$	65
SP-20	21.5	12.6	0.62	$2.48 \times 10^{-3}$	72
SP-30	23.0	14.3	0.86	$4.05 \times 10^{-3}$	80
SPW-1	25.8	16.2	1.75	$3.78 \times 10^{-2}$	111
SPW-3	28.4	18.3	3.14	$4.65 \times 10^{-2}$	125
SPW-5	32.3	19.6	2.17	$3.23 \times 10^{-2}$	130

### Membranes Characterizations

Physicochemical behaviour of prepared nanocomposite membranes are shown in the Table 1. Water uptake, ion exchange capacity, proton conductivity are very important parameters

for PEMs. Water molecules are essential for proton transferring in membranes. The available water molecules have an important role in proton conductivity of membrane by proton transferring Vehicle and Grotthuss mechanisms. Water uptake of the PEMs were increased by the introduction of hydrophilic PVA as well as hydrogen bonding of WS<sub>2</sub>. IEC shows the density of proton exchangeable group in membrane. IEC values of SPES/PVA membranes were decreased due to the absence of exchangeable proton group (SO<sub>3</sub>H) in PVA, however IEC values were increased when WS<sub>2</sub> was added in the SPES/PVA matrix [3]. It is due to the sulfur is commonly regarded as hydrogen bonding acceptor and forming a hydrogen bonding between OH group of SPES/PVA and sulfur atom of WS<sub>2</sub> which leads to high proton conductivity [2]. Mechanical and thermal stability also enhances in modified nanocomposite membrane due to the effective dispersion of WS<sub>2</sub> into SPES/PVA matrix enhance the stability of the membrane.

### Conclusions

The WS<sub>2</sub> incorporated SPES/PVA nanocomposite membranes were successfully fabricated through facile solution casting method. The modified PEMs showed high water uptake, IEC, and proton conductivity than those of SPES and SPES/PVA membranes. The introduction of WS<sub>2</sub> reorganize the aromatic polymer chains through H-bonding interaction which strengthen the membrane thermally and mechanically and also reduce the methanol crossover. The present study affords useful information about the fabrication and physicochemical, thermo mechanical, and proton conduction properties of SPES/PVA/WS<sub>2</sub> nanocomposite PEMs. Therefore, this study might help to realize the significances of nanocomposite PEMs in the applications of DMFCs.

### References

- Novel nanocomposite membranes based on blended sulfonated poly (ether ether ketone)/poly (vinyl alcohol) containing sulfonated graphene oxide/Fe<sub>3</sub>O<sub>4</sub> nanosheets for DMFC applications, *RSC Adv.*, **5**, 74054-74064.
- A. Muthumeenal, Neelakandan, S., Rana, D., Matsuura, T., Kanagaraj, P., Nagendran, A., Sulfonated poly ether sulfone (SPES)- Charged surface macromolecules (cSMMs) blends as a cation selective membrane for fuel cells, *14*, 853-861.
- Sung-Kon Kim, Jeong Jae Wie, Qasim Mahmooda and Ho Seok Park Anomalous nano-inclusion effects of 2D MoS<sub>2</sub> and WS<sub>2</sub> nanosheets on the mechanical stiffness of polymer nanocomposites, *Nanoscale*, **6**, 2014, 7430-7435.

## **OP 4** Novel Approach For Substituting Hazardous Additives In Zinc Electrode For Alkaline Silver Oxide-Zinc Battery

**K. Rathinakumar<sup>1</sup>, G.A. Pathanjali<sup>2</sup> and R.Karvembu<sup>3</sup>**  
*National Institute of Technology, Tiruchirappalli*  
*krkumar1969@yahoo.com*

Historically, toxic heavy metals such as Mercury (Hg), Cadmium (Cd) and Lead (Pb) were used as alloying additives to the zinc electrode in alkaline cells. The corrosion behavior of

the baser metal such as Zn altered, with the inclusion of more electropositive metals thus stabilizing both the corrosion cum electro deposition steps that take place during the charging cum discharging of secondary rechargeable cells. The formation of the zinc amalgam with mercury improves the contact between zinc powder grains, improving current collection and reducing gas evolution of the alkaline cells. The zinc amalgam with mercury also increases the hydrogen overvoltage, inhibiting corrosion of the zinc and hydrogen gas evolution. Due to environmental crisis and concerns, mercury has been eliminated in all usable application. In this study, the negative electrodes (zinc anode) are made using additives and the electrodes are assembled with positive silver electrode and formed as cell. During the electrical performance tests, the capacity and gasometric estimation are studied.  $\text{Bi}_2\text{O}_3$  additive has shown the best performance equivalent to mercury and reduces the corrosion of the zinc electrode and minimizes hydrogen gas production.

**Key words:** silver oxide-zinc, lead monoxide, bismuth oxide, cadmium oxide.

### Introduction:

The Zinc electrode is a negative (anode) active material, which is very suitable for use in aqueous electrolytes due to its high energy per unit volume and high hydrogen over potential. This instability becomes apparent in the internal pressure, which is often accompanied by self-discharging due to cell distortion. Gas could form in all of these types of batteries due to the corrosion of zinc. This corrosion can cause electrolysis, with the generation of hydrogen gas in the canister. The build-up of hydrogen gas can cause limits the ability of the battery to function. In alkaline batteries, mercury is the most useful additive to the zinc anode material for suppressing hydrogen gas evolution that is caused by self-discharge reactions [1-4]. Multiple components, such as viz., indium, lead, bismuth, and cadmium, to zinc particles is effective in suppressing hydrogen gas evolution zinc has been added with bismuth to suppress evolution of hydrogen gas due to the self discharge reaction of zinc and by the increase in internal cell impedance. The use of mercury has become an environment issue and attention has been focused on developing mercury free batteries [5].

### Methodology

Zinc negative electrodes are manufactured by wet coating process. Ratio of additives used in Zinc mix is as per Table - 1

Additives	Weight		
	Zn	O	Additive
PbO	57%	42%	1%
$\text{Bi}_2\text{O}_3$	74%	22%	4%
CdO	54%	43%	3%
HgO	53%	46%	1%

TABLE:1. MIXING RATIO

Cellulosic thin paper was placed in the cavity of 38 mm x 44 mm size mould. 1.5 g of prepared mix was evenly spread over the paper and perforated silver grid to which is attached a silver tab for current collection, was placed over the ZnO mix and further another portion of 1.5 g of ZnO was spread over the silver grid. Then, 4 sides of the paper were folded to cover the ZnO and pressed at 204 kg/cm<sup>2</sup> to achieve 0.65 mm thickness of pressed electrode. The Negative electrode was placed in centre of a 'U' wrap so that two positive electrodes faced either side of the single negative electrode. The entire assembly was inserted into a cell case and terminals were connected to the cell cover. The cell cover was sealed with case using binder. The cells were tested to ensure leak free cell case to cell cover joint. The assembled cells were subjected to electrical tests.

### Findings

Cells with different additives such as PbO, Bi<sub>2</sub>O<sub>3</sub>, CdO and HgO in a range of compositions varying from 1% upto 5% were prepared and subjected to electrochemical tests and gas measurement studies. Gas Evolution and Capacity of Cell with Control Cell during charge and discharge are tabulated in Table – 2.

Test Parameters	Charging Details		Control Sample	Additives		
	Current-A (I)	End Voltage V	1% HgO	4% Bi <sub>2</sub> O <sub>3</sub>	1% CdO	1% PbO
TC-1 – Charging Gas volume, cc.	0.0625	2.05	1.40	1.50	2.40	2.40
TC-1– Discharging Gas Volume, cc.	0.625	1.1	1.80	1.60	1.40	1.40
Capacity, Ah.			1.27	1.04	1.30	1.25
TC-2 Charging Gas Volume, cc.	0.0625	2.05	1.20	1.60	4.00	3.10
TC-2 Discharging Gas Volume, cc.	3.125	1.1	1.20	1.20	1.30	1.40
Capacity, Ah.			0.833	0.83	0.93	0.78

**Table – 2 Cell Performance Characteristics**

### Conclusion

Generally during charging, gas volume of cells with lead oxide & Cadmium oxide additives were found to be more than the control cell, whereas the gas volume of 4% Bismuth oxide was found to be less than that of control cell. During discharging gas volume of lead oxide & Cadmium oxide was found to be more than the control cell, whereas the gas volume of Bismuth oxide was found to be less. Based on the performance evaluation and data analysis, the gas volume in cells using Bismuth oxide additive is comparable with that of control cell with Mercury

Oxide. Hence Bismuth oxide can be considered as a suitable alternate additive to replace the hazardous heavy metal.

### Reference:

- M. Yano, S. Fujitani, K. Nishio, Y. Akai, and M. Kurimura, *J. Power Sources*, 74, (1998) 129.  
Y. D. Cho and G. T. Fey, *J. Power Sources*, 184, 610 (2008).  
M.H.S. Andrade, M. L. Acioli, J.G.S. Júnior, J.C.P. Silva, E. O. Vilar, and J. Tonholo, *Int. J. Hydrogen Energy*, 29, (2004) 235.  
Cornell, G. Lindbergh, and D. Simonsson, *Electrochim. Acta*, 37, (1992) 1873.  
M. Yano, S. Fujitani, K. Nishio, Y. Akai, Storage characteristics of mercury-free alkaline manganese batteries, *J. of Applied Electrochemistry*, (1998) 1221-25

## **OP-5** Antimicrobial activity of cerium oxide nanoparticle synthesized by green approach

S. Induja<sup>a</sup>, G.V. Geetha<sup>a</sup>, M. Periyanyaki<sup>a</sup> and R. Sivakumar<sup>a,\*</sup>

<sup>a</sup>*Department of physics, Alagappa University, Karaikudi-630 003*

\**Corresponding author email: krsivakumar1979@yahoo.com*

Metal oxide nanoparticles have attracted great interest due to their various applications. In the present work, we focused on the research work concerning antimicrobial activity of cerium oxide nanoparticles. The synthesis of cerium oxide nanoparticle was carried out from *Acalypha indica* leaf extract by co-precipitation method. Aqueous solution of 0.1 M cerium chloride heptahydrate [CeCl<sub>3</sub>.7H<sub>2</sub>O] was used for the synthesis. The powdered sample was calcined at 400°C for 2 hr in air to get cerium oxide nanoparticles. The structural and optical properties of the synthesized product were studied using various characterization techniques. X-ray diffraction analysis showed the presence of cubic phase CeO<sub>2</sub>. The crystallite size of the particle is about 16 nm as calculated by Scherrer formula. From the optical absorbance data, the energy band gap of the sample was found to be 2.5 eV.

**Keywords:** Green synthesis, Cerium oxide, *Acalypha indica*, Antibacterial property.

### Introduction

Nanotechnology and biomedical sciences open the possibility for a wide variety of biological research topics and medical uses at the molecular and cellular level. The biosynthesis of nanoparticles has been proposed as a cost effective and environmental friendly alternative to chemical and physical methods. Plant mediated synthesis of nanoparticles is a green chemistry approach that connects nanotechnology with plants. Among the biological alternatives, plants and plant extracts seem to be the best option. They are cost efficient and require low maintenance. Novel methods of ideally synthesizing nanoparticles are thus thought that are formed at ambient temperatures, neutral pH, low cost and environmental friendly fashion. Keeping these goals in



view metal oxide nanomaterials have been synthesized using plant extract using co-precipitation method[1].

### **Materials and methods**

The present study reports the biosynthesis of a pure CeO<sub>2</sub> nanoparticle by the co-precipitation method using *Acalypha indica* leaf extract. It acts as a capping and reducing agent so as to reduce the particle size. The cerium chloride hepta hydrate [CeCl<sub>3</sub> .7H<sub>2</sub>O] was directly used without further purification. The leaves of *Acalypha indica* were collected, washed thoroughly with double distilled water and dried for a week at room temperature.

### **Preparation of plant extract**

The dried and finely cut leaves (20 g) were boiled in a 250 ml Erlenmeyer flask with 100 ml of double distilled water for ten minutes. Then the extract was filtered through ordinary filter paper and through Whatman No. 1 filter paper. The filtrate was collected and it was kept in a refrigerator at 4° C for further proceedings.

### **Synthesis of cerium oxide nanoparticle**

Aqueous solution of 0.1 M cerium chloride hepta hydrate (CeCl<sub>3</sub> . 7H<sub>2</sub>O) was used as the prime precursor for the synthesis of cerium oxide nanoparticles. 10 ml of *Acalypha indica* leaf extract was added to 50 ml of 0.1 M CeCl<sub>3</sub>. 7H<sub>2</sub>O in a 250 ml beaker and stirred at 80° C for two hours. After adequate time of stirring the particles were precipitated at the bottom of the beaker. The precipitated particles were washed with water and dried in air oven at 100°C for few hours for complete dehydration. The dried sample was powdered using mortar and pestle and subjected to calcination at 300° C , 400° C for two hours to get cerium oxide nanoparticles. The same experiment was repeated with 0.2 M of CeCl<sub>3</sub>. 7H<sub>2</sub>O and the obtained particles were calcined at 300° C and 400° C for two hours. Thus cerium oxide nanoparticles for different concentrations of precursors and different annealing temperatures were obtained.

### **Results and discussion**

The crystalline nature of the as-prepared sample was identified using the X-ray diffractometer as shown in figure 1. The peaks corresponding to (111), (200), (220), (311), (400) and (331) planes were located at angles (2θ) of 28.71°, 33.4°, 47.68°, 56.45°, 76.75° respectively. From the X-ray diffraction pattern it is confirmed that the cerium oxide nanoparticles belongs to face centered cubic structure (JCDPS card no.34-0394).The crystallite size of the nanoparticle was estimated by using scherrer's formula as 16 nm.

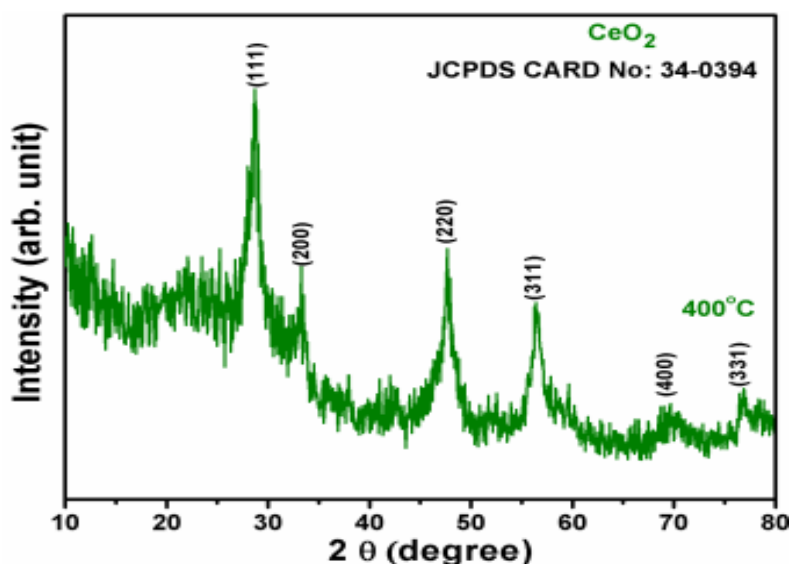


**Figure 1: X-ray diffraction pattern of the as prepared sample**

UV visible analysis showed that absorption peak shifted into UV-visible region. The optical energy band gap of nano-ceria was estimated using Tauc's equation

$$\alpha h\nu = A(h\nu - E_g)^{1/2}$$

The estimated band gap of the CeO<sub>2</sub> sample is 2.5 eV. It can be seen that the CeO<sub>2</sub> sample shows a decrease in  $E_g$  by a value 0.69 eV, compared to the bulk CeO<sub>2</sub> powders ( $E_g = 3.19\text{eV}$ ).

The photoluminescence spectra of CeO<sub>2</sub> nanoparticles were recorded with the excitation wavelength of 330 nm. The PL emission observed for CeO<sub>2</sub> nanoparticles is covering from the very short wavelength of 360 nm to long wavelength 520 nm. A good fit of five peaks Gaussian function is obtained for CeO<sub>2</sub> nanoparticles. The emission spectra of the CeO<sub>2</sub> nanoparticles are emphasized five peaks at 363, 412, 440, 488 and 520 nm. These bands are corresponding to near band edge emissions, violet emission, blue emission, blue-green emission and green emission, respectively [2].

## Conclusion

Cerium oxide nanoparticles were successfully synthesized using *Acalypha indica* leaf extract as precipitating agent. XRD, UV-Vis and PL studies clearly revealed the formation of CeO<sub>2</sub> nanoparticles. The smaller size and large surface area of the particle leads to high antimicrobial property. This was tested using Gram positive and Gram negative bacteria.

## Reference

- S.K.Kannan and M. Sundrarajan, *International Journal of Nanoscience*, 13, (2014) 1450018-1450025.
- Ayyakannu Arumugam Chandrasekaran Karthikeyan, Abdulrahman syedahamed, *Material Science and Engineering : C*, 49, 2015, 408-415.

## **OP-6** Physical and Electrochemical Characterization of Direct Current Electrodeposited Ni-Tin Nanocomposite Coatings

S. Kasturibai<sup>1</sup> and G. Paruthimal Kalaignan<sup>2\*</sup>

<sup>1</sup> Dept of Chemistry, Alagappa Government Arts College, Karaikudi-630 003, Tamilnadu, India

<sup>2</sup> Dept of Industrial Chemistry, Alagappa University, Karaikudi-630 003, Tamilnadu, India

E mail: pkalaignan@yahoo.com and kasturibai2007@gmail.com

### **Abstract**

In the present investigation, TiN reinforced nickel composite coatings were deposited on a mild steel substrate using direct current electrodeposition process employing a nickel acetate bath. Smooth composite deposits containing well-distributed Titanium nitride particles were obtained. The crystallite structure was fcc for electrodeposited nickel and Ni- TiN nanocomposite coatings. The corrosion potential ( $E_{\text{corr}}$ ) in the case of Ni-TiN nanocomposite had shown a negative shift, confirming the cathodic protective nature of the coating.

**Key words:** Electrodeposition, Nanocomposite coating, XRD, SEM, Micro hardness.

### **Introduction**

The expansion of current machinery requires metallic materials with better surface properties. The development of modern technology requires metallic materials with better surface properties. Particle-reinforced metal matrix composites generally exhibited wide engineering applications due to their enhanced hardness, better wear and corrosion resistance when compared to pure metal or alloy [1]. Acetate-based baths are environmental friendly compared to other baths [1, 2]. Titanium nitride (TiN) is a very hard ceramic material and possesses excellent dimensional stability.

### **Experimental Details**

Nickel bar of high purity (99.9%) was used as the anode and pre-treated MS plate specimen (4 cm X 2.5 cm) was used as cathode. Myriad bipolar pulsed power supply was used as current power source for all deposition studies. Surface morphology, microstructure and crystal orientation of the Ni and Ni – TiN nanocomposites were investigated by SEM and X-ray diffraction analysis respectively. Vickers Hardness was measured at an applied load of 50g for 15s. Potentiodynamic polarization and Impedance measurements were conducted using an electrochemical analyzer (EG&G – Auto lab Analyzer Model: 6310) connected to a PC for potential control and data acquisition.

### **Results and Discussion**

Smooth composite deposits containing uniformly distributed Titanium nitride particles were obtained. The crystal grains on the surface of Ni– TiN composite coating are compact. The preferred growth direction was also influenced by Titanium nitride nano-particles. Therefore, the preferred growth process of the nickel matrix in crystallographic directions  $\langle 111 \rangle$ ,  $\langle 200 \rangle$  and

<220> is strongly influenced at a concentration of 9 g/l. The structure of electrodeposited nickel and nickel nanocomposite coatings were face centered cubic (fcc). It was confirmed from ICDD-JCPDS standards [87-0712]. The effect of incorporation is maximum at a current density of 8 A/dm<sup>2</sup>. The microhardness values of the Ni- TiN nanocomposite coatings (840HV) were higher than that of pure nickel (310HV) due to dispersion-strengthening; matrix grain refining and increased with the increase of incorporated TiN particles content [3]. The corrosion potential ( $E_{\text{corr}}$ ) in the case of Ni- TiN nanocomposite coatings had shown a negative shift, confirming the cathodic protective nature of the coatings [4]. The corrosion rates of Ni- TiN nanocomposite coatings (1.45 milliinch/yr) were lower than that of electrodeposited pure nickel coating (67.69 milliinch/yr) in 3.5% NaCl solution. The impedance spectra has showed a depressed semicircle at the centre of real axis, which has been attributed to the roughness and inhomogeneity of the solid surfaces. The charge transfer resistance ( $R_{\text{ct}}$ ) values for Ni- TiN nanocomposite coatings were increased and the constant phase element (CPE) values decreased with increased TiN content in the composite coatings due to the distribution of relaxation times as a result of inhomogeneities present at a micro level or nano level such as the surface roughness and porosity. The enhancement in the corrosion resistance may be due to physical barriers produced by TiN to the corrosion process by filling crevices, gaps, and micron holes on the surface of the composite coatings.

## Conclusions

Pure nickel and Ni- TiN composite coatings were successfully fabricated using electrodeposition process employing an Acetate bath. The reinforcement of TiN in the composite coating has prohibited the columnar growth of the nickel grains resulting in random texture and smaller coating thickness in the composite coatings. The better corrosion resistance of the Ni- TiN nanocomposite coatings may be ascribed to the favourable chemical stability of the TiN nanoparticles, which help to reduce the hole size in the nanocomposite coatings and prevent the corrosive pits from growing up.

## References

- R. Bose and G. Paruthimalkalaignan, *Ionics*, 17(2011) 495-499.
- S Kasturibai, G Paruthimal Kalaignan *Materials chemistry and physics*, 147 (2014) 1042-1045
- M.A.K. Hazrayie, A.R.S. Aghdam, *Trans. Nonferrous. Mater. Soc. China* vol.20 (2010) 1017-1020
- S. Ramalingam, V.S. Muralidharan, A. Subramania, *J. Solid State Electrochemistry*, 13 (2009) 1777-1780.

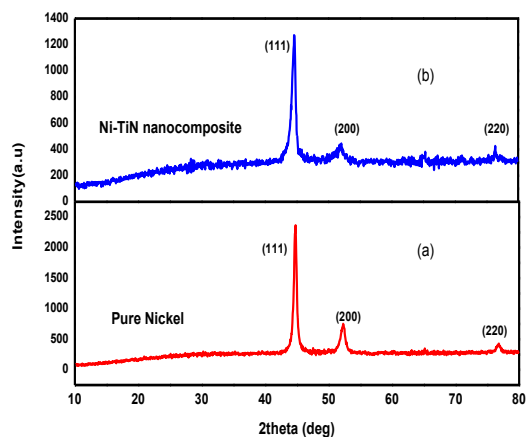


**Fig 1 XRD patterns of Direct current (a) Electrodeposited Nickel and (b) Ni-TiN nanocomposite coatings**

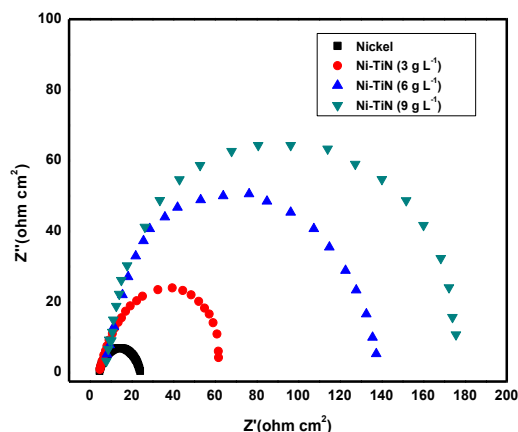


**Fig. 2 Impedance spectrum of Direct current deposited Nickel and Ni-TiN nanocomposite coatings**

facilitates redox reaction of CuS and gives rise to an additional pseudo-capacitance. The shape of CVs depicts pseudo-capacitive behaviour, showing an anodic peak at around  $\sim 0.6/0.57$  V and cathodic peak at  $\sim 0.25/0.23$  V for CuS and C-Dot/CuS respectively. The redox peaks indicate the Faradaic reaction happens during the cyclic process. Fig 2 shows the EIS results of CuS and C-Dot/CuS. It clearly reveals that, C-Dot/CuS have higher ionic conductivity than bare CuS.

## **OP 7 C-Dot/CuS Nanocomposite for Energy Storage Devices**

**P. Naveenkumar and G. Paruthimal Kalaigan\***

*Materials Research Laboratory, Department of Industrial Chemistry, Alagappa University, Karaikudi-630 003, Tamilnadu, India.*

*\*Corresponding Author Phone No: +91-9443135307, Fax: +914565 225202.*

*Email id: pkalaigan@yahoo.com*

### **Abstract**

In recent years, transition metal sulfides have much attraction to the researchers, because it has higher electronic conductivity, surface area, better safety and cheaper than the corresponding transition metal oxides.[1] Therefore, different metal sulfides were analyzed for the electrode materials of the supercapacitors. Among them, CuS is one of the significant transition metal sulfides belongs to the p-type semiconductor. It is most abundant and low-priced materials for various applications such as chemical sensors, Li-ion batteries, catalyst, solar cells and so on. So many efforts have been made to explore CuS as an electrode material for supercapacitors due to its high theoretical capacity.[2][3]

Carbon dots (CDs), a new generation of zero-dimensional carbon nanomaterials, have drawn intense attention in recent years, owing to their attractive properties and applications in

the fields of bio-imaging, photodetectors, optical sensing, photovoltaic devices, and photocatalysis.[4] More recently, CDs were emerged in the fields of energy storage such as lithium ion batteries and supercapacitors. CDs usually exhibited strong hydrophilicity, which can improve the wettability of the electrolyte.[5]

In this present work, we have prepared the nanocomposite of C-Dot/CuS by solvothermal method. The prepared materials were characterized by XRD, FTIR, UV-DRS, and SEM with EDAX. The electrochemical performance was evaluated by three electrode systems consist of active materials coated nickel foam as working electrode, Pt foil as counter electrode and Ag/AgCl as reference electrode in 1M KOH electrolyte.

Fig. 1 Shows the cyclic voltammetry curve of the bare CuS and C-Dot/CuS nanocomposite. As perceived in the curves, the CV curve area of the C-Dot/CuS is slightly higher than that of as-synthesized bare CuS. The result clearly depicts that the C-Dot/CuS exhibited high specific capacitance when compared to the as-synthesized CuS, which is due to the synergistic effect between CuS, C-Dot. Again, the existence of surface functional groups on C-Dot facilitates redox reaction of CuS and gives rise to an additional pseudo-capacitance. The shape of CVs depicts pseudo-capacitive behaviour, showing an anodic peak at around  $\sim 0.6/0.57$  V and cathodic peak at  $\sim 0.25/0.23$  V for CuS and C-Dot/CuS respectively. The redox peaks indicate the Faradaic reaction happens during the cyclic process. Fig 2 shows the EIS results of CuS and C-Dot/CuS. It clearly reveals that, C-Dot/CuS have higher ionic conductivity than bare CuS.

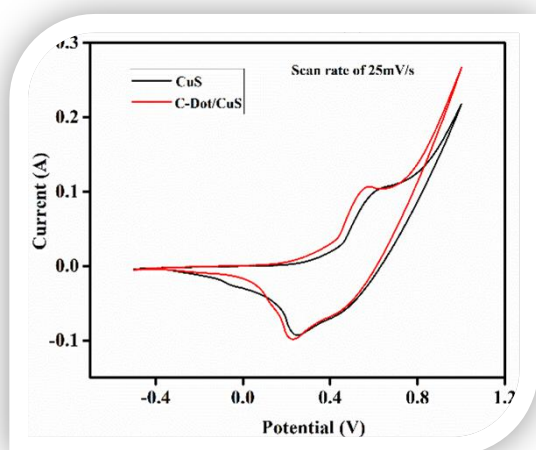


**Fig.1 Comparison CV graph of CuS, and C-Dot/CuS at 25mV/s.**

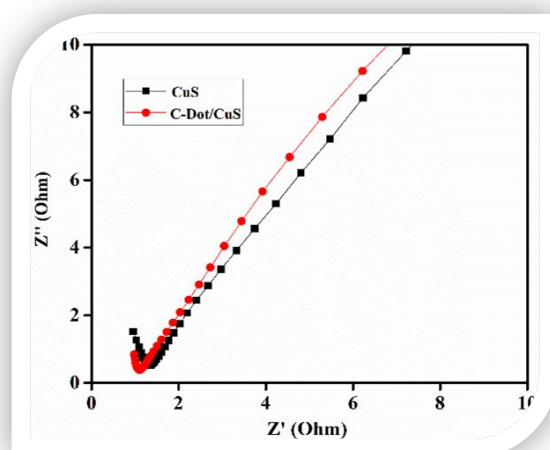


**Fig.2 EIS spectrum of CuS, and C-Dot/CuS**

## References

- C. Justin Raj, B.C. Kim, W.J. Cho, W.G. Lee, Y. Seo, K.H. Yu, *J. Alloys Compd.* 586 (2014) 191–196.
- W. Fu, W. Han, H. Zha, J. Mei, Y. Li, Z. Zhang, E. Xie, *Phys. Chem. Chem. Phys.* 18 (2016) 24471–24476.
- Y. Zhang, J. Xu, Y. Zheng, X. Hu, Y. Shang, Y. Zhang, *RSC Adv.* 6 (2016) 59976–59983.

- X. Jian, J. gang Li, H. min Yang, L. le Cao, E. hui Zhang, Z. hai Liang, Carbon N. Y. 114 (2017) 533–543.
- J. Xu, Y. Xue, J. Cao, G. Wang, Y. Li, W. Wang, Z. Chen, RSC Adv. 6 (2016) 5541–5546.

## **OP 8** *Dodonaea viscosa* Leaf Extract Mediated Synthesis of Silver Nanoparticles and its Characterization

**M. Anandan and H. Gurumalles Prabu\***

*Department of Industrial Chemistry, School of Chemical Sciences, Alagappa University, Karaikudi - 630 003, India*

*\* Corresponding author. Tel.: +919443882946; Fax: +91 4565225202*

*E-mail address: hgprabu2010@gmail.com, hgprabhu@alagappauniversity.ac.in*

### **Abstract**

Stable silver nanoparticles were prepared from the precursor solution by reduction of silver ions using the leaf extract of *Dodonaea viscosa* plant. The *Dodonaea viscosa* leaves were extracted using acetonitrile as a solvent. The extract acts as both reducing (from  $\text{Ag}^+$  to  $\text{Ag}^0$ ) and capping agent in the reduction process. The synthesized nanoparticles were characterized by UV-Vis, FT-IR, X-Ray diffraction (XRD) methods and Scanning Electron microscopy (SEM) coupled with EDX. The XRD and SEM results reveal nano size (12 nm) with spherical morphology of the nanoparticles. The revealed that the nanoparticles synthesized from *Dodonaea viscosa* leaves could inhibit the growth of A549 NSCLC cells effectively with  $\text{IC}_{50}$  values of 80  $\mu\text{g/ml}$ .

**Keywords:** Silver nanoparticles, *Dodonaea viscosa*, XRD, MTT assay.

### **Introduction**

Nano sized materials find great interest in the emerging field of science and curative medicines. Silver nanoparticles (AgNPs) possess potential applications in the fields of agriculture, waste management, forensic science, pollution control, solar cells, and medicine [1]. Conventional methods for synthesis of AgNPs require hazardous chemicals as reducing agents and formation of hazardous byproducts. Thus, Now-a-days, plants seem to be the best green resource which is suitable for a large-scale biosynthesis of nanoparticles. Thus, there is a growing interest in the use of natural compounds to develop safe and more effective therapeutic drugs for cancer treatments [2]. In the present study, green synthesis and characterization of stable colloidal silver nanoparticles was carried out using leaf extracts of *Dodonaea viscosa* as a reducing agents and assessed for its anticancer properties by MTT assay.

### **Experimental Details**

#### **Synthesis of silver nanoparticles**

Screening of active components from the leaves was employed by extraction with acetonitrile. The fresh plant leaves were collected, washed and dried. 5 g of leaves were crushed well in a mortar and 50 ml of solvent was added and extracted using soxhlet apparatus for about 2

h. Then, the extract was filtered through Whatmann filter paper and stored in a desiccator for further use. A 5 ml of leaf extract was added to  $\text{AgNO}_3$  (1 mM, 25 ml) solution in 2.5 ml of freshly prepared pH buffer at room temperature and allowed to stir for 2 h. The colorless solution of  $\text{AgNO}_3$  turned to brown after addition of the extract and it was finally turned to black color due to the formation of AgNPs. The synthesized nanoparticles were characterized by UV-Vis, FT-IR, XRD and SEM coupled with EDX. MTT assay was performed to access the cytotoxicity of the nanoparticles against A549 cancer cells.

## Results and Discussion

The UV-Vis spectrum of the reaction mixture was recorded at different time intervals to monitor the completion of the reduction process. The results were presented in terms of the maximum absorbance values ( $\lambda_{\text{max}}$ ) of SPR phenomenon. The UV-Vis results reveal that the SPR absorption peak ( $\lambda_{\text{max}}$ ) was observed as 440 nm. The similarities between the spectra of neat extract and extract with synthesized AgNPs have some marginal shifts in peak position which clearly indicate the presence of the residual plant extract in the sample as a capping agent. Four distinct peaks at  $2\theta$  values of  $38.12^\circ$ ,  $44.31^\circ$ ,  $64.45^\circ$  and  $77.41^\circ$  were indexed with the planes (111), (200), (220) and (311) for FCC silver as per the JCPDS file no. 01-087-0717 [3] which was shown in the figure 1. SEM results reveal nano size (12 nm) with spherical morphology of the nanoparticles and EDX spectrum confirms that the presence of a strong silver peak at 3.25 keV. The revealed that the nanoparticles synthesized from *Dodonaea viscosa* leaves could inhibit the growth of A549 NSCLC cells effectively with  $\text{IC}_{50}$  values of 80  $\mu\text{g/ml}$ .

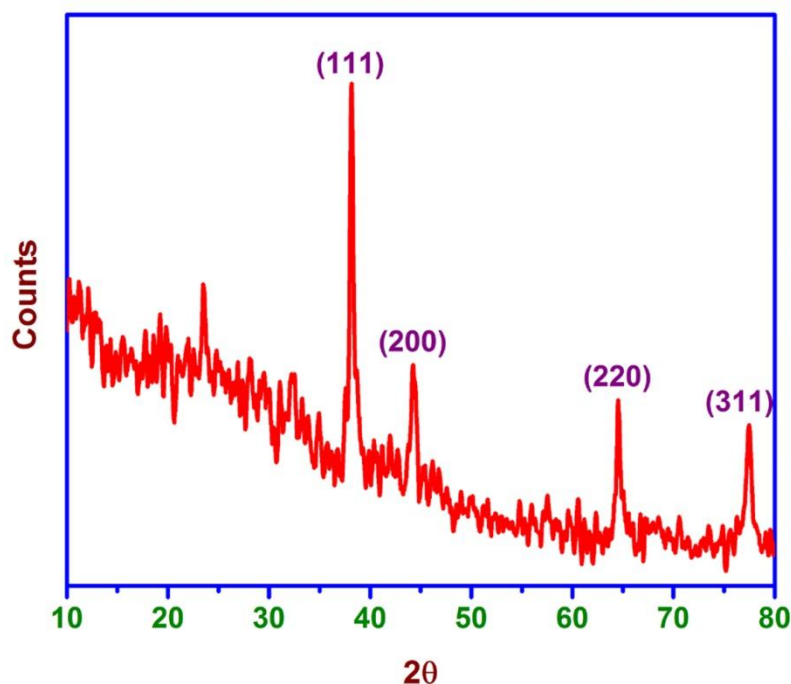


**Figure 1:** XRD pattern AgNPs of synthesized using leaf extracts of *Dodonaea viscosa*



## Conclusion

The silver nanoparticles were successfully synthesized using the leaf extracts of *Dodonaea viscosa* and characterized by optical and microscopic methods. The cytotoxic property of the extract mediated nanostructures showed  $IC_{50}$  values at very low concentrations proved that the AgNPs combined with the extracts have good inhibition efficiency against the A549 NSCLC cells.

## References

- K.M. Metz, S.E. Sanders, J.P. Pender, M.R. Dix, D.T. Hinds, S.J. Quinn, A.D. Ward, P. Duffy, R.J. Cullen, P.E. Colavita, *ACS Sustainable Chemistry & Engineering*. 3 (2015) 1610–1617.
- E.C. Njagi, H. Huang, L. Stafford, H. Genuino, H.M. Galindo, J.B. Collins, G.E. Hoag, S.L. Suib, *Langmuir*. 27 (2011) 264–271.
- P. Sivasankar, P. Seedeivi, S. Poongodi, M. Sivakumar, T. Murugan, L. Sivakumar, K. Sivakumar, T. Balasubramanian, *Carbohydrate Polymers*. (2017).

## OP 9 Multifunctional Application of Iron Oxide – Chitosan Composite

AL. Kavitha\*<sup>1</sup> and H. Gurumallesh Prabu \*<sup>2</sup>

<sup>1</sup>Department of Chemistry, Kings College of Engineering, Punalkulam – 613303,

<sup>2</sup>School of Chemistry, Alagappa University, Karaikudi.

\*Corresponding author: [alkavitha82@gmail.com](mailto:alkavitha82@gmail.com), [hgprabu2010@gmail.com](mailto:hgprabu2010@gmail.com)

### Abstract

This work was aimed to develop reusable iron oxide – chitosan composite for multifunctional applications.  $\gamma\text{-Fe}_2\text{O}_3$  and  $\alpha\text{-Fe}_2\text{O}_3$  particles were synthesized by two different methods such as Microwave and Self assembly. Chitosan is to be prepared and characterized by using XRD and SEM techniques. Glucose oxidase(GOx) enzyme was used to prepare  $\gamma\text{-Fe}_2\text{O}_3$ -chitosan composite(1:3) containing carbon paste electrode for sensitive detection of glucose. The immobilized enzyme retained its bioactivity, exhibited a surface confined reversible electron transfer reaction, and had good stability. The surface parameters like surface coverage ( $\tau$ ), Diffusion coefficient ( $D_0$ ), and rate constant ( $k_s$ ) were studied. The shelf life of the developed electrode system is about 12 weeks under refrigerated conditions.

**Keywords:**  $\gamma\text{-Fe}_2\text{O}_3$ ,  $\alpha\text{-Fe}_2\text{O}_3$ , Chitosan, Composite, Glucose Biosensor, Glucose Oxidase

### Introduction

In recent years, iron oxide nanoparticles have attracted the interest of researchers from various fields such as physics, medicine, and material science due to their multifunctional properties with small size, superparamagnetism, and low toxicity [1–5]. chitosan (CH) along with nanoparticles has been utilized as a stabilizing agent due to its excellent film forming ability,

mechanical strength, biocompatibility, non-toxicity, high permeability towards water, susceptibility to chemical modifications, cost effectiveness, etc. In the present work, the synthesized iron oxide – chitosan composite for imparting dye decolourization and glucose biosensor applications.

## Experimental

The iron oxide nanoparticles were synthesized by Microwave and self assembly method. The chitosan were prepared from the crab shells. The synthesized iron oxide and chitosan were characterized and applied to dye decolourization and glucose biosensor.

## Results and Discussion

### Dye decolourization with $\alpha$ -Fe<sub>2</sub>O<sub>3</sub>, chitosan and $\alpha$ -Fe<sub>2</sub>O<sub>3</sub>-chitosan composite

Synthesized  $\alpha$ -Fe<sub>2</sub>O<sub>3</sub>, chitosan and  $\alpha$ -Fe<sub>2</sub>O<sub>3</sub>-chitosan composite (1:3) were subjected to dye decolourization at various pH conditions (3, 7, 10) to assess the potential role of chitosan. The results obtained are given below;

COD of dye solutions before and after treatment were analyzed (Table 1). It is found that COD reduction is significant in treatment with  $\alpha$ -Fe<sub>2</sub>O<sub>3</sub>, chitosan and  $\alpha$ -Fe<sub>2</sub>O<sub>3</sub>-chitosan at all pH systems studied.  $\alpha$ -Fe<sub>2</sub>O<sub>3</sub>-chitosan composite has decolourized the dye more effectively than the pristine  $\alpha$ -Fe<sub>2</sub>O<sub>3</sub> and pristine chitosan.

**Table 1. Percentage COD reduction in dye decolourization**

Substrate	pH		
	3	7	10
$\alpha$ -Fe <sub>2</sub> O <sub>3</sub>	62	55	58
Chitosan	40	35	37
$\alpha$ -Fe <sub>2</sub> O <sub>3</sub> -chitosan composite	78	65	69

Based on the above results, it is concluded that  $\alpha$ -Fe<sub>2</sub>O<sub>3</sub>-chitosan composite is found to be effective for the decolourization of dye.

## Development of Biosensor

### Cyclic voltammetric investigation of carbon paste electrode

Cyclic voltammetry was performed using carbon paste electrode in phosphate buffer (50 mM, pH 7) medium at 50 mV/s scan rate. The cyclic voltammogram thus obtained for bare carbon paste electrode. No redox peak is observed in the potential window between -0.4 V and 1.2 V.

In the presence of either  $\gamma$ -Fe<sub>2</sub>O<sub>3</sub> or chitosan on the electrode surface, no redox peak is observed (curves a and b). But, in the presence of  $\gamma$ -Fe<sub>2</sub>O<sub>3</sub> particles incorporated into the chitosan matrix on the modified electrode, a redox peak is obtained (curve c). This may be due to the interaction of  $\gamma$ -Fe<sub>2</sub>O<sub>3</sub> particles with chitosan that resulted into the increased electron mobility at the electrode surface.

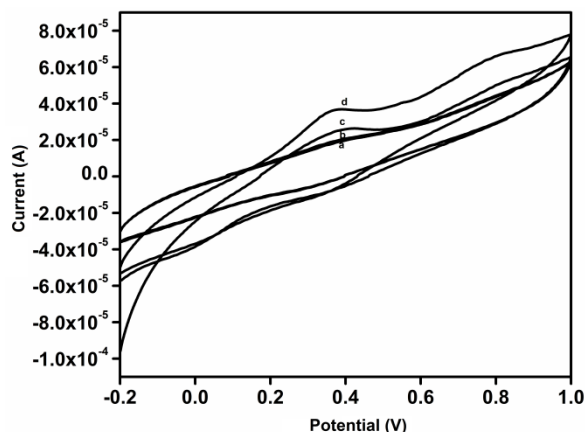


**Figure 1: Cyclic voltammograms of carbon paste electrode containing (a)  $\gamma$ - $\text{Fe}_2\text{O}_3$ , (b) chitosan, (c)  $\gamma$ - $\text{Fe}_2\text{O}_3$ -chitosan composite, (d)  $\gamma$ - $\text{Fe}_2\text{O}_3$ -chitosan-GOx at 50 mV/s scan rate in phosphate buffer solution (50 mM, pH 7).**

## Conclusion

**Application of synthesized compounds:** The synthesized compounds were subjected to applications in diverse fields. The findings are summarized below:

- **Dye decolourization:** The decolourization of Direct Red 7 dye was tested with the synthesized magnetite and  $\alpha$ - $\text{Fe}_2\text{O}_3$ . Results showed that the  $\alpha$ - $\text{Fe}_2\text{O}_3$ - $\text{H}_2\text{O}_2$  could decolourize the dye effectively than magnetite.
- **Development of biosensor:**  $\gamma$ - $\text{Fe}_2\text{O}_3$  particles were successfully embedded in the chitosan matrix separately. GOx was immobilized on CPE containing the composite. Cyclic voltammetric and EIS results indicated better electron transfer of GOx. Bioelectrode containing  $\gamma$ - $\text{Fe}_2\text{O}_3$ -chitosan-GOx composite showed high sensitivity and fast response for glucose determination. In addition, this bioelectrode exhibited good reproducibility, better shelf-life (30 days of study) and interference-free analysis. It is observed that  $\gamma$ - $\text{Fe}_2\text{O}_3$ -chitosan composite (1:3) modified CPE showed better electron transfer capability in modified CPE.

The shelf-life of the bioelectrode was checked. It is found that the bioelectrode containing  $\gamma$ - $\text{Fe}_2\text{O}_3$ -chitosan composite maintained its 99% of its initial activity even after 30 days, but the electrode containing either  $\gamma$ - $\text{Fe}_2\text{O}_3$  or chitosan only did not produce better activity. Improved stability and better shelf-life of this bioelectrode is noted when compared with the previous report [22]. This could be due to the excellent biocompatibility effect of  $\gamma$ - $\text{Fe}_2\text{O}_3$ -chitosan and  $\gamma$ - $\text{Fe}_2\text{O}_3$ -chitosan-GOx.

## References

- Y.S.Kang, S. Risbud, J.F. Rabolt, and P. Stroeve, *P. Chem. Mater.*, 8, 220(1996).  
 M.Racuciu, *Curr. Appl. Phys.*, 9, 1062(2009).  
 I.Willner., and E. Katz, *Angew. Chem. Int. Ed.*, 42, 4576(2003).

J. Dobson, *Drug. Dev. Res.*, 67, 55(2006).

S.I.Park, J.H. Lim, and C.O.Kim, *Curr. Appl. Phys.*, 8, 706(2008).

## **OP 10** Synthesis and Characterization of Seaweed Biopolymer Based ZnO Composite

**S. Rajaboopathi, S. Thambidurai\***

*Department of industrial chemistry, school of chemical sciences,*

*Alagappa university, Karaikudi - 630003, Tamil nadu, India.*

*Email:siva.raja2389@gmail.com*

### **Abstract**

In the present study, seaweed bio-polymer based ZnO composite was synthesized by the simple chemical precipitation method, seaweed component was taken as a biosurfactant. The functional groups of respective components of seaweed and metal oxide was characterized and confirmed by FTIR and UV-Visible spectroscopy. The crystallite size was confirmed by X-ray diffraction analysis (XRD). The optical activity of the composites was tested by using absorbance and transmittance spectra. Thermal characteristics of the composite was analyzed by TG-analysis, the seaweed-ZnO composite showing enhanced thermal stability than seaweed. The results demonstrate that higher ZnO intercalated seaweed matrix has the reinforced effect than compared to among the other three components. Therefore, biopolymer based seaweed-ZnO matrix can be promising materials for optically active sensors and super capacitors applications.

**Key words:** Seaweed, Zinc oxide, thermal stability, optical property

### **Materials**

Zinc chloride, Sodium hydroxide, Ethanol, Seaweed, Millipore water was used for all the preparation process.

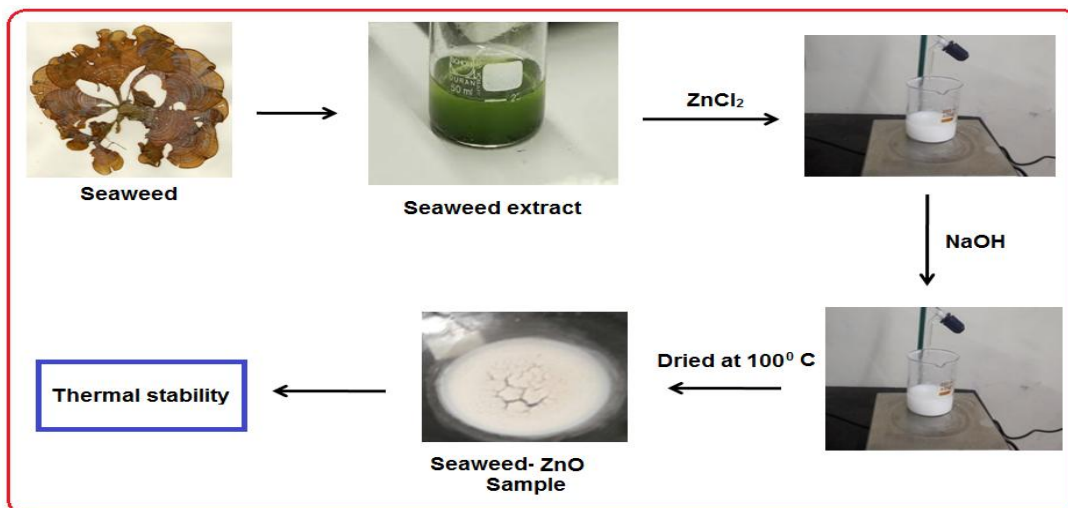
### **Experimental Methods**

Aqueous seaweed extracts preparation, Chemical precipitation method

### **Introduction**

Marine algae are the important and inexpensive constituent due to their occurrence in all existing ecological units on earth [1-2]. Macro algae extracts contain a wide variety of bioactive components with different health benefits. These were due to the presence of many functional sites, such as sulphonate, carboxyl, amine and hydroxyl groups in their structural edges [3]. Furthermore, these can be exhibited the good anti-diabetic and nutritional properties, which are extensively used in various applications [4-6]. Zinc oxide (ZnO) nano-crystalline material has the potential exciting properties of bio compatibility, ultraviolet protection, biosafety, high refractive index and antimicrobial activity with new potential applications in sensors, solar cells and electric materials [7]

## Scheme:



Schematic formation of biopolymer based SW-ZnO hybrid composite.

## References

- M. Song, H. D. Pham, J. Seon, H. C. Woo, *Renew. Sustain. Energy Rev.* 50 (2015) 782–792.  
 L. Zheng, G. Zhang, M. Zhang, S. Guo, Z. –H. Liu, J. *Power Sources.* 201 (2012) 376-381.  
 J. Shen, M. Shi, N. Li, B. Yan, H. Ma, Y. Hu, M. Ye, *Nano Res.* 3 (2010) 339-349.  
 M. T. Ale, J. D. Mikkelsen, A. S. Meyer, *Mar. Drugs.* 9 (2011) 2106-2130.  
 G. Bedoux, K. Hardouin, A. S. Burlot, N. Bourgougnon, *Adv. Bot. Res.* 71 (2014) 345-378.  
 S. N. Fedorov, S. P. Ermakova, T. N. Zvyagintseva, V. A. Stonik, *Mar. Drugs.* 11 (2013) 4876-4901.  
 I. Perelshtein, G. Applerot, N. Perkas, J. Grinblot, E. Wehrschuetz-Sigl, A. Hasmann, G. Guebitz, A. Gedanken, *Surf. Coat. Technol.* 204 (2009) 54-57.

### OP 11 Study on the Corrosion behaviour of Mild Steel using an Aqueous Leaf Extract *Cissus quadrangularis*

K Anuradha<sup>a</sup>, V Maasilamani<sup>b</sup> and K Velmanirajan<sup>c</sup>

<sup>a</sup>Department of Chemistry, Alagappa government Arts college, Karaikudi, Tamil Nadu - 630 003, India

<sup>b</sup>Research scholar, Department of Chemistry, Alagappa government Arts college, Karaikudi, Tamil Nadu - 630 003, India

<sup>c</sup>Department of Mechanical engineering, VSVN Polytechnic College, Virudhunagar, Tamilnadu, India

email: [anuvmrajan@yahoo.co.in](mailto:anuvmrajan@yahoo.co.in)

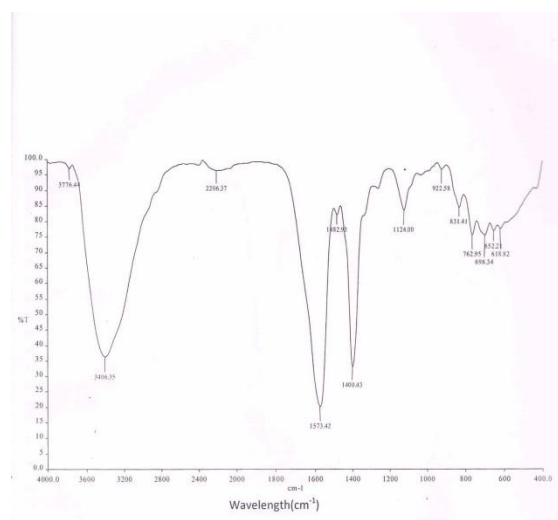
## Abstract

In nature, metals are present in the form of chemical compounds i.e., Minerals: Some amount of energy is needed to extract metals from their ores and the same amount of energy is evolved during the chemical or electrochemical reaction involving corrosion. The study of corrosion inhibition is significant in the field of research due to its usefulness in various industries. An increasing concern in human health and risks has drawn attention in the

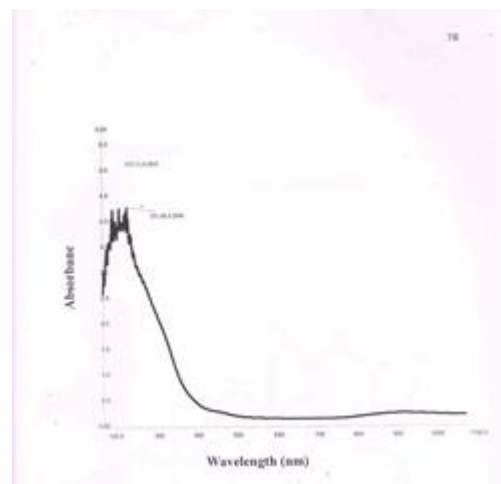
development of mild steel corrosion. Mild steel in acid medium is widely used in various industrial processes. Sea water finds extensive application as coolant in various exothermic reactions. Sea water constitutes a rich source of various commercially important chemical elements. Depending upon the metal /environment combinations different types of inhibitors are used in suitable concentrations. Zinc ions have long been considered as valuable corrosion inhibitors for protection afforded by a cathodic polarization mechanism. One of the effective methods to prevent corrosion is the addition of natural inhibitors. Most of the natural products are non-toxic, biodegradable and really available in plenty. In the present investigation, leaves of *Cissus quadrangularis* extract (CQE) have been used as corrosion inhibitor for mild steel in sea water medium. The inhibition efficiency was found to increase with increase in concentration of the leaf extract. The formulation consisting of 6 ml of CQE and 10 ppm of  $Zn^{2+}$  has 92 % inhibition efficiency (IE). A study on the effect of immersion period on the CQE-  $Zn^{2+}$  showed an IE that decreased from five days. UV-Visible spectra revealed the formation of a protective film on the metal surface. The same is confirmed through FT-IR spectrum. From the surface examination studies, it could be confirmed that the corrosion inhibition was due to the formation of a protective film consists of  $Fe^{2+}$ - CQE complex.

**Key words:** Corrosion inhibition, surface examination, eco-friendly, sea water.

### CQE



FTIR- CQE



FTIR, CQE+  $FeSO_4$

### Conclusion

The weight loss study reveals that the formulation consisting of 6 ml of *Cissus quadrangularis* extract (CQE) and 10 ppm of  $Zn^{2+}$  has 92 % inhibition efficiency in controlling the corrosion of mild steel immersed in an aqueous solution containing sea water. A study of the effect of immersion period on the *Cissus quadrangularis* extract (CQE) -  $Zn^{2+}$  system shows an inhibition efficiency that decreases as the immersion period increases. UV-Visible spectra reveal

that a protective film is formed on the metal surface. The FTIR spectrum also reveals the formation of protective film that consists of  $\text{Fe}^{2+}$ -CQE complex.

## **OP 12** Chromium Removal From Aqueous Solution Using *Prosopis juliflora* Biochar and Its Disposal Study in MFC

**D. Krishnaveni and A.N. Senthilkumar\***

*PG & Research Department of Chemistry, Alagappa Government Arts College,  
Karaikudi – 630 003.*

*\*Corresponding Author email: [ansent@gmail.com](mailto:ansent@gmail.com)*

### **Introduction**

In the present study *Prosopis juliflora* was used as biomass for preparing biochar. *Prosopis juliflora* stalks were charred at 450°C by slow thermal pyrolysis process and the obtained product was labelled as PSB. The obtained PSB was subjected to physico-chemical, morphological and functional groups analysis using standard methods. Latter phenomena lead to depletion of active sites in adsorbent whose restitution was attempted using microbes in microbial fuel cell. Characterization of PSB lime lighted its soil modifying and sorptive tendencies. Further study concluded PSB as adsorbent for removing phosphate from synthetic aqueous solution. Desorption of chromium ions from PSB's active sites were effectively assisted by microbes with simultaneous power generation in microbial fuel cell.

### **Experimental Techniques**

#### **Pyrolysis and preparation of biochar**

*Prosopis juliflora* was collected from in and around villages of Sivagangai district. Collected stalks were dried under mild sunlight for 7 days and then shredded, charred in a slow pyrolysis unit.

#### **Characterization Techniques**

Surface functional group of biochar was analysed by fourier transform infrared (FT-IR) spectrometer of Bruker Optik GmbH of model No TENSOR 27. Scanning electron microscopy (SEM) was done by using Hitachi, Japan instrument of model S-3000H to investigate the surface morphology of prepared biochar samples.

#### **Chromium adsorption isotherm**

The chromium concentrations of the liquid phase samples were then determined by Diphenyl Carbazide method.

#### **Construction of MFC**

Soil microbial fuel cell was constructed using 150 mL glass beaker. 100 g of sandy loamy soil used in the present study served as fuel in MFC. Soil was moisturised with 40 mL of distilled

water and packed into beaker in such a way that 30g of it was loaded at the bottom of the beaker over which anode was placed. Anode was then covered the remaining amount of soil above which the cathode was allowed to float in 25 mL of distilled water. Mild steel specimens of dimension 3 X 3 X 0.2 cm were used as electrodes. Soil bacteria served as biocatalyst. The constructed MFC was used as control, labelled as CMFC. Two similar MFC were constructed and one out of it was packed with 0.5 g of RSB near the anode (PMFC) and another MFC's anode was packed with RSB used for phosphate adsorption from aqueous solution of 40 ppm concentration (PCMFC). The open circuit potential offered by the three MFC's were measured using digital multimeter individually.

## Results and Discussion

Surface morphology of PSB is presented in Figure 1. Visible macro porosity observed in PSB. The smaller sized pores which were resulted due to volatilization of organic compounds. The shift of the vibration bands assigned to hydroxyl, carboxyl and amino group indicates their involvement in the removal of Cr (VI). The experimental values obeyed well with empirical Freundlich isotherm as evidenced from Fig.2 ( $R^2=0.923$ ). Hence PSB provides heterogeneous site for chromium adsorption in non-uniform layer with reversibility [3]. The free energy of adsorption ( $\Delta G_{ads} < -20$  kJ) calculated from equilibrium constant ( $K_c$ ) values showed physical mode of phosphate adsorption on PSB [4]

## Phosphate recycling in MFC

Open circuit potential discharged by PCMFC last upto 24 days and then falls steeply due to chromium intolerance. PMFC offered steady potential from the eighth day of MFC operation and last longer upto 40 days with gradual fall in potential. CMFC offered low potential value (around 180 mv) and delivered potential upto 15 days. Electricity generation is dependent on fuel concentration and microbial activity till a plateau region is reached. At the saturation point, maximum rate of electron transfer is achieved by microbial metabolic mechanism and/or by an increase in alternate electron acceptor that compete with anode [5]. Higher potential offered by PMFC may be due to better microbial activity on soil organic matter. PMFC undergoes progressive decrease of potential by slow microbial acclimation process.

## Conclusion

The study concluded that PSB effectively adsorbs chromium from synthetic aqueous solution obeying Freundlich adsorption isotherm. The calculated free energy of adsorption supported physical mode of binding between PSB and chromium. The adsorbed chromium ion was disposed in MFC with power generation.



## References

- D.S. Bhargava, S.B. Sheldarkar, Use of TNSAC in phosphate adsorption studies and relationships-literature, experimental methodology, justification and effects of process variables, *Water Res.* 27 (1993) 303–312.
- C.P. Huang, Removal of phosphate by powdered aluminum-oxide adsorption, *J. Water Pollut. Control Fed.* 49 (1977) 1811–1817.
- Hu Tang, Weijie Zhou, Lina Zhang, Adsorption isotherms and kinetics studies of malachite green on chitin hydrogels, *J. Hazardous Materials*, 209-210 (2012)218-225.
- Senthilkumar, A.N., Kumaravel, T., Gopalakrishnan, S.M., 2012. Steric effect of alkyl substituted piperidin-4-one oximes for corrosion control of mild steel in H<sub>2</sub>SO<sub>4</sub> medium. *Acta Phys. Chim. Sin.* 28, 399–406.
- Y. Zuo, P. Maness, B. Logan, Electricity production from steam-exploded corn stover biomass, *Energ. Fuel.* 20 (2006) 1716–1721.

## **OP 13** Room Temperature Fiber Optic Gas Sensor Technology Based on Co<sub>2</sub>VO<sub>4</sub> Nanoplatelets

**M. Subramanian, V. Violet Dhayabaran and M. Shanmugavadivel**

*PG and Research Department of chemistry, Bishop Heber College (Autonomous),  
Tamilnadu-620 017, India.*

*E-mail: y2ksubramani@yahoo.com*

### Abstract

A highly sensitive fiber-optic technique for the detection of VOCs is described and preliminary results obtained using these sensors is reported. Cobalt vanadate nanopowder was obtained by surfactant assisted solution combustion method. Scanning electron microscopy, transmission electron microscopy, X-ray diffraction analyses, FT-IR and diffuse reflectance spectra were used to characterize the structures of the synthesized products. The fiber optic gas sensing properties of the clad modified Co<sub>2</sub>VO<sub>4</sub> were tested with volatile organic compounds such as, ammonia, acetone, methanol and ethanol. Results reveal that the Co<sub>2</sub>VO<sub>4</sub> nanoplatelets has the highest sensitivity to ethanol with a fast response and a recovery time of 38.6 and 45.5 minutes respectively.

**Keywords:** Cobalt vanadate nanocrystals, Solution combustion synthesis, Evanescent wave absorption, Fiber optic gas sensor.

### Introduction

Despite their toxicity and hazard, VOCs are still used in industries as intermediates to produce other chemicals and as solvents in research laboratories and the probabilities of over exposure to such toxic agents are very high. Therefore, the development of gas sensors for early detection of toxic gases is necessary. Now a day, there has been a great deal of research toward the development of miniaturized gas-sensing devices and the improvement of sensor performance, particularly for toxic gas detection and for environmental pollution monitoring. Among various

sensors, fiber optic sensors are attractive and powerful because of their inherent advantages over the conventional electrical measurement based semiconductor sensors. The focal reason is fiber optic sensors are immune to electromagnetic interference, explosion proof, small size, light weight, compact, flexible, room temperature operation and low cost.

## Experimental

$\text{Co}_2\text{VO}_4$  nanopowder was obtained by surfactant mediated solution combustion method. Analar grade cobalt nitrate dihydrate and ammonium meta vanadate were dissolved in the aqueous solution of tartaric acid in the mole ratio of [TA] : [Zn&V] = 2:1. The surfactant solution was prepared by dissolving the surfactants cetyl trimethylammoniumbromide (CTAB) and Triton X-100 in water. These metal and surfactant solutions were mixed and stirred for one hour at room temperature. Ethylene glycol was added drop wise to this solution under stirred condition. The pH of the final solution mixture was adjusted to 7 by the addition of aqueous ammonia. This resultant solution was heated at about  $200^\circ\text{C}$  to get the dried precursor sample. The obtained precursor powder was then calcined at  $600^\circ\text{C}$  for two hours in air to get  $\text{Co}_2\text{VO}_4$  nanopowder.

The heart of the sensor is the multimode plastic step index optical fiber having a length 42 cm and diameter 750 micron with a sensing region of about 3 cm at the center of the fiber. This fiber made up of polymethylmethacrylate (PMMA) is cleaved at both ends to have flat edges. A red was used as light source and focused onto one end of the fiber. The output light from the other end of the fiber was detected using a photodiode detector. The output light intensity from the optical fiber is measured after the time interval of 10 minutes. The change in output light intensity is measured by the multimeter in terms of change in voltage. The signal from the multimeter is interfaced with the computer and the graphs are recorded separately.

The gas sensing region (of about 3 cm) is obtained by completely removing the clad part with the careful use of a cleaver without affecting the core of the fiber. The uniformity of the clad removed sensing region was monitored by an optical microscope.  $\text{Co}_2\text{VO}_4$  nanopowder was mixed with isopropyl alcohol to form a paste like material and coated for a thickness of about 3 cm of the clad removed sensing region by dip coating method and dried at room temperature.

## Results and Discussion

The XRD pattern was indexed to a cubic unit cell corresponding to  $\text{Co}_2\text{VO}_4$ . The sharp and high intensity peaks indicate the high crystallinity and high purity of the  $\text{Co}_2\text{VO}_4$  prepared by the facile solution combustion method. All diffraction peaks are in agreement with the JCPDS file (JCPDS Card no. 73-1633), indicating that the prepared  $\text{Co}_2\text{VO}_4$  nanomaterial is single phase in nature. The average crystallite size was calculated using the Scherrer formula and it was found to be 60 nm.

SEM results revealed that the material surface is highly porous with fine nanoparticle structures. The high density nanoparticles are uniformly dispersed on the surface and the particle

sizes were found to be around 60 nm. The elemental signals seen in the EDS spectrum confirm the existence of V, Co and O and no other peaks due to impurities were observed. The elemental data indicates the formation of  $\text{Co}_2\text{VO}_4$  in a perfect stoichiometric composition.

TEM results showed that the particles are mostly uniform in size and homogeneously distributed. The individual nanoplatelets formed thick junctions and many of them are combined together with neighbors accommodating pores in the middle. The average particle sizes determined by TEM are very close to the crystallite size calculated from XRD results. The highly crystalline nanoplatelets with a clear lattice pattern are also observed in the TEM selected area electron diffraction.

In clad modified fiber optics sensors, the variations in light intensity with various analyte gases could generally be attributed to evanescent wave absorption in the modified cladding or changes in the effective refractive index. Based on the light reflecting nature of the sensing material, the measured total light output varies with different gases and this denotes the response characteristics of the sensor.

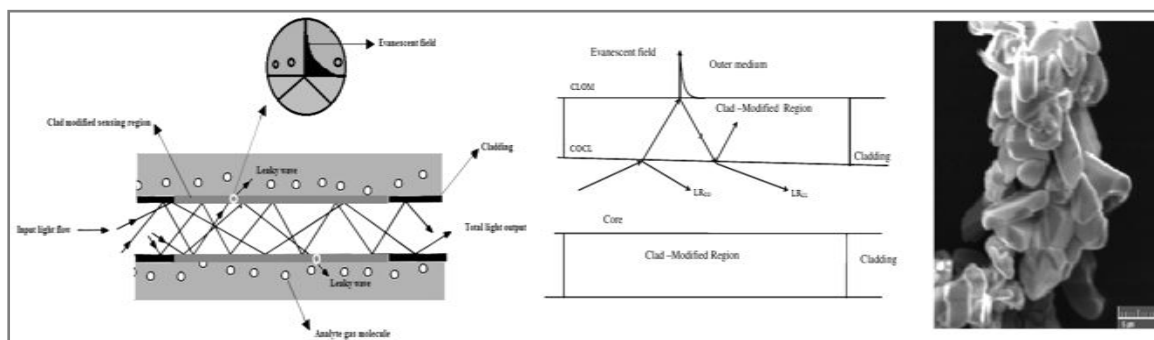
The charge transfer process occurs over the large surface area of  $\text{Co}_2\text{VO}_4$  and effectively modifies the refractive index of the cladding region. The evanescent wave absorption by the gas molecules depends upon the interaction of the gas molecules at the interface and it may be higher or lower than the absorption by the air. The intensity of the reentered leaked light is modulated by the evanescent wave absorption by the gas molecules interacting with the  $\text{Co}_2\text{VO}_4$  modified cladding. The gas response value is measured as voltage output and it depends on the amount of evanescent wave absorption by the test gas present at the interface.

The response is defined as the change in voltage in the presence of the test gas compared to the voltage in air at constant current. Generally, sensitivity is the measure of change in output signal per concentration unit of the analyte gas. Sensitivity of the gas is derived from the relative change in intensity of the total light output measured in terms of voltage change in comparison with the reference value.

Generally the response of a sensor depends upon the rapid removal of adsorbed oxygen by the robust interaction of target gas molecules and the consecutive generation of electrons. From the results  $\text{Co}_2\text{VO}_4$  is found to be more sensitive towards ethanol and having greater response than ammonia, methanol and acetone.

## Conclusion

This study reports a facile and effective method for the preparation of  $\text{Co}_2\text{VO}_4$  nanoplatelets for evanescent wave fiber optic gas sensor application. The solid response characteristics and enhanced sensitivity towards ethanol vapors found through this investigation are mainly attributed to the phase composition, high surface area and highly porous nature of the  $\text{Co}_2\text{VO}_4$  nanoplatelets. The superior ethanol-sensing performance of the  $\text{Co}_2\text{VO}_4$  nanoplatelets suggested that they may be suitable for use in alcohol sensing.



## OP 14 Photoluminescence Studies on Oxide and Borate Phosphors: Surface Modified - $\text{Y}_2\text{O}_3:\text{Eu}^{3+}$ and $\text{Ba}_2\text{Mg}(\text{BO}_3)_2:\text{Bi}^{3+}$

N. Radha\* and K. Prabhavathi

Asst. Professor of Chemistry, Alagappa Govt. Arts College, Karaikudi – 3  
[Chemradha74@gmail.com](mailto:Chemradha74@gmail.com)

### Abstract

Phosphors are inorganic luminescent materials. They consist of an activator ion that is responsible for emission properties, in a host lattice. Phosphors are either crystalline or amorphous materials. In general, the activator ion absorbs the energy in the ultra violet (UV) region and emits in the visible region. The present study has two components. The first one deals with the synthesis of nanoparticles of  $\text{Y}_2\text{O}_3:\text{Eu}^{3+}$  phosphor and its surface modification using oleic acid (OA) by hydrothermal method. The second part of this work involves the synthesis of  $\text{Ba}_{2-2x}\text{Bi}_x\text{K}_x\text{Mg}(\text{BO}_3)_2$  [ $x = 0.001, 0.01, 0.02$  and  $0.05$ ] phosphors by solid state reaction method. The synthesized phosphors were characterized by powder x-ray diffraction, FT-IR, Diffuse reflectance UV-Visible (DRUV-Vis), and laser Raman spectroscopic techniques. The morphologies of  $\text{Y}_2\text{O}_3:\text{Eu}^{3+}$  phosphors were analyzed using scanning electron microscopic (SEM) technique. The photoluminescence (PL) properties of synthesized materials were studied at room temperature. These samples with different  $\text{Bi}^{3+}$  content were synthesized using conventional high temperature solid state reaction method. The lattice vibrations were understood using laser Raman and FT-IR spectroscopic techniques. The PL studies revealed a UV emission

at 370 nm when excited using 304 nm wavelengths. The PL emission intensity decreased as  $\text{Bi}^{3+}$  content increases due to concentration quenching.

**Key words:** Phosphors, inorganic luminescent, amorphous materials, photoluminescence, activator ions, emission properties.

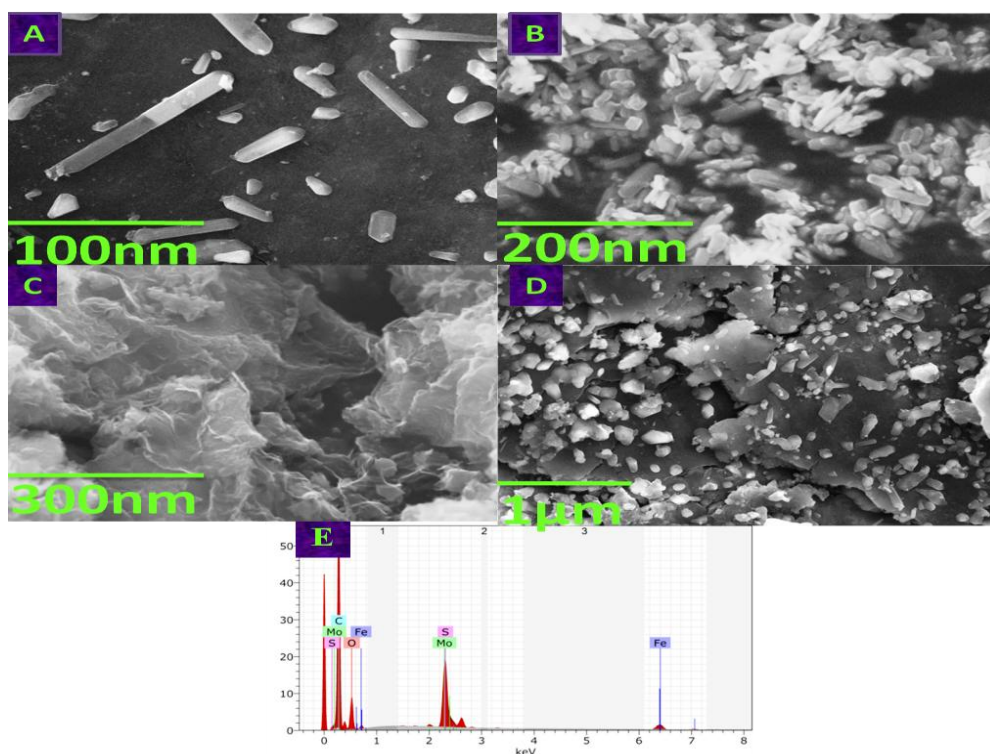
## **OP 15** Environmental pollutants simultaneous determination: Polyaniline composite $\alpha\text{-Fe}_2\text{O}_3$ on $\text{MoS}_2$ binder free hybrid nanostructures

**P. Thivya and J. Wilson\***

*Polymer Electronics Lab, Department of Bioelectronics and Biosensors, Alagappa University, Karaikudi-630 004, Tamilnadu, India  
Mail Id: dddivyaec@gmail.com*

### **Abstract**

In this work,  $\alpha\text{-Fe}_2\text{O}_3$  and Polyaniline (PANi) nanotubes strongly mounted on the  $\text{MoS}_2$  sheet as a versatile platform for the detection of environmental pollutants. PANi- $\alpha\text{-Fe}_2\text{O}_3$ - $\text{MoS}_2$  hybrid structure significantly exhibited better electro catalytic activity toward simultaneous detection of pollutants such as hydroquinone (HQ), catechol (CC), resorcinol (RS) and nitrite ( $\text{NO}_2^-$ ).



SEM images of (A) PANi nanotubes (B)  $\alpha\text{-Fe}_2\text{O}_3$  nanorods (C)  $\text{MoS}_2$  nanosheets (D) PANi- $\alpha\text{-Fe}_2\text{O}_3$ - $\text{MoS}_2$  composite (E) EDAX spectrum of hybrid structure

The PANi- $\alpha$ -Fe<sub>2</sub>O<sub>3</sub>-MoS<sub>2</sub> composite demonstrated significant wider range 500 nM-300  $\mu$ M, 400 nM-300  $\mu$ M, 200 nM-300  $\mu$ M and 300 nM-300  $\mu$ M with lowest detection limits 180, 178, 95 and 102 nM and also importantly reduced the oxidation potential of analytes by 6, 2.5, 5 and 7mV. The intercalated interaction between PANi and MoS<sub>2</sub> improves the conductivity and thermal stability of MoS<sub>2</sub>/PANi nanocomposites with the increasing fraction of MoS<sub>2</sub>. This architecture is also advantageous for enhancing the capacitance properties and cyclic stabilities of MoS<sub>2</sub>/PANi electrodes. The proposed sensor also exhibited good sensitivity, stability and reproducibility in real sample analysis.

## **OP 16** Synthesis, Characterization and inhibitive evaluation of 2-(4,5-diphenyl-1H-imidazol-2-yl)phenol on mild steel in 1.0 M Hydrochloric acid

**K.T. Loganathan K T,<sup>a\*</sup> and Natarajan<sup>b</sup>**

<sup>a</sup>Department of Chemistry, Alagappa Chettiar College of Engineering & Technology, Karaikudi – 630003, Tamilnadu, India

<sup>b</sup>P.G. & Research Department of Chemistry, Alagappa Government Arts College, Karaikudi – 630003, Tamilnadu, India

\*Corresponding author E-Mail id: [logchem80@gmail.com](mailto:logchem80@gmail.com)

### **Abstract**

2-(4,5-diphenyl-1H-imidazol-2-yl) phenol was synthesized by microwave assisted synthetic method and characterized by UV-Visible, FT-IR, <sup>1</sup>H & <sup>13</sup>C NMR spectroscopic techniques. Inhibitor evaluations on mild steel in 1.0 M HCl of different concentrations (1, 3, 5, 7 & 10  $\mu$ M) were examined using weight loss measurements, Tafel polarization and electrochemical impedance spectroscopic techniques. The corrosion rate is found to decrease with increased inhibition efficiency with concentration and reasoned due to adsorption phenomena. The maximum surface coverage observed is 0.88 at a 10  $\mu$ M concentration of inhibitor addition. The adsorbed compound formed a layer on the mild steel surface and act as a barrier coating in the corrosive environment. From the Tafel polarization curve, it is observed that the inhibitor compound act as both anodic and cathodic inhibitor.

The polarization resistance ( $R_p$ ) and the percentage of (IE) inhibitor efficiency also increased with inhibitor concentrations. The high efficiency was attributed through bonding of adsorbed film of the inhibitor on the mild steel surface. The enhancement of capacitance ( $C_{dl}$ ), polarization resistance ( $R_p$ ), charge transfer resistance ( $R_{ct}$ ) and inhibition efficiency (IE) values were noticed from EIS study and it showed good agreement with the Tafel polarization and weight loss measurement studies. The inhibitor obeyed Langmuir adsorption isotherm. The achievement of restriction of corrosion process and maintenance of smooth surface also noticed through SEM studies.

## **OP 17** Biomimetic and Cell-Mediated Mineralization of graphene by Ionic liquid Assisted Nitrogen, phosphate, fluorine tri doped ternary nanocomposite

**M. Balaji<sup>a</sup>, S. Jegatheeswaran<sup>b</sup>, S. Selvam<sup>c</sup> and M. Sundrarajan<sup>a\*</sup>**

<sup>a</sup>*Advanced Green Chemistry Lab, Department of Industrial Chemistry, School of Chemical Sciences, Alagappa University, Karaikudi - 630 003, Tamil Nadu, India.*

<sup>b</sup>*The Key Laboratory of Advanced Textile Materials and Manufacturing Technology of the Ministry of Education, College of Materials and Textiles, Zhejiang, Sci-Tech University, Hangzhou, China.*

<sup>b</sup>*Laser and Sensor Application Laboratory, Engineering Building, Pusan National University, Busan - 609735, South Korea.*

*\*Corresponding author: Dr. M. Sundrarajan,*

*Email: [sundrarajan@yahoo.com](mailto:sundrarajan@yahoo.com); [drmsgreenchemistrylab@gmail.com](mailto:drmsgreenchemistrylab@gmail.com)*

### **Abstract**

In bone tissue engineering, it is imperative to design multifunctional biomaterials that can induce and assemble bone-like materials that are close to natural bone. In this study, graphene was functionalized by ionic liquid. The resulting nitrogen, phosphate, fluorine tri-doped graphene (NPF-graphene) was further used as a substrate for biomimetic and cell-mediated mineralization of bone tissue engineering. It was confirmed that NPF-graphene surface facilitated the growth of bone tissues. The observation of the effect of the NPF- graphene was analyzed by morphology, and- proliferation of MG-63 cell line derived from human osteoblast was investigated. In vitro studies clearly, show the effectiveness of NPF- graphene provide the mineralization and cell differentiation. The results of this study suggested that the NPF- graphene hybrid will be a promising material for bone regeneration and implantation.

**Keywords:** Graphene, Ionic liquid, Biomimetic mineralization, MG-63 cell line, Bone tissue engineering.

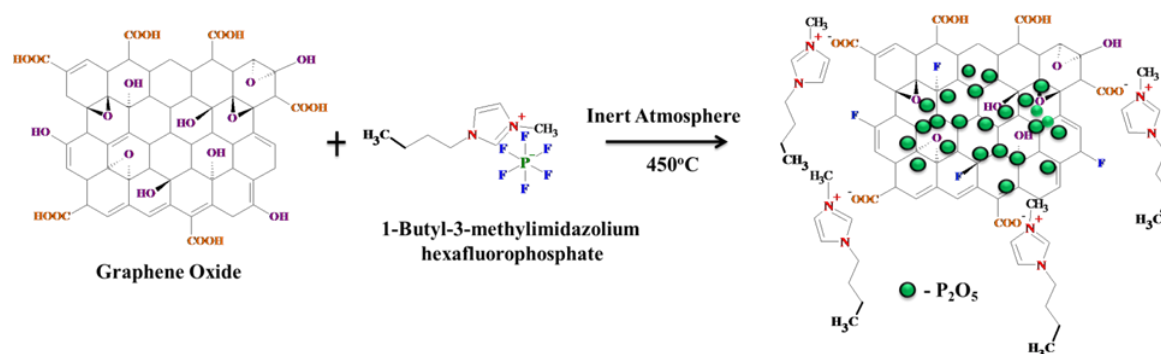
### **Introduction**

Tissue engineering is an attractive interdisciplinary field that combines the basic principles and techniques of material science, biology, and manufacturing to fabricate various substitutes for regenerating damaged tissues and organs. As the major component of natural bone contains phosphate ions exhibits excellent biocompatibility and bioactivity and it has been widely used in bone replacement systems. In this record ionic liquid is used for functionalization of graphene due to its higher amount of functionalities and its low coordination nature.

## Experimental Details

First, graphene oxide was prepared from commercial graphite powder by an improved Hummers' method. As to the tri doping of N, P and F atoms into the carbon frameworks, 100 mL as-synthesized graphene oxide ( $0.5 \text{ mg mL}^{-1}$ ) aqueous dispersion was mixed with 100 mg of 1-Butyl-3-methylimidazolium hexafluorophosphate by sonication for 2 h. Afterward, the mixture was freeze-dried at  $50 \text{ }^\circ\text{C}$  for 12 h to remove the water and then the resulting GO-ionic liquid samples were placed in a tube furnace and heated at  $400 \text{ }^\circ\text{C}$  in N atmosphere. During the thermal annealing process N, P and F atoms can be interacted with the functional groups and doped into the lattices of carbon layers, and simultaneously GO was reduced to graphene, forming the desired NPF-G ternary composite.

## Results and Discussion



FE-SEM clearly shows the graphene sheets under close inspection, the N, and F dual-doped carbon sheets are decorated uniformly by numerous small P<sub>2</sub>O<sub>5</sub> NPs with sizes below 50-60 nm. The tri doping carbon frameworks are forming the mineralization of osteoblast cell line. In XRD spectrum the characteristic broad peak at  $2\theta=25.6^\circ$  refer the generation of graphene structure to this additional peaks observed at  $31.6^\circ$ ,  $37.7^\circ$  and  $40.9^\circ$  indexed to the P<sub>2</sub>O<sub>5</sub> NPs (JCPDS no. 87-0952). The Raman spectra of NPF-G displayed two prominent scattering peaks at  $1340$  and  $1580 \text{ cm}^{-1}$  are evident the D and G bands of distorted graphitic carbon materials. Remarkably, the D/G intensity ratio ( $I_D/I_G$ ) for Pd/NS-G (1.15) is much higher than those for graphene (0.79), demonstrating a higher defect density in NPF-G sheets because of the N, P and F dopants.

In XPS measurements four characteristic peaks located at the binding energies of 285.6, 400.1, 165.0, 133.2 and 687.8 eV are clearly observed, belonging to the C 1s, N 1s, P 2p and F 1s signals, respectively. After 7day incubation, the MG-63 cell lines area on NPF-G is broader than the other two substrates. The cells exhibited better adhesion than the undoped. The cell adhesion and proliferation assay indicated that the prepared substrates show a very good biocompatibility. It is reported that the cell behavior can be also influenced by the presence of P, N, and F in the nanocomposite.

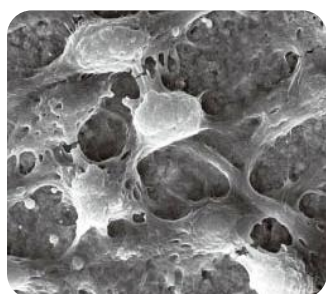


## Conclusion

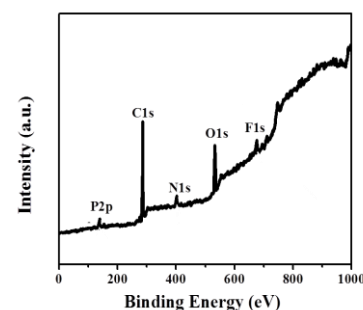
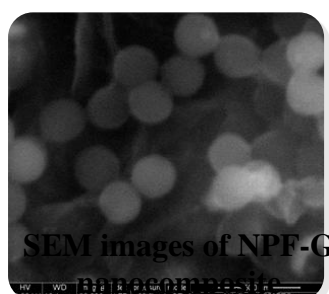
In conclusion, we have presented a combined thermal annealing and hydrothermal method for the deposition of ultrafine  $P_2O_5$  on N and F dual-doped graphene sheets. That gives to the distinct structural advantages, such as large surface area, coexistence of N and F atoms, homogeneous dispersion of small  $P_2O_5$  particles with improved morphology. The NPF-G exhibits bio interface that promoted the mineralization both in simulated physiological condition and cell-mediated condition. The hybrid material exhibited good cellular activities including cell attachment, cell proliferation, which suggested that it is a promising substrate for induced synthesis of biomaterials in bone tissue regeneration and implantation.

## References

- Debe, M. K. Electrocatalyst Approaches and Challenges for Automotive Fuel Cells. *Nature* 2012, 486, 43-51.
- Huang, H. J.; Wang, X., Recent Progress on Carbon-Based Support Materials for Electrocatalysts of Direct Methanol Fuel Cells. *J. Mater. Chem. A* 2014, 2, 6266-6291



Osteoblast cell proliferation of MG-63 cell line on NPF-G



XPS spectrum of NPF-G nanocomposite

## OP 18 Ionic liquid Mediated Green Synthesis of Strontium Cerium Core Nanoparticles and its Antibacterial Activity

P. Nithya<sup>a</sup>, M. Balaji<sup>a</sup>, S. Jegatheeswaran<sup>a</sup>, A. Surya<sup>a</sup>, V. MuthuLakshmi<sup>a</sup>, A. Keerthana<sup>a</sup>, A. Herculin Arun Baby<sup>a</sup>, A. Mayakrishnan<sup>a</sup>, S. Selvam<sup>a</sup> and M. Sundrarajan<sup>a\*</sup>

<sup>a</sup>Advanced Green Chemistry Lab, Department of Industrial Chemistry, School of Chemical Sciences, Alagappa University, Karaikudi - 630 003, Tamil Nadu, India.

<sup>b</sup>Laser and Sensor Application Laboratory, Engineering Building, Pusan National University, Busan - 609735, South Korea.

\*Corresponding author: Tel: + 91 94444 96151

E-mail: [drmsgreenchemistrylab@gmail.com](mailto:drmsgreenchemistrylab@gmail.com)

## Abstract

Green synthesis of metal and metal oxide Nanoparticles (NPs) is an emerging field of nanoscience and technology. The metal and metal oxide Nanoparticles can exhibit significantly physical, chemical and biological properties. SrO/CeO<sub>2</sub> NPs synthesis in *Petalium murexplant* extract in (IL) medium, which is confirmed by XRD, FT-IR, UV-DRS, Raman Spectroscopy,

SEM with EDX and TEM. The synthesized SrO/CeO<sub>2</sub> core NPs exhibit good antibacterial activity.

**Key words:** *Pedaliium murex*; SrO/CeO<sub>2</sub>; core metal oxide; Antibacterial;

## Introduction

Nanoparticles exhibit significantly novel and improved properties. Nano-scale particles based on specific characteristics such as size distribution, shape, morphology, composition and crystalline phase. Ionic liquids (ILs) are employed in the creation of nanostructure materials because of their unique properties such as good dissolving ability, excellent and high ionic conductivity. ILs assisted green synthesis of SrO/CeO<sub>2</sub> core metal oxide NPs prepared greener method by using environment benign *P.murex* plant extract and [BMIM] PF<sub>6</sub> (IL) is a capping agent. Strontium cerium core metal oxide (SrO/CeO<sub>2</sub>) NPs is combinatorial chemistry technique which exhibit luminescence under excitation of cathode and X-rays [1].

## Experimental Details

SrO/CeO<sub>2</sub> core metal oxide nanoparticles (**Figure: 1**) prepared by greener method by strontium nitrate [Sr(NO<sub>3</sub>)<sub>2</sub>], Cerium chloride [CeCl<sub>3</sub>.7H<sub>2</sub>O] used as a precursor with environment benign *Pedaliium murex* plant extract and [BMIM] PF<sub>6</sub> (IL) is a capping agent. Strontium nitrate solution (0.1 N), Cerium chloride (0.1 N) solution and 1 mL [BMIM]PF<sub>6</sub> (IL) were added to the ethanolic solution of *Pedaliium murex* plant extract and stirred for 6 hours continuously at room temperature. The resulting sample were filtered, washed with distilled water and dried at 100 °C. The powered sample was calcinated in a muffle furnace at 700 °C to get SrO/CeO<sub>2</sub> core metal oxide nanoparticles.

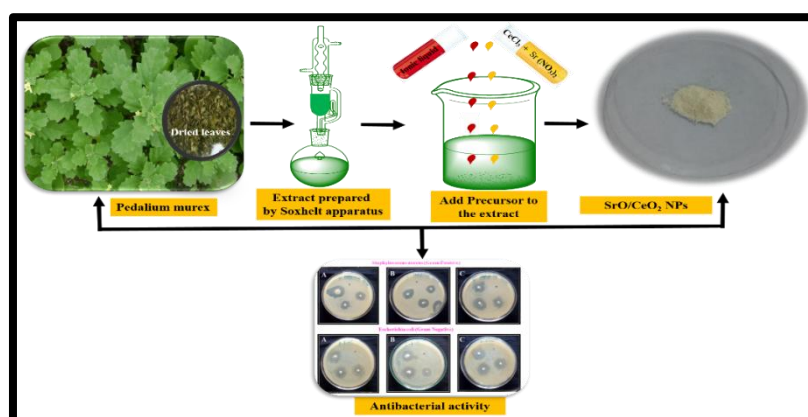


**Figure: 1** Preparation of SrO/CeO<sub>2</sub> core metal oxide nanoparticles

## Results and Discussion

The green synthesized SrO/CeO<sub>2</sub> core metal oxide NPs system displaying nano rod like structure with 10-15 nm and high crystallinity that are confirmed by SEM and XRD studies. GC-MS spectroscopy confirms the presence of N- Hexadecanoic acid (29%), 6-Octadecenoic acid (13%) present in the plant extract that are capable to convert the corresponding metal ion

precursor to SrO/CeO<sub>2</sub> core metal oxide NPs. In FTIR spectral studies the peak at 451 and 856 cm<sup>-1</sup> that are characteristic peaks of Ce-O and Sr-O respectively. Raman spectroscopy give stretching frequency at 457 and 159 cm<sup>-1</sup> that proofs the presence of CeO<sub>2</sub> and SrO present in core metal oxide. The band gap energy of the SrO/CeO<sub>2</sub> core metal oxide NPs was estimated as 3.17eV from the UV- DRS spectroscopy. The anti-bacterial studies performed against a set of bacterial strains *S. aureus* and *E-coli*, the result showed that SrO/CeO<sub>2</sub> core metal oxide NPs more susceptible for gram positive (G+) bacteria than gram negative (G-) bacteria. The toxicology behavior of SrO/CeO<sub>2</sub> core metal oxide NPs found due to the high oxygen site vacancies, reactive oxygen species (ROS) formation, smallest particle size and higher surface area [2].

## Conclusion

Herein, we successfully, facile and ecofriendly synthesized the SrO/CeO<sub>2</sub> core metal oxide NPs in the presence of ionic liquid (IL) medium by ethanolic solution of *P.murex* leaves extract. In green synthesis IL align the structure of NPs and act as a capping agent without affect the environment. The anti-bacterial studies performed against a set of bacterial strains the result showed that SrO/CeO<sub>2</sub> core metal oxide NPs more susceptible for Gram positive (G+) bacteria than Gram negative (G-) bacteria.

## References

- S.B. Khan, M. Faisal, M.M. Rahman and Jamal, Journal of Sci. Total Environ, 409[15]2011, 2987- 2922.
- S. Patil, A. Sandberg, E. Heckert, W. Self and S.Seal, Journal of Biomaterials, 28[31] 2007, 4600-4607.

## **OP 19** Effect of mixed halide ions induced the inorganic cesium lead iodide light harvester photo-anode for perovskite solar cell application

**K. Sakthi velu, B. Suganya bharathi, G. Vignesh Kumar and T. Stalin\***

*Photochemistry Lab, Department of Industrial Chemistry, School of Chemical Sciences, Alagappa University, Karaikudi-03, Tamilnadu-India.*

*\* Corresponding Author: Dr.T.Stalin*

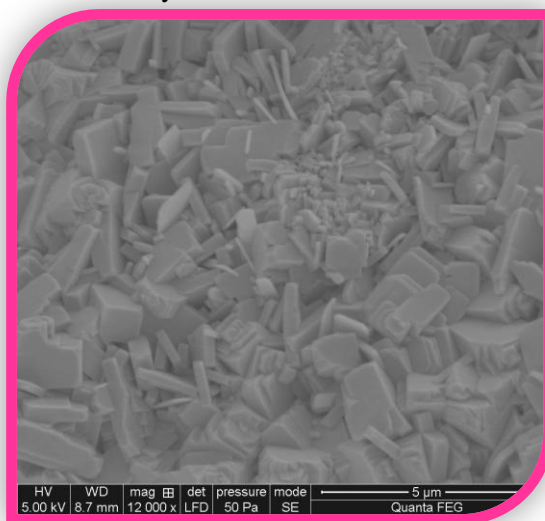
*Email Address: [tstalinphd@reddiffmail.com](mailto:tstalinphd@reddiffmail.com), [drstalin76@gmail.com](mailto:drstalin76@gmail.com).*

## Abstract

The inorganic perovskite solar cells were fabricated with mixed halide ions of iodide and chloride. Effect of mixed halide (Iodide/Chloride) ions based perovskite solar cell was improved their internal stability and performance of the device. The mixed halide ions were present in the composition were determined that the power X-ray diffraction pattern. The functional group of iodide and chloride present in the cesium based inorganic perovskite light absorber were identified by the ATR-FTIR spectroscopy. The absorption maximum of the mixed halide based

perovskite photo-anodes were analysis by the Diffused-reflectance spectroscopy (UV-DRS). The electrical conductivity of the chloride and iodide used in the preparation of the inorganic perovskite solar cell was achieved the higher compared with pristine cesium lead iodide and cesium lead chloride perovskite solar cell. The surface morphology of mixed halide ions based FE-SEM images shown in uniform multicrystalline growth.

The perovskite solar cell were fabricated with mixed halide ions coated on the FTO/TiO<sub>2</sub> used as photo-anode, Spiro-OMeTAD used as hole transport materials and Gold used as back electrode (Counter electrode). Finally, mixed halide ions coated on the FTO/TiO<sub>2</sub> photo-anode give higher power conversion efficiency of 9.4%.



**FE-SEM image mixed halide based CsPbI<sub>3</sub> light absorber**

**Keywords:** Cesium lead iodide, Cesium lead chloride, Photo-anode, Perovskite Solar Cell.

## **OP 20** Comparative Studies on Dissociation Constant Values of 4-Ethylbenzoic Acid Derivatives with DFT/HF Theories - Computational Approach

**M. Nalini, C. Shanthi, S. Karthick and G. Gopu\***

*Department of Industrial Chemistry, Anacapa University, Karaikudi – 630003*

*\*E-mail: nggopi79@gmail.com*

### **Abstract**

In this work, calculations of Dissociation constant (pK<sub>a</sub>) values of 4-ethylbenzoic acid derivatives have been performed by using Quantum chemical calculation methods. Gas-phase Optimizations were calculated with HF theory by using the basis set 6-31G\*\*. The CBS-QB3 method was used to calculate the gas-phase free energy of 4-ethylbenzoic acid derivatives and their respective anion, and the CPCM continuum solvation method was applied to calculate the free energy differences of solvation for the 4-ethylbenzoic acid and their anion. Thermodynamic cycle was used for the calculation of gas-solvent phase free energy. Absolute pK<sub>a</sub> calculations

with solvated phase optimized structures for the CPCM calculations yielded standard deviations and root-mean square errors of less than 0.4 pKaunits. The results that show the calculated pKa values using the HF are better than those using the corresponding B3LYP. From the results observed, the value of 4-ethylbezoic acid obtained as 5.1 which nearly to the experimental evidence. For the investigated compound, a good agreement between the experimental and the calculated pKa values were also observed.

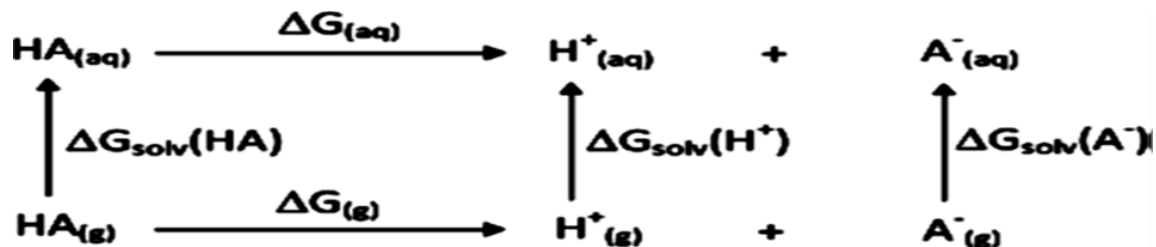


Figure 1: Thermodynamic Cycle A

**Keywords:** Quantum Chemistry, Dissociation Constant, Ionization Constant, CBS-QB3 and CPCM model

## References

Ao Yu, Yuanhai Liu, Zucheng Li, and Jin-Pei Cheng, *J. Phys. Chem. A*, 111 39 2007, 9978–9987  
 Bahram Ghalami-Chooabar, Ali Ghiami-Shomami and Paria Nikparsa, *J. Theor. Comput. Chem.* 11, (2012), 283.

## OP 21 Voltammetric simultaneous determination of vitamin B<sub>2</sub> and B<sub>6</sub> using Gd-ZnO:f-MWCNT nanocomposite modified electrode

N. Dhanalakshmi<sup>a</sup>, T. Priya<sup>a</sup>, S. Thennarasu<sup>b</sup> and N. Thinakaran<sup>a\*</sup>

<sup>a</sup>Environmental Research Lab, PG and Research Department of Chemistry, Alagappa Government Arts College, Karaikudi- 630 003, Tamil Nadu, India.

<sup>b</sup>School of Chemistry, Bharathidasan University, Thiruchirapalli – 620024, Tamil Nadu, India.

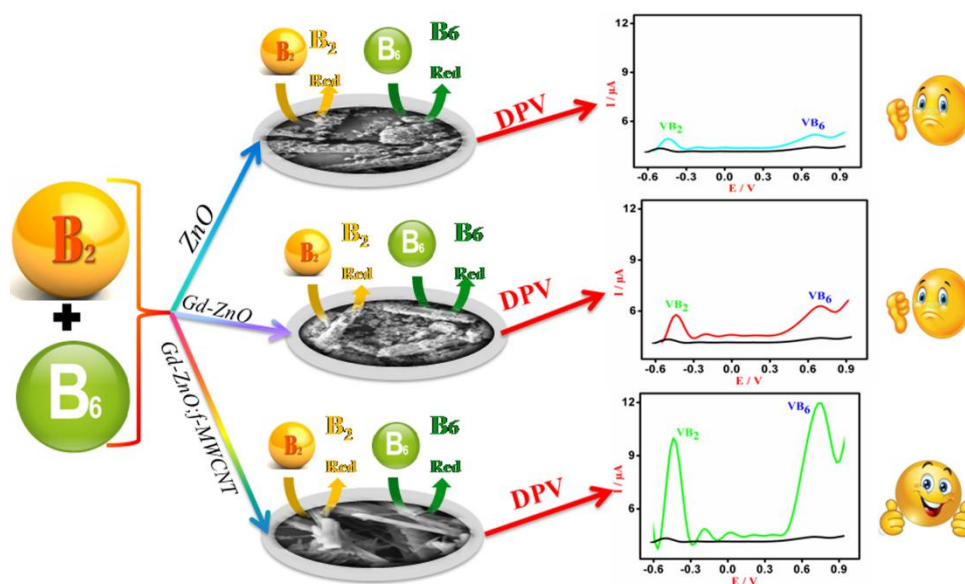
\*Corresponding author.

E-Mail addresses: thinakaran2k@yahoo.com (Thinakaran)

## Abstract

In the present work, rare earth element gadolinium doped Zinc oxide and functionalized Multiwalled Carbon Nanotube containing nanocomposites (Gd-ZnO:f-MWCNT) modified glassy carbon electrode has been constructed for simultaneous determination of vitamins B<sub>2</sub> and B<sub>6</sub>. The surface morphologies of the nanocomposites were characterized by Field Emission Scanning Electron Microscopy, Energy Dispersive Spectrum, X-Ray Diffraction and Fourier Transformed Infrared Spectrum (FTIR) techniques. The electrochemical properties are evaluated by the Cyclic Voltammetry (CV) Differential Pulse Voltammetry (DPV) and Electrochemical Impedance Spectroscopy (EIS). The optimal pH value was determined as 7. The oxidation peak current of

VB<sub>2</sub> and VB<sub>6</sub> showed a linear relationship with concentration over the range from 0.05 to 10 μM with detection limit 0.009 and 0.001 μM for VB<sub>2</sub> and VB<sub>6</sub> respectively. The sensitivities calculated were 1.05 μA.μM<sup>-1</sup>.cm<sup>-2</sup> (VB<sub>2</sub>) and 1.79 μA.μM<sup>-1</sup>.cm<sup>-2</sup> (VB<sub>6</sub>). Furthermore the modified electrode exhibited good reproducibility and long-term stability, as well as high selectivity. Finally, the proposed electrode was successfully applied to the determination of VB<sub>2</sub> and VB<sub>6</sub> in practical samples (pharmaceutical tablet and commercial orange juice) and the results obtained are validated with HPLC.



## OP 22 Steric group in tripodal molecules enforces cyclic aromatic trimer conformer

Deval Sathiyashivan Shankar<sup>a</sup>, Chakka kirankumar<sup>b</sup>, M. Sathiyendiran<sup>\*b</sup> and Dhanraj T. Masram<sup>\*a</sup>

<sup>a</sup> Department of Chemistry, University of Delhi-110007.

<sup>b</sup> School of Chemistry, University of Hyderabad, Hyderabad- 500046.

Email: dhanraj\_masram27@rediffmail.com; mvdiran@yahoo.com

### Abstract

The C–H···π and π···π interactions between aromatic clusters are vital in stabilizing biomolecular structures, and functions.<sup>1</sup> Theoretical models as well as synthetic molecules for benzene dimers are prevalent.<sup>1-3</sup> However, beyond the dimers such as aromatic trimers, tetramers and oligomers are highly limited.<sup>1-3</sup> A family of new tripodal molecules (1-6) possessing the cyclic aromatic trimer motif (CATs) was synthesized and characterized using with/without steric ethyl group at the central benzene scaffold and with the furan/thiophene/pyridyl group at the 2-position of the benzimidazolyl unit. Molecular structures of 1, 3, and 5 were further confirmed by SC-XRD method. Further all molecules were thoroughly studied using NMR analysis. The studies reveal that introduction of three ethyl groups into a central benzene scaffold of

furan/thiophene/pyridyl substituted benzimidazolyl based tripodal molecule enhances the *edge-to-face* C–H··· $\pi$  interactions, thereby favour the aromatic cyclic trimer motif, in the solution and the solid state. The unsubstituted central benzene scaffold allows the furan/thiophene substituted benzimidazolyl units in the tripodal molecule to move freely thereby weakening the *edge-to-face* C–H··· $\pi$  interactions between the aromatic cyclic trimer motifs. The DFT calculations indicate that the energy minimized structures of the tripodal molecules adopt the symmetric (*syn*) cyclic aromatic trimer motif conformation i.e. cylinder like conformation. To the best of our knowledge, the work demonstrates that the discrete molecules with aromatic cyclic trimer motif arrangement both in solid and solution state can be designed and prepared.

**Fig 1.** Chemdraw structure of synthesized (1-6) tripodal molecules.

Recently, nine new family of tripodal molecules have been synthesized and characterized using mono-/di-/tri-methoxyphenyl substituted benzimidazolyl based molecules with/without alkyl substituted spacer. To the best of our knowledge, one of our molecules (7) is the first crystallographic evidence possessing perfect symmetrical CATs motif (distance 4.8 Å, centroid to centroid, and interplanar angle 60° between any two aromatic units in the trimer motif) as predicted theoretically for low-energy cyclic benzene trimer (CBT) motif (fig. 2). Whereas, the literature data discloses the cyclic benzene trimer (CBT) motif in the supramolecular structure **II** with metric parameters ( $d_{\text{COM}\cdots\text{COM}} = 4.97/4.62/5.00$  Å;  $\tau = 68/33/59^\circ$ ) which are close to the calculated distance for the optimized geometry of the  $C_{3h}$ -symmetric CBT motif ( $d_{\text{COM}\cdots\text{COM}} = 4.8$  Å).<sup>4</sup>

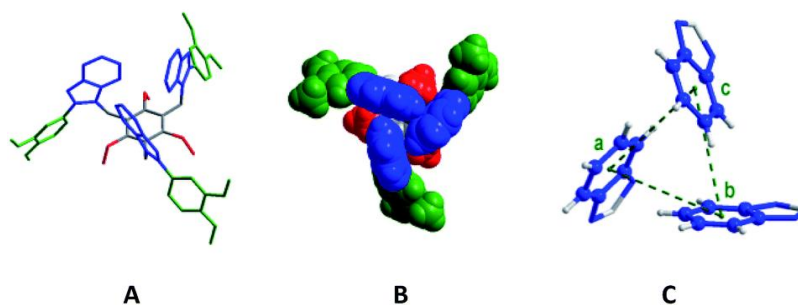


**Fig 2.** Molecular structures of 7 (A: stick model; H-atoms are removed; B: space-filling model; C: three benzimidazolyl units of 7), and a, b and c are the COM points of the benzene ring.

## References

- (a) T. P. Sauer and C. D. Sherrill, *J. Phys. Chem. A.*, 2005, **109**, 10475; (b) E. Lanzarotti, R. R. Biekofsky, D. A. Estrin, M. A. Marti and A. G. Turjanski, *J. Chem. Inf. Model.*, 2011, **51**, 1623 and references therein;
- (a) B. W. Van De Waal, *Chem. Phys. Lett.*, 1986, **123**, 69; (b) A. De Meijere and F. Huisken, *J. Chem. Phys.*, 1990, **92**, 5826; (c) H. Krause, B. Ernstberger and H. J. Neusser, *Chem. Phys. Lett.*, 1991, **184**, 411
- (a) T. Imori, Y. Aoki and Y. Ohshima, *J. Chem. Phys.*, 2002, **117**, 3675; (b) X. Ye, Z. Li, W. Wang, K. Fan, W. Xu and Z. Hua, *Chem. Phys. Lett.*, 2004, **397**, 56
- T. Morimoto, H. Uno and H. Furuta, *Angew. Chem., Int. Ed. Engl.*, 2007, **46**, 3672.

## **OP 23** Synthesis and Antimicrobial Screening of Thiadiazolyl Coumarins

Ganesh N Alawandi<sup>a</sup>, Kiran K Pujar<sup>b</sup> and Manohar V Kulkarni<sup>b</sup>

1. Sigma-Aldrich chemicals Pvt Ltd, No. 12, Bommasandra–Jigani Link road, Bangalore-560100

2. Department of Chemistry, Karnatak University, Dharwad- 580 003, Karnataka, India

\* **correspondence Author:** Ganesh N Alawandi. E-Mail: [dralawandi@gmail.com](mailto:dralawandi@gmail.com)

Cell No.: 9448360681

## Abstracts

(2-oxo-2H-chromen-4-ylmethyl sulphanyl/sulfonyl)-acetic acid hydrazides (**4a-f**) reacts with alkyl or aryl isothiocyanate resulted in the formation of corresponding thiosemicarbazides (**5a-l**) were then subsequently cyclized with concentrated sulfuric acid at 80°C to afforded corresponding 4-(5-substituted amino-[1,3,4]-thiadiazole-2-ylmethyl sulfanyl/sulfonyl methyl)-chromen-2-ones or thiadiazolylcoumarins (**6a-l**). All newly synthesized compounds have been characterized by IR, <sup>1</sup>H NMR, Mass and elemental analysis. All the synthesised thiazolylcoumarins have been screened for their antimicrobial activity against gram – ve bacterium *Escherishia coli*, gram + ve bacterium *Bacillus staphylococci* and fungi *Penicilium* and *Aspergillus*, .

**Key Words:** Thiosemicarbazides, Coumrin, Cyclized and Antimicrobial activity.



# Sche

## **OP 24** Synthesis and Characterization of Novel Acrylamide Copolymers

**S. Bharathi<sup>a\*</sup> and P. Pazhanisamy<sup>b</sup>**

<sup>1</sup>Department of Chemistry, Saveetha Engineering College, Chennai-602 105, India

<sup>2</sup>Department of Chemistry, Sir Theagaraya College, Chennai-600 021, India

\*Corresponding author: E-Mail: bharathimuhesh@gmail.com

### **Abstract**

Copolymer, N-tert-butylacrylamide (NTB) with 2-methyl-N-1, 3-thiazole-2-acrylamide (TMA) was synthesized with different monomer-to-monomer ratios in the feed. The resulting copolymers were characterized and the copolymer compositions were determined by <sup>1</sup>H-NMR data. Fineman-Ross, Kelen-Tudos and extended Kelen-Tudos methods were employed to calculate the reactivity ratios of monomer (NTB) and comonomer (TMA). The reactivity ratios were found to be  $r_1 = 2.5$  and  $r_2 = 0.70$  by Fineman-Ross,  $r_1 = 2.5$  and  $r_2 = 0.70$  by Kelen-Tudos and  $r_1 = 2.5$  and  $r_2 = 0.70$  by Extended Kelen-Tudos method. The product of  $r_1, r_2 > 1$  (1.75) shows weakly ordered and predominantly random distribution in nature. The Value of  $r_1$  shows that NTB favours homopropagation over cross-propagation and  $r_2$  shows that TMA favours cross-propagation over homopropagation. Thus values suggest that NTB is more reactive than TMA. Mean sequence lengths of copolymers were estimated from  $r_1$  and  $r_2$  values. It shows that the NTB units increase in a linear fashion in the polymer chain as the concentration of NTB increases in the monomer feed. Thermogravimetric analysis shows that all the copolymers underwent

triplestage thermal degradation. Glass transition temperatures of the copolymer were found to increase with increasing feed content of NTB. The increase in  $T_g$  may be due to reduction in segmental mobility of the polymer chain and reveals that the thermal stability of the copolymers increases with increases in the mole fraction of NTB in the copolymers. Antimicrobial activity of the polymers prepared were also investigated against various micro-organisms like bacteria (*Escherichia coli*, *Pseudomonas Aeruginosa* and *Klebsiella pneumonia*) and fungi (*AspergillusFlavus*, *Candida albicans* and *Cryptococcus Neoformans*) by using standard agar well diffusion method. It shows moderate activity and may be used as a drug for curing the microbial infection.

**Keywords:** Copolymer composition, Reactivity ratios, Mean sequence lengths, Antimicrobial activity.

**OP 25** **Analysis of inorganic toxic ions in environmental pollutants caused by the dyes used in korai mat weaving cottage industries in Ayyanaruthu, Kayatharu Taluk, Tuticorin District, Tamil Nadu: A case study**

**S. Subbiah Thangadurai<sup>a</sup> and K. Gurusamy<sup>b</sup>**

*Post Graduate Studies and Research Department of Chemistry,  
Raja Doraisingam Government Arts College, Sivagangai – 630 561.*

*<sup>#</sup>Toxicology Division, Regional Forensic Science Laboratory,  
Government of Tamil Nadu, Madurai-625 020.*

**Abstract**

A case study on water pollution of ground water in Ayyanaruthu village, Tuticorin district, Tamil Nadu is presented to highlight the need for the remedial measures. Based on the printed media's information, we have undertaken this study to find out the potential pollutant of this village. We have collected the bore well water samples from the vicinity to the korai mat weaving tiny industries and remote from these industries residence areas. Also, we have encountered certain inorganic ions *viz.* sodium ( $\text{Na}^+$ ), potassium ( $\text{K}^+$ ), chloride ( $\text{Cl}^-$ ), cyanate ion ( $\text{OCN}^-$ ), phosphate ( $\text{PO}_4^{3-}$ ), thiocyanate ( $\text{SCN}^-$ ), nitrate ( $\text{NO}_3^-$ ), sulphite ( $\text{SO}_3^{2-}$ ), sulphate ( $\text{SO}_4^{2-}$ ) and perchlorate ( $\text{ClO}_4^-$ ) by sensitive micro chemical tests and FTIR methods. The nitrate ( $\text{NO}_3^-$ ) ion has been estimated by UV-Vis Spectrophotometry and the alkali metals have been estimated by Flame Photometry. Most of the bore water samples in Ayyanaruthu areas are not suitable for drinking purpose. In the cottage industrial belt up of Ayyanaruthu, the bore water gets more polluted than other sampling sites due to the direct discharge of industrial untreated wastewater and intrusion of polluted cottage industries water. The human exposure to  $\text{NO}_3^-$  and  $\text{NO}_2^-$  and the relative contribution of drinking water to that exposure were assessed. Hence, it is recommended that suitable water quality management is essential to avoid any further contamination.

**Keywords:** Ayyanaruthu village, FTIR, UV-vis spectrophotometry, flame photometry, IC.

*\*Author for correspondence ; E-mail: [drsdurai@mail.com](mailto:drsdurai@mail.com)*

**OP 26** **Analysis of chlorate, perchlorate and nitrate by TLC, FTIR, Powder XRD and IC in Irrigation water, soil debris and sewage sludge samples from Fireworks and Safety Matches manufacturing areas in Sivakasi, Virudhunagar District, Tamil Nadu, India**

**S. Thangadurai\* and Karthikprabu**

*Post Graduate Studies and Research Department of Chemistry  
Raja Doraisingam Government Arts College, Sivagangai – 630 561.*

**Abstract**

Water is an important source of life. Without water there is no life and no development. Water has been featuring prominently both on national and international agenda. An efficient wastewater disposal is important to the health of any community. Stress on water resources is from multiple sources such as urbanization, increased industrial activities, heavy use of fertilizers and pesticides in agricultural activities, discharge of untreated sewage and industrial effluents into environment. All these activities ultimately leads to both surface and groundwater pollution. Effective collection and treatment of wastewater is a critical problem especially in developing countries like India. It is therefore necessary that the quality of water should be monitored at regular intervals. In this study, our aim was to assess the nitrate ( $\text{NO}_3^-$ ), chlorate ( $\text{ClO}_3^-$ ) and perchlorate ( $\text{ClO}_4^-$ ) contamination in soil debris, irrigation water and sewage sludge samples from fireworks and safety matches manufacturing areas in Sivakasi. Sensitive micro chemical analyses were carried out for the aforementioned samples. Then thin-layer chromatography (TLC), Fourier Transform infrared spectrometry (FTIR), and powder X-ray diffraction (XRD) and Ion Chromatography (IC) methods for confirming the presence of the toxic ions in the aforementioned samples. The TLC systems developed provide numerous possibilities for rapid, reproducible and clean separations of  $\text{ClO}_3^-$  and  $\text{ClO}_4^-$  from the aforementioned samples. The high concentration of  $\text{NO}_3^-$ ,  $\text{ClO}_3^-$  and  $\text{ClO}_4^-$  detected in irrigation water was mainly due to the industrial units and firework manufacturing and display sites. Vicinity to these industrial units agricultural well water has been affected, they became unsuitable for irrigation due to the contamination of potential pollutant *viz.*  $\text{NO}_3^-$ ,  $\text{ClO}_3^-$  and  $\text{ClO}_4^-$ , plethora of agricultural well water and agricultural lands have become dry land.

**Keywords:** Inorganic ions, Fireworks, Match industries, TLC, FTIR, Powder XRD, IC

*\*Author for correspondence: [drstdurai@gmail.com](mailto:drstdurai@gmail.com)*

## **OP 27** Enzyme-Free Glucose Sensor Based on Copper Based Metal-Organic Framework/ rGO Composite

**T. Ponnuthuselvi and S. Viswanathan\***

*Department of Industrial Chemistry, Alagappa University, Karaikudi-630 003, Tamil Nadu.*

*\*Corresponding Author E-mail: [rsviswa@gmail.com](mailto:rsviswa@gmail.com)*

### **Abstract**

Enzyme-free electrochemical glucose sensor based on a Cu-based metal-organic framework (Cu-MOF) with reduced graphene oxide (rGO) modified electrode was developed. The Cu-MOF/rGO was prepared by a simple solvothermal synthesis, and the characterizations of the Cu-MOF/rGO were studied by Fourier transform infrared spectroscopy (FT-IR), scanning electron microscopy (SEM), and thermogravimetric analysis (TGA) and X-ray powder diffraction (XRD). Electrochemical behaviors of the Cu-MOF modified electrode to glucose were measured by amperometric technique. The electrochemical results showed that the Cu-MOF/rGO modified electrode exhibited an excellent electro-catalytic oxidation towards glucose in the range of 1  $\mu$ M to 300  $\mu$ M and a detection limit of 66  $\mu$ M. prominently; good reproducibility, long-time stability, and excellent selectivity were obtained within the as-fabricated glucose sensor.

**Keywords:** Metal-organic framework, Enzyme-free sensor, glucose, amperometric method.

### **Introduction**

Metal-Organic Frameworks (MOFs) are a class of novel porous, three-dimensionally linked coordination network materials, which are composed of metal ions and organic ligands by strong coordination bonds. MOFs have similar structure contrasted to zeolites or alumina silicates unlike zeolites which are purely inorganic; MOFs are hybrids of inorganic and organic materials. MOFs have greater advantage than well-known nonporous zeolites because of its structural and functional group tenability [1]. MOFs have been widely used in the areas of catalysis, drug delivery, and gas adsorption. MOFs also are good electrode materials and have been applied in energy storage, fuel cells, solar cells, lithium-ion rechargeable batteries, and sensors [2].

### **Experimental**

Cu-MOF/rGO composites containing copper MOF with reduced graphene oxide were synthesized by Solvothermal method from the precursors of copper nitrate and benzene tricarboxylic acid (BTC) and graphene oxide. The electrochemical sensing property of Cu-MOF/rGO composite was investigated by drop caste method on a Carbon paste electrode (CPE).

### **Result and Discussion**

As prepared Cu-MOF and Cu-MOF-rGO was characterized by SEM to investigate the surface morphology. The image shows that the sheet like structure onto square pyramidal shape of crystal. Crystallinity and the functional groups presence in the MOF samples was successfully

proved by powder XRD and ATR-FTIR spectroscopy respectively. To investigate the electrocatalytic activity of as-prepared Cu-MOF/rGO composites toward glucose oxidation, Cu-MOF/rGO composites were dispersed in Nafion/ethanol solution and immobilized onto CPE. The CVs technique is applied to investigate the electrochemical behavior of the Cu-MOF/rGO/CPE in NaOH (0.1 M) with the presence and absence of glucose. A pair of well-defined redox peaks appeared in the absence of glucose for Cu-MOF/rGO/CPE and Cu-MOF/CPE (Fig a). Further, the phenomenon of oxidation current response increasing with the concentration of glucose is observed on the Cu-MOF/rGO/CPE, proving that glucose can be easily oxidized on Cu-MOF/rGO/CPE over a wide concentration window Fig. (b). The enhancement of anodic current is due to the electro-oxidation of glucose with the participation of Cu (III).

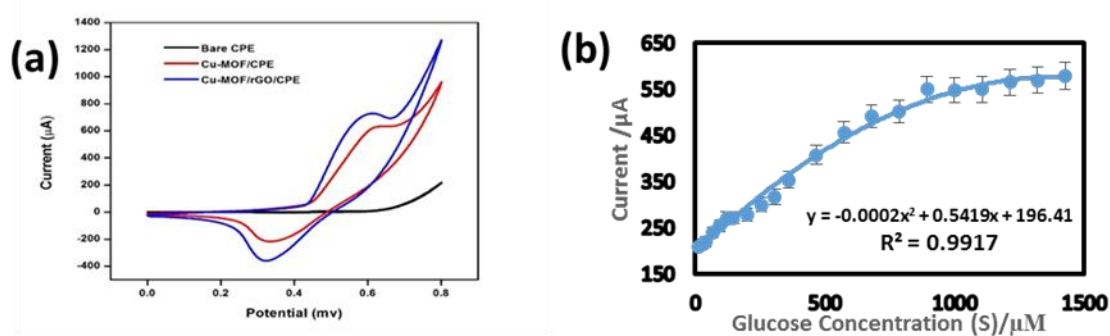


**Fig: (a)** CVs of bare CPE, Cu-MOF/ CPE, and Cu-MOF/rGO CPE in NaOH (0.1 M) with 50  $\mu\text{M}$  glucose (scan rate: 50 mV/S) **(b)** Calibration curve of current versus glucose concentrations for Cu-MOF/rGO/CPE by Amperometric method. Error bars are the standard error of the mean (three parallel electrodes)

## Conclusion

A novel Cu-MOF material was synthesized and used to fabricate a sensitive and selective electrochemical non-enzymatic glucose sensor. The structural features of Cu-MOF were characterized by XRD, FT-IR, SEM and TGA. We demonstrate the exploitation of a porous Cu-based metal-organic framework (Cu-MOF) with large pore size as non-enzymatic sensors for the electrochemical determination of glucose. The results showed that the non-enzymatic sensors based on the rGO modified Cu-MOF display excellent analytical performances with a wide linear range from 1  $\mu\text{M}$  to 300  $\mu\text{M}$  and a detection limit of 66  $\mu\text{M}$ . It is due to easy fabrication, adequate robustness, renewability, good reproducibility and stability.

## References

- Wang, X.; Wang, Q.; Wang, Q.; Gao, F.; Gao, F.; Yang, Y.; Guo, H. Highly Dispersible and Stable Copper Terephthalate Metal-Organic Framework-Graphene Oxide Nanocomposite for an Electrochemical Sensing Application. *ACS Appl. Mater. Interfaces* 2014, 6, 11573–11580.
- Kim, E.; Yoon, M. Facile Synthesis of  $\gamma\text{-Fe}_2\text{O}_3$ @Porous Carbon Materials Using an Fe-based Metal-organic Framework: Structure and Porosity Study. *J. Porous Mater.* 2015, 22, 1495–1502.

**OP 28** Microwave assisted synthesis of gold microcubes: Greener approach

M. Kiruba, R. Mangaiyarkarasi and S.Umadevi\*

*Liquid Crystal Lab, Department of Industrial Chemistry, School of Chemical Sciences, Alagappa University, Karaikudi -3, Tamil Nadu, India.*

*Email: [kiruba101195@gmail.com](mailto:kiruba101195@gmail.com), [mangairajkumarchem@gmail.com](mailto:mangairajkumarchem@gmail.com) and [umadevilc@gmail.com](mailto:umadevilc@gmail.com)*

**Abstract**

In this current work, gold micro cubes have been successfully prepared by microwave heating of  $\text{HAuCl}_4$  in an ionic liquid crystal (ILC), as reaction medium without any additional templating agent. The synthesized ILC was chemically characterised by nuclear magnetic resonance spectroscopy and Fourier transformer infra-red spectroscopy while mesophase behaviour was confirmed by polarising optical microscopic and differential scanning calorimetry techniques. Morphology and size of the resulting gold particles were analysed using scanning electron microscopy (SEM) studies. It was demonstrated that the ILC could act as a reaction medium as well as templating agent for the formation of cube-shaped gold microparticles. The present synthesis route is very simple, faster and can be extended to the synthesis of other metal nano/microstructures in the ILC medium.

**Keywords:** Ionic liquid crystal, microwave irradiation, templating agent, organized reaction medium, gold micro cubes, greener approach

**Introduction**

Gold nanoparticles (AuNPs) are most extensively studied because of their unique optical, electrochemical, biological properties that give importance to them in the areas ranging from chemical and biological sensors, electronic materials, fundamental research and even catalysis [1]. Several methods have been already reported for the synthesis of these nanomaterials. However, controlled growth of the particles with desired morphology is still challenging in the synthesis of nanomaterials.[2] Microwave assisted synthesis of gold nanoparticles using ILCs is an efficient greener approach. It reduces the reaction time from several hours to a few minutes in a process that avoids the use of external templating agent. In view of the emerging importance of the ILC as reaction media for nanomaterial synthesis, combination of microwave properties and ionic liquid behavior in this approach is an efficient greener strategy for nanomaterial synthesis.

**Experimental Details**

An appropriate amount of chloroauric acid ( $\text{HAuCl}_4 \cdot 3\text{H}_2\text{O}$ ) was mixed with a 2-fold of synthesized ILC (Fig 1a) and heated in a microwave oven for 5 minutes at 140 W.

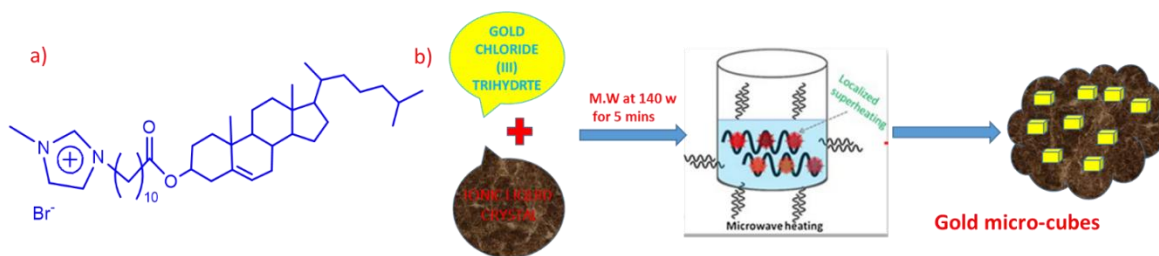


**Figure 1. a) Structure of synthesized ILC; b) Graphical representation of synthesis of AuNPs**

## Results and Discussion

Microwave (MW) dielectric heating is a new promising technique for preparation of size-controlled metallic nanostructures due to its rapid heating and penetration. A suitable amount of  $\text{HAuCl}_4 \cdot 3\text{H}_2\text{O}$  was mixed with 2-fold of synthesized ILC and heated in a microwave oven for 5 minutes at a power of 140 W.

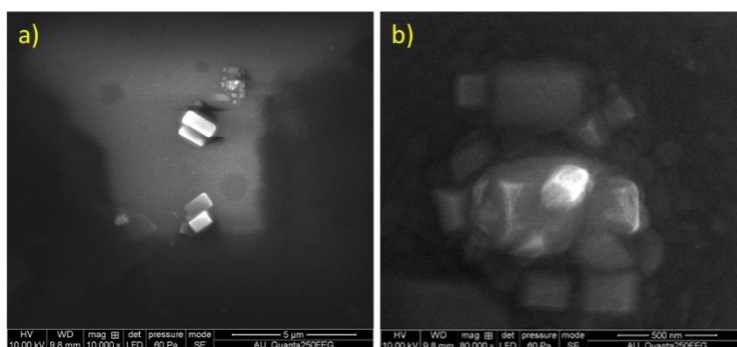


**Figure 2: (a) and (b) SEM images of gold microcubes at different magnification**

Upon microwave irradiation, colour of the mixture changed from yellow to bright red indicating the formation of nanoparticles. The nanomaterials with interesting non-conventional morphologies are expected since the nucleation and growth process takes place in a structurally ordered ILC medium. Accordingly, cube-shaped particles were obtained in this synthesis which was confirmed through scanning electron microscopy images (SEM). Figure 2 shows SEM images of gold cube-like structures embedded in the ILC medium.

## Conclusion

In summary, we have developed an effective greener approach for the synthesis of gold nano cubes using microwave irradiation by employing an ILC. ILC acted as a reaction medium and a templating agent in this synthesis process and assisted the formation of cube-like microstructures. Such a simple synthetic procedure is a versatile approach that can be extended to the synthesis of other metal nano/micro particles of varying size having unusual morphologies.

## References

- M. C. Daniel and D. Astruc, *Chem. Rev.* **104**, 2004, 293-346  
 Q. Ji, S. Acharya, G. J. Richards and S. Zhang, *Langmuir*, **29**, 2013, 7186-7194  
 Z. Li, Z. Liu, J. Zhang, B. Han and J. Du, *J. Phys. Chem. B*, **109**, 2005, 14445-14448

## OP 29 Interaction Study of Palladium(II) Ion with Coumarin 460 : An NMR Approach

B. M. Ashwin, M. Vinothini, M. Suganthi and P. Muthu Mareeswaran\*

Department of Industrial Chemistry, Alagappa University, Karaikudi - 630003, Tamilnadu, India.

E-mail: [muthumareeswaran@gmail.com](mailto:muthumareeswaran@gmail.com)

### Abstract

The fluorescent molecule coumarin 460 (C460) sense  $\text{Pd}^{2+}$  metal ion by quenching process. Here, the mechanism for the C460 and  $\text{Pd}^{2+}$  interaction is studied and explained by the  $^1\text{H}$  NMR titration. The changes in the NMR peaks are attributed to the mode of binding of  $\text{Pd}^{2+}$  with C460.

**Keywords:** Coumarin 460, Palladium ion, NMR titration.

### Introduction

Palladium is an active metal belongs to transition metals group due to its physicochemical properties. Palladium have negative impacts on human health by disturbing a variety of cellular processes by its binding tendency towards thiol-containing amino acids, proteins, DNA and other macromolecules present inside cell.<sup>1</sup> Owing to its hazardous effect, strict restrictions are implemented on the level of residual heavy metals in end products (less than 5– 10 ppm).<sup>2</sup> Therefore the detection of palladium even at lower molar concentration at all environmental conditions receives importance.

The coumarins are adaptable to aqueous systems.<sup>3</sup> They are highly luminescent organic molecules having excellent optical properties and readily available.<sup>4</sup> Many reports are available on highly conjugated coumarin derivatives for sensor applications for cation by internal charge transfer (ICT) mechanism has been widely exploited.<sup>5</sup> The coumarin 460 (C460) is a highly fluorescent readily available probe for  $\text{Pd}^{2+}$  metal ion. The fluorescence of C460 quenched in the presence of  $\text{Pd}^{2+}$  ion. Herein we report the binding/interaction of  $\text{Pd}^{2+}$  with C460 to explore the quenching mechanism.

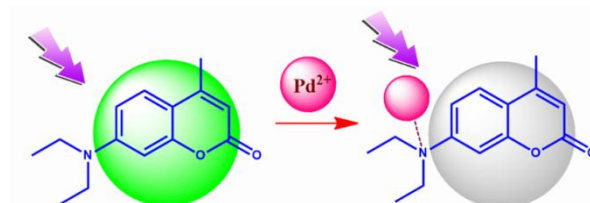


**Figure 1. Fluorescence quenching of C460 in the presence of  $\text{Pd}^{2+}$**

### Experimental Details

$^1\text{H}$  NMR titration is carried out using DMSO- $d_6$  solvent in Bruker 500 MHz NMR Spectrometer. 0.01 M of C460 is fixed and  $\text{PdCl}_2$  is varied from 0.5 - 2.0 equivalents for the  $^1\text{H}$  NMR titrations.



## Results and Discussion

On addition of  $\text{Pd}^{2+}$  ion with C460, there is no changes were observed in the aromatic protons. It confirms that there is no interaction between  $\text{Pd}^{2+}$  and the aromatic moiety. On increasing the  $\text{Pd}^{2+}$  concentration a new peak at 2.1 ppm is appeared corresponding to the upfield shift of methylene ( $-\text{CH}_2-$ ) from 3.4 ppm. This may be due to the interaction of  $\text{Pd}^{2+}$  with the lone pairs of nitrogen atom which is neighbour to the methylene proton.<sup>6</sup> The close proximity of  $\text{Pd}^{2+}$  ion and the loss of electrons by nitrogen atom is the reason for the shift. The rotation of the N-C could be restricted in the presence of  $\text{Pd}^{2+}$ . These results explains the binding site of  $\text{Pd}^{2+}$  with C460 by strong interaction.

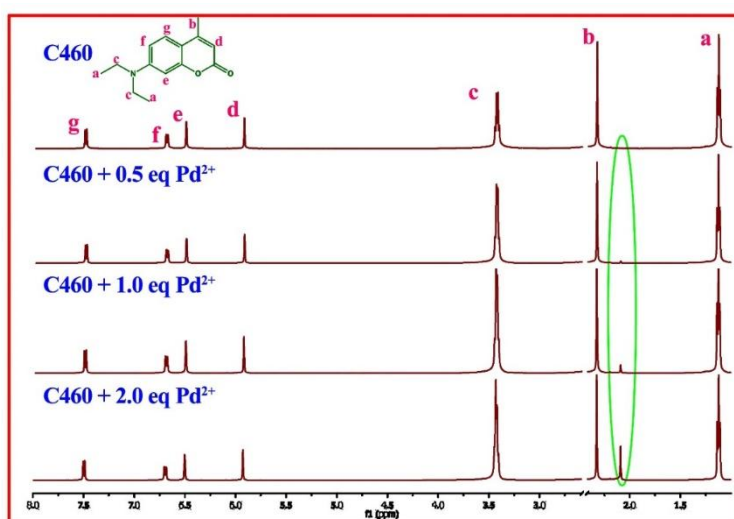


**Figure 2.**  $^1\text{H}$  NMR titration of C460 with  $\text{Pd}^{2+}$  in DMSO-d<sub>6</sub> (Solvent peak is removed for clarity)

C460 is a 'push-and-pull' type of fluorophore. Diethylamino group of C460 is pushing an electron, while carbonyl groups are pulling the  $\pi$ -electrons to afford a strong fluorescence emission at  $\lambda_{\text{max}} = 470$  nm. When adding  $\text{Pd}^{2+}$  to C460, the fluorescence intensities of C460 decreased, which is due to the restriction of electron transfer from nitrogen atom. The binding of  $\text{Pd}^{2+}$  with C460's nitrogen lone pair is also well explained in the  $^1\text{H}$  NMR spectral studies. Hence, this sensor system works in the basis of simple internal charge transfer (ICT) mechanism.<sup>6</sup> The sensing mechanism is illustrated in the Figure 1.

## Conclusion

The quenching mechanism of  $\text{Pd}^{2+}$  with C460 is clearly interpreted with the help of  $^1\text{H}$  NMR titration. The sensing mechanism behind  $\text{Pd}^{2+}$  ion detection by C460 is internal charge transfer (ICT). The appearance of new peak is due to the binding of  $\text{Pd}^{2+}$  in the vicinity of nitrogen. The mode of binding is established using this study.

## References

J. Kielhorn, C. Melber, D. Keller, I. Mangelsdorf, Int. J. Hyg. Environ. Health, 205 [6] 2002, 417-432.

- C.E. Garrett, K. Prasad, *Adv. Synth. Catal.*, 346 [8] 2004, 889-900.  
V.M. Malikov, A.I. Saidkhodzhaev, *Chem. Nat. Compd.*, 34 [3] 1998, 345-409.  
M. Tasior, D. Kim, S. Singha, M. Krzeszewski, K.H. Ahn, D.T. Gryko, J. Mater. Chem. C, 3 [7] 2015, 1421-1446.  
H.S. Jung, P.S. Kwon, J.W. Lee, J.I. Kim, C.S. Hong, J.W. Kim, S. Yan, J.Y. Lee, J.H. Lee, T. Joo, J.S. Kim, *J. Am. Chem. Soc.*, 131 [5] 2009, 2008-2012.  
C. Lu, Z. Xu, J. Cui, R. Zhang, X. Qian, *J. Phys. Chem.*, 72 [9] 2007, 3554-3557.

### **OP 3** Copper (II) L-Tryptophan Schiff Base Complexes: Synthesis, Spectral Studies and Its Biological Evaluation

**N. Kavitha, Fidali Stanley Edwin, P. Rajeshwari, Fathima Farhana, N. Pavithra, K. Suganya and N. Sengottuvelan\***

*Department of Industrial Chemistry, Alagappa University, Karaikudi.*

*Email :nsvelan@gmail.com*

#### **Abstract**

Transition metal complexes have been a large area of research interest for many decades, because of their efficient DNA binding and cleavage properties under physiological conditions [1]. L-Tryptophan (L-Trp) is a large neutral amino acid present in living organisms having biological importance. In this present work we have synthesized Copper(II) tryptophan Schiff base complexes  $[\text{Cu}(\text{Msal})(\text{L-Trp})(\text{H}_2\text{O})]$  (**1**),  $[\text{Cu}(2\text{-HNP})(\text{L-Trp})(\text{H}_2\text{O})]$  (**2**), and  $[\text{Cu}(\text{NB})(\text{L-Trp})(\text{H}_2\text{O})(\text{N}_3)]$  (**3**) and characterized using spectroscopic techniques. The IR spectra of complexes (**1-3**) shows sharp bands resulting from the C=N stretching vibration at  $1648\text{ cm}^{-1}$ ,  $1638\text{ cm}^{-1}$  and  $1625\text{ cm}^{-1}$  suggesting the presence of azomethine functional group in complexes. In the UV absorption spectra, peak near 657 nm, 610 nm and 570 nm for complexes **1**, **2** & **3** respectively, is assigned to a d-d transition, which is consistent with the square-planar geometry of the Copper(II) complexes [2]. The EPR spectra of the copper (II) complexes were recorded at liquid nitrogen temperature, the results shows well-resolved four lines due to hyperfine splitting with nuclear hyperfine spin 3/2 [3]. The intrinsic binding constant to ctDNA was obtained by monitoring the absorption intensity of the charge transfer spectral bands near 271, 289 and 273 nm for the complexes of **1**, **2** & **3** respectively. Upon addition of increasing amounts of ctDNA, a significant 'hypochromic' effect in the intraligand bands was observed for complexes, this may be due to the square planar geometry of complexes and presence of planar aromatic chromophore that facilitates a strong binding interaction of the complexes with ctDNA via insertion of the aromatic moiety in between the stacking base pair. The results indicated that the three complexes are able to bind to DNA with different binding affinity as  $8.56 \times 10^{-7}$ ,  $2.68 \times 10^{-5}$ ,  $1.47 \times 10^{-6}\text{ M}^{-1}$  respectively, in the order as **2** > **3** > **1**. The antibacterial activity was confirmed for a Gram-positive bacteria *Staphylococcus mutans* (*S.mutans*) and a Gram-negative bacteria *Escherichia coli* (*E.coli*) on nutrient agar medium by the disc diffusion method. On comparing the Gram-negative

and positive bacteria, the complexes exhibit higher efficiency for Gram-positive bacteria than Gram negative bacteria. We conclude that the synthesized complexes (**1-3**) are biologically active Schiff base complexes having selective binding affinity with DNA, thus these complexes can be studied for further therapeutical activities.

## Reference

- G. Prati, J. Bernadou and B. Meunier, *Adv. Inorg. Chem.*, 45 (1998) 251.  
A. Bencini, C. Benelli, D. Gatteschi, C. Zanchini, A.C. Fabretti, G.C. Franchini, *Inorg. Chim. Acta* 86 (1984) 169–172.  
V. Suresh Babu, A. Ramesh, P. Raghuram, R. Raghava Naidu, *Polyhedron* 16, 1997a, 607–612.

## **OP 31** Biological screening studies of DNA relate metal complexes from Benzalidene-4-imino-2,3-dimethyl-1-phenyl-3-pyrazolin-5-one and 2-aminothiazole

A. Palanimurugan and A. Kulandaisamy\*

PG and Research Department of Chemistry, Raja Doraisingam Government Arts College, Sivagangai-630 561, Tamilnadu, India.

\*Corresponding Author email id: [kulandai.kvn@gmail.com](mailto:kulandai.kvn@gmail.com), +91-94420 12970.

## Abstract

Novel terdentate cationic complexes of Cu(II), Ni(II), Co(II), Mn(II) and Zn(II) ion have been prepared using a Schiff base derived from Benzalidene-4-imino-2,3-dimethyl-1-phenyl-3-pyrazolin-5-one and 2-aminothiazole. The structural features of the chelates have been confirmed by micro-analytical data, FAB-Mass spectra, Powder XRD, SEM, FTIR, UV-Vis., <sup>1</sup>H-NMR, EPR, CV and thermal analysis techniques. The analytical data of the complexes correspond well with the general formula [ML<sub>2</sub>]Cl<sub>2</sub>. The high conductance of the chelates supports their electrolytic nature. The magnetic susceptibility and electronic absorption spectra of the complexes indicate that all the complexes exhibit octahedral geometry around the central metal ion. From Powder XRD, the average crystallite size of Schiff base and its [CuL<sub>2</sub>]Cl<sub>2</sub>, [MnL<sub>2</sub>]Cl<sub>2</sub> and [ZnL<sub>2</sub>]Cl<sub>2</sub> complexes are 57, 56, 42 and 36 nm respectively. The minimum crystalline size was observed for [ZnL<sub>2</sub>]Cl<sub>2</sub> complexes and it has better crystalline nature than other complexes. From the SEM image of the Schiff base and its [CuL<sub>2</sub>]Cl<sub>2</sub>, [MnL<sub>2</sub>]Cl<sub>2</sub> and [ZnL<sub>2</sub>]Cl<sub>2</sub> complexes, irregular spherical grain structure for Schiff base, cloud like model for [CuL<sub>2</sub>]Cl<sub>2</sub>, well dispersed, heterogeneous sized with highly agglomerated grains for [MnL<sub>2</sub>]Cl<sub>2</sub> and cauli flower model like structure for [ZnL<sub>2</sub>]Cl<sub>2</sub> complex was observed.

From <sup>1</sup>H NMR spectra, The Schiff base exhibits the following signals: phenyl as multiplet at 7.53–7.58 δ, =C–CH<sub>3</sub> at 2.60 δ, –N–CH<sub>3</sub> at 3.18–3.30 δ, –CH– at 5.78 δ, –N–C=CH at 7.93–8.23 and –C–S–CH– at 7.69–7.71 δ (thiazole ring). A slight downfield shift was observed in all the signals in the spectrum of zinc complex which clearly indicated that the coordination ligand

system with metal ion. The EPR spectra of the  $[\text{CuL}_2]\text{Cl}_2$  complex was recorded in DMSO. The observed spin Hamiltonian parameters values  $A_{\parallel}$  ( $151 \times 10^4\text{-cm}^{-1}$ )  $>$   $A_{\perp}$  ( $71 \times 10^4 \text{ cm}^{-1}$ );  $g_{\parallel}$  (2.31)  $>$   $g_{\perp}$  (2.075)  $>$  2 ensures that the system coincides well with axially elongated octahedral geometry. The spin Hamiltonian parameters of  $[\text{MnL}_2]\text{Cl}_2$  complex in DMSO solution at 77 K ( $A_{\text{iso}} = 110 \times 10^4\text{cm}^{-1}$  and  $g_{\text{iso}} = 1.99 < 2$ ). It shows a six-line hyperfine splitting due to Mn(II) ( $I = 5/2$ ) ion. This fact is also supported by the magnetic susceptibility data of the complexes. DNA interaction studies of  $[\text{CuL}_2]\text{Cl}_2$  complex have been done by electronic spectral and cyclic voltametric measurements which reveal that the binding occurs through intercalation between complex and DNA interaction of  $[\text{CuL}_2]\text{Cl}_2$  complex with CT-DNA leads to hypochromism. Cyclic voltammogram pattern of  $[\text{CuL}_2]\text{Cl}_2$  complex was totally altered due to strong binding of CT-DNA. The *in-vitro* biological screening effects of the investigated compounds were tested against various bacteria and fungi. The MIC values against the growth of microorganisms are lower for metal chelates than the ligand. The minimum inhibitory concentration values indicate that most of the complexes have higher toxicity than the ligand against the microorganisms.

# Poster

# Presentation

**PP 1**      **Microwave Assisted Pyrazole Derivative Synthesis****N. Radha\*\* and V. Suganya***\*Asst. Professor of Chemistry, Alagappa Govt. Arts College, Karaikudi – 3,  
Chemradha74@gmail.com*

This eco-friendly solvent-free approach using microwave irradiation opens numerous possibilities for conducting rapid heterocyclic synthesis using a variety of supported reagents on mineral oxides and phase transfer catalysis conditions.

The use of multimode oven, monomode reactor and conventional glass apparatus, demonstrates the numerous practical applications in laboratory scale experiments. Furthermore, there are different advantages of these solvent-free protocols as “*Green Chemistry*” since they provide absence of solvent thereby preventing pollution in organic synthesis.

The absence of solvent clearly reduces the reaction time and generally improves the yields. In fact it is noticeable that in several cases thermal effects play a determinant part in the rates and in the chemio and regio- or stereo selective heterocyclic synthesis.

Additionally, there are many heterocyclic reactions with great potential for automated medicinal and combinatorial chemistry which traditionally have been performed with long reaction times that might be dramatically accelerated by solvent-free microwave irradiation.

Today, new therapeutic hetero-macromolecular targets are increasingly being identified as drug targets. The lead generation and lead optimization processes must be accelerated.

Traditional methods of organic heterocyclic synthesis are simply too slow to satisfy the future demand for compounds.

Microwave assisted solvent-free chemistry is a technique that has the power to accelerate the generation of organic molecules.

**Keywords:** Microwave irradiation, solvent-free microwave irradiation, hetero-macromolecular, Optimization processes, *Green Chemistry* synthesis

**PP 2**      **Corrosion Inhibition by Leaves Extract of Vitex Doniana for Mild Steel in HCl Solution****K. Akila and S. Kasturibai\****\*PG & Research department of chemistry, Alagappa government arts college,  
Karaikudi -630 003, Tamilnadu, India.  
E mail: kasturibai2007@gmail.com***Abstract**

Corrosion inhibition efficiency of Vitex Doniana leaves extract in 1M HCl medium was investigated by weight loss and temperature studies. Effect of temperature (303-333 K) on the corrosion behavior of mild steel in the presence of plant extract was studied. Inhibition was found

to increase with increase in concentration of the extract. The FTIR results shows that the extracts contains the peaks of O-H, C-N and unsaturated C=C functional groups, which were identified as contributing to the inhibition exhibited by the extracts. Langmuir isotherm best fits the data suggesting physical adsorption as the adsorption mechanism between the extract and mild steel substrate.

**Keywords:** Vitex Doniana, plant extract, corrosion inhibitor, mild steel, HCl medium.

## Introduction

Mild steel is known to be a very versatile ferrous alloy utilized for a wide range of applications because of its excellent combination of mechanical properties, ease of fabrication, excellent weldability and low purchasing cost [1]. However it has low corrosion resistant in acidic environment [2]. The use of inhibitors has been widely explored to militate against corrosion of mild steel utilized in acidic environment. In the present study, the corrosion inhibition, adsorption characteristics and spectral analysis of Vitex Doniana leaves extract in 1M HCl solution was investigated. However its use as corrosion inhibitor has not been reported in the literature.

## Experimental Details

Mild steel specimens of area  $4 \times 2 \text{ cm}^2$  have been used. During the study the samples were pretreated, dried, weighed and stored in desiccators for further use. The leaves were collected, shade dried and powdered. Plant materials are dried in shade so as to enrich the active principles in them, by reducing their moisture content. The extract was prepared by refluxing 25 g of powdered dry leaves in 200 ml of water for 2 hour and kept overnight. Then it was filtered and dried to solid mass. Weighed samples are immersed in 100 ml of the acid (1 M HCl) without and with different concentrations (50 ppm -250 ppm) of the inhibitor for various intervals of time. They are then taken out and then washed thoroughly with tap water, rinsed with distilled water, dried, stored in desiccators and reweighed.

## Results and Discussion

The extract of Vitex Donianais a good inhibitor for the corrosion of mild steel in 1M HCl. The inhibition efficiency increases with the increase in inhibitor concentration and thus increases the protective action of the inhibitor on mild steel. The compound seems to function as inhibitor by being adsorbed on the metal surface. The inhibitor showed maximum inhibition efficiency of 91.43% at 200 ppm concentration for an immersion period of 12 hours at 303K. Inhibition efficiency increases from 3 hours to 12 hours and at 24 hours it decreases. Increase in inhibitor efficiency from 1- 12 hours shows the strong adsorption of constituents present in the plant extract on the surface of mild steel giving it a protective layer. Immersion for a longer period leads to desorption of plant constituents. Adsorption of extract molecules on mild steel surface obeyed the Langmuir, Temkin, adsorption isotherms.

The percentage of Inhibitor efficiency increases with increase in temperature, which confirms that Plant *Vitex doniana* acts as an effective inhibitor at high temperature also. The result showed that as the temperature increases the inhibition efficiency reaches maximum of 93.1% at 323 K for 200ppm and then decreases. At elevated temperature as timelag between adsorption and desorption of inhibitor over metal surface becomes shorter, so the % of inhibitor efficiency decreases.

UV-Visible spectra (Fig1) of  $\text{Fe}^{2+}$  ion in the presence of *Vitex Doniana* inhibitor in the HCl medium gives additional peaks at 255nm, 295nm and 439 nm. Among these 255nm peak is very pronounced and may be due to metal ion–inhibitor complex formation in the medium and secondary inhibition by such a complex not be ruled out [3]. FTIR spectra (Fig2) of HCl extract of *Vitex Doniana* showed the presence of oxygen and nitrogen atoms in functional groups of O-H, N-H and unsaturated group C=C. The presence of oxygen and nitrogen atoms in the extract met the general characteristics of typical corrosion inhibitors. There is shift in the spectra of the extract when mild steel was immersed in it to corrosion product, which shows that there is interaction between the extract and mild steel specimen which resulted in inhibition [4,5].

## Conclusion

The present study shows that acid extract of *Vitex Doniana* is a good inhibitor for the corrosion of mild steel in 1MHCl. The inhibition efficiency increases with the increase in inhibitor concentration and thus increases the protective action of the inhibitor on mild steel. The compound seems to function as inhibitor by being adsorbed on the metal surface. The inhibitor showed maximum inhibition efficiency of 91.43% at 200 ppm inhibitor concentration for an immersion period of 12 hours at 303K. SEM studies revealed that the smooth surfaces appeared by formation of a protective film on the metal surface. The inhibitor was found to obey Langmuir and Temkin adsorption isotherm from the fit of experimental data.

## References

- V.G. Vasudha and K. Shanmuga Priya, *Research Journal of Chemical Sciences* Vol. 3(1), 2013, 21-26,
- J. Rosaline Vimala, A. Leema Rose, and S. Raja *International Journal of Chem Tech Research*, Vol.3, (4), 2011, 1791-1801.
- S. Kasturibai, T. Vasudevan, *Bulletin of materials Chemistry*, 8, 1992, 107-110
- K.Kanayo Alaneme, S. Joseph, *Alexandria Engineering journal*, <http://dx.doi.org/10.1016/a.aej.2015.10.009>
- A.F Guldoin, A.N. Becerra, *Journal of Materials Environmental Science*, 4(1), 2013, 143-158.



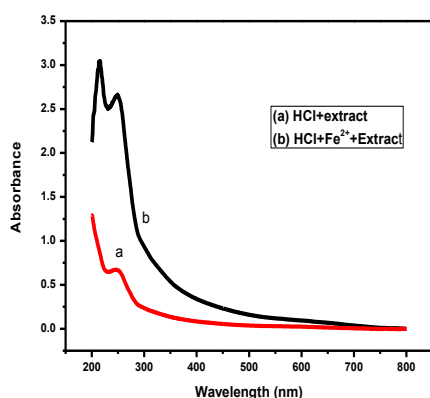


Fig:1 UV-Visible Spectrum

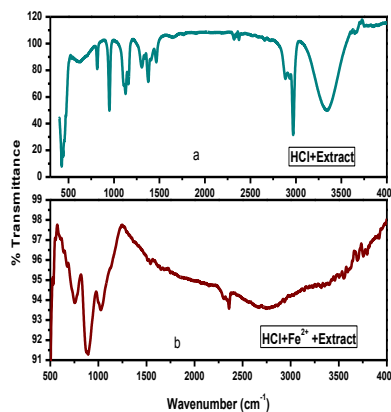


Fig:2 FTIR Spectrum

### PP 3 Enhanced Electrochemical performances of Al-doped $\text{LiNi}_{1/3}\text{Mn}_{1/3}\text{Co}_{1/3}\text{O}_2$ cathode materials for Lithium-ion batteries

V. Abinaya, K. Kalaiselvi, G. Paruthimal Kalaignan\*

*Advanced Materials Laboratory, Department of Industrial Chemistry, Alagappa University, Karaikudi-630 003, Tamil Nadu, India*

#### Abstract

$\text{LiNi}_{1/3-x}\text{Mn}_{1/3}\text{Co}_{1/3}\text{Al}_x\text{O}_2$  ( $0.00 \leq x \leq 0.05$ ) cathode materials were synthesized by sol-gel method using aqueous solutions of metal nitrates and tartaric acid as chelating agents. Their morphology, structure and electrochemical properties were characterized by SEM, XRD, charge-discharge tests, Cyclic Voltammetry (CV) and electrochemical impedance spectroscopy (EIS). The surface morphology and composition analysis were characterized by taking SEM with EDAX. XRD studies revealed a well defined layer structure and linear variation of lattice parameters with the addition of Aluminium confirmed phase pure compounds in a rhombohedral structure without impurities. SEM analysis shows that  $\text{LiNi}_{1/3-0.05}\text{Mn}_{1/3}\text{Co}_{1/3}\text{Al}_x\text{O}_2$  has smaller particle size and more regular morphological structure with narrow size distribution than those of  $\text{LiNi}_{1/3}\text{Mn}_{1/3}\text{Co}_{1/3}\text{O}_2$ . The electrochemical properties of  $\text{LiNi}_{1/3-x}\text{Mn}_{1/3}\text{Co}_{1/3}\text{Al}_x\text{O}_2$  ( $0.00 \leq x \leq 0.05$ ) samples were monitored using 2032 coin-type by galvanostatic charge/discharge and cycling test. Among them,  $\text{LiNi}_{1/3-0.05}\text{Mn}_{1/3}\text{Al}_{0.05}\text{O}_2$  behaved much better, losing about 7% of its initial capacity ( $208 \text{ mAhg}^{-1}$ ) after 50 cycles at  $192 \text{ mAhg}^{-1}$ . While the pristine  $\text{LiNi}_{1/3}\text{Mn}_{1/3}\text{Co}_{1/3}\text{O}_2$  loss about 13% of its initial capacity ( $148 \text{ mAhg}^{-1}$ ).  $\text{LiNi}_{1/3-0.05}\text{Mn}_{1/3}\text{Co}_{1/3}\text{Al}_{0.05}\text{O}_2$  has high charge/discharge capacity, low irreversible capacity and superior electrochemical performance.

**Keywords:**  $\text{LiNi}_{0.3-x}\text{Mn}_{0.3}\text{CoAl}_x\text{O}_2$ , XRD, SEM, Charge/discharge

## Introduction

Li-ion batteries are the most suitable power supplies for many portable electronic devices, such as cellular phones, digital cameras and notebooks, because of their high energy and power density [1-2]. In this Present work,  $\text{LiNi}_{1/3-x}\text{Mn}_{1/3}\text{Co}_{1/3}\text{AlO}_2$  by sol - gel chelation method for use as a Cathode material in Li ion battery. Element Al is adopted to substitute Nickel in the calcining process to prepare  $\text{LiNi}_{1/3-0.05}\text{Mn}_{1/3}\text{Co}_{1/3}\text{Al}_{0.05}\text{O}_2$ . Crystal structure, Lattice parameters, Morphology structure, Electrochemical performances and the charging / discharging process of Al-substituted cathode are thoroughly studied.

## Experimental Details

$\text{LiNi}_{1/3-x}\text{Mn}_{1/3}\text{Co}_{1/3}\text{Al}_x\text{O}_2$  were synthesized by sol-gel method. Stoichiometric amount of lithium nitrate, nickel (II) nitrate hexahydrate, Manganese (II) nitrate hydrate and aluminium (III) nitrate monohydrate were dissolved in distilled water. The resulting metal ions in the solution were stirred well. Then, one molar solution of tartaric acid was dissolved by using deionized water, added drop by drop with continuous stirring, pH of the resulting solution was maintained between 8-9. The temperature of the solution increased to 80 °C, when coloured ionic solution was obtained. After 10 hours of continuous stirring at 80 °C, coloured, highly viscous gel was obtained. The gel was dried in air oven at 120 °C for 12 hours. It was slightly ground and calcined at 800 °C for 12 hours in air to obtain phase pure nano powder is obtained.

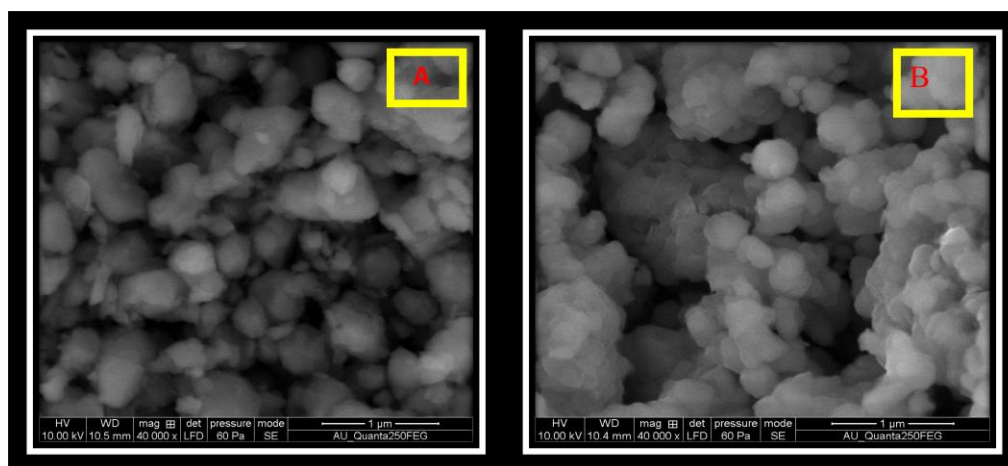


**Figure: SEM images of bare and  $\text{LiNi}_{1/3-0.05}\text{Mn}_{1/3}\text{Co}_{1/3}\text{Al}_{0.05}\text{O}_2$  powders sintered at 800 °C in oxygen**

## Results and discussion

The XRD patterns of bare and Al doped  $\text{LiNi}_{1/3}\text{Co}_{1/3}\text{Mn}_{1/3}\text{O}_2$  cathode material powders. All the diffraction peaks are identical with respect to the pristine sample and can be indexed to a hexagonal  $\alpha\text{-NaFeO}_2$  structure with an R-3m space group. Observed narrow 006/102 and 108/110 couplet splitting peaks are evidence of the formation of a well-defined crystalline structure. The morphological investigations showed rhombohedral particles with in the range 100-200nm. The

electrochemical studies show that initial and final discharge capacities of 208 mAhg<sup>-1</sup> and 192mAhg<sup>-1</sup> at 0.01 with voltage range 2.0–4.2V.

## Conclusion

LiNi<sub>1/3-x</sub>Mn<sub>1/3</sub>Co<sub>1/3</sub>AlO<sub>2</sub> synthesized by sol-gel method using tartaric acid as a chelating agent. The XRD pattern indicates the crystalline nature of the cathode materials followed by SEM with EDAX confirmed the surface morphology and particle size. Electrochemical properties are characterized by charge/discharge tests, Cyclic Voltammetry (CV) and electrochemical impedance spectroscopy. Finally, Al-doped LiNi<sub>1/3</sub>Mn<sub>1/3</sub>Co<sub>1/3</sub>O<sub>2</sub> is a promising cathode material for Lithium-ion batteries.

## References

- S.S. Zhang, The effect of the charging protocol on the cycle life of a Li-ion battery. *J. Power Sour.* 2006, 161, 1385–1391.
- S.S. Zhang; K. Xu; T.R. Jow Charge and discharge characteristics of a commercial LiCoO<sub>2</sub> based 18650 Li-ion battery. *J. Power Sour.* 2006, 160, 1403–1409

## PP 4 Improved high Rate Electrochemical performances of Zr-doped LiNi<sub>1/3</sub>Mn<sub>1/3</sub>Co<sub>1/3</sub>O<sub>2</sub> cathode materials for Rechargeable Lithium-ion batteries

**P. Gokila, K. Kalaiselvi, G. Paruthimal Kalaignan\***

*Advanced Materials Laboratory, Department of Industrial Chemistry, Alagappa University, Karaikudi-630 003, Tamil Nadu, India*

*\*Corresponding author mail id : [pkalaigan@yahoo.com](mailto:pkalaigan@yahoo.com)*

## Abstract

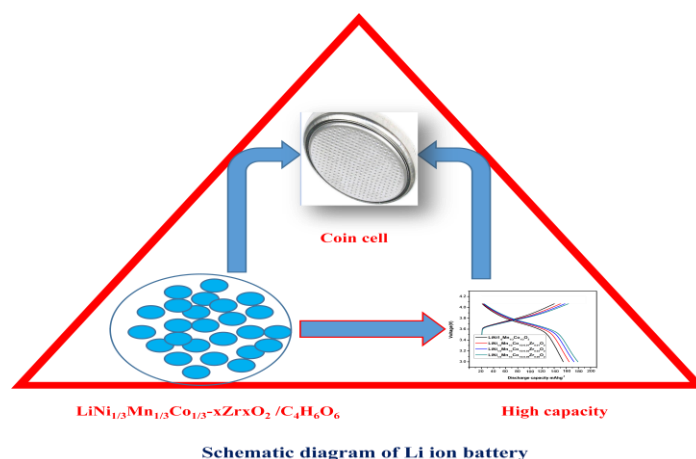
Layered mixed oxides LiNi<sub>1/3</sub>Mn<sub>1/3</sub>Co<sub>1/3-x</sub>ZrxO<sub>2</sub> (x=0, 0.01, 0.03, 0.05) synthesized by a sol-gel method using citric acid as a chelating agent. The analysis of electrochemical properties is investigated by XRD, SEM and TEM. The Electrochemical behavior of so synthesized cathode materials is evaluated by galvanostatic charge/discharge studies using coin type of cathode material cells. The obtained cathode materials discharge specific capacity of 180mAhg<sup>-1</sup> at the Rate of 0.1C. The cycling studies are carried out in the voltage range of 2.4 V to 4.2V. However, the doped sample has better cyclic stability than the Pristine sample. After 100 cycles, the capacity remains 100 and 88mAhg<sup>-1</sup> for the doped and the Pristine samples, respectively. The electrochemical tests show that it has the highest the results from EIS show that the doped sample has a process for Li-ion intercalation/de-intercalation than the undoped cathode material. Herein, we report on the synthesis of a series LiNi<sub>1/3</sub>Mn<sub>1/3</sub>Co<sub>1/3-x</sub>ZrxO<sub>2</sub> cathode materials and their promising application exhibited enhanced cyclic stability compared with the pristine LiNi<sub>1/3</sub>Mn<sub>1/3</sub>Co<sub>1/3</sub>O<sub>2</sub>.

## Introduction

Lithium-ion secondary batteries are the development of the promising high energy storage technology for electric vehicles (EVs) and hybrid electric vehicles (HEVs) in the next decades. To meet the necessities of EVs and HEVs, Li-ion batteries want to possess the following characteristics: low cost, high rate capability, large energy intensity, long cycle life, and nontoxic. The limited specific capacity of the developing cathode materials for advanced rechargeable to increasing the high energy densities of recent Lithium-ion batteries [1-2]. In this study, we synthesized the Zr-doped  $\text{LiNi}_{0.3}\text{Mn}_{0.3}\text{Co}_{0.3}\text{O}_2$  materials are directly synthesized followed by the effects of Zr doping, structure, morphology of modified materials and electrochemical performance of pristine and Zr doped  $\text{LiNi}_{1/3}\text{Mn}_{1/3}\text{Co}_{1/3-x}\text{Zr}_x\text{O}_2$  ( $x=0.01, 0.03, 0.05,$ ) samples have been characterized by the analytical instrumentations such as XRD, SEM, TEM and electroanalytical techniques vice versa.

## Experimental section

The Zr doped cathode material was prepared by the following sol-gel technique. First, an aqueous solution of reaction mixture was prepared by dissolving stoichiometric amounts of anhydrous Lithium nitrate, Nickel (II) nitrate, Cobalt (II) nitrate hexahydrate, Manganese (II) nitrate and Zirconium nitrate hexahydrate were dissolved in deionized water and addition of tartaric acid solution with continuous stirring. Ammonium hydroxide was then used to adjust the pH 8. The solution was then heated and stirred at  $80\text{ }^\circ\text{C}$  until the gels were formed after 8 hrs. The gel was dried in hot air oven at  $120\text{ }^\circ\text{C}$  to obtain the form of powder. These powders were calcined in air at  $800\text{ }^\circ\text{C}$  for 10h. The calcined powders were thoroughly ground in an agate mortar. Then, Collected and stored in the separate vessel.



## Results and discussion

The crystal nature of the so prepared by powder samples was analyzed by XRD, as the diffraction patterns are well indexed to a layered hexagonal  $\alpha\text{-NaFeO}_2$  structure with  $R\text{-}3m$  group. Furthermore, distinct splitting of (006)/(102) and (108)/(110) peaks were observed without any

impurities reflections, indicating the formation of the homogenous layered structure of zirconium doping. The morphology of the synthesized powders was observed using SEM. The SEM images of bare  $\text{LiNi}_{1/3}\text{Mn}_{1/3}\text{Co}_{1/3}\text{O}_2$  and  $\text{LiNi}_{1/3}\text{Co}_{1/3}\text{Mn}_{1/3}\text{Zr}_{0.01}\text{O}_2$  samples there exist small agglomerates for both the powders. All primary particles show spherical shape and a narrow particle size distribution ranging from 50 nm to 100 nm. The CV curves of the pristine electrodes and  $\text{LiNi}_{1/3}\text{Mn}_{1/3}\text{Co}_{1/3}\text{Zr}\text{O}_2$  between 2.5 V and 4.2 V for the first five cycles at a scanning rate of  $0.1 \text{ ms}^{-1}$  at room temperature. The Redox behavior has been successfully characterized by the voltammetric technique.

## Conclusion

$\text{LiNi}_{1/3}\text{Mn}_{1/3}\text{Co}_{1/3-x}\text{O}_2$  ( $x=0, 0.01, 0.03$  and  $0.05$ ) cathode materials were successfully prepared by sol-gel method. The effect of Zr substitution on the structure, morphology and electrochemical properties of  $\text{LiNi}_{1/3}\text{Co}_{1/3}\text{Mn}_{1/3}\text{O}_2$  was investigated in detail. The results indicate that Zr substitution has an effective effect on the improvement of cycling performance of  $\text{LiNi}_{1/3}\text{Co}_{1/3}\text{Mn}_{1/3}\text{O}_2$ . Moreover, the Zr-doped sample has the best cycling performance at 0.1 C under the potential of 2.4–4.2 V among all the doped samples. EIS results indicate that Zr substitution has an obvious effect on restraining the increase of charge transfer impedance of  $\text{LiNi}_{1/3}\text{Co}_{1/3}\text{Mn}_{1/3}\text{O}_2$  during cycling. XRD analysis indicates that Zr-doped sample has a slighter structure change so that it has the best cycling performance.

## References

- J.M. Tarascon; M. Armand, Issues and Challenges Facing Rechargeable Lithium Batteries. *Nature* 414 (2001) 359–367.
- A. Manthiram; A. Vadivel Murugan; A. Sarkar; T. Muraliganth Nanostructured Electrode Materials for Electrochemical Energy Storage and Conversion. *Energy Environ. Sci.* 1 (2008) 621–638.

## PP 5 Dodonaea Viscosa as a Corrosion Inhibitor for Mild Steel in HCl Solution

S. Nirosha and S. Kasturibai\*

\*PG & Research department of chemistry, Alagappa government arts college,  
Karaikudi -630 003, Tamilnadu, India.  
E mail: [kasturibai2007@gmail.com](mailto:kasturibai2007@gmail.com)

## Abstract

Corrosion inhibition of mild steel 1M HCl by leaves extract of *Dodonaea viscosa* was investigated by Weight loss and spectroscopic studies (UV-Visible and FTIR) techniques at 303-333K. It was found that the leaves extract of *Dodonaea viscosa* inhibited the acid induced corrosion of mild steel. The inhibition efficiency increases with increasing inhibitor concentration of the extract. The FTIR results show that the extracts contain the peaks of O-H, C-N and

unsaturated C=C functional groups, which were identified as contributing to the inhibition exhibited by the extracts. Langmuir isotherm best fits the data suggesting physical adsorption as the adsorption mechanism between the extract and mild steel substrate.

**Keywords:** Dodonaeaviscosa, plant extract, corrosion inhibitor, mild steel, HCl medium.

## Introduction

Mild steel is known to be a very versatile ferrous alloy utilized for a wide range of applications because of its excellent combination of mechanical properties, ease of fabrication, excellent weldability and low purchasing cost.. However it has low corrosion resistant in acidic environment [2]. The use of inhibitors has been widely explored to militate against corrosion of mild steel utilized in acidic environment. In the present study, the corrosion inhibition, adsorption characteristics and spectral analysis of Dodonaea viscosa leaves extract in 1M HCl solution as investigated. However its use as corrosion inhibitor has not been reported in the literature.

## Experimental Details

Mild steel specimens of area  $4 \times 2 \text{ cm}^2$  have been used. During the study the samples were pretreated, dried, weighed and stored in desiccators for further use. The leaves were collected, shade dried and powdered. Plant materials are dried in shade so as to enrich the active principles in them, by reducing their moisture content. The extract was prepared by refluxing 25 g of powdered dry leaves in 200 ml of water for 2 hour and kept overnight. Then it was filtered and dried to solid mass. Weighed samples are immersed in 100 ml of the acid (1 M HCl) without and with different concentrations (50 ppm -250 ppm) of the inhibitor for various intervals of time. They are then taken out and then washed thoroughly with tap water, rinsed with distilled water, dried, stored in desiccators and reweighed.

## Results and Discussion

The extract of Dodonaea viscosa is a good inhibitor for the corrosion of mild steel in 1M HCl. The inhibition efficiency increases with the increase in inhibitor concentration and thus increases the protective action of the inhibitor on mild steel. The compound seems to function as inhibitor by being adsorbed on the metal surface. The inhibitor showed maximum inhibition efficiency of 91.64 % at 200 ppm concentration for an immersion period of 12 hours at 303K. Inhibition efficiency increases from 3 hour to 12 hours and at 24 hours it decreases. Increase in Inhibition efficiency from 1- 12 hours shows the strong adsorption of constituents present in the plant extract on the surface of mild steel giving it a protective layer. Immersion for a longer period leads to desorption of plant constituents. Adsorption of extract molecules on mild steel surface obeyed the Langmuir, Temkin adsorption isotherms.

The % inhibitor efficiency increases with increase in temperature, which confirms that Dodonaea viscosa extract acts as an effective inhibitor at high temperature also. The results shows that as the temperature increases the inhibition efficiency increases reaches maximum of 92.41%

at 328 K for 200 ppm and then decreases. At elevated temperature as time lag between adsorption and desorption of inhibitor over metal surface becomes shorter the inhibitor efficiency decreases.

UV-Visible spectra (Fig1) of  $\text{Fe}^{2+}$  ion in the presence of Dodonaeaviscosainhibitor in the HCl medium gives additional peaks at 245 nm, 295 nm and 439 nm. Among these 245 nm peak is very pronounced and may be due to metal ion –inhibitor complex formation in the medium and secondary inhibition by such a complex not be ruled out [3]. FTIR spectra (Fig2) of HCl extract of Dodonaea viscose showed the presence of oxygen and nitrogen atoms in functional groups of O-H, N-H and unsaturated group C=C. The presence of oxygen and nitrogen atoms in the extract met the general characteristics of typical corrosion inhibitors [4,5]. There is shift in the spectra of the extract when mild steel was immersed in it to corrosion product. Which shows that there is interaction between the extract and mild steel specimen which resulted in inhibition.

### Conclusions

The present study shows that acid extract of Dodonaea viscose is a good inhibitor for the corrosion of mild steel in 1M HCl. The inhibition efficiency increases with the increase in inhibitor concentration and thus increases the protective action of the inhibitor on mild steel. The compound seems to function as inhibitor by being adsorbed on the metal surface. The inhibitor showed maximum inhibition efficiency of 91.64% at 200 ppm inhibitor concentration for an immersion period of 12 hours at 303K. SEM studies revealed that the smooth surfaces appeared by formation of a protective film on the metal surface. The inhibitor was found to obey Langmuir and Temkin adsorption isotherm from the fit of experimental data.

### References

- V.G. Vasudha and K. Shanmuga Priya, Research Journal of Chemical Sciences 3(1), 2013, 21-26,  
J. Rosaline Vimala, A. Leema Rose, and S. Raja, International Journal of Chem Tech Research, 3  
(4), 2011, 1791-1801.  
S.Kasturibai, T. Vasudevan, Bulletin of materials Chemistry. 8, 1992, 107-110  
K. KanayoAlaneme, S. Joseph, Alexandria Engineering journal, <http://dx.doi.org/10.1016/a.aej.2015.10.009>  
A.F. Guldoin, A.N. Becerra, Journal of Materials Environmental Science, 4(1), 2013, 143-158.

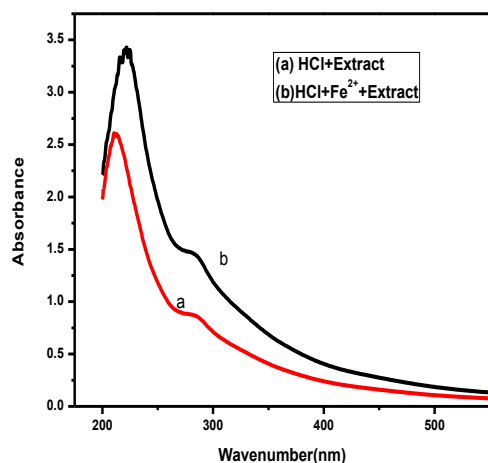


Figure: 1 UV-Visible Spectrum

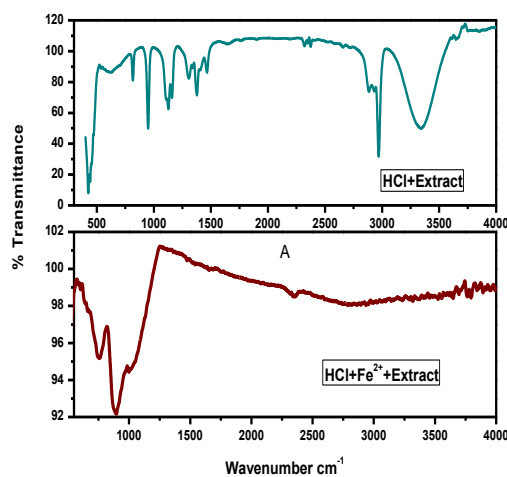


Figure: 2 FTIR Spectrum

## PP 6 Synthesis and electrochemical characterization of $\text{CuCo}_{2-x}\text{Ni}_x\text{S}_4$ for supercapacitors

S. Gausalya, P. Naveenkumar and G. Paruthimal Kalaigan\*

Materials Research Laboratory, Department of Industrial Chemistry, Alagappa University,  
Karaikudi-630 003, Tamilnadu, India.

\*Corresponding Author Phone No: +91-9443135307, Fax: +914565 225202.

Email id: pkalaigan@yahoo.com

### Abstract

The limited availability of the fossil fuels and the continuous usage of fossil fuels leads to the severe environmental issues like global warming, ocean layer depletion etc. The above issues, to motivate the researcher to focus the environmental benign energy storage and conversion devices for the future. Supercapacitor has been considered as reliable energy storage devices, owing to the higher power density and long-life span. While compare the specific capacitance behavior of the carbon-based materials (EDLCs) with metal oxide, metal hydroxide and metal sulfide (Pseudocapacitors). Pseudocapacitors have offer higher specific capacitance due to the efficient reversible redox reaction. Nowadays, metal sulfides such as  $\text{NiS}_2$ ,  $\text{CoS}$ ,  $\text{NiCo}_2\text{S}_4$  and  $\text{FeNi}_2\text{S}_4$ , have been received wide attention due to the higher conductivity and better electrochemical performance, when compared to the corresponding metal oxides. Among various Bimetal sulfides,  $\text{CuCo}_2\text{S}_4$  shows higher electrical conductivity and possesses richer electroactive sites in comparison with single-component sulfides or their oxide counterparts.

In this present work, we have studied effect of nickel doping at cobalt site of the  $\text{CuCo}_2\text{S}_4$ . The mixing of the transition metal is an effective way improve capacitance behavior of the materials. The synthesized electrode materials were characterized by XRD, FTIR, and UV-DRS. The morphology and elemental composition of the materials was analyzed by SEM with EDAX. The electrochemical performances were evaluated in 3M KOH electrolyte with a three-electrode



system on electrochemical workstation where active material coated Ni-foam as working electrode Pt foil as and Ag/AgCl as reference electrode, respectively. Cyclic voltammetry (CV) and Galvanostatic charge–discharge (GCD) tests were carried out with in a voltage range  $-0.1$  to  $0.6$  V. Electrochemical impedance spectroscopy (EIS) tests were conducted with a sine wave with  $5$  mV amplitude in a frequency range  $100$  kHz to  $0.1$  Hz. The CV results suggest that nickel doping have improved the specific capacitance and reversibility of the electrode materials. The EIS results clearly indicated that  $\text{CuCo}_{1.0}\text{Ni}_{1.0}\text{S}_4$  materials have higher ionic conductance than  $\text{CuCo}_{1.5}\text{Ni}_{0.5}\text{S}_4$  and  $\text{CuCo}_2\text{S}_4$ .

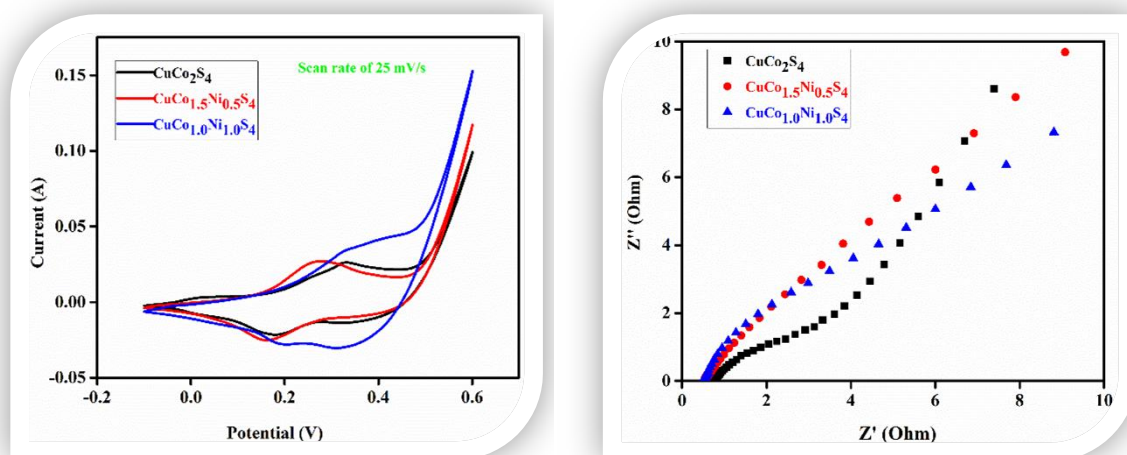


**Figure 1:** Comparison CV curve of **Figure 2:** EIS spectrum of  $\text{CuCo}_2\text{S}_4$ ,  $\text{CuCo}_{1.5}\text{Ni}_{0.5}\text{S}_4$ , and  $\text{CuCo}_{1.0}\text{Ni}_{1.0}\text{S}_4$  at  $25$  mV/s.

**Keywords:** Metal Doping,  $\text{CuCo}_2\text{S}_4$ , Hydrothermal Method.

## References

- H. You, L. Zhang, Y. Jiang, T. Shao, M. Li, J. Gong, *J. Mater. Chem. A*. 0 (2018) 1–6.  
 S.K. Shinde, D.P. Dubal, G.S. Ghodake, D.Y. Kim, V.J. Fulari, 6 (2016) 5–13.  
 S.K. Shinde, D.P. Dubal, G.S. Ghodake, D.Y. Kim, V.J. Fulari, *J. Electroanal. Chem.* 732 (2014) 80–85.  
 Y. Xu, T. Zhou, X. Cao, W. Zhao, J. Chang, W. Zhu, W. Guo, W. Du, *Mater. Res. Bull.* 91 (2017) 68–76.

## **PP 7** Structure and Electrochemical performances of Ru-doped $\text{LiNi}_{1/3}\text{Mn}_{1/3}\text{Co}_{1/3}\text{O}_2$ cathode materials for Rechargeable Lithium-ion batteries

**K. Kalaiselvi, G.ParuthimalKalaigan\***

*Advanced Materials Laboratory, Department of Industrial Chemistry, Alagappa University, Karaikudi-630 003, Tamil Nadu, India*

*\*Corresponding author mail id : pkalaigan@yahoo.com*

### **Abstract**

$\text{LiNi}_{1/3}\text{Mn}_{1/3}\text{Co}_{1/3}\text{RuO}_2$  Cathode materials were synthesized by sol-gel method using aqueous solutions of metal nitrates and citric acid as chelating agent. Thermal analysis, XRD, SEM with EDAX and TEM experiments are used to characterize their physical and structural properties. The electrochemical characterizations were investigated by Galvanostatic charge/discharge, Cyclic Voltammetry, and AC Impedance techniques. XRD studies revealed a well-defined layer structure and a linear variation of lattice parameters with the addition of Ruthenium, confirming the formation of phase pure compound. SEM analysis showed that the synthesized cathode material had a smaller particle size and more regular morphological structure with narrow size distribution. Electrochemical Impedance spectroscopy of  $\text{LiNi}_{1/3}\text{Mn}_{1/3}\text{Co}_{1/3}\text{RuO}_2$  electrode has exhibited improved charge transfer resistance values upon cycling. The as prepared cathode has shown superior electrochemical properties, such as high charge/discharge capacity, good electrochemical conductivity and improved cycling.

**Keywords:** Positive electrode materials, Cyclic Voltammetry, Charge – Discharge, SEM, TEM

### **Introduction**

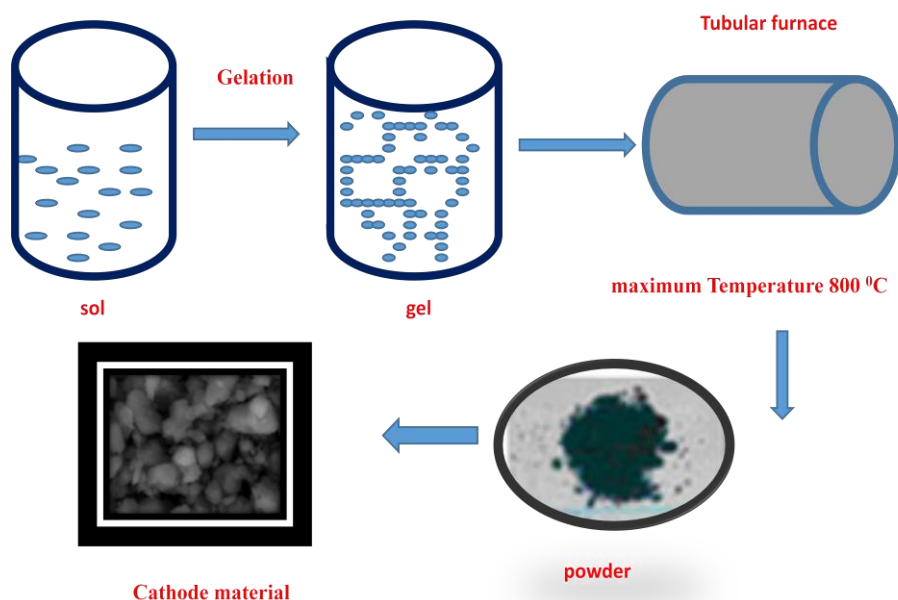
The development of cathode materials for lithium-ion batteries providing a high energy density at fast charge/discharge rates become imperative due to high power requirements for hybrid electric vehicles and power tools [1-3]. We have therefore designed and synthesized the novel  $\text{LiNi}_{1/3}\text{Mn}_{1/3}\text{Co}_{1/3-x}\text{RuO}_2$  by simple sol-gel method. The synthesized pristine and  $\text{LiNi}_{1/3}\text{Mn}_{1/3}\text{Co}_{1/3-x}\text{RuO}_2$  demonstrate excellent rate capability and cyclic performance at high current density.

### **Experimental**

Lithium nitrate  $\text{LiNO}_3$ , Nickel (II) nitrate  $\text{Ni}(\text{NO}_3)_2$ , Cobalt (II) nitrate hexahydrate  $\text{Co}(\text{NO}_3)_2 \cdot 6\text{H}_2\text{O}$ , Manganese (II) nitrate  $\text{Mn}(\text{NO}_3)_2 \cdot 4\text{H}_2\text{O}$  and Ruthenium nitrate  $\text{Ru}(\text{NO}_3)_2$  were dissolved in deionized water and addition of citric acid solution with continuous stirring. Ammonium hydroxide was then used to adjust the pH 8. The solution was then heated and stirred at  $80^\circ\text{C}$  until the gels were formed after 8 hrs. The gel was dried in hot air oven at  $120^\circ\text{C}$  to obtain the form of powder. The mixture was calcined in air at  $400^\circ\text{C}$  for 5 h followed by grinding,

and then calcined again at 800 °C for 10 h to get the final products of pristine and  $\text{LiNi}_{1/3}\text{Mn}_{1/3}\text{Co}_{1/3-x}\text{Ru}_x\text{O}_2$ .

### Synthesis of Ru– doped cathode material



### Conclusions

In summary, to improve the rate capability and cyclic performance of the electrode material pristine, we have developed high-performance  $\text{LiNi}_{1/3}\text{Mn}_{1/3}\text{Co}_{1/3-x}\text{Ru}_x\text{O}_2$  by simple sol-gel technique. The XRD analysis exhibit a well defined crystalline nature of the material whereas SEM with EDAX clearly indicate the surface morphology with appropriate composition of the cathode material. Further, the electrochemical features and redox behavior are characterized by various electro analytical techniques such as impedance spectroscopy and cyclic voltammetry. Thus, the Ru doped  $\text{LiNi}_{1/3}\text{Mn}_{1/3}\text{Co}_{1/3}\text{O}_2$  cathode material has been used as promising material for Li-ion batteries.

### References

- K. Kang, Y.S. Meng, J. Breger, C.P. Grey, G. Ceder, *Science* 311 (2006) 977.
- J. Molenda, J. Marzec, *Funct. Mater. Lett.* 1 (2008) 91–96.
- J. Liu, Z. Sun, J. Xie, H. Chen, N. Wu, B. Wu, *J. Power Sources* 240 (2013) 95.

## PP 8 Corrosion Behaviour of Mild Steel using an Aqueous Leaf Extract of Cynodon Dactylon

K. Anuradha<sup>1</sup>, C. Sathya<sup>2</sup>, S. Keerthanapriya<sup>2</sup> and K. Velmanirajan<sup>3</sup>

<sup>1</sup>Department of Chemistry, Alagappa government Arts college, Karaikudi, Tamil Nadu - 630 003.

<sup>2</sup> Research scholar, Department of Chemistry, Alagappa government Arts college, Karaikudi, Tamil Nadu - 630 003, India

<sup>3</sup> Department of Mechanical engineering, VSVN Polytechnic College, Virudhunagar, Tamilnadu.  
mail id: [anuvmrajan@yahoo.co.in](mailto:anuvmrajan@yahoo.co.in)

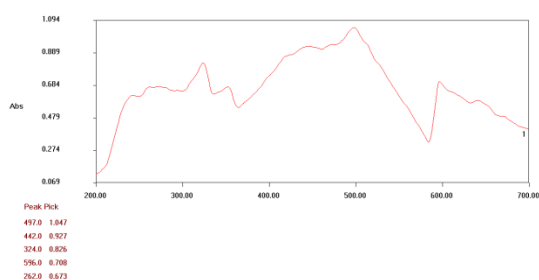
### Abstract

The study of corrosion inhibition is significant in the field of research due to its usefulness in various industries. An increasing concern in human health and risks has drawn attention in the development of mild steel corrosion. Mild steel in acid medium is widely used in various industrial processes. Sea water finds extensive application as coolant in various exothermic reactions. Sea water constitutes a rich source of various commercially important chemical elements. Depending upon the metal /environment combinations different types of inhibitors are used in suitable concentrations. Zinc ions have long been considered as valuable corrosion inhibitors for protection afforded by a cathodic polarization mechanism. One of the effective methods to prevent corrosion is the addition of natural inhibitors. Most of the natural products are non-toxic, biodegradable and really available in plenty. In the present investigation, leaves of cynodon dactylon extract (CDE) have been used as corrosion inhibitor for mild steel in sea water medium. The inhibition efficiency was found to increase with increase in concentration of the leaf extract. The formulation consisting of 8 ml of CDE and 10 ppm of  $Zn^{2+}$  has 85 % inhibition efficiency (IE). A study on the effect of immersion period on the CDE-  $Zn^{2+}$  showed an IE that decreased from five days. UV-Visible spectra revealed the formation of a protective film on the metal surface. The same is confirmed through FT-IR spectrum. From the surface examination studies, it could be confirmed that the corrosion inhibition was due to the formation of a protective film consists of  $Fe^{2+}$ - CDE complex.

**Keywords:** Corrosion inhibition, Surface examination, Eco-friendly, Sea water.

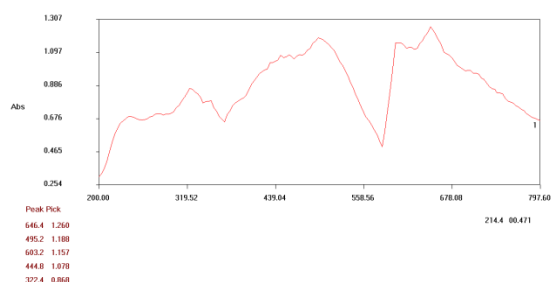
CDE

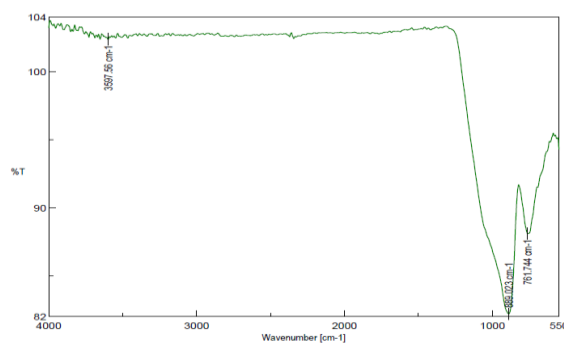
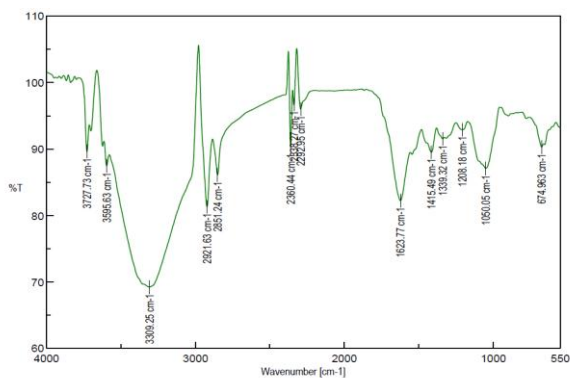
FTIR - CDE



CDE + FeSO<sub>4</sub>

FTIR, CDE+ FeSO<sub>4</sub>





## Conclusions:

The weight loss study reveals that the formulation consisting of 8 ml of cynodon dactylon extract (CDE) and 10 ppm of  $Zn^{2+}$  has 85 % inhibition efficiency in controlling the corrosion of mild steel immersed in an aqueous solution containing sea water. A study of the effect of immersion period on the cynodon dactylon extract (CDE)- $Zn^{2+}$  system shows an inhibition efficiency that decreases as the immersion period increases. UV-Visible spectra reveal that a protective film is formed on the metal surface. The FTIR spectrum also reveals the formation of protective film that consists of  $Fe^{2+}$  - CDE complex.

## PP 9 Synthesis and characterization of rGO/MnS for supercapacitors

**S. Manoj, P. Naveenkumar and G. Paruthimal Kalaigan\***

*Materials Research Laboratory, Department of Industrial Chemistry, Alagappa University, Karaikudi-630 003, Tamilnadu, India.*

*\*Corresponding Author Phone No: +91-9443135307, Fax: +914565 225202.*

*Email id: pkalaigan@yahoo.com*

### Abstract

We have prepared the MnS on reduced Graphene oxide wrapped Ni-foam by electrodeposition method. Recently, Transition metal sulfide like  $Co_2S_3$ , CuS,  $Ni_3S_2$ ,  $CoNi_2S_4$ ,  $MoS_2$ ,  $FeS_2$  have been emerged as a reliable and next generation of electrode material for supercapacitor applications. It has high electronic conductivity and better cyclic performances than metal oxides. In various metal sulfides, MnS is a p-type semiconductor with band gap of 3.1 to 3.7eV. It has the higher electronic conductivity than their corresponding metal oxides or metal hydroxides. Electrodeposition is a simple technique to deposit directly electrode materials on the surface of the Ni-Foam. The as deposited electrode materials were characterized by XRD, FTIR, Raman spectroscopy and UV-DRS. The morphology and elemental composition of the materials was analyzed by SEM with EDAX. The grain size of the materials was measured by TEM analysis.

The electrochemical measurements of the working electrodes were carried out in 3M KOH electrolyte with a three-electrode system on electrochemical workstation where Pt foil and Ag/AgCl electrodes were used as counter electrode and reference electrode respectively. Cyclic voltammetry (CV) and galvanostatic charge–discharge (GCD) tests were carried out within a voltage range  $-0.2$  to  $0.7\text{V}$ . Electrochemical impedance spectroscopy (EIS) tests were conducted with a sine wave with  $5\text{mV}$  amplitude in a frequency range  $100\text{ kHz}$  to  $0.1\text{ Hz}$ . The discharge-specific capacitances of tested electrodes were calculated by using the following equation

$$C = \frac{I\Delta t}{m\Delta V} \quad (1)$$

where  $C_{\text{sp}}$  is specific capacitance (F/g),  $m$  is mass of active materials in electrode (g),  $\Delta V$  is the potential window,  $I$  is discharge current (A) and  $\Delta t$  is the discharge time (s). Using galvanostatic charge–discharge (GCD) results, we have calculated the  $C_{\text{sp}}$  of the MnS and rGO/MnS is  $1848\text{ F/g}$  and  $2087\text{ F/g}$  at a current density of  $1\text{ A/g}$ .

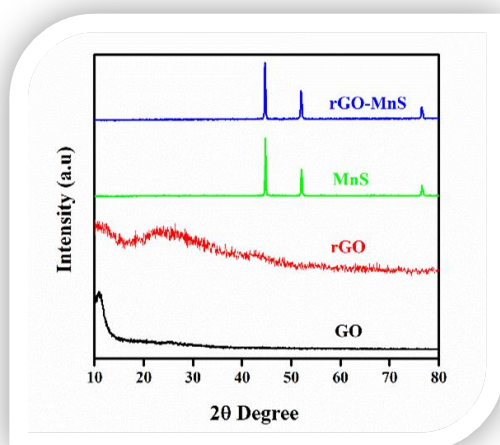


**Figure 1: XRD pattern of the synthesized GO, rGO, MnS and rGO-MnS.**

**Keywords:** Electrodeposition, rGO/MnS, Supercapacitor.

## References

- R. Ramachandran, M. Saranya, A.N. Grace, F. Wang, RSC Adv. 7 (2017) 2249–2257.  
Y. Tang, T. Chen, S. Yu, Y. Qiao, S. Mu, J. Hu, F. Gao, J. Mater. Chem. A. 3 (2015) 12913–12919.  
Shi, X. Li, G. He, L. Zhang, M. Li, J. Mater. Chem. A. 3 (2015) 20619–20626.

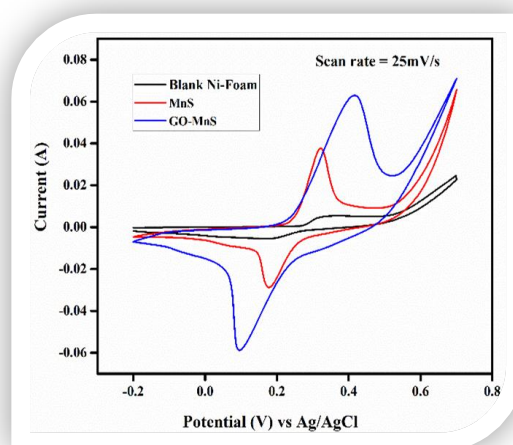


**Figure 2: Comparison CV of MnS and rGO-MnS at  $25\text{mV/s}$ .**

**PP-10**    **Synthesis and Electrochemical Characterization of  $\text{CuCo}_2\text{S}_4$  @  $\text{NiCo}(\text{OH})_2$  for Supercapacitors****B. Priyadharshini, P. Naveenkumar and G. Paruthimal Kalaignan\****Materials Research Laboratory, Department of Industrial Chemistry, Alagappa University, Karaikudi-630 003, Tamilnadu, India.**\*Corresponding Author Phone No: +91-9443135307, Fax: +914565 225202.**Email id: pkalaignan@yahoo.com***Abstract**

With the increasing demands on the clean energy to solve these serious pollution issues and to achieve a sustainable world, several energy-generating and energy-storing devices were developed intensively. Bimetallic transition metal sulfides have been greatly studied as the electroactive materials for the pseudocapacitors due to the multiple oxidation states for the Faradaic redox reactions and the high electronic conductivity because of the coupling of bimetallic transition metal species. NiCo Layered double hydroxide also have enhanced electrical conductivity and electrochemical properties due to the synergistic effects between Ni and Co elements and numerous electroactive sites arising from the multiple oxidation states.

In this present work, we have prepared the  $\text{CuCo}_2\text{S}_4$  by two step hydrothermal method.  $\text{NiCo}(\text{OH})_2$  was deposited by chronoamperometric technique using 1:1 mol ratio of  $\text{NiCl}_2 \cdot 6\text{H}_2\text{O}$  and  $\text{Co}(\text{NO}_3)_2 \cdot 4\text{H}_2\text{O}$  in 50 ml Millipore water. The prepared electrode materials were characterized by XRD, FT-IR, UV-DRS and SEM with EDAX. Electrochemical characterizations were carried out in 3M KOH electrolyte with a three-electrode system consist of active material coated Ni-foam as working electrode, Pt foil as counter electrode and Ag/AgCl as reference electrode, respectively. Cyclic voltammetry (CV) and Galvanostatic charge-discharge (GCD) tests were carried out with in a voltage range  $-0.1$  to  $0.6\text{V}$ . Electrochemical impedance spectroscopy (EIS) tests were conducted with a sine wave with  $5\text{mV}$  amplitude in a frequency range  $100\text{ kHz}$  to  $0.1\text{ Hz}$ .

Fig.1 Shows the comparison cyclic voltammetry curve of  $\text{CuCo}_2\text{S}_4$ ,  $\text{NiCo}(\text{OH})_2$ , and  $\text{CuCo}_2\text{S}_4/\text{NiCo}(\text{OH})_2$ , at  $25\text{mV/s}$ . The results suggested that all materials having the redox and reversibility nature and the current capability of the composite having higher than bare  $\text{CuCo}_2\text{S}_4$  and  $\text{NiCo}(\text{OH})_2$ . Fig.2 shows the EIS spectrum of  $\text{CuCo}_2\text{S}_4$ ,  $\text{NiCo}(\text{OH})_2$ , and  $\text{CuCo}_2\text{S}_4/\text{NiCo}(\text{OH})_2$ . The EIS results exposed the composite  $\text{CuCo}_2\text{S}_4/\text{NiCo}(\text{OH})_2$  have higher ionic conductivity than  $\text{CuCo}_2\text{S}_4$  and  $\text{NiCo}(\text{OH})_2$ . The above results show the composite of  $\text{CuCo}_2\text{S}_4/\text{NiCo}(\text{OH})_2$  is most promising candidate for supercapacitors.

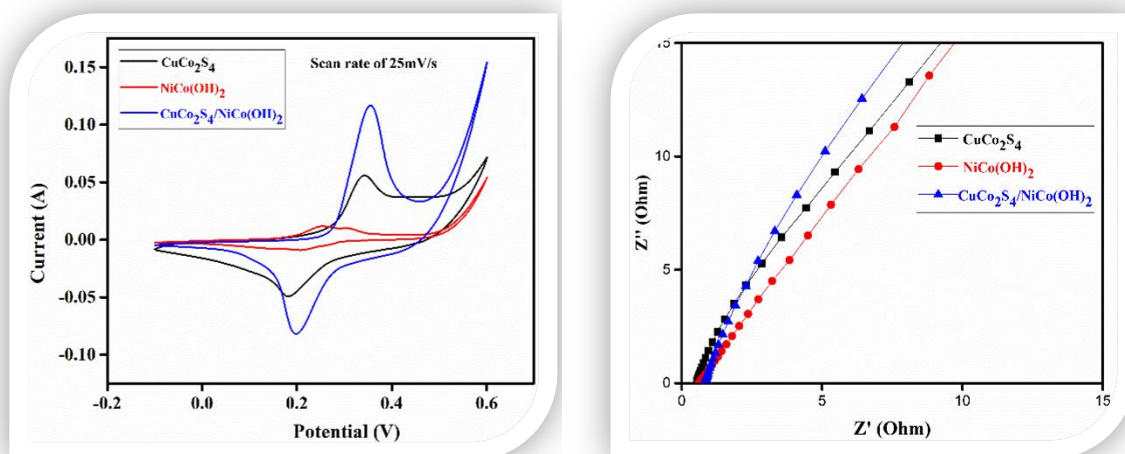


**Figure 1:** Comparison CV curve of  $\text{CuCo}_2\text{S}_4$ ,  $\text{NiCo}(\text{OH})_2$ , and  $\text{CuCo}_2\text{S}_4/\text{NiCo}(\text{OH})_2$ , at  $25\text{mV/s}$ . **Figure 2:** EIS spectrum of  $\text{CuCo}_2\text{S}_4$ ,  $\text{NiCo}(\text{OH})_2$ , and  $\text{CuCo}_2\text{S}_4/\text{NiCo}(\text{OH})_2$ .

**Keywords:** Nanocomposite,  $\text{CuCo}_2\text{S}_4$  Layered Double Hydroxide.

## References

- Y. Wang, D. Yang, T. Zhou, J. Pan, T. Wei, Y. Sun, *Nanotechnology*. 28 (2017) 465402.  
 S. Liu, K.S. Hui, K.N. Hui, V. V. Jadhav, Q.X. Xia, J.M. Yun, Y.R. Cho, R.S. Mane, K.H. Kim, *Electrochim. Acta*. 188 (2016) 898–908.  
 D. Zha, H. Sun, Y. Fu, X. Ouyang, X. Wang, *Electrochim. Acta*. 236 (2017) 18–27.

## PP 11 A study On The Corrosion Behaviour of Mild Steel Using an Aqueous Leaf Extract of *Lagenaria Siceraria*

K. Anuradha<sup>1</sup>, S. Keerthanapriya<sup>2</sup>, C. Sathya<sup>2</sup> and K. Velmanirajan<sup>3</sup>

<sup>1</sup>Department of Chemistry, Alagappa government Arts college, Karaikudi, Tamil Nadu - 630 003.

<sup>2</sup>Research scholar, Department of Chemistry, Alagappa government Arts college, Karaikudi, Tamil Nadu - 630 003, India

<sup>3</sup> Department of Mechanical engineering, VSVN Polytechnic College, Virudhunagar, Tamilnadu, India  
 email: anuvmrajan@yahoo.co.in

## Abstract

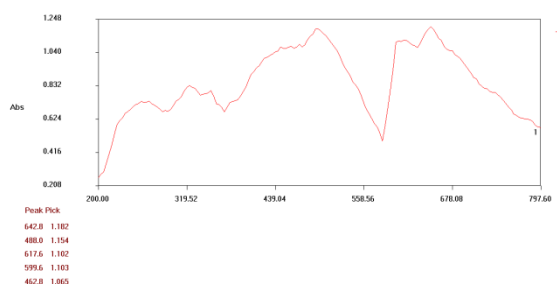
Mild steel in acid medium is widely used in various industrial processes. Sea water finds extensive application as coolant in various exothermic reactions. Sea water constitutes a rich source of various commercially important chemical elements. Depending upon the metal/environment combinations different types of inhibitors are used in suitable concentrations. The study of corrosion inhibition is significant in the field of research due to its usefulness in various industries. An increasing concern in human health and risks has drawn attention in the development of mild steel corrosion. Zinc ions have long been considered as valuable corrosion



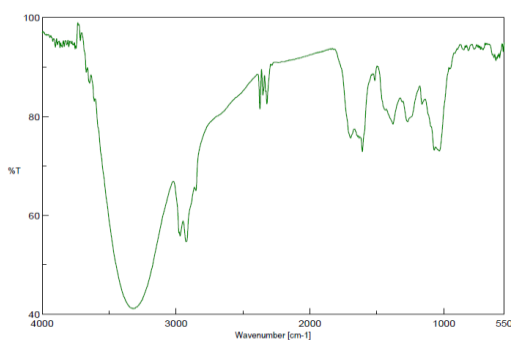
inhibitors for protection afforded by a cathodic polarization mechanism. One of the effective methods to prevent corrosion is the addition of natural inhibitors. Most of the natural products are non-toxic, biodegradable and really available in plenty. In the present investigation, leaves of *lagenaria siceraria* extract (LSE) have been used as corrosion inhibitor for mild steel in sea water medium. The inhibition efficiency was found to increase with increase in concentration of the leaf extract. The formulation consisting of 8 ml of LSE and 15 ppm of  $Zn^{2+}$  has 91 % inhibition efficiency (IE). A study on the effect of immersion period on the LSE-  $Zn^{2+}$  showed an IE that decreased from five days. UV-Visible spectra revealed the formation of a protective film on the metal surface. The same is confirmed through FT-IR spectrum. From the surface examination studies, it could be confirmed that the corrosion inhibition was due to the formation of a protective film consists of  $Fe^{2+}$  - LSE complex.

**Keywords:** Corrosion inhibition, Surface examination, Eco-friendly, Sea water.

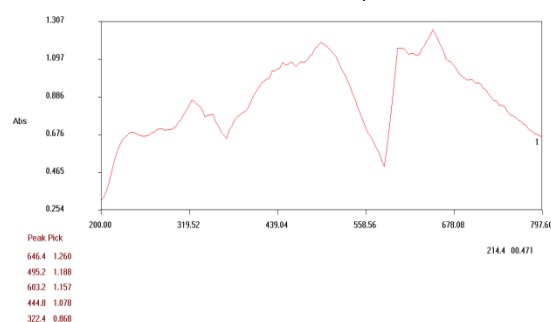
### LSE



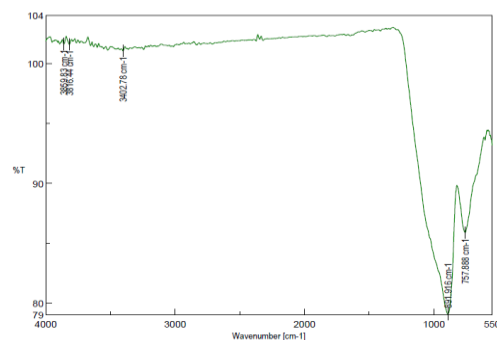
### FTIR, LSE



### LSE + FeSO<sub>4</sub>



### FTIR, LSE + FeSO<sub>4</sub>



## Conclusions

The weight loss study reveals that the formulation consisting of 8 ml of *lagenaria siceraria* extract (LSE) and 15 ppm of  $Zn^{2+}$  has 91 % inhibition efficiency in controlling the corrosion of mild steel immersed in an aqueous solution containing sea water.

A study of the effect of immersion period on the *lagenaria siceraria* extract (LSE)- $Zn^{2+}$  system shows an inhibition efficiency that decreases as the immersion period increases.

UV-Visible spectra reveal that a protective film is formed on the metal surface.

The FTIR spectrum also reveals the formation of protective film that consists of Fe<sup>2+</sup>-LSE complex.

## **PP 12** Bio Synthesis of Silver Nanoparticles Using *Musa Paradisiaca* Flower Extract and its Antibacterial Activity

Aiswarya Pandian and Gurumallesh Prabu Halliah \*

Department of Industrial Chemistry, School of Chemical Sciences, Alagappa University,  
Karaikudi - 630 003, India

\* Corresponding author. Tel.: +919443882946; Fax: +91 4565225202

E-mail address: hgprabu2010@gmail.com, hgprabhu@alagappauniversity.ac.in

### **Abstract**

Colloidal silver nanoparticles (AgNPs) were prepared from the precursor solution by reduction of silver ions using the flower extract of *Musa paradisiaca*. The effect of pH was also studied in the synthesis process. The formation of silver nanoparticles was visibly identified by the colour changes (colorless to brown). The extract acts as both reducing (from Ag<sup>+</sup> to Ag<sup>0</sup>) and capping agent in the reduction process. The synthesized silver nanoparticles were characterized by UV-Vis, FT-IR, XRD and SEM coupled with EDX. The synthesized silver nanoparticles show adsorption peak at 435 nm in the UV-Vis spectrum. The XRD result reveals that four distinct peaks at 2θ values of 38.3°, 44.5°, 64.6° and 77.6° were indexed with the planes (111), (200), (220) and (311) for FCC silver as per the JCPDS file no. 01-087-0719. The synthesized particles will be assessed to its catalytic performance and bacterial filtration efficacy.

**Keywords:** AgNPs, XRD, *Musa paradisiaca*, Antibacterial activity.

### **Introduction**

Currently, improving and protecting our environment using green chemistry have become important issues in many fields of research. The noble metal nanoparticles exhibit new physico-chemical properties which are not observed either in individual molecules or bulk metals. Among noble metal nanoparticles, silver nanoparticles in particular are known for their versatile applications in medical industries. Silver nanoparticles were most efficient as good antimicrobials and antioxidants. In the field of nano-science, the use of various biological units instead of toxic chemicals for the reduction and stabilization of metal nanoparticles, has received extensive attention. Biological entities, such as bacteria, fungi, yeasts, algae or plants, have been reported as serving as both reducing and stabilizing agents. Among these possible bio- resources, biologically active products from plant resources represent excellent scaffolds for this purpose. *Musa* flowers have been traditionally used to alleviate dysentery, diabetes, heart pain, stomach cramps.

In the present study, green synthesis and characterization of stable colloidal silver nanoparticles was carried out using flower extract of *Musa paradisiaca* as reducing agents. The synthesized particles will be assessed to its catalytic performance and bacterial filtration efficacy.

## Experimental Details

### Materials

Silver nitrate ( $\text{AgNO}_3$ ) and pH buffer tablets were purchased from Merck, Chennai, India. All chemicals and reagents were of AR grade, which are used without any further purification. Millipore water was used throughout the experiments.

### Extract preparation

Screening of active components from the leaves was employed by extraction with water. The fresh plant leaves were collected, washed and dried. 5 g of leaves were crushed well in a mortar and 50 ml of solvent was added and extracted using soxhlet apparatus for about 2 h. Then, the extract was filtered through Whatmann filter paper and stored in a desiccator for further use.

### Synthesis of silver nanoparticles

A 5 ml of leaf extract was added to  $\text{AgNO}_3$  (1 mM, 25 ml) solution in 2.5 ml of freshly prepared pH buffer at room temperature and allowed to stir for 2 h. The colorless solution of  $\text{AgNO}_3$  turned to brown after addition of the extract and it was finally turned to black color due to the formation of AgNPs.

## Results and Discussion

*UV-Vis spectroscopy analysis:* The UV-Vis results were presented in terms of the maximum absorbance values ( $\lambda_{\text{max}}$ ) of SPR phenomenon. The UV-Vis results reveal that the SPR absorption peak ( $\lambda_{\text{max}}$ ) was observed as 435 nm as shown in figure 1.

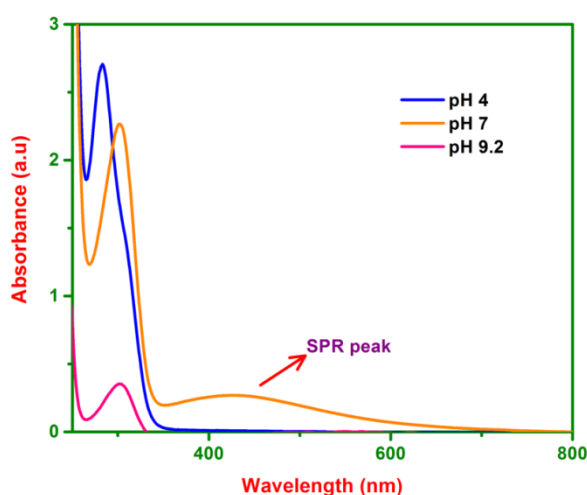


**Figure 1: UV-Vis spectrum of AgNPs synthesized using leaf extract with different pH**

### FT-IR analysis

The similarities between the spectra of neat extract and extract with synthesized AgNPs have some marginal shifts in peak position which clearly indicate the presence of the residual plant extract in the sample as a capping agent. When compared to FT-IR spectra of neat extracts, shifts in the peaks with decreased band intensity were observed.

### X-ray diffraction (XRD) analysis

Four distinct peaks at  $2\theta$  values of  $38.3^\circ$ ,  $44.5^\circ$ ,  $64.6^\circ$  and  $77.6^\circ$  were indexed with the planes (111), (200), (220) and (311) for FCC silver as per the JCPDS file no. 01-087-0719.

### Conclusions

The silver nanoparticles were successfully synthesized using the flower extract of *Musa paradisiaca* and characterized by optical and microscopic methods. The formation of AgNPs (from  $\text{Ag}^+$  to  $\text{Ag}^0$ ) is confirmed by the observed surface plasmon resonance ( $\lambda_{\text{max}}$  at 435 nm) in UV-Vis spectra. The XRD shows crystalline nature of FCC silver with the respective planes of (111), (200), (220) and (311) at an angle of  $38.3^\circ$ ,  $44.5^\circ$ ,  $64.6^\circ$  and  $77.6^\circ$ , respectively.

### References

- H. Veisi, S. Azizi, P. Mohammadi, *Journal of Cleaner Production*. 170 (2018) 1536–1543.  
M. Vanaja, G. Annadurai, *Applied Nanoscience*. 3 (2013) 217–223.

## **PP 13** Synthesis and Characterisation of Silver Nanoparticles Using *Tectona Grandis* Leaf Extract and its Antibacterial Activity

**Manjuladevi Subramaniyan and Gurumallesh Prabu Halliah\***

*Department of Industrial Chemistry, School of Chemical Sciences, Alagappa University, Karaikudi - 630 003, India*

\* Corresponding author. Tel.: +919443882946; Fax: +91 4565225202

E-mail address: hgprabu2010@gmail.com, hgprabhu@alagappauniversity.ac.in

### Abstract

Medicinally active silver nanoparticles were synthesized using *Tectona grandis* leaf extract. Bioactive compounds in the leaves act as reducing (from  $\text{Ag}^+$  to  $\text{Ag}^0$ ) and stabilizing agent in the AgNPs synthesis. The synthesized silver nanoparticles were characterized by UV-Vis, FT-IR, XRD and SEM coupled with EDX. FTIR results revealed the extract functional groups which are responsible for the synthesis of AgNPs. XRD patterns confirmed the crystalline AgNPs in the colloidal solution. X-ray diffraction (XRD) result reveals that four distinct peaks at  $2\theta$  values of  $38.26^\circ$ ,  $44.42^\circ$ ,  $64.69^\circ$  and  $77.50^\circ$  were indexed with the planes (111), (200), (220) and (311) for FCC silver as per the JCPDS file no. 01-087-0718. The synthesized silver nanoparticles using teak leaf extract were also successfully evaluated for their antibacterial activity and its catalytic performance.

**Keywords:** AgNPs, XRD, *Tectona grandis*, Antibacterial activity

## Introduction

Nano sized materials find great interest in the emerging field of science and curative medicines. Silver nanoparticles (AgNPs) possess potential applications in the fields of agriculture, waste management, forensic science, pollution control, solar cells, and medicine. Conventional methods for synthesis of AgNPs require hazardous chemicals as reducing agents and formation of hazardous byproducts. Now-a-days, plants seem to be the best green resource for a large-scale biosynthesis of nanoparticles.

In the present study, green synthesis and characterization of stable colloidal silver nanoparticles was carried out using leaf extracts of *Tectona grandis* as reducing agents. The synthesized particles will be assessed to its catalytic performance and bacterial filtration efficacy.

## Experimental Details

### Materials

Silver nitrate ( $\text{AgNO}_3$ ) and pH buffer tablets were purchased from Merck, Chennai, India. All chemicals and reagents were of AR grade, which are used without any further purification. Millipore water was used throughout the experiments.

### Extract preparation

Screening of active components from the leaves was employed by extraction with water. The fresh plant leaves were collected, washed and dried. 5 g of leaves were crushed well in a mortar and 50 ml of solvent was added and extracted using soxhlet apparatus for about 2 h. Then, the extract was filtered through Whatmann filter paper and stored in a desiccator for further use.

### Synthesis of silver nanoparticles

A 5 ml of leaf extract was added to  $\text{AgNO}_3$  (1 mM, 25 ml) solution in 2.5 ml of freshly prepared pH buffer at room temperature and allowed to stir for 2 h. The colorless solution of  $\text{AgNO}_3$  turned to brown after addition of the extract and it was finally turned to black color due to the formation of AgNPs.

## Results and Discussion

### UV-Vis spectroscopy analysis

The UV-Vis results were presented in terms of the maximum absorbance values ( $\lambda_{\text{max}}$ ) of SPR phenomenon. The UV-Vis results reveal that the SPR absorption peak ( $\lambda_{\text{max}}$ ) was observed as 342 nm as shown in figure 1.

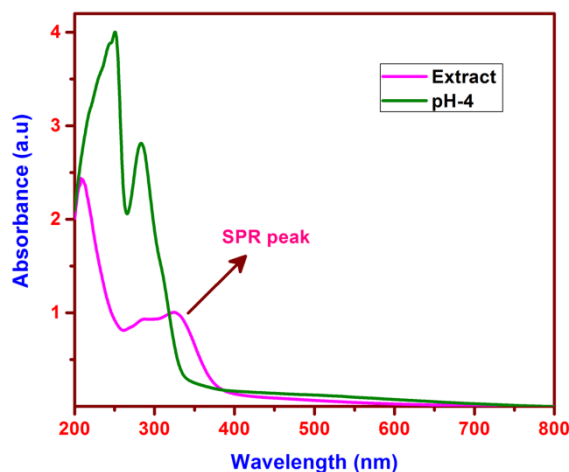


**Figure 1: UV-Vis spectrum of leaf extract and AgNPs synthesized with pH 4.**

### FT-IR analysis

The similarities between the spectra of neat extract and extract with synthesized AgNPs have some marginal shifts in peak position which clearly indicate the presence of the residual plant extract in the sample as a capping agent. When compared to FT-IR spectra of neat extracts, shifts in the peaks with decreased band intensity were observed.

### X-ray diffraction (XRD) analysis

Four distinct peaks at  $2\theta$  values of  $38.26^\circ$ ,  $44.42^\circ$ ,  $64.69^\circ$  and  $77.50^\circ$  were indexed with the planes (111), (200), (220) and (311) for FCC silver as per the JCPDS file no. 01-087-0718.

### Conclusion

The silver nanoparticles were successfully synthesized using the leaf extract of *Tectona grandis* and characterized by optical and microscopic methods. The formation of AgNPs (from  $\text{Ag}^+$  to  $\text{Ag}^0$ ) is confirmed by the observed surface plasmon resonance ( $\lambda_{\text{max}}$  at 342 nm) in UV-Vis spectra. The XRD shows crystalline nature of FCC silver with the respective planes of (111), (200), (220) and (311) at an angle of  $38.26^\circ$ ,  $44.42^\circ$ ,  $64.69^\circ$  and  $77.50^\circ$ , respectively.

### References

S. Basu, P. Maji, J. Ganguly, Applied Nanoscience. 6 (2016) 1–5.

## **PP-14 Bio-Power from Chromium Sorbed Helianthus Annuus Biochar**

**A. Muthu and A.N. Senthilkumar\***

*PG & Research Department of Chemistry, Alagappa Government Arts College,  
Karaikudi – 630 003.*

*\*Corresponding Author email: [ansent@gmail.com](mailto:ansent@gmail.com)*

### **Introduction**

Biochar is a biomass derived carbonaceous material burnt under limited supply of oxygen through a process known as pyrolysis. The release of chromium from point and non-point sources causes threat to environmental health. It is therefore very important to develop an effective technology to remove chromium from aqueous solutions prior to their discharge. Surface functional groups and macro pores present in the biochar are considered as a promising candidate for chromium removal. Helianthus annuus biochar (HNB) is investigated for chromium ion adsorbing capacity from synthetic aqueous solution and subsequently the work was extended to find a viable solution for disposing the HNB absorbed chromium through microbes in microbial fuel cell (MFC).

### **Experimental**

#### **Pyrolysis and preparation of biochar**

Helianthus annuus stalks were collected from farm holdings of Karaikudi town. Collected stalks were dried under mild sunlight for 7 days and then shredded, prepared in a slow pyrolysis unit.

#### **Techniques**

The chromium concentrations of the liquid phase samples were then determined by diphenyl carbazide method [3] with aid of a spectrophotometer systronic C120.

#### **Microbial fuel cell (MFC) construction**

Soil microbial fuel cell was constructed using 150 mL glass beaker. 100 g of sandy loamy soil used in the present study served as fuel in MFC. Soil was moisturised with 40 mL of distilled water and packed into beaker in such a way that 30g of it was loaded at the bottom of the beaker over which anode was placed. Anode was then covered the remaining amount of soil above which the cathode was allowed to float in 25 mL of distilled water. Mild steel specimens of dimension 3 X 3 X 0.2 cm were used as electrodes. Soil bacteria served as biocatalyst. The constructed MFC was used as control, labelled as CMFC. Two similar MFC were constructed and one out of it was packed with 0.5 g of HNB near the anode (HMFC) and another MFC's anode was packed with HNB used for chromium adsorption from aqueous solution of 40 ppm concentration (CrMFC).

The open circuit potential offered by the three MFC's were measured using digital multimeter individually.

## Results and Discussion

### Chromium sorption study

The experimental values obeyed well with empirical Freundlich isotherm ( $R^2=0.923$ ). Hence HNB provides heterogeneous site for chromium adsorption in non-uniform layer with reversibility. FTIR evidenced the existence of N-H moiety in HNB which on protonation in aqueous medium could cause physical interaction on chromate ions leading to the formation of non uniform layer. The free energy of adsorption ( $\Delta G_{ads} < -20 \text{ kJ}$ ) calculated from equilibrium constant ( $K_c$ ) values showed physical mode of chromium adsorption on HNB.

### Chromium discharging in MFC

Open circuit potential discharged by CrMFC last up to 24 days and then falls steeply. HMFC offered steady potential from the eighth day of MFC operation and last longer upto 40 days with gradual fall in potential. CMFC offered low potential value (around 180 mv) and delivered potential upto 15 days. Electricity generation is dependent on fuel concentration and microbial activity till a plateau region is reached. At the saturation point, maximum rate of electron transfer is achieved by microbial metabolic mechanism and/or by an increase in alternate electron acceptor that compete with anode. Higher potential offered by HMFC may be due to better microbial activity on soil organic matter which was triggered by HNB. In each study a sharp demise of OCP occurred after stable plateau is reached. HMFC undergoes progressive decrease of potential by slow microbial acclimation process.

## Conclusion

The study concluded that HNB effectively adsorbs chromium from synthetic aqueous solution obeying Freundlich adsorption isotherm. The calculated free energy of adsorption supported physical mode of binding between HNB and chromium. The adsorbed chromium was discharged in MFC with subsequent power generation.

## References

- D.S. Bhargava, S.B. Sheldarkar, Use of TNSAC in chromium adsorption studies and relationships-literature, experimental methodology, justification and effects of process variables, *Water Res.* 27 (1993) 303–312.
- C.P. Huang, Removal of chromium by powdered aluminum-oxide adsorption, *J. Water Pollut. Control Fed.* 49 (1977) 1811–1817.
- S.R. Olsen, L.E. Sommers, Phosphorus. In: Page, A.L., Miller, R.H., Keeney, D.R. (Eds.), *In: Methods of Soil Analysis, Part 2: Chemical and Microbiological Properties.* Agronomy Monograph 9, ASA and SSSA, Madison, WI, USA. 1982
- Hu Tang, Weijie Zhou, Lina Zhang, Adsorption isotherms and kinetics studies of malachite green on chitin hydrogels, *J. Hazardous Materials*, 209-210 (2012) 218-225.



Y. Zuo, P. Maness, B. Logan, Electricity production from steam-exploded corn stover biomass, *Energ. Fuel.* 20 (2006) 1716–1721.

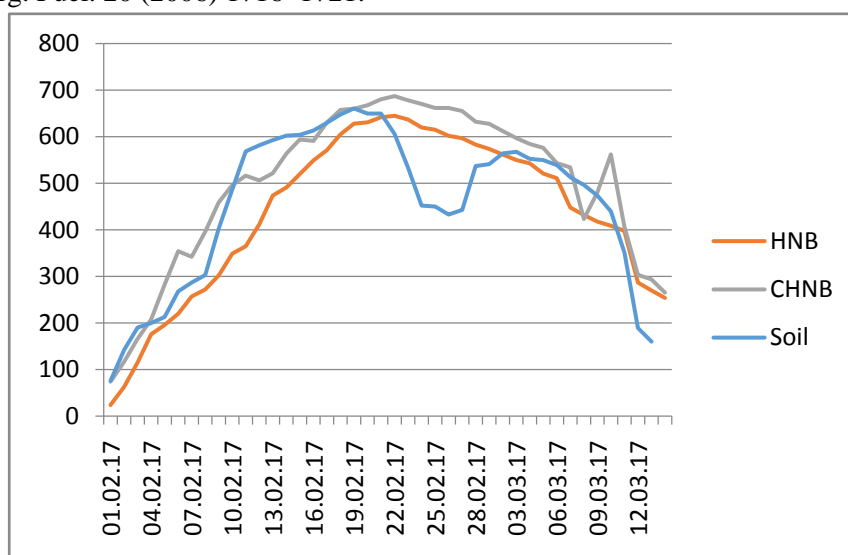


**Figure 1: Observed OCP values during MFC operation**

## **PP-15** Bio Synthesis of Silver Nanoparticles Using *Azadirachta Indica* Leaf Extract and its Antibacterial Activity

**Manoj kumar Sekar and Gurumallesh Prabu Halliah\***

*Department of Industrial Chemistry, School of Chemical Sciences, Alagappa University, Karaikudi - 630 003, India*

\* Corresponding author. Tel.: +919443882946; Fax: +91 4565225202

E-mail address: hgprabu2010@gmail.com, hgprabhu@alagappauniversity.ac.in

### **Abstract**

Synthesis of nanocomposites using green route is a major focus of modern nanotechnology. Herein we demonstrate the synthesis of silver based chitosan bionanocomposite using the stem extract of *Azadirachta indica*. The extract acts as both reducing (from  $\text{Ag}^+$  to  $\text{Ag}^0$ ) and capping agent in the reduction process. The synthesized silver nanoparticles were characterized by UV-Vis, FT-IR, XRD and SEM coupled with EDX. The absorbance at 302 nm in the UV-Vis spectrum reveals the synthesis of silver nanoparticles due to its characteristic surface plasmon resonance (SPR). The presence of possible functional group involved in the reduction of silver metal ions into silver nanoparticles was identified by Fourier transform infrared spectroscopy (FT-IR) analysis. X-ray diffraction (XRD) result reveals that four distinct peaks at  $2\theta$  values of  $36.5^\circ$ ,  $42.4^\circ$ ,  $61.4^\circ$  and  $74.1^\circ$  were indexed with the planes (111), (200), and (311) for FCC silver as per the JCPDS file no. 01-087-0718. The synthesized silver nanoparticles using *A. indica* leaf extract were also successfully evaluated for their antibacterial activity and its catalytic performance.

**Keywords:** Green synthesis, Nanocomposites, Chitosan, *Azadirachta indica*, Antibacterial activity.

## Introduction

Synthesis of metal nanocomposites is one of the emerging research areas in the arena of modern nanoscience and nanotechnology. Due to their distinct physicochemical properties, metal nanocomposites have been used in variety of applications such as adsorption, water purification, antimicrobial activity, biomedicine and sensors. Nanocomposites are defined as the dispersion of inorganic nanoparticles in a polymeric compound. Chitosan (poly (1-4) 2 amino 2-deoxy  $\beta$ -D glucan), is a natural, non-toxic, microbial resistant and biodegradable polymer used for the template in the bionanocomposite synthesis.

In the present study, green synthesis and characterization of stable colloidal silver nanoparticles and silver based chitosan nanocomposite were carried out using leaf extract of *Azadirachta indica* as reducing agents. The synthesized composite will be assessed to its catalytic performance and bacterial filtration efficacy.

## Experimental Details

### Materials

Silver nitrate ( $\text{AgNO}_3$ ) and pH buffer tablets were purchased from Merck, Chennai, India. All chemicals and reagents were of AR grade, which are used without any further purification. Millipore water was used throughout the experiments.

### Extract preparation

Screening of active components from the leaves was employed by extraction with water. About 5g of sliced pieces were added to 20 ml of deionized water and boiled for 30 minutes in a Soxhlet extractor for about 2 h. Then, the extract was filtered through Whatmann filter paper and stored in a desiccator for further use.

### Synthesis of silver/Chitosan nanocomposite

A 5 ml of leaf extract was added to  $\text{AgNO}_3$  (1 mM, 100 ml) solution in 2.5 ml of freshly prepared pH buffer at room temperature and allowed to stir for 2 h followed by sonication for 60 min. The color changes from pale yellow to brown indicate the formation of silver nanoparticles. About 1g of chitosan was mixed with 0.5ml of acetic acid and made up volume to 20ml for dissolving the powdered chitosan. Then colloidal silver nanoparticles (5ml) solution was added to the chitosan solution. The suspension was stirred by using magnetic stirrer for 2h at 80°C.

## Results and Discussion

*UV-Vis spectroscopy analysis* : The UV-Vis results were presented in terms of the maximum absorbance values ( $\lambda_{\text{max}}$ ) of SPR phenomenon. The UV-Vis results reveal that the SPR absorption peak ( $\lambda_{\text{max}}$ ) was observed as 302 nm as shown in figure 1.

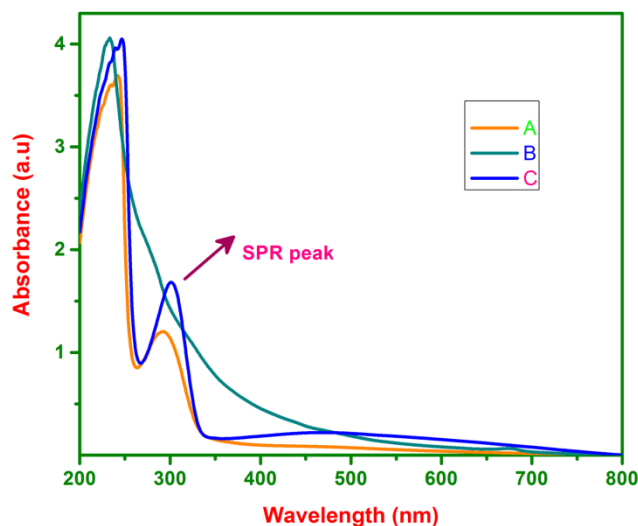


**Figure 1: UV-Vis spectrum of A) Extract B) Extract with AgNPs C) AgNPs/Chitosan nanocomposite**

*FT-IR analysis* :The similarities between the spectra of neat extract and extract with synthesized AgNPs have some marginal shifts in peak position which clearly indicate the presence of the residual plant extract in the sample as a capping agent. When compared to FT-IR spectra of neat extracts, shifts in the peaks with decreased band intensity were observed.

*X-ray diffraction (XRD) analysis* : Four distinct peaks at  $2\theta$  values of  $36.5^\circ$ ,  $42.4^\circ$ ,  $61.4^\circ$  and  $74.1^\circ$  were indexed with the planes (111), (200), (220) and (311) for FCC silver as per the JCPDS file no. 01-087-0718.

## Conclusion

The silver nanoparticles and silver/Chitosan nanocomposite were successfully synthesized using the leaf extract of *Azadirachta indica* and characterized by optical and microscopic methods. The formation of AgNPs (from  $\text{Ag}^+$  to  $\text{Ag}^0$ ) is confirmed by the observed surface plasmon resonance ( $\lambda_{\text{max}}$  at 302 nm) in UV-Vis spectra. The XRD shows crystalline nature of FCC silver with the respective planes of (111), (200), (220) and (311) at an angle of  $36.5^\circ$ ,  $42.4^\circ$ ,  $61.4^\circ$  and  $74.1^\circ$  respectively.

## References

- M. Kumar, K. Bansal, V.S. Gondil, S. Sharma, D.V.S. Jain, S. Chhibber, R.K. Sharma, N. Wangoo, *Journal of Molecular Liquids*. 249 (2018) 1145–1150.
- A. Regiel-Futyra, M. Kus-Liśkiewicz, V. Sebastian, S. Irusta, M. Arruebo, A. Kzyziół, G. Stochel, *RSC Advances*. 7 (2017) 52398–52413.

**PP 16**    **Synthesis and Characterisation of Silver Nanoparticle using *Ocimum Basilicum* Leaf Extract and its Antibacterial Activity****Ramamani Mohanram and Gurumallesh Prabu Halliah\****Department of Industrial Chemistry, School of Chemical Sciences, Alagappa University,  
Karaikudi - 630 003, India**\* Corresponding author. Tel.: +919443882946; Fax: +91 4565225202**E-mail address: hgprabu2010@gmail.com, hgprabhu@alagappauniversity.ac.in***Abstract**

Plant mediated synthesis of nanoparticles has been considered as green route of synthesis due to its eco-friendly approach. The Silver nanoparticles were synthesized by using *Ocimum basilicum* (sweet basil) leaf extract as a reducing agent. The completion of reduction reaction (from  $\text{Ag}^+$  to  $\text{Ag}^0$ ) was monitored by UV-Vis spectroscopy. The color change from light yellow to grey with  $\lambda_{\text{max}}$  of 280nm confirmed the formation of AgNPs. The synthesized nanoparticles were further characterized by UV-DRS, XRD, FT-IR and SEM with EDAX analyses. The FT-IR spectra of neat extract and extract with synthesized AgNPs have some marginal shifts in peak position which clearly indicate the presence of the residual plant extract in the sample as a capping agent. The XRD result reveals that four distinct peaks at  $2\theta$  values of  $38.23^\circ$ ,  $44.12^\circ$ ,  $64.63^\circ$  and  $77.63^\circ$  were indexed with the planes (111), (200), (220) and (311) for FCC silver as per the JCPDS file no. 01-087-0717. The synthesized particles will be assessed to its catalytic performance and bacterial filtration efficacy.

Keywords: AgNPs, FT-IR, *Ocimum basilicum*, Antibacterial activity

**Introduction**

In modern research, nanotechnology plays a vital role; it involves the manipulation of particles at the nano-scale range (1-100 nm). Metallic nanoparticles possess unique optical, electrical and photo thermal properties and the silver nanoparticles are exploited widely because of their excellent antibacterial properties. Silver nanoparticles are used in the development of new technologies in the areas of electronics, material sciences and medicine. Several methods have been introduced to prepare metallic nanoparticles such as physical, chemical, photochemical and biological. Biosynthetic green methods used for synthesis of nanoparticles using of medicinal plants and microorganisms such as fungi and algae to synthesize nanoparticles. It is eco-friendly, cost effective as compared to the other chemical and physical methods. In the present study, green synthesis and characterization of stable colloidal silver nanoparticles was carried out using leaf extracts of *Ocimum basilicum* as reducing agents. The synthesized particles will be assessed to its catalytic performance and bacterial filtration efficacy.

## Experimental Details

### Materials

Silver nitrate ( $\text{AgNO}_3$ ) and pH buffer tablets were purchased from Merck, Chennai, India. All chemicals and reagents were of AR grade, which are used without any further purification. Millipore water was used throughout the experiments.

### Extract preparation

Screening of active components from the leaves was employed by extraction with water. The fresh plant leaves were collected, washed and dried. 5 g of leaves were crushed well in a mortar and 50 ml of solvent was added and extracted using sonication for about 30 mins. Then, the extract was filtered through Whatmann filter paper and stored in a desiccator for further use.

### Synthesis of silver nanoparticles

A 5 ml of leaf extract was added to  $\text{AgNO}_3$  (1 mM, 25 ml) solution in 2.5 ml of freshly prepared pH buffer at room temperature and allowed to stir for 2 h. The colorless solution of  $\text{AgNO}_3$  turned to light yellow after addition of the extract and it was finally turned to black color due to the formation of AgNPs.

## Results and Discussion

*UV-Vis spectroscopy analysis:* The UV-Vis results were presented in terms of the maximum absorbance values ( $\lambda_{\text{max}}$ ) of SPR phenomenon. The UV-Vis results reveal that the SPR absorption peak ( $\lambda_{\text{max}}$ ) was observed as 280 nm as shown in figure 1.

*FT-IR analysis:* The FT-IR spectra of neat extract and extract with synthesized AgNPs have some marginal shifts in peak position which clearly indicate the presence of the residual plant extract in the sample as a capping agent. When compared to FT-IR spectra of neat extracts, shifts in the peaks with decreased band intensity were observed.

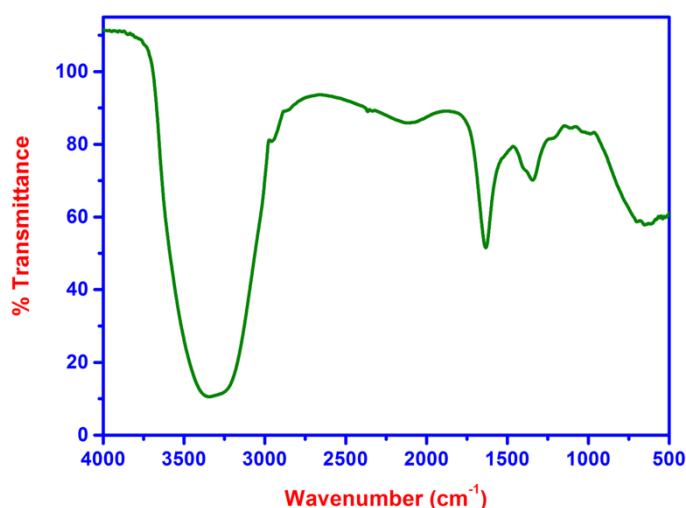


**Figure 1: FT-IR spectrum of AgNPs synthesized using *Ocimum basilicum* leaf extract**

*X-ray diffraction (XRD) analysis:* Four distinct peaks at  $2\theta$  values of  $38.23^\circ$ ,  $44.12^\circ$ ,  $64.63^\circ$  and  $77.63^\circ$  were indexed with the planes (111), (200), (220) and (311) for FCC silver as per the JCPDS file no. 01-087-0717.

## Conclusion

The silver nanoparticles were successfully synthesized using the leafextract of *Ocimum basilicum* and characterized by optical and microscopic methods. The formation of AgNPs (from  $\text{Ag}^+$  to  $\text{Ag}^0$ ) is confirmed by the observed surface plasmon resonance ( $\lambda_{\text{max}}$  at 280 nm) in UV-Vis spectra. The XRD shows crystalline nature of FCC silver with the respective planes of (111), (200), (220) and (311) at an angle of  $38.23^\circ$ ,  $44.12^\circ$ ,  $64.63^\circ$  and  $77.63^\circ$ , respectively.

## References

- G. Muhammad, M.A. Hussain, M. Amin, S.Z. Hussain, I. Hussain, S.N. Abbas Bukhari, M. Naeem-ul-Hassan, RSC Adv. 7 (2017) 42900–42908.
- N. González-Ballesteros, J.B. Rodríguez-González, M.C. Rodríguez-Argüelles, Journal of Photochemistry and Photobiology B: Biology. 178 (2018) 302–309.

## **PP 17** Characterization and Water Holding Potential of Peanut Shell Biochar

**K . Rajeshwari and A.N. Senthilkumar\***

*PG & Research Department of Chemistry, Alagappa Govt. Arts College, Karaikudi-630 003.*

*\*Corresponding Author email: [ansent@gmail.com](mailto:ansent@gmail.com)*

### Introduction

Biochar is produced by thermal decomposition of biomass under oxygen-limited conditions. The characteristics of biochar are influenced mainly by the preparation temperature and biomass. Biochars derived from various source materials show different properties of surface area, porosity and the amount of functional groups which influences the properties of biochar. Biochar has been proved to be effective in improving soil properties and increasing crop biomass. Biochar is increasingly receiving attention and highly recommended as soil amendment because it cannot only mitigate climate change by sequestering C from atmosphere into soil but also improve soil properties and enhance soil fertility by improving moisture and nutrients retention and microbial activity. In the present study peanut shell were subjected to slow thermal pyrolysis at  $350^\circ\text{C}$ . The resulting biochar (PNB) physical and chemical properties were analyzed. Characterized PNB's soil water holding nature was examined

### Experimental Details

#### Materials and preparation of biochar

Peanut shells were collected from in and around the farm holdings of Karaikudi town, Sivaganga district and collected stalks were dried under mild sunlight for 7 days to remove

unbound moisture and then shredded. The shredded stalks were pyrolyzed at 350°C. After the pyrolysis biochar was grounded to small granules and pass through 2 mm sieve in order to have the same particle size as that of the soil.

### Physico-chemical characterization

The prepared PNB was mixed with water in the ratio of 1:5 by mass to measure pH and EC in ELICO instrument of model LI 617. The organic carbon was determined by wet digestion method. Total organic carbon (TOC), total nitrogen, phosphorous and potassium content, water soluble cations and exchangeable cations were analysed as reported elsewhere.

2.3 FTIR analysis: Surface functional group of biochar was analysed by fourier transform infrared (FT-IR) spectrometer of BrukerOptik GmbH of model No TENSOR 27. Biochar was pelleted with potassium bromide for experimental use.

### Water holding capacity measurements

Sandy loamy soils were conditioned with various amounts of PNB by mass to assess the effects on the water holding capacity at different mixture rates. The homogenized 2 mm size of 50g soil was filled in 200 ml capacity container and different proportions between 0 -10% were mixed to soil individually. Water was slowly applied to each mixture present in the container, by gentle agitation until super saturation. Then these mixtures were allowed to settle for 24 h to ensure homogeneity and the saturated samples were weighed to determine wet mass. The samples were then dried at 110°C for 24 h using a hot air oven and weighed for dry mass.

## Results and Discussion

### Physico-chemical characteristics of biochar

Physico-chemical parameters of the PNB are given in the Table1. PNB was possessing alkaline pH due to the presence of organic anions, carbonates and other alkali metal ions. Appreciable quantities of dissolved ions were responsible for electrical conductivity (EC) [3]. The presence of nitrogen in studied biochar is likely due to amino group as evidenced from FTIR. However, this N content cannot be completely utilized by crops because it exists in inaccessible forms as functional groups in the skeleton of carbon chain. Lower temperature pyrolysis produces higher amount of nitrogen as evident from Table1.

### Water holding capacity

The following equation was used to determine the water holding capacity of PNB

$$\text{Waterholdingcapacity}(\%) = \frac{\text{masswet} - \text{massdry}}{\text{massdry}} \times 100$$

Standard deviation was determined from the three replicate samples for each mixture. Experimental results revealed that the 9% PNB soil mixture's (by mass) whose water holding capacity doubled as compared to control treatment. It was reported that mixture rates of less than

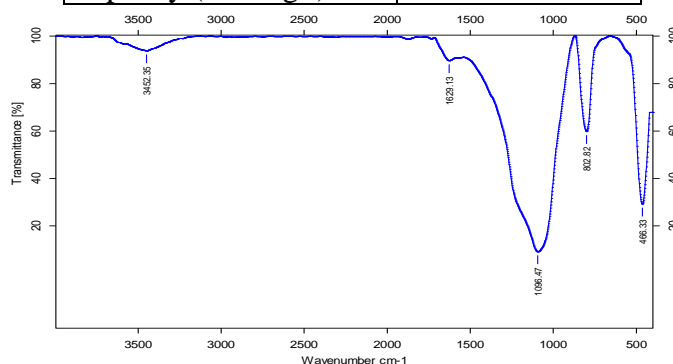
10% were safe for agricultural purposes to loamy sand soil [4]. The higher water holding capacity was mainly due to its higher carbon and pore space of the studied biochar.

## Conclusion

The study concluded that PNB increased the water holding capacity of sandy loamy soil. 9% addition by mass of PNB enhanced water holding capacity doubly. Hence the biochars can effectively supplement the sandy loamy soil for irrigation purpose.

**Table-1:Physio-chemical properties of PNB**

Property	MeasuredValues
Bulk density (Mg m-3)	0.46
Particle density (Mg m-3)	0.569
Per cent pore space	35
Moisture content (%)	4.5
pH	8.7
EC(dS m <sup>-1</sup> )	0.65
Organic carbon (gkg <sup>-1</sup> )	80
Total Carbon (%)	65
Total N (%)	0.48
Total P (%)	0.20
Total K (%)	1.1
Total Na (%)	0.72
Total Ca (%)	1.2
Total Mg (%)	1.0
Exchangeable Ca	3.00
Exchangeable Mg	1.4
Exchangeable Na	1.3
Exchangeable K	2.3
Cation exchange capacity (cmolk <sup>-1</sup> )	34



Sample Name: Rice-Ash 28-02-13

## Physical and chemical properties of PNB

**Figure 1: FTIR analysis of PNB**



## References

- E. Marris, Putting the carbon back: black is the new green, *Nature*, 442 (2006) 624-626.
- J. Lehmann, A handful of carbon, *Nature*, 447 (2007) 143-144.
- Basile-Doelsch, W.E.E. Amudson, R. Stone, D. Borschneck, J.Y. Bottero, T. Moustier, F. Masin, F. Colin, Mineral control of carbon pools in a colcanic horizon, *Geoderma*, 137 (2007) 437-489.
- P. Jha, A. Biswas, B. Lakaria, A.S. Rao, Biochar in agriculture - prospects and related implications. *Current science*, 99 (2010) 1218-1225.

## **PP 18** Synthesis and Characterization of Silver Nanoparticle using *Solanum Trilobatum* Leaf Extract and its Antibacterial Activity

Gomathi Shanmugam and Gurumallesh Prabu Halliah\*

Department of Industrial Chemistry, School of Chemical Sciences, Alagappa University,  
Karaikudi - 630 003, India

\* Corresponding author. Tel.: +919443882946; Fax: +91 4565225202

E-mail address: hgprabu2010@gmail.com, hgprabhu@alagappauniversity.ac.in

### Abstract

The present investigation describes the simple and effective method for synthesis of silver nanoparticles using *Solanum trilobatum* leaf extract as a reducing agent. The synthesized silver nanoparticles were characterized by UV-Vis, FT-IR, XRD and SEM coupled with EDX. The completion of reduction reaction (from  $\text{Ag}^+$  to  $\text{Ag}^0$ ) was monitored by UV-Vis spectroscopy. The color change from colorless to grey with  $\lambda_{\text{max}} \sim 300\text{nm}$  due to its characteristic surface plasmon resonance (SPR) confirmed the formation of AgNPs. Fourier Transform Infrared Spectroscopy (FT-IR) results confirmed the presence of the residual plant extract in the sample acts as a reducing (from  $\text{Ag}^+$  to  $\text{Ag}^0$ ) and capping agent in the synthesis process. The X-ray diffraction (XRD) result reveals that four distinct peaks at  $2\theta$  values of  $38.26^\circ$ ,  $44.42^\circ$ ,  $64.66^\circ$  and  $77.71^\circ$  were indexed with the planes (111), (200), (220) and (311) for FCC silver as per the JCPDS file no. 01-087-0717. The synthesized particles will be assessed to its catalytic performance and bacterial filtration efficacy.

**Keywords:** AgNPs, SEM, *Solanum trilobatum*, Antibacterial activity

### Introduction

Nanotechnology deals with the synthesis and stabilization of matters at the nanoscale ranging from 1 to 100 nm. Silver metal has been used widely across the civilization for different purpose. Silver is a well known antibacterial agent against a wide range of over 650 microorganisms from different classes such as gram-negative to gram positive bacteria, fungi and viruses. Silver Nanoparticles (AgNPs) have been extensively used in food packaging, food and seed preservation, bio-fertilizers and medicines. Plants seem to be a good alternative for the synthesis of metal nanoparticles.

In the present study, green synthesis and characterization of stable colloidal silver nanoparticles was carried out using leaf extracts of *Solanum trilobatum* as reducing agents. The synthesized particles will be assessed to its catalytic performance and bacterial filtration efficacy.

## Experimental Details

### Materials

Silver nitrate ( $\text{AgNO}_3$ ) and pH buffer tablets were purchased from Merck, Chennai, India. All chemicals and reagents were of AR grade, which are used without any further purification. Millipore water was used throughout the experiments.

### Extract preparation

Screening of active components from the leaves was employed by extraction with water. The fresh plant leaves were collected, washed and dried. 5 g of leaves were crushed well in a mortar and 50 ml of solvent was added and extracted using soxhlet apparatus for about 30 min. Then, the extract was filtered through Whatmann filter paper and stored in a desiccator for further use.

### Synthesis of silver nanoparticles

A 5 ml of leaf extract was added to  $\text{AgNO}_3$  (1 mM, 25 ml) solution in 2.5 ml of freshly prepared pH buffer at room temperature and allowed to stir for 2 h. The colorless solution of  $\text{AgNO}_3$  turned to brown after addition of the extract and it was finally turned to black color due to the formation of AgNPs.

## Results and Discussion

### UV-Vis spectroscopy analysis

The UV-Vis results were presented in terms of the maximum absorbance values ( $\lambda_{\text{max}}$ ) of SPR phenomenon. The UV-Vis results reveal that the SPR absorption peak ( $\lambda_{\text{max}}$ ) was observed as 300 nm as shown in figure 1.

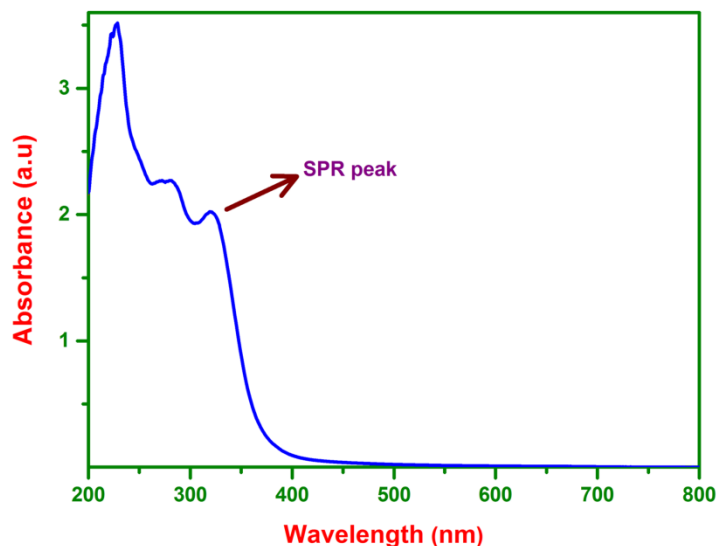


**Figure 1: UV-Vis spectrum AgNPs synthesized using *Solanum trilobatum* leaf extract**

*FT-IR analysis:* The similarities between the spectra of neat extract and extract with synthesized AgNPs have some marginal shifts in peak position which clearly indicate the presence of the residual plant extract in the sample as a capping agent. When compared to FT-IR spectra of neat extracts, shifts in the peaks with decreased band intensity were observed.

*X-ray diffraction (XRD) analysis:* Four distinct peaks at  $2\theta$  values of  $38.26^\circ$ ,  $44.42^\circ$ ,  $64.66^\circ$  and  $77.71^\circ$  were indexed with the planes (111), (200), (220) and (311) for FCC silver as per the JCPDS file no. 01-087-0717.

## Conclusion

The silver nanoparticles were successfully synthesized using the leaf extract of *Solanum trilobatum* and characterized by optical and microscopic methods. The formation of AgNPs (from  $\text{Ag}^+$  to  $\text{Ag}^0$ ) is confirmed by the observed surface plasmon resonance ( $\lambda_{\text{max}} \sim 300$  nm) in UV-Vis spectra. The XRD shows crystalline nature of FCC silver with the respective planes of (111), (200), (220) and (311) at an angle of  $38.26^\circ$ ,  $44.42^\circ$ ,  $64.66^\circ$  and  $77.71^\circ$ , respectively.

## References

S. Ahmed, M. Ahmad, B.L. Swami, S. Ikram, Journal of Advanced Research. 7 (2016) 17–28.

**PP 19** Total synthesis of pyrazole pyrimidine and thienopyridines derivatives as inhibitor for KSP and its anticancer agents

P. Muthuraja<sup>a</sup>, A. Susaimanickam<sup>b</sup>, S. Prakash<sup>a</sup> P. Manisankar<sup>a\*</sup>

Correspondence to: Prof. P. Manisankar ([manisankarp@alagappauniversity.ac.in](mailto:manisankarp@alagappauniversity.ac.in))

<sup>a</sup>Address of corresponding author: Former Syndicate Member, Former Dean, Faculty of Science

Professor & Head (Rtd.), Department of Industrial Chemistry, Alagappa University, Karaikudi 630003, Tamil Nadu, INDIA \*Tel: +91 4565 228836, Fax: +91 4565 225202

<sup>b</sup>Department of Chemistry, Arumugam Pillai Seethai Ammal College, Tiruppattur, Tamilnadu

**Abstract**

Both the pyrazole pyrimidine and thienopyridines derivatives were tested for activity against human mitotic kinesin eg5. Three compounds (12, 25 and 27) showed to inhibit the eg5 activity at micromolar concentration. Molecular docking studies suggest that they have higher binding affinity to site 1 of eg5 by interacting with the hotspot residues such as Trp127 and Arg119. These compounds also interact with Tyr352 by forming three hydrogen bonds in the site 2 allosteric binding site of Eg5. The pyrazole pyrimidine derivatives can be used as temple to further structure based drug discovery in order to design more inhibitors with improved potency. The present work forms the basis for carrying out *in vivo* and structural studies of these compounds and developing them further as lead compounds for cancer chemotherapy.

*in vivo* activity,

**Keywords:** KSP, Pyrazole Pyrimidine.

## **PP 20** Adsorption of Phosphate by Biochar Derived From Acacia Nilotica Leaf

**K. Shanthi and A.N. Senthilkumar\***

*PG & Research Department of Chemistry, Alagappa Government Arts College, Karaikudi.*

*\*Corresponding Author email: [ansent@gmail.com](mailto:ansent@gmail.com)*

### **Abstract**

The aim of the present study was to prepare a biochar from agricultural residues. In the present study Acacia nilotica leaf was used as biomass for preparing biochar (ANBC). Laboratory experiments were conducted to remove phosphate from aqueous solution by using the prepared biochar. Freundlich isotherm model fitted the experimental isotherm of phosphate adsorption better than Langmuir model. Our results suggest that ANBC can be used as an alternate adsorbent to reclaim phosphate from aqueous solution.

### **Introduction**

Biochar is a biomass derived carbonaceous material burnt under limited supply of oxygen through a process known as pyrolysis. The release of phosphate from point and non-point sources causes threat to environmental health. It is therefore very important to develop an effective technology to remove phosphate from aqueous solutions prior to their discharge. Surface functional groups and macro pores present in the biochar are considered as a promising candidate for phosphate removal. ANBC was investigated for phosphate ion adsorbing capacity from synthetic aqueous solution.

### **Experimental Techniques**

#### **Pyrolysis and preparation of biochar**

Acacia Nilotica was collected from in and around the Karaikudi town. Collected leaves were dried under mild sunlight for 7 days and then shredded, prepared in a slow pyrolysis unit.

#### **Characterization and experimental Techniques**

Surface functional group of biochar was analysed by fourier transform infrared (FT-IR) spectrometer of Bruker Optik GmbH of model No TENSOR 27. The phosphate  $\text{KH}_2\text{PO}_4$  concentrations of the liquid phase samples were then determined by the ascorbic acid method [3] with aid of a spectrophotometer systronic C120.

### **Results and Discussion**

#### **Characteristics of biochar**

FTIR spectroscopy of RHB showed 3 important characteristics peaks. A band at  $3452\text{ cm}^{-1}$  proves the existence of hydroxyl group. The band at  $1629\text{ cm}^{-1}$  corresponds to amide and amine functional group. A well stretched band at  $1098\text{ cm}^{-1}$  is attributed to C-O vibrational

stretching frequency of aliphatic ethers. Thus hydroxyl, amide, amine and aliphatic ethers are present in the ANBC which is shown in fig.1

### Adsorption Study

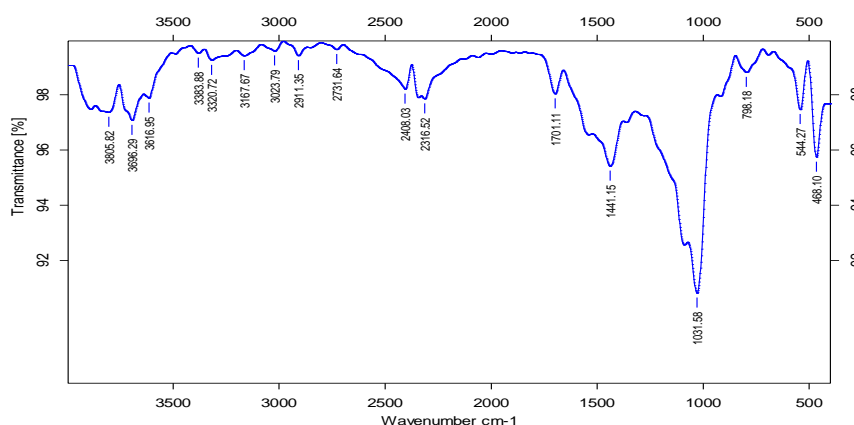
The experimental values obeyed well with empirical Freundlich isotherm as evidenced from Fig.2 ( $R^2=0.979$ ). Hence ANB provides heterogeneous site for phosphate adsorption in non-uniform layer with reversibility [4]. FTIR evidenced the existence of N-H moiety in ANBC which on protonation in aqueous medium could cause physical interaction on phosphate ions leading to the formation of non uniform layer. The free energy of adsorption ( $\Delta G_{ads} < -20 \text{ kJ}$ ) calculated from equilibrium constant ( $K_c$ ) values showed physical mode of phosphate adsorption on ANB.

### Conclusions

The study concluded that ANBC effectively adsorbs phosphate from synthetic aqueous solution obeying Freundlich adsorption isotherm. The calculated free energy of adsorption supported physical mode of binding between ANBC and phosphate.

### References

- D.S. Bhargava, S.B. Sheldarkar, Use of TNSAC in phosphate adsorption studies and relationships-literature, experimental methodology, justification and effects of process variables, *Water Res.* 27 (1993) 303–312.
- C.P. Huang, Removal of phosphate by powdered aluminum-oxide adsorption, *J. Water Pollut. Control Fed.* 49 (1977) 1811–1817.
- S.R.Olsen, L.E.Sommers, Phosphorus. In: Page, A.L., Miller, R.H., Keeney, D.R. (Eds.), In: *Methods of Soil Analysis, Part 2: Chemical and Microbiological Properties*. Agronomy Monograph 9, ASA and SSSA, Madison, WI, USA.1982
- Hu Tang, Weijie Zhou, Lina Zhang, Adsorption isotherms and kinetics studies of malachite green on chitin hydrogels, *J.Hazardous Materials*, 209-210 (2012)218-225.



Sample Name: Ad 1

**Figure 1: FTIR spectra of ANBC**

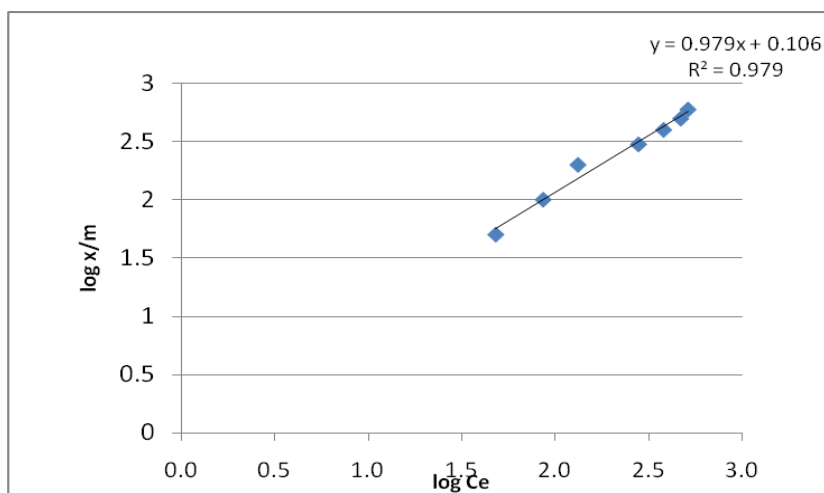


Figure 2: Freundlich graph for ANBC

## PP-21 Copper-based metal-organic framework for electrochemical detection of tryptophan

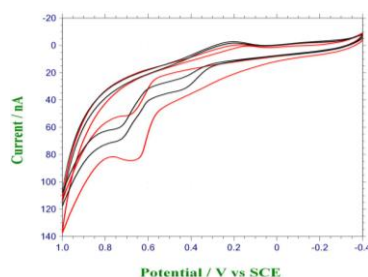
S. Yogesh<sup>a</sup>, S. Prakash<sup>a</sup>, P. Muthuraja<sup>a</sup>, P. Manisankar<sup>a\*</sup>

<sup>a</sup>Department of Industrial Chemistry, Alagappa University, Karaikudi(TN), India.

\*<sup>a</sup>E-mail: manisankarp@alagappauniversity.ac.in

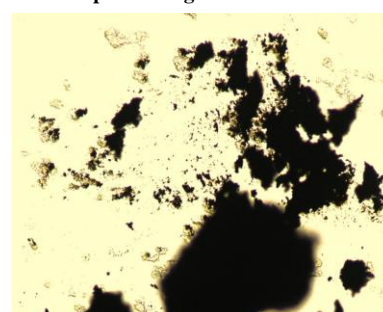
### Abstract

Tryptophan is an essential amino acid. Liver cells take it and use it to synthesize other important molecules such as niacin and serotonin. The amount of Trp reflects liver cell function from different sides. If the amount of Trp in liver cells could be obtained, a more accurate conclusion on cell function would be drawn. It is very difficult to culture the primary liver cell in vitro, because a homogeneous population (cell line) obtained from one cell in a liver tissue by tissue culture techniques must be different from the primary liver cell and must have lost some of its characteristics. So, electrochemical determination of Trp is important and significant work. In this work, we developed a method for electrochemical determination of Trp



Cyclic voltammery of Cu-MOF electrode in the presence of 1mM Trp using 0.1 M NaOH electrolytes (black line: no Trp and redline: presence of Trp).

Optical image of Cu-MOF



at a Cu-based metal-organic framework (Cu-MOF) modified electrode. The Cu-MOF was prepared by a simple hydrothermal synthesis, and the characterizations of the Cu-MOF were studied by Fourier transform infrared spectroscopy (FT-IR), scanning electron microscopy (SEM), and X-ray powder diffraction (XRD). Electrochemical behaviors of the Cu-MOF modified electrode to Trp were measured by amperometry. The electrochemical results showed

that the Cu-MOF modified electrode exhibited an excellent electro-catalytic oxidation towards Trp in 0.1M NaOH. Moreover, the fabricated sensor showed a high selectivity to the oxidation of Trp. The sensor was satisfactorily applied to the determination of Trp.

**Keywords:** Tryptophan, Cu-MOF, Sensor, Electrochemistry.

## **PP-22** Synthesis and Characterization of Seaweed-PVA/Zno Composite for Better Thermal Stability and Antibacterial Activity

**R. Aiswarya, S. Rajaboopathi, S. Thambidurai\***

*\*Department of industrial chemistry, school of chemical sciences,  
Alagappa university, Karaikudi - 630003, Tamil nadu, India.*

*Email:aisramamoorthy@gmail.com*

### **ABSTRACT**

Seaweed is a large group of multicellular algae, seaweed located in colder northern hemisphere waters. It can be classified into brown algae (Phaeophyta), red algae (Rhodophyta), and green algae (Chlorophyta). In our present study, we had taken the brown seaweed of (*Padina tetrastratica*) as a biopolymer template component. Poly vinyl alcohol is a water-soluble synthetic polymer; it is applied in papermaking, textiles, and a variety of coatings. This is taken as a capping agent. In the current scenario, metal nanoparticles have gained more attention in many fields due to their unique interaction with biomolecules. Zinc oxide is a most studied metal oxide in a wide range of applications. In the present study SW-PVA/ZnO hybrid composite was synthesized by using seaweed extract and PVA synthetic polymer solution. The synthesized hybrid composites are characterized by using UV-visible, FTIR, and XRD spectroscopy. The prepared nanocomposites were used as antibacterial agents tested against the Gram positive (*S.aureus*) and Gram negative (*E. coli*) bacterial pathogens.

**Keyword:** Seaweed, Composite, Crystalline size, Antibacterial activity, Thermal stability.

### **Introduction**

Seaweed isolates are typically used industrially. Seaweed is a loose colloquial term encompassing macroscopic, multicellular, benthic marine algae. The term includes some members of the red, brown and green algae. Seaweeds can also be classified by use (as food, medicine, fertilizer, industrial, etc.).

### **Experimental Details**

0.5g of seaweed powder poured into 50ml of 0.25M ZnCl<sub>2</sub> solution and it was allowed to continuously stirred for 2h. then add 0.5g of PVA dissolved with distilled water with 1h constant stirring. To filter the solution, To add NaOH from the burette, the formed white coloured precipitated was allowed to continuously stirred for 4h. The obtained precipitated was settled for



1day. It was washed with Millipore water. The obtained precipitated is tried in an oven for 6h. The product was grind well with mortar.

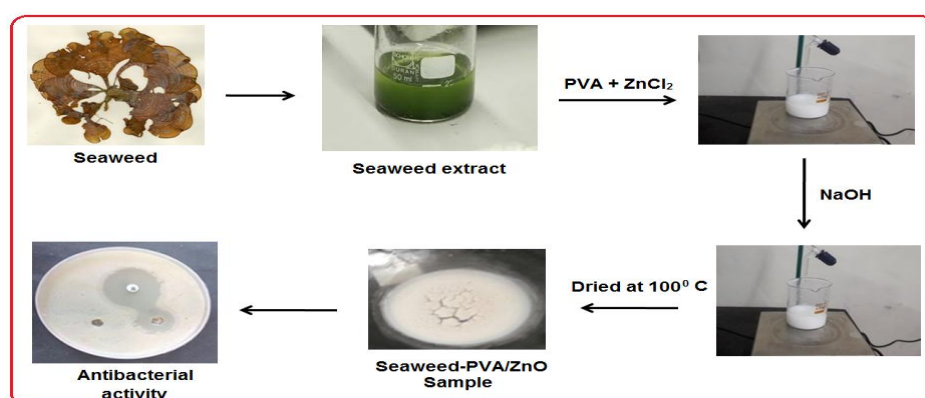
## Results and Discussion

In the present investigation SW-PVA-ZnOcomposites was prepared from Seaweed,  $ZnCl_2$  and NaOH source materials. The prepared composites structure was characterized by different analytical techniques.

## Conclusion

The nanocomposites materials are synthesized by precipitation method and the structure was confirmed by FT-IR, UV-Vis and XRD analysis.

## Graphical Abstract



## References

- RF Patarra, L. Paiva, AI. Neto, E. Lima, J.J. Baptista Appl. Phycol. (2010):1.  
 P. MacArtain, CIR Gill, M. Brooks, R. Campbell, IR. Rowland. Nutr. Rev. (2007); 65:535.  
 Department of Biological Sciences, Faculty of Science, Niger Delta University, Wilberforce Island, Bayelsa State, Nigeria.  
 Department of Science laboratory Technology, School of Applied Science, Rivers State Polytechnic, Bori, Rivers State, Nigeria.

## PP 23 Understanding the antibacterial activities of Terpenoids against Gram Positive & Negative bacteria through Biofilms

P.Venmathy<sup>1</sup>, J. Jeya sundari<sup>1</sup>, V. S. Vasantha<sup>2\*</sup>

<sup>1</sup>Nadar Mahajana Sangam S. Vellaichamy Nadar College, Nagamalai, Madurai,

<sup>2</sup>Department of Natural Products Chemistry, School of Chemistry, Madurai Kamaraj University, Madurai - 625021, India.

\* Email: vasantham999@yahoo.co.in

**Keywords:** Betulinic acid, Ursolic acid, Antibacterial, Biofilm, SEM, EPS.

## Introduction

The aim of this study is to evaluate the bacterial activity of medicinal plants and biofilm of two types of bacteria species. The growth inhibitory concentration (MIC), effects on biofilm

formation and in the absence and presence of the extracts by confocal laser-scanning microscopy were performed by two types of bacteria.

### Experiment Details:

Anti bacterial activity of two different terpenoids compounds against four pathogens namely *Staphylococcus aureus*, *Staphylococcus sp.*, *Escherichia coli* and *Pseudomonas aeruginosa* were studied by plate diffusion method. Briefly, the overnight grown fresh test culture of pathogens were taken (0.1 mL) and swabbed on the sterile LB agar plates. Wells of about 1mm diameter were bored into the plates at a uniform gap on the plates swabbed with the pathogenic culture. Five different concentrations of the 2 test compounds (0-100 $\mu$ M) i.e, 0, 25, 50, 75 and 100  $\mu$ M were prepared in DMSO using their stock solutions (1mM) for each compound. Each test compound was tested on all 4 pathogens. The antibacterial activity was screened by observing for the zone of inhibition of growth of the test pathogen around the wells filled with the test compound. Kanamycin (50  $\mu$ M) was used as positive control in each plate. The plate assay was performed in duplicates for each test compound and test pathogen.

### Results and Discussions:

Final report was gathered from scanning electron microscopy and exo-polysaccharides studies. Biofilm formation is a multi-step process starting with attachment to a surface then formation of micro-colony that leads to the formation of three dimensional structures and finally ending with maturation followed by detachment. During biofilm formation many species of bacteria are able to communicate with one another through specific mechanism called quorum sensing. It is a system of stimulus to co-ordinate different gene expression. Bioassay results indicated that bioactive terpenoids such as Betulinic acid and Ursolic acid significantly reduced the biofilm formation of the bacteria.

### Plate diffusion method

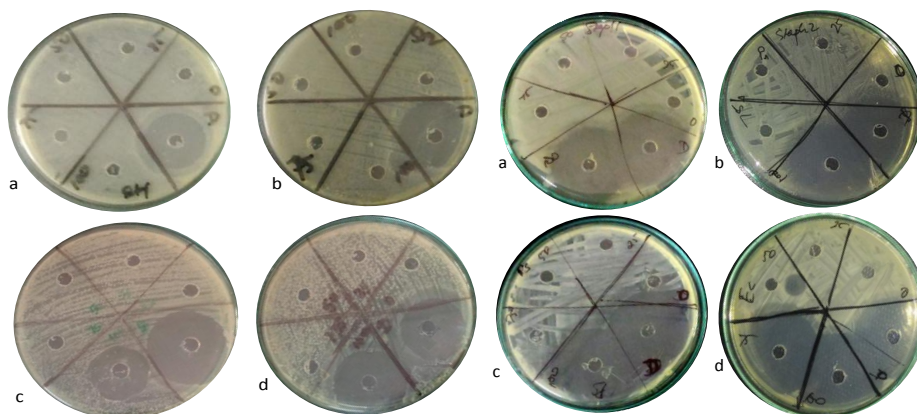
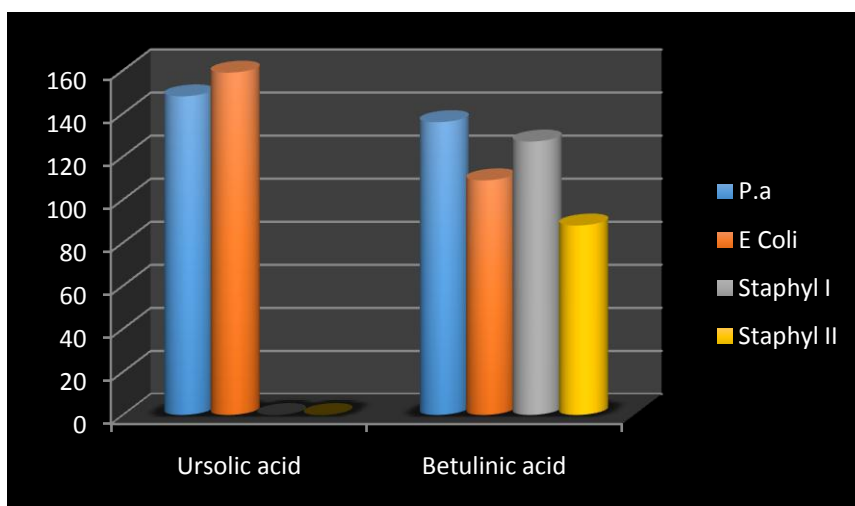


Fig. 1: Anti-bacterial activity of Ursolic acid

Fig. 2: Anti-bacterial activity of Betulinic acid

**EPS Study:****Conclusion**

Bioassay results indicated that bioactive terpenoids such as Betulinic acid and Ursolic acid significantly reduced the biofilm formation of the bacteria.

**References**

- Jayant S. Raut , Ravikumar B. Shinde , Nitin M. Chauhan & S. Mohan Karuppaiyl Terpenoids of plant origin inhibit morphogenesis, adhesion, and biofilm formation by *Candida albicans* Biofouling, 2013 29, 1, 87–96, <http://dx.doi.org/10.1080/08927014.2012.749398>.
- Yong-Guy Kim, Jin-Hyung Lee<sup>1</sup>, Giyeon Gwon<sup>1</sup>, Soon-Il Kim, JaeGyu Park & Jintae Lee Essential Oils and Eugenols Inhibit Biofilm Formation and the Virulence of *Escherichia coli* O157:H7 Scientific Reports | 6:36377 | DOI: 10.1038/srep36377

**PP 24 Preparation and Characterization of Chitin-CdO Composite for Better Antibacterial Activity**

**S. Ilamathi, T. Revathi, S. Thambidurai\***

*Department of Industrial Chemistry, School of Chemical Sciences,  
Alagappa University, Karaikudi - 630003, Tamil Nadu, India.*

*Email: sthambi01@yahoo.co.in*

**Abstract**

The present study explores the possibilities of using locally available inexpensive waste crab shell derived chitin. Composites are prepared by chemical precipitation method. The composites were prepared by using chitin as biosurfactant, cadmium nitrate as a source material and NaOH as a precipitating agent. The prepared composite was characterized and the functional groups confirmed by Fourier transform infrared spectroscopy (FT-IR). The optical properties of composite are studied by UV-Vis DRS spectroscopy. The crystalline size of composite was calculated by X-ray diffraction analysis (XRD). The surface morphology was analyzed by Scanning Electron Microscopy (SEM). The chitin-CdO composite exhibited antibacterial activity

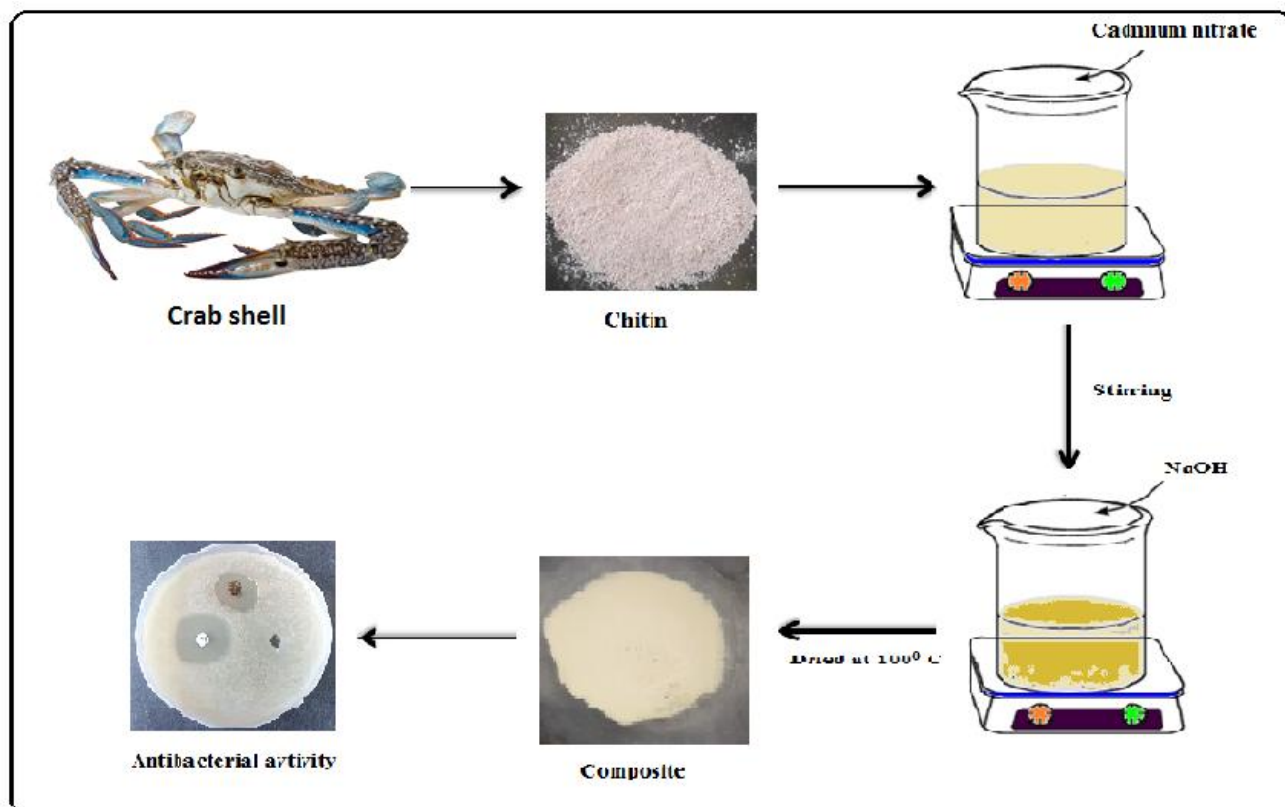
against gram positive as well as gram negative microorganisms. The composite material has higher antibacterial activity compared to chitin. The improvement of mechanical properties and the results of antimicrobial of the composites also evaluated and revealed the composite would be a suitable candidate for implant application in biomedical field.

**Keywords:** Chitin, CdO, Composite, Antibacterial activity.

## Introduction

Chitin ( $\beta$ -(1-4)-linked 2-acetamido-2-deoxy-d-glucose units) is the second most important natural polymer in the world and its main sources exploited are two marine crustaceans, shrimp and crabs. It is less toxic, biodegradable in nature, capable of wound healing and also inert in the gastrointestinal tract of mammals. The last two decades witnessed extensive research on semiconductor nanostructured materials especially on Cd based CdO, CdS and CdSe because of their unique size and shape dependent properties and making them potential candidates for optical, electronics, optoelectronic, sensor and biomedical device application. Cadmium oxide (CdO), an n-type semiconductor with a wide direct band gap (2.77 eV) and a narrow indirect band gap (0.55 eV).

## Experimental Details



## Result and Discussion

In this work, demineralization and deproteinization process were applied for crab shell and chitin was obtained. The prepared chitin- CdO composite have been characterized. The functional groups of resultant matrix from chitin, cadmium oxide were characterized and confirmed by FTIR, UV-Vis DRS. The chitin-CdO composite has good crystalline structure. The surface morphology was determined by SEM analysis. The composite showed high antibacterial efficiency against *S. aureus* and *E. coli*. The results demonstrate that the composite would be a suitable candidate for implant application in biomedical sector.

## Conclusion

In this study, a simple and economic biological process has been developed to prepared chitin- CdO composite. Antibacterial activity of chitin- CdO composite exhibit pronounced skill against the pathogenic bacteria.

## Reference

- Romana Nasrin, Shanta Biswas, Taslim Ur Rashid, Sanjida Afrin, Rumana Akhter Jahan, Papia Haque, Mohammed Mizanur Rahman, Preparation of Chitin-PLA laminated composite for implantable application, *Bioactive Materials*, 2 (2017) 199-207..
- Chattopadhyay, P.K., Price, D.K., Harper, T.F., Betts, M.R., Yu, J., Gostick, E., Perfetto, S.P., Goepfert, P., Koup, R.A., De Rosa, S.C., Bruchez, M.P., Roederer, M. Quantum dot semiconductor nanocrystals for immunophenotyping by polychromatic flow cytometry. *Nat. Med.* 12 (2006) 972–977.

## PP 25 Synthesis and Characterization of Chitin-Zno Composite for Better Antibacterial Activity

**Kanimozhi. S, Revathi.T, Thambidurai.S\***

*\*Department of Industrial Chemistry, School of Chemical Sciences,  
Alagappa University, Karaikudi - 630003, Tamil Nadu, India.*

*Email:sthambi01@yahoo.co.in*

## ABSTRACT

In this work, Chitin was isolated from crab shell wastes. Chitin-ZnO composites are prepared by the chemical precipitation method. chitin was taken as the biosurfactant, zinc nitrate as the source material and NaOH as the precipitating agent. The prepared composite was characterized and the functional groups confirmed by Fourier transform infrared spectroscopy (FT-IR). The optical properties of composite are studied by UV-Vis DRS spectroscopy. The crystalline properties and surface morphology of the composite powder were characterized with X-ray diffraction (XRD), scanning electron microscopy (SEM) and Transmission electron microscopy (TEM). The thermal stability of the composite were analysed by Thermal gravimetric analysis (TGA). The advantages of these biomaterials, they can be easily processed into different

forms such as membranes, sponges, gels, microparticles, nanoparticles and nanofibers for applied into a variety of biomedical applications such as drug delivery, gene therapy, and wound healing fields.

**Keywords:** Chitin, ZnO, Thermal stability, Biomedical application, Optical property.

## Introduction

Chitin is a widespread polysaccharide in nature and produced annually as much as cellulose. The chemical structure of chitin is comparable to that of cellulose and the 2-hydroxy group on each sugar unit of cellulose is replaced with acetamido to give chitin, i.e.,  $\beta$ -(1 $\rightarrow$ 4)-linked N-acetylglucosamine polymer. Chitin is found in many places throughout the natural world, especially in the shells of crustaceans such as crabs, lobsters and shrimps. Zinc oxide (ZnO) nanoparticles are used as a semiconductor with wide band gap of 3.2–3.37 eV. ZnO is a polar crystal with hexagonal phase, air-stable and environmental friendly, which has been explored for a wide range of applications in nano scale devices such as nano generators, sensors, field-emission transistors ultra violet photo-detectors and in biomedical systems as ultra sensitive DNA sequence detectors.

## Experimental Details

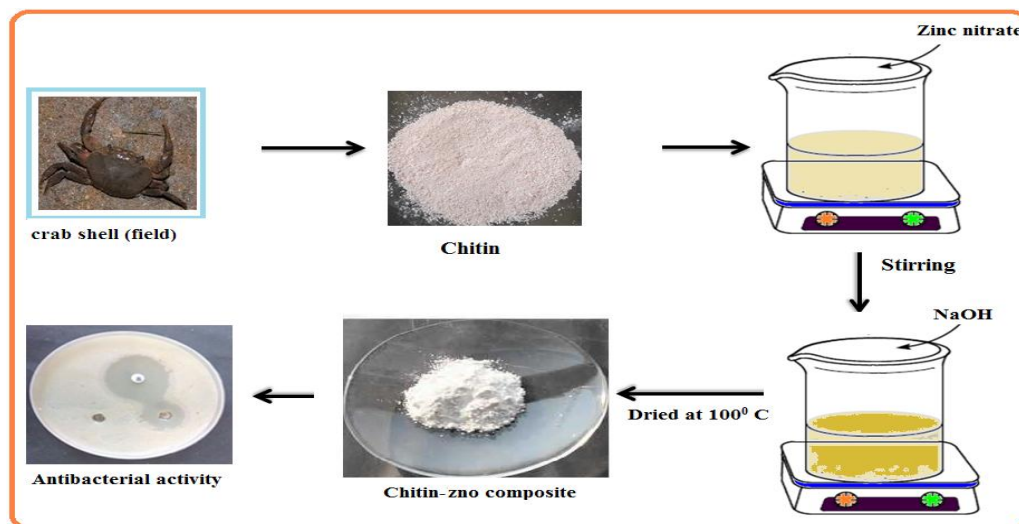


**Figure 1: Schematic diagram of formation of chitin-ZnO composite**

## Results and Discussion

In this study, demineralization and deproteinization process were carried out for crab shell and chitin was obtained. The synthesized chitin- ZnO composite have been characterized. The functional groups of resultant matrix from chitin, zinc oxide were characterized and confirmed by FTIR, UV-Vis DRS, SEM, TEM and TGA. The antimicrobial activity of the chitin-ZnO composite was tested against the gram positive and gram negative bacterial species.

## Conclusion

In this study, a simple and economic biological process has been developed to synthesized chitin- ZnO composite. The inorganic-natural polymer materials would have great potential in biomedical applications.

## References

- A. Sila, N. Mlaik, N. Sayari, R. Balti, A. Bougatef, Chitin and chitosan extracted from shrimp waste using fish proteases aided process: efficiency of chitosan in the treatment of unhairing effluents, *J. Polym. Environ.* 22 (2014) 78-87.
- S. Anandhavelu, S. Thambidurai, Effect of zinc chloride and sodium hydroxide concentration on the optical property of chitosan–ZnO nanostructure prepared in chitin deacetylation, *Materials Chemistry and Physics* 131 (2011) 449–454.

## **PP 26** Electron beam-irradiated Polypyrrole decorated with Bovine serum albumin pores: Simultaneous determination of Epinephrine and L-Tyrosine

**R. Ramya<sup>1</sup> and Dr. J. Wilson<sup>1\*</sup>**

<sup>1</sup>*Polymer Electronics Lab, Department of Bioelectronics and Biosensors, Alagappa University, Karaikudi - 630004, Tamilnadu, India.  
Email: mramya155@gmail.*

## Abstract

In current work highly sensitive and stable electrochemical sensor for simultaneous non-enzymatic detection of epinephrine (EP), L-tyrosine (L-Tyr) is constructed based on Electron beam irradiated Polypyrrole (EB-Ppy) nanospheres (Zeta potential 33.69 mV at pH 7) embedded over bovine serum albumin (BSA) (Zeta potential -11.54 mV at pH 7) porous structure, fabricated by simple chemical routes. The BSA structure has the advantages of large surface area, excellent structure stability, rich pore channels and redox mediator role. The constructed sensor exhibited excellent sensor performances by the combination of protein with NH group and recorded the linear response of EP, L-Tyr individual in the concentration range of 100 nM–1 mM, 100 nM–800  $\mu$ M, with detection limit 7.1 nM, 8.8 nM ( $S/N=3\sigma/b$ ). The EB-Ppy-BSA/GCE electrochemical sensor manifests intriguing application with good sensitivity, selectivity and reproducibility towards the EP, L-Tyr detection. The practical analytical utility provides great promise by selective measurements in tea, and chicken extract which has a promising future for biological and healthcare applications.

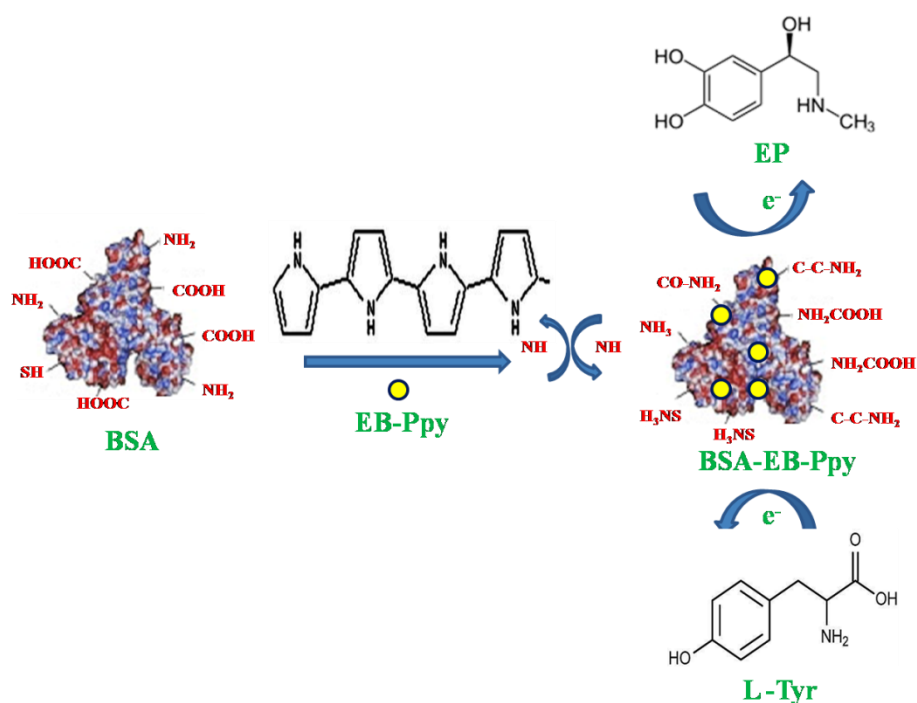


Figure 1: Mechanism of EB-Ppy-BSA interaction with EP and L-Tyr

## PP 27 Synthesis and Characterization of Bi Doped ZnO–RGO/Pani Hybrid Composite For Supercapacitor Applications

Karthik R, Thambidurai S\*

\*Department of Industrial Chemistry, School of Chemical Sciences, Alagappa University, Karaikudi-630 003, Tamil Nadu, India.

Email: sthambi01@yahoo.co.in (S.Thambidurai)

### Abstract

We aimed to develop bismuth doped-reduced graphene oxide-ZnO (RGO) by chemical precipitation method using Bismuth nitrate, Zinc nitrate, NaOH, and RGO as a precursors and followed by polymerized with aniline monomer by in-situ polymerization method. Fourier transform spectroscopy (FTIR) and X-ray diffraction spectroscopy were employed to investigating the presence of functional group and crystallinity of the hybrid composite. Homogeneously distributed metal oxide particles are viewed and observed by scanning electron microscope (SEM). Elemental composition of the hybrid composite was investigated by EDX analysis. Finally, electrochemical properties of Bi doped RGO-ZnO/PANI hybrid composite was investigated by cyclic voltammetry (CV), electrochemical impedance spectroscopy (EIS) and galvanostatic charge discharge (GCD) method. The GCD measurements showed that specific capacitance of RGO-BZO/PANI (In three electrode system  $604.5 \text{ F g}^{-1}$  and two electrode system  $237 \text{ F g}^{-1}$ ) is greater than that of RGO-ZnO/PANI (In three electrode system  $265.32 \text{ F g}^{-1}$  and two electrode system  $81.74 \text{ F g}^{-1}$ ) which is due to the synergistic effects of small size and good redox



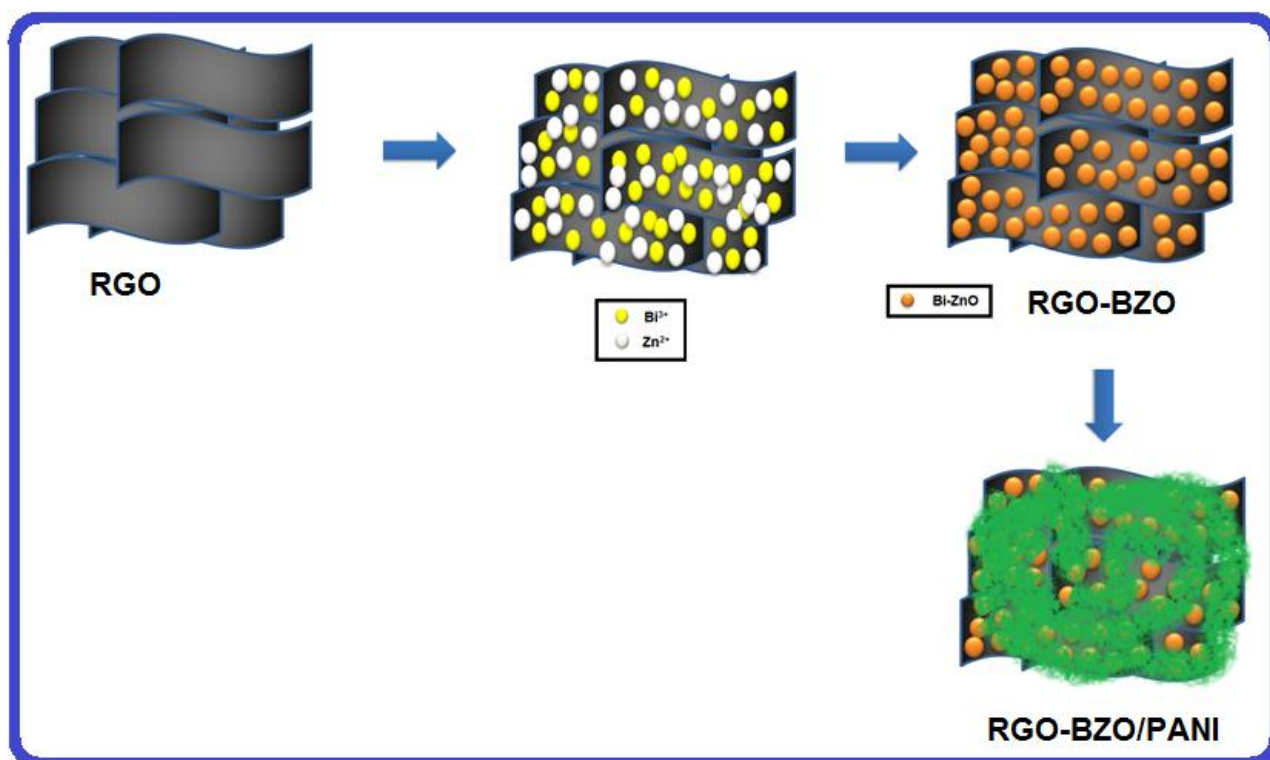
activity of bismuth doped ZnO particles are combined with the high electronic conductivity of the RGO and PANI chains. Hence, the synthesized RGO-BZO/PANI hybrid composite is considered as a potential electrode material for supercapacitor

**Keywords:** Bismuth nitrate, FTIR, RGO, ZnO, SEM.

## Introduction

Electrochemical capacitors (often called supercapacitors) are novel energy storage systems that have been applied in many fields because of their long cycle-life, excellent reversibility and high power density. However, their widespread use is limited by their lower energy storage density and relatively higher effective series resistance than that of batteries. Therefore, many researchers in this area have focused on the development of different electrode materials such as various forms of carbon, conducting polymers, and transition metal oxides. Electrically conducting polymers have attracted worldwide research interest because of their high flexibility and relatively high specific capacitance as one of the main electrode materials for supercapacitors. Among various polymers, polyaniline (PANI) is extremely attractive as electrode materials for supercapacitors due to high electrochemical activity, chemical stability and ease of synthesis as well as relatively low cost. But it can produce volume expansion and contraction sometimes, low intensity of cycle stability, easy to collapse when in charge and discharge. So it is needed to be studied further to improve the cycle performance of PANI electrode materials. In order to overcome this drawback, all kinds of carbon materials, such as porous carbon, mesoporous carbon and carbon nanotube, have been investigated due to their good conductivity, stable physicochemical properties, low cost, and long cycle life. Graphene oxide (GO) surface contains a large number of functional groups (carboxyl, hydroxyl, epoxy group, etc.). These unique functional groups make it good dispersion and hydrophilic in the water, which make it as a promising candidate for the fabrication of supercapacitor electrode materials.

## EXPERIMENTAL DETAILS



## Reference

- R.Karthik, S. Thambidurai, Synthesis of RGO– Co doped ZnO / PANI hybrid composite for supercapacitor application, *Journal of Materials Science: Materials in Electronics*. 28 (2017) 9836–9851.
- Z.F. Li, H. Zhang, Q. Liu, L. Sun, L. Stanciu, J. Xie, Fabrication of high-surface-area graphene/polyaniline nanocomposites and their application in supercapacitors, *ACS Applied Materials and Interfaces*. 5 (2013) 2685–2691.
- S. Vijayakumar, S. Nagamuthu, S.H. Lee, K.S. Ryu, Porous thin layered nanosheets assembled ZnCo<sub>2</sub>O<sub>4</sub> grown on Ni-foam as an efficient electrode material for hybrid supercapacitor applications, *International Journal of Hydrogen Energy*. 42 (2017) 3122–3129.
- B. Ma, X. Zhou, H. Bao, X. Li, G. Wang, Hierarchical composites of sulfonated graphene-supported vertically aligned polyaniline nanorods for high-performance supercapacitors, *Journal of Power Sources*. 215 (2012) 36–42.
- D. Gui, C. Liu, F. Chen, J. Liu, Preparation of polyaniline/graphene oxide nanocomposite for the application of supercapacitor, *Applied Surface Science*. 307 (2014) 172–177.

## PP 28 Synthesis and Characterization of Chitosan-Bi<sub>2</sub>O<sub>3</sub>-Sodium Alginate Hybrid Composite for Photocatalytic Applications

K. Mariyappan, R. Karthik, S. Thambidurai\*

*Department of Industrial Chemistry, School of Chemical Sciences, Alagappa University,  
Karaikudi-630 003, Tamil Nadu, India.*

*Email: sthambi01@yahoo.co.in (S.Thambidurai)*

### Abstract

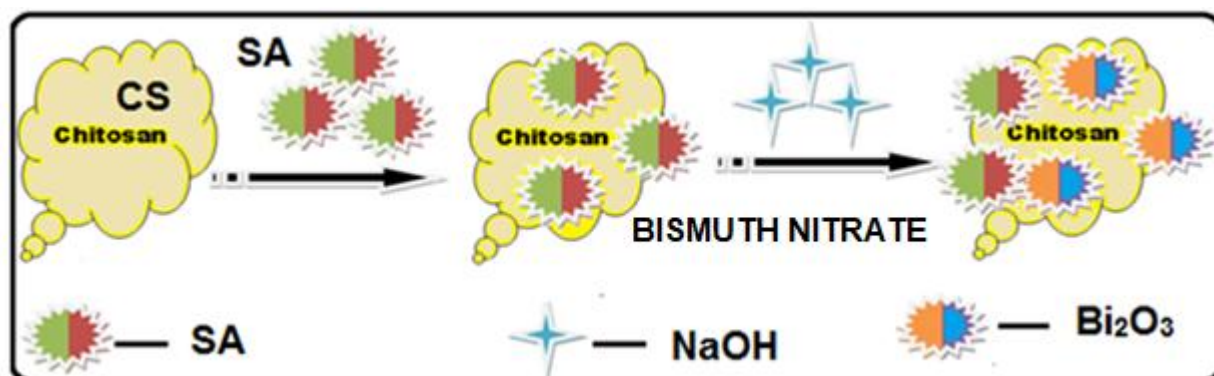
In this paper, we used two polyelectrolytes, chitosan (CS) and sodium alginate (SA), as templates to synthesize CS-Bi<sub>2</sub>O<sub>3</sub>-SA nanocomposites. Both chitosan (CS) and sodium alginate (SA) are naturally occurring polysaccharides, and widely investigated for photocatalytic applications. Grafting of Bi<sub>2</sub>O<sub>3</sub> in positively-charged CS and SA by electrostatic attraction. Their morphologies, structures, and photocatalytic performance in the degradation of methylene blue (MB) was characterized by scanning electron microscopy, transmission electron microscopy, X-ray diffraction spectroscopy, UV-vis absorption spectroscopy, and electrochemical impedance spectroscopy, respectively. The results show that the SA addition can enhance the photocatalytic performance of CS-Bi<sub>2</sub>O<sub>3</sub>-SA nanocomposites

**Keywords:** Chitosan, Bi<sub>2</sub>O<sub>3</sub>, Sodium alginate, Photocatalytic, Methylene blue

### Introduction

Sodium alginate (SA) and chitosan (CH) are very important biopolymers, with many relevant industrial applications, such as in the pharmaceutical industry where they are widely used as biomaterials, especially when intrinsic viscosity [ $\eta$ ] and viscosity average molar mass ( $M_v$ ) are known [1, 2]. Sodium alginate is an anionic polysaccharide formed by linear and unbranched chains of amorphous copolymers composed of two monomeric units, (1,4)- $\beta$ -linked D mannuronic acid (M) and (1,4)- $\alpha$ -linked L-guluronic acid (G), obtained from brown seaweeds [3]. Chitosan, a crystalline cationic polysaccharide, is produced commercially by deacetylation of chitin, with deacetylation degree (DD) ranging from 70 to 95% and molar mass in the range of 104-106 g/mol. Chitosan chains are composed essentially of (1,4)- $\beta$ -linked D-glucosamine units together with some proportion of N-acetyl- $\beta$ -D-glucosamine units [5]. The efficacy of chitosan depends on the respective molar mass and polydispersion values. If the former is known and there good understands of the conformation of the polymer in the solvent medium, the rheological and mechanical properties can be estimated [6]. Bi<sub>2</sub>O<sub>3</sub> has attracted considerable attention due to its high refractive index, dielectric permittivity, thermal stability and wide application in photocatalysis, gas sensors, capacitors, optical coatings, and photovoltaic cells. The band gap of Bi<sub>2</sub>O<sub>3</sub> is 2.58-2.85 eV, which has been proved to be good visible light driven photocatalyst for water splitting and pollutant decomposition. However, the quick recombination of photo-generated charge carriers has significantly decreased the photocatalytic performance of Bi<sub>2</sub>O<sub>3</sub> [7].

## Experimental Details



## Results and Discussion

The prepared hybrid composite CH-Bi<sub>2</sub>O<sub>3</sub>-SA was characterized and the functional groups of resultant for confirmed by FTIR, UV-vis. the CH-Bi<sub>2</sub>O<sub>3</sub> composite has good crystalline structure analysed by XRD. The surface morphology and photocatalytic performance in the degradation of methylene blue (MB) was determined by SEM analysis. The hybrid composite developed at photocatalytic degradation. The results demonstrate that the composite would be suitable for implant application in agricultural and biomedical sector.

## Conclusion

In this work, simple and economic, CH-Bi<sub>2</sub>O<sub>3</sub>-SA composite was photocatalytic activity in the degradation Of methylene blue under UV irradiation.

## Reference

- D. Gomez-Diaz, J.M. Navaza, Rheology of aqueous solutions of food additives Effect of concentration, temperature and blending, *J. Food Eng.* 56 (2003) 387-392.
- M.P.M. Costa, I.L.M. Ferreira, M.T.M. Cruz, New polyelectrolyte complex from pectin/chitosan and montmorillonite clay, *Carbohydr. Polym.* 146 (2016) 123-130.
- J. Comaposada, P. Gou, B. Marcos, J. Arnau, Physical properties of sodium alginate solutions and edible wet calcium alginate coatings, *LWT - Food Sci. Technol.* 64 (2015) 212-219.
- F. Belalia, N-E. Djelali, Rheological properties of sodium alginate solutions, *Rev.Roum. Chim.* 59 (2014) 135-145.
- J. Yang, J. Chen, D. Pan, Y. Wan, Z. Wang, PH-sensitive interpenetrating network hydrogels based on chitosan derivatives and alginate for oral drug delivery, *Carbohydr.Polym.* 92 (2013) 719– 725.
- M.R. Kassai, Calculation of Mark–Houwink–Sakurada (MHS) equation viscometric constants for chitosan in any solvent–temperature system using experimental reported viscometric constants data, *Carbohydr. Polym.* 68 (2007) 477–488.
- X. Liu, L. Pan, T. Lv, Z. Sun, C.Q. Sun, Visible light photocatalytic degradation of dyes by bismuth: Oxide-reduced graphene oxide composites prepared via: Microwave-assisted method, *Journal of Colloid and Interface Science.* 408 (2013)

**PP 29**    **Fibrous Silicon nanosphere tethered N-Heterocyclic Carbene complexes: Synthesis and its Catalytic application****Saravanakumar Shanmuganathan<sup>\*§</sup>,**<sup>§</sup>*Department of Energy Science, Alagappa University, Karaikudi, India.*

Combing the advantage of homogenous catalysis on heterogeneous surface might provide an ultimate momentum in the field of sustainable catalytic technologies [1]. For versatile catalytic application, single-site catalyst on solid supports can be protected with covalently linked organic molecules to may provide enhanced dispersity in solvents [2]. Among the nanostructure supported single site catalysts have drawn considerable attention recently [1]. The stability of inorganic matrix is important in redox environment, therefore the majority of heterogeneous catalysts come from silica supports [3]. Silica supported catalysts are advantageous over zeolite encapsulated catalysts [4]. Notably high surface area silica nanosphere (KCC) displays excellent properties such as high surface area, pore volume, pore size and durable mechanical properties [5a-b]. Particularly KCC shows excellent fibrous morphology which may attributes its high performance as catalyst support in overall. In this work, we have prepared fibrous silica nanosphere on covalently grafted Ruthenium/Copper/Silver N-Heterocyclic Carbene complexes **Figure 1** [6]. The synthesis was achieved by convenient direct transmetallation and followed sol-gel process. Different synthetic routes to these complexes will be outlined. The structural morphology of these new materials will be presented along with preliminary results from their catalytic testing.

**Figure 1: Fibrous Nanosphere Silica Supported Metal-N-heterocyclic Carbene Complexes.****Reference**

- C. Christophe, C.V Aleix, C.P Matthew, D.P Estes, A. Fedorov, V. Mougel, H. Nagae, F. Núñez-Zarur, P. A. Zhizhko *Chem. Rev.*, 2016, 116 (2), 323–421
- MacQuarrie, S.; Nohair, B.; Horton, J. H.; Kaliaguine, S. *Crudden, C. M J. Phys. Chem. C* 2010, 114, 57–64.
- M. Opanasenko, P. Stepnicka, J. Cejka., *RSC Adv.* 2014, 4, 65137–65162.
- S Saravanakumar, L. Greiner, P. Dominguez, *Tetrahedron letters* 2010, 51, 6670-6672.

- C. T. Kresge, M. E. Leonowicz, W. J. Roth, J. C. Vartuli, J. S. Beck, *Nature* 1992, 359, 710–712;  
V. Polshettiwar, D. Cha, X. Zhang, J. M. Basset, *Angew. Chem. Int. Ed.* 2010, 49, 9652–  
9656; *Angew. Chem.* 2010, 122, 9846–9850.  
S. Saravanakumar, manuscript in preparation.

## **PP 30** Preparation and Characterization of Chitin-Bi<sub>2</sub>O<sub>3</sub> Composite for Higher Antibacterial Activity

**Pragathambal. M, Revathi. T, Thambidurai. S\***

*Department of Industrial Chemistry, School of Chemical Sciences,  
Alagappa University, Karaikudi - 630003, Tamil Nadu, India.*

*Email:sthambi01@yahoo.co.in*

### **Abstract**

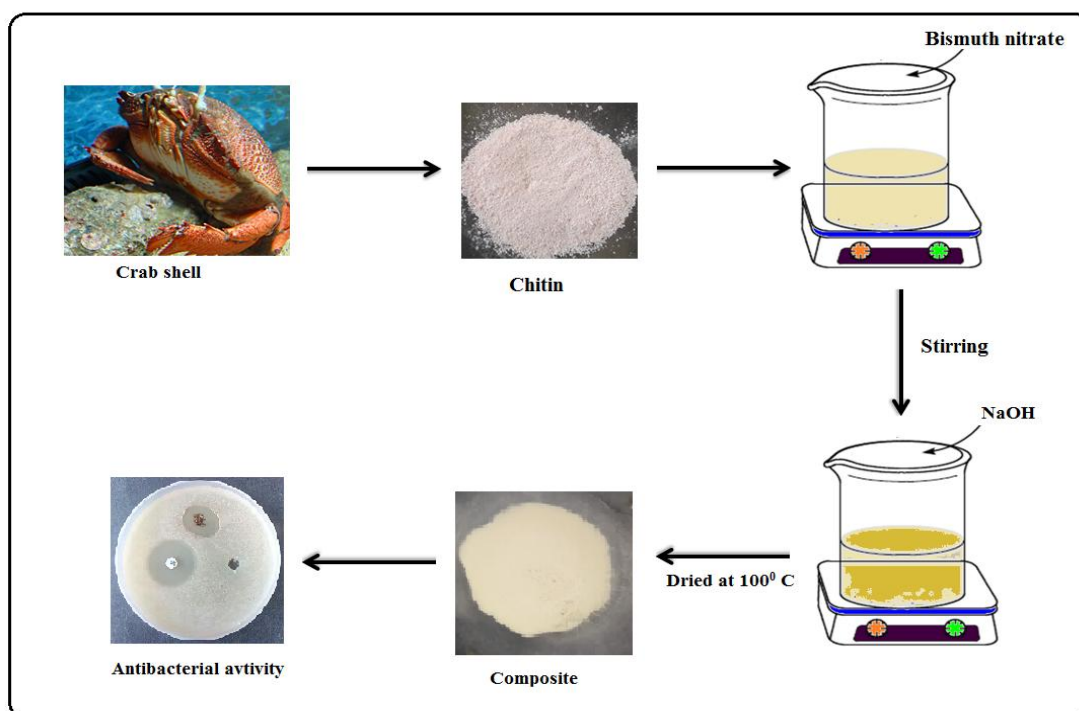
In the present work, composites are prepared by co-precipitation method. The composites were prepared by using chitin as biosurfactant, bismuth oxide as a source material and NaOH as a precipitating agent. The prepared composite was characterized and the functional groups confirmed by Fourier transform infrared spectroscopy (FT-IR). The optical properties of composite are analyzed by UV-Vis DRS spectroscopy. The crystalline size of composite was calculated by X-ray diffraction analysis (XRD). The surface morphology was analyzed by Scanning Electron Microscopy (SEM). The chitin-Bi<sub>2</sub>O<sub>3</sub> composite exhibited antibacterial activity against gram positive as well as gram negative microorganisms. The composite material has higher antibacterial activity compared to chitin. The results demonstrate that composite can be promising materials for medical and tissue engineering applications.

**Keywords:** Chitin, Bismuth Oxide, Composite, Antibacterial activity.

### **Introduction**

Chitin is a linear polysaccharide composed of  $\beta$ -(1-4)-linked 2-acetamido-2-deoxy-d-glucose units, and is insoluble in common solvents, when has limited the further utilization of the natural biopolymer to a small area and biological activities. It is the main structural component of the exoskeletons of animals like insects and crustaceans. Crab, shrimp and fish scale waste is ideal raw material for chitin production. Bi<sub>2</sub>O<sub>3</sub> is a well-popular transition metal oxide. It has been investigated extensively due to its optical and electrical properties such as refractive index, large energy band gap, dielectric permittivity as well as remarkable photoluminescence and photoconductivity. Several organometallic bismuth compounds are used in bactericidal and fungicidal applications.

## Experimental Details



## Result and Discussion

In this work, demineralization and deproteinization process were applied for crab shell and chitin was obtained. The prepared chitin-  $\text{Bi}_2\text{O}_3$  composite have been characterized. The functional groups of resultant matrix from chitin, metal oxide were characterized and confirmed by FTIR, UV-Vis DRS and XRD analysis. Evaluating the antibacterial activity of biopolymer connected on bismuth oxide and surface morphology was analyzed by SEM. The results demonstrate that the composite can be promising materials for medical and tissue engineering applications.

## Conclusion

The prepared chitin-  $\text{Bi}_2\text{O}_3$  composite exhibited excellent crystallinity and antibacterial activities. It is concluded that these composite may be applied for biomedical applications.

## References

- A. Sila, N. Mlaik, N. Sayari, R. Balti, A. Bougatef, Chitin and chitosan extracted from shrimp waste using fish proteases aided process: efficiency of chitosan in the treatment of unhairing effluents, *J. Polym. Environ.* 22 (2014) 78-87.
- Hilip Domenico, Richard J. Salo, Sabrina G. Novick, Paul E. Schoch, Ken Van Horn, And Burke A. Cunha, Enhancement of Bismuth Antibacterial Activity with Lipophilic Thiol Chelatorss, antimicrobial agents and chemotherapy, 41 (1997) 1697–1703.

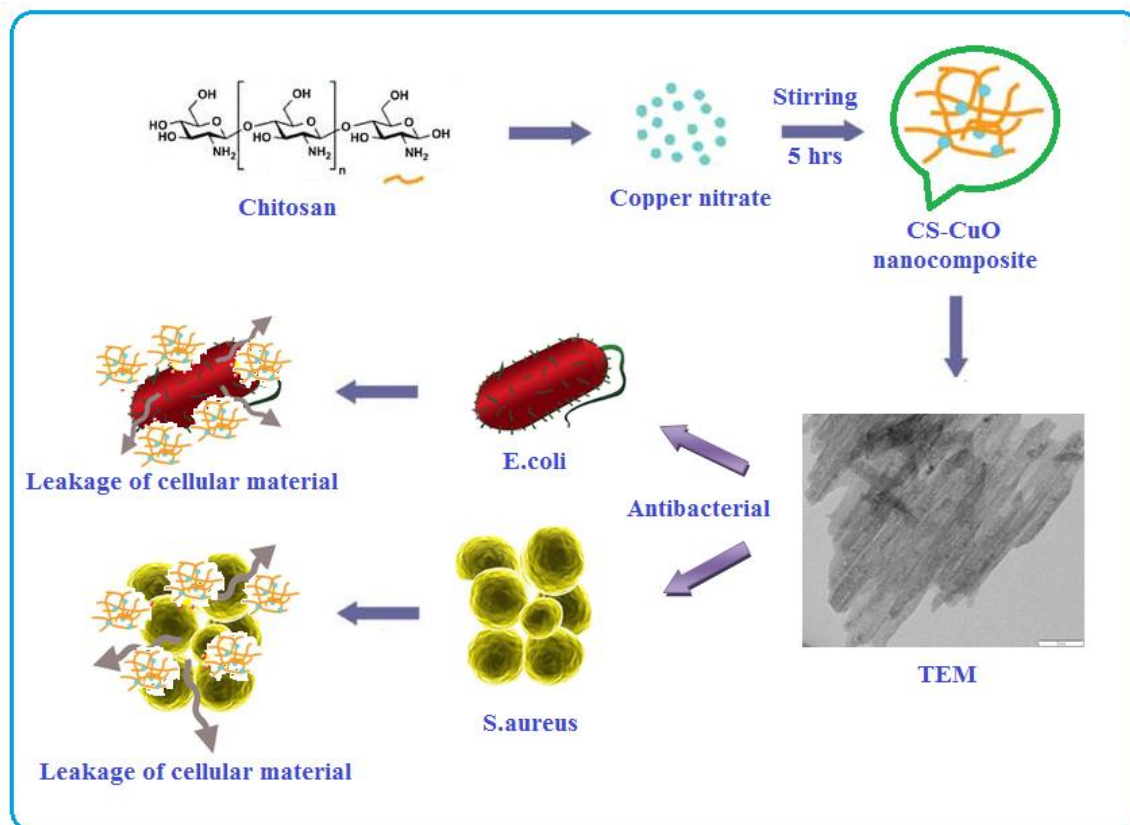
**PP 31** Layer Structured Chitosan-Copper Oxide Nanocomposites for Better Thermal and Antibacterial Activity**T. Revathi, S.Thambidurai\****Bio-nanomaterials Research Lab, Department of Industrial Chemistry,  
School of Chemical Sciences, Alagappa University,  
Karaikudi-630003, Tamil Nadu, India.**Email: [sthambi01@yahoo.co.in](mailto:sthambi01@yahoo.co.in), [revathimahesh22@gmail.com](mailto:revathimahesh22@gmail.com)***Abstract**

Recently, microbial threats on human health and safety have become a serious public threat. To fight and prevent disease, a great effort has been devoted to the development of new and efficient antimicrobial materials. Particularly, inorganic antibacterial agents exhibit better performance than organic ones in durability, heat resistant and low occurrence of antibiotic-resistant bacteria, which open the possibility of formulation of a new generation of bactericidal materials. Chitosan is a fully biodegradable and biocompatible natural polymer and can be used as an adhesive as well as antibacterial and antifungal agent. The primary amine and hydroxyl groups of chitosan exhibit very strong affinity towards metal ions for the control of particle size and prevent its agglomeration. CuO is a p-type semiconductor with narrow band gap of 1.2eV. Copper oxide nanoparticles are attractive due to their easy availability, low cost and good thermal conductivity besides their use in areas such as catalysis, electronics and coating.

A natural and inorganic material of chitosan-copper oxide (CS-CuO) nanocomposite was prepared by simple co-precipitation method. The synthesized nanocomposites were analyzed by X-ray diffraction (XRD), Fourier transform infrared spectroscopy (FT-IR), Ultraviolet visible spectroscopy (UV-Vis), Higher resolution scanning electron microscopy (HR-SEM), Transmission electron microscopy (TEM) and Thermal gravimetric analysis (TGA). From the results, the CS-CuO nanocomposite showed layer and rod like structure confirmed by HR-SEM and TEM analysis. From the FTIR spectra, the various functional groups present in the CS-CuO nanocomposite were observed. The crystalline structure of CS-CuO nanocomposite was confirmed in XRD patterns. Thermo gravimetric analysis showed that the as-prepared CS-CuO nanocomposite possessed better thermal stability than chitosan. The antibacterial activities were tested against gram-positive *Staphylococcus aureus* (*S. aureus*) and gram negative *Escherichia coli* (*E.coli*) bacteria by agar well diffusion method and a better antibacterial activity was observed in CS-CuO nanocomposite. Thus the CS-CuO has enhanced antibacterial activity and can be suggested as a promising material for numerous biomedical applications.

**Keywords:** Chitosan, CuO, TEM, Thermal stability, Antibacterial activity.





## References

- N. Cioffi, L. Torsi, N. Ditaranto, G. Tantillo, L. Ghibelli, L. Sabbatini, T. Bleve-Zacheo, M. D'Alessio, P. Zambonin, E. Traversa, Copper nanoparticle/polymer composites with antifungal and bacteriostatic properties, *Chem. Mater.* 17 (2005) 5255–5262.
- S. Mallick, S. Sharma, M. Banerjee, S.S. Ghosh, A. Chattopadhyay, A. Paul, Iodine-stabilized Cu nanoparticle chitosan composite for antibacterial applications *ACS Appl. Mater. Interfaces* 4 (2012) 1313–1323.
- M.N.V.R. Kumar, A review of chitin and chitosan applications, *Reactive Functional Polymers* 46 (2000) 1–27.
- J. Lee, J.S. Choi, M. Yoon, Fabrication of ZnO nanoplates for visible light-induced imaging of living cells, *J. Mater. Chem. B* 2 (2014) 2311–2317.
- A. Angi, D. Sanli, C. Erkey, O. Birer, Catalytic activity of copper (II) oxide prepared via ultrasound assisted Fenton-like reaction, *Ultrason. Sonochem.* 21(2014) 854–859.

**PP 32**    **Synthesis and Characterization of Chitin-ZnO Composite for Excellent Antibacterial Activity****Roshni. A, Revathi.T, Thambidurai.S\****\*Department of Industrial Chemistry, School of Chemical Sciences,  
Alagappa University, Karaikudi - 630003, Tamil Nadu, India.**Email: sthambi01@yahoo.co.in***Abstract**

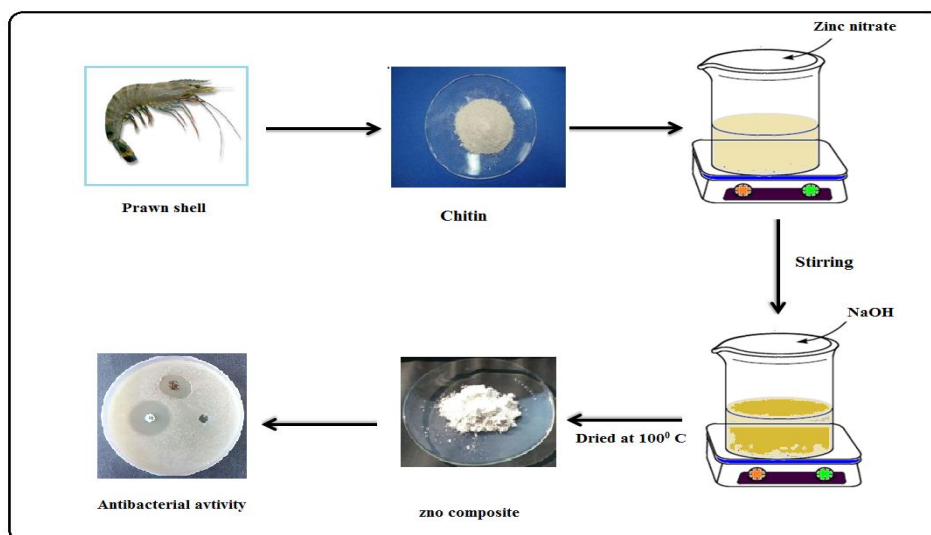
In this work, Chitin was isolated from prawn shell wastes. The chitin-ZnO Composites are prepared by chemical precipitation method. The composites were prepared by using chitin as biosurfactant, zinc nitrate as a source material and NaOH as a precipitating agent. The prepared composite was characterized and the functional groups confirmed by fourier transform infrared spectroscopy (FT-IR). The optical properties of composite are studied by UV-Vis DRS spectroscopy. The structure and properties of the composite membranes were characterized with X-ray diffraction (XRD), scanning electron microscopy (SEM). The chitin-ZnO composite exhibited antibacterial activity against gram positive (*S.aureus*) as well as gram negative (*E.coli*) microorganisms. The chitin-ZnO composite material showed excellent antibacterial activity. The enhancement of mechanical properties and the results of antibacterial of the composites also evaluated and revealed the composite would be a suitable candidate for implant application in biomedical field.

**Keywords:** Chitin, ZnO, Composite, Antibacterial activity.

**Introduction**

Chitin is the second most abundant natural biopolymer after cellulose. The chemical structure of chitin is comparable to that of cellulose and the 2hydroxy group on each sugar unit of cellulose is replaced with acetamido to give chitin, i.e., $\beta$ -(1 $\rightarrow$ 4)-linked N-acetylglucosamine polymer. Chitin is found in many places throughout the natural world, especially in the shells of crustaceans such as crabs, lobsters and shrimps. Zinc oxide (ZnO) nanoparticles are used as a semiconductor with wide band gap of 3.2–3.37 eV. ZnO is a polar crystal with hexagonal phase, air-stable and environmental friendly, which has been explored for a wide range of applications in nano scale devices such as nano generators, sensors, field-emission transistors ultra violet photo-detectors and in biomedical systems as ultra sensitive DNA sequence detectors.

## Experimental Details



## Results and Discussion

In this study, demineralization and deproteinization process were carried out for prawn shell and chitin was obtained. The synthesized chitin-ZnO composite have been characterized. The functional groups of resultant matrix from chitin, zinc oxide were characterized and confirmed by FTIR, UV-Vis DRS. The chitin-ZnO composite has good crystalline structure. The surface morphology was studied by SEM analysis. The chitin-ZnO composite exhibited good antibacterial activity against *S. aureus* and *E. coli*.

## Conclusion

In this study, a simple and economic biological process has been developed to synthesized chitin-ZnO composite. The inorganic-natural polymer materials would have great potential in biomedical applications.

## References

- S. Ifuku, S. Morooka, A.N. Nakagaito, M. Morimoto, H. Saimoto, Preparation and characterization of optically transparent chitin nanofiber/(meth)acrylic resin composites, *Green. Chem.* 13 (2011) 1708–1711.
- S. Anandhavelu, S. Thambidurai, Effect of zinc chloride and sodium hydroxide concentration on the optical property of chitosan-ZnO nanostructure prepared in chitin deacetylation, *Materials Chemistry and Physics* 131 (2011) 449–454.

## **PP 33** An Ionic Liquid Mediated Synthesis of Silver/Zinc Oxide Nanoparticles Intercalated into Bentonite and Their Biological Activities

**K. Bama and M. Sundrarajan\***

*\*Advanced Green Chemistry Lab, Department of Industrial Chemistry, School of Chemical Sciences, Alagappa University, Karaikudi -3, Tamil Nadu, India.*

### **Abstract**

In ionic liquid mediated synthesized of silver/zinc oxide/bentonite clay inorganic hybrid nanocomposite were prepared via thermal decomposition method. The synthesized nanocomposite was analyzed by using suitable characterizations. Furthermore, the thermal decomposition method indicated that  $\text{Ag}^+/\text{ZnO}$  were not released from the nanocomposite and agar well diffusion method confirmed that nanocomposite were active against the Gram-positive, Gram-negative bacteria and cytotoxicity behavior. In general, these results revealed that the new and excellent  $\text{Ag}/\text{ZnO}/\text{bent}/\text{IL}$  nanocomposite could be a low releasing nanocomposite with excellent antibacterial and cytotoxicity activity.

**Keywords:**  $\text{Ag}/\text{ZnO}/\text{bent}$  nanocomposite, Ionic liquid, Antibacterial activity, Cytotoxicity behavior.

### **Introduction**

$\text{Ag}/\text{ZnO}$  nanoparticles could be widely applied in environmental remediation because of their easy availability, stability, nontoxicity, cost-effective, and eco-friendly nature [1]. However, antibacterial and cytotoxicity behavior of  $\text{Ag}/\text{ZnO}$  nanoparticles have not been extensively studied, likely due to an increased tendency of aggregation, which decreases its long-term biological applications. Bentonite (bent), which consists of more than 70 % predominate compound of montmorillonite clay material, it has 2:1 layer of aluminosilicate structure and it is composed of two tetrahedral sheets sandwiched by an octahedral sheet [2]. Bentonite clay minerals are widely used as a filler/substrate with many metal and metal oxides. Bentonite clay is exceptional eco-friendly and cost-effective filler/substrate for  $\text{Ag}/\text{ZnO}$  composite. N-trimethyl-N-propylammonium bis(trifluoromethanesulfonyl) imide (IL -  $\text{C}_8\text{H}_{16}\text{F}_6\text{N}_2\text{O}_4\text{S}_2$ ) ionic liquid, its act as a capping agent for the synthesis of  $\text{Ag}/\text{ZnO}$  nanoparticles in  $\text{Ag}/\text{ZnO}/\text{bent}/\text{IL}$  nanocomposite. In this innovative work and newly approach, we have been advanced and introduced the green synthesis of silver/zinc oxide/bentonite/ionic liquid ( $\text{Ag}/\text{ZnO}/\text{bent}/\text{IL}$ ) nanocomposite by advanced method of thermal decomposition technique as shown in Figure 1.

### **Results and discussion**

The synthesized  $\text{Ag}/\text{ZnO}$  nanocomposite supported on bent was characterized by XRD, FT-IR, UV-DRS, SEM with EDX-mapping, and TEM techniques. Quasi-spherical sizes of Ag coated on ZnO nanoparticles intercalated into the bent layers were studied through SEM and TEM

analysis. The major peak of XRD at  $2\theta = 38.3^\circ$ ,  $44.3^\circ$ ,  $31.5^\circ$ , and  $47.5^\circ$ , which overlaps with the reflections of Ag and ZnO nanoparticles in Ag/ZnO/bent/IL nanocomposite [1]. The nanocomposite lattice plane of fcc of Ag and hexagonal phase of ZnO and average crystalline size of nanoparticles is 11.4 nm was calculated by Scherrer equation. In FT-IR analysis shows Ag/ZnO/bent/IL nanocomposite were confirm the presence of Ag and ZnO nanoparticles peaks at  $1383\text{ cm}^{-1}$ ,  $901\text{ cm}^{-1}$ , and  $835\text{ cm}^{-1}$  corresponds to the Ag/ZnO/bent/IL nanocomposite. In SEM and TEM analysis result shows the clearly exposes the size of nanoparticles were around ca. 50-100 nm in excellent spherical shape. The optical band-gap energies for Ag/ZnO/bent/IL nanocomposites, as estimated from the reflectance onset,  $E_g = 3.1\text{ eV}$  for an indirect band gap are higher than of bulk ZnO nanoparticles ( $E_g = 2.8\text{ eV}$ ), which is attributed to the quantum confinement effect arising from the small crystal size. Antibacterial activity was carried out using agar well diffusion method for human pathogenic bacteria like Gram-positive *Staphylococcus aureus* and Gram-negative *Escherichia coli*. The obtained results suggested that the Ag/ZnO/bent/IL nanocomposite have excellent antibacterial activity and cytotoxicity toward the HEK 293 cell line and  $IC_{50}$  values were calculated [2]. These results showed that this nanocomposite has probable to be used as antibacterial materials with cytotoxicity behavior.

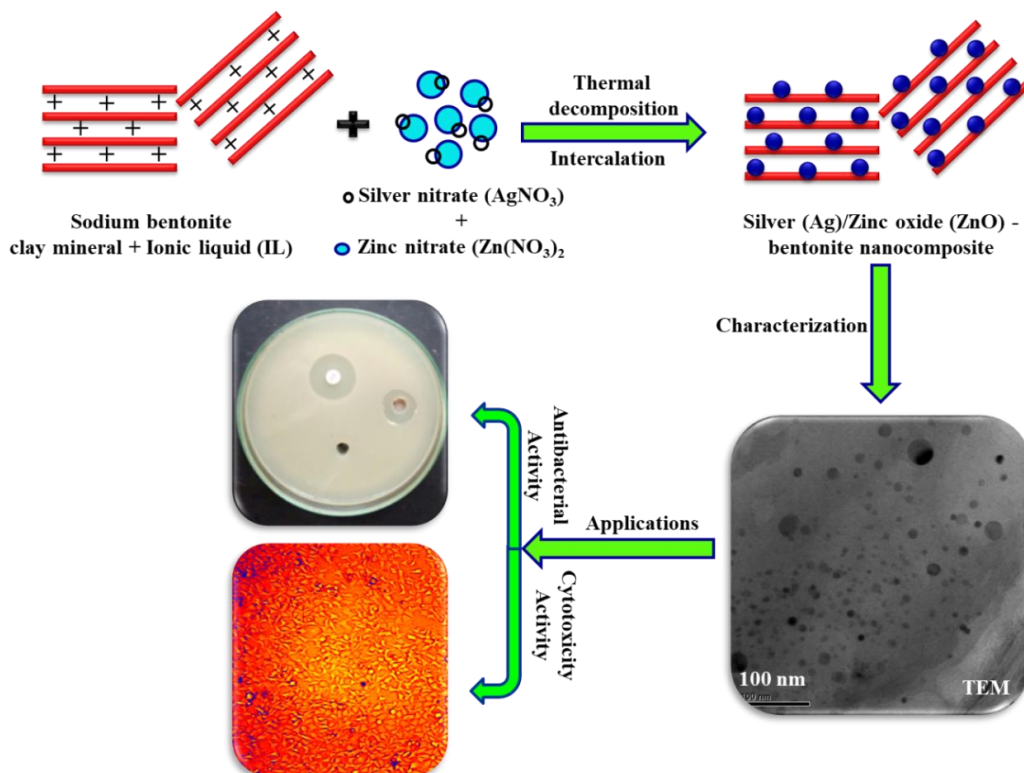


**Figure 1: Schematic representation of synthesized Ag/ZnO/bent/IL nanocomposite by thermal decomposition method**

## Conclusion

In conclusion, a single step, efficient, environment-friendly, fast and novel Ag/ZnO/bent nanocomposites have successfully synthesized in the presence of IL by thermal decomposition method. *S. aureus* has given excellent result than *E. coli* bacteria. In vitro studies showed that nanocomposite exhibited non-toxic effect against HEK 293 cell lines. It has potential applications in a wide variety of fields such as sportswear, socks, and medical textile.

## References

- Sarah C. Motshekga, Suprakas S. Ray, Maurice S. Onyango, Maggie N.B. Momba, Microwave-assisted synthesis, characterization and antibacterial activity of Ag/ZnO nanoparticles supported bentonite clay, *Journal of Hazardous Materials* 262 (2013) 439-446.
- Sh. Sohrabnezhad, M.J. Mehdipour Moghaddam, T. Salavatiyan, Synthesis and characterization of CuO-montmorillonite nanocomposite by thermal decomposition method and antibacterial activity of nanocomposite, *Spectrochimica Acta Part A: Molecular and Biomolecular Spectroscopy* 125 (2014) 73-78.

## PP 34 Green Synthesis of Silver Nanoparticles using *Morinda Citrifolia* Leaves Extract and their Antifungal Activity

P. Suganya<sup>a</sup>, K. Bama<sup>a</sup>, M. Bhavani<sup>a</sup>, K. Bharathi<sup>b</sup>, M. Sundrarajan<sup>a\*</sup>

<sup>a</sup>Advanced Green Chemistry Lab, Department of Industrial Chemistry, School of Chemical Sciences, Alagappa University, Karaikudi - 600 003, Tamil Nadu, India.

\*Corresponding author: [drmsgreenchemistrylab@gmail.com](mailto:drmsgreenchemistrylab@gmail.com)

<sup>b</sup>Department of Chemistry, Poompohar college (Autonomous), Melaiyur 609107, Tamil Nadu.

## Abstract

In the present work, we describe the synthesis of silver (Ag) nanoparticles using an aqueous leaves extract of *Morinda citrifolia*. XRD, FT-IR, and SEM were performed to characterize the formation of Ag nanoparticles. In addition these biologically synthesized nanoparticles were also proved to exhibit excellent antifungal activity on *Candida albicans* fungi.

**Keywords:** *Morinda citrifolia*, silver nanoparticles, Hydrothermal method.

## Introduction

Silver nanoparticles have proved to be most effective as it has good efficacy against fungi, bacteria, viruses and other eukaryotic micro-organisms [1]. Silver nanoparticles have been studied for their antimicrobial potential and have proven to be antibacterial agents against both bacteria and antiviral agents against the HIV-1 hepatitis B virus respiratory syncytial virus herpes simplex virus type and monkey pox virus. Green synthesis of silver nanoparticles was carried out using boiling extract of *Morinda citrifolia* as capping and reducing agents [2]. In this work, we synthesized silver (Ag) nanoparticles using leaf extract of *Morinda citrifolia* by the hydrothermal method.

## Experimental Details

Silver nitrate ( $\text{AgNO}_3$ ) was purchased from Sigma Aldrich Pvt. Ltd. Aqueous solution of 1mM  $\text{AgNO}_3$  was used for the synthesis of silver nanoparticles. The reaction mixture as prepared by adding 5 ml of the plant crude extracts to 95 ml of 1mM  $\text{AgNO}_3$  solution in a 100 ml Teflon stainless steel vessel. Then, the resulting mixture was sealed in a stainless steel autoclave and maintained at  $180^\circ\text{C}$  for 3 h. After the reaction was completed, the autoclave was cooled down to room temperature naturally. The products were collected by centrifuged and washed with water and ethanol five times, respectively. Then, they were dispersed in ethanol for further characterization. Schematic illustration of silver nanoparticles using leaves extract by hydrothermal method as shown in Figure 1.

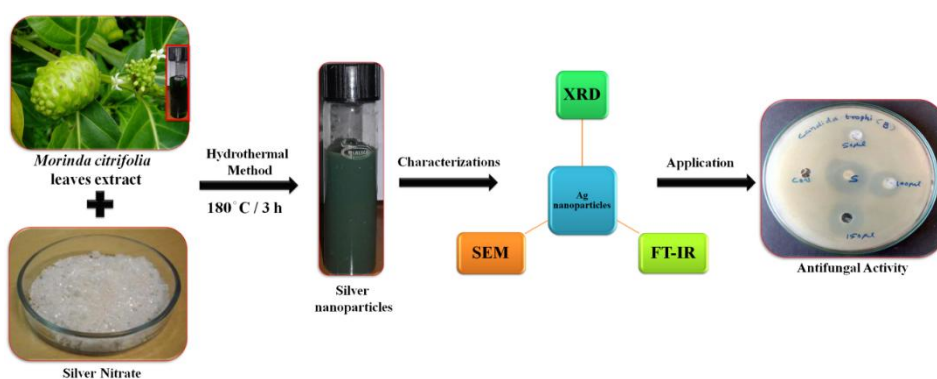


**Figure 1: Synthesis of silver nanoparticles using *M. citrifolia* leaves extract by hydrothermal method**

## Results and Discussion

The synthesized silver nanoparticles were characterized by X-ray Diffraction (XRD), Fourier Transmission Infrared (FT-IR), and Scanning Electron Microscope (SEM). The synthesized Ag nanoparticles were characterized by major peak at  $38.5^\circ$ ,  $44.6^\circ$ ,  $64.5^\circ$  and  $78.2^\circ$  corresponds to the (111), (200), (220), and (311) lattice plane of face centred cubic (fcc - JCPDS card no: 87-0720) Ag phase and average crystalline size of nanoparticles is 10 nm. The XRD pattern synthesized Ag nanoparticles using the leaves extract of *Morinda citrifolia* is depicted. The FT-IR result showed that Ag nanoparticles synthesized by *Morinda citrifolia* leaves extract showed band at  $1380\text{ cm}^{-1}$  and  $460\text{ cm}^{-1}$  due to Ag nanoparticles. In SEM analysis, the synthesized *Morinda citrifolia* Ag nanoparticles shows less aggregation with particles are spherical in shape and the size ranges from 10 to 30 nm in diameter with an average size of 20 to 30 nm. The results medicated, that the Ag nanoparticles observed inhibitory actions against harmful human pathogens. Antifungal activity was carried out using potato dextrose agar method for human pathogenic fungal such as *Candida albicans*[2]. The zone of inhibition was observed and expressed in millimetre (mm). Ag nanoparticles are effective bactericidal effect. Hence, in the

present investigation, green synthesis of silver nanoparticles using the leaf extract of *Morinda citrifolia* and their antifungal activities are presented and discussed.

### Conclusion

The present study investigated a simple eco-friendly approach for synthesis of Ag nanoparticles using aqueous plant extracts of *Morinda citrifolia* leaves. The *M. citrifolia* leaves powder extracts containing Ag nanoparticles were characterized by the XRD, FT-IR and SEM. Hence, in the present investigation, antifungal activities are presented and discussed.

### Reference

- Asha R Pai, Kavitha S, Shweta Raj S, Priyanka P, Vrindha A, Vivin T. S, Silpa Sasidharan, Green Synthesis and Characterization of Silver Nanoparticles Using Fresh Leaf Extract of *Morinda citrifolia* and its Anti-microbial Activity Studies, International of Journal Pharmaceutical Science, 7 (2015) 0975-1491.
- M. Sundrarajan, K. Bama, M. Bhavani, S. Jegatheeswaran, S. Ambika, A. Sangili, P. Nithya, R.Sumathi, Obtaining Titanium Dioxide Nanoparticles with Spherical Shape and Antimicrobial Properties using *M. Citrifolia* Leaves Extract by Hydrothermal Method, Journal of Photochemistry and Photobiological, B: Biology, 171 (2017) 117-124.

## **PP 35** Analysis of toxic inorganic ions by FTIR, AAS, ICP-AES and IC in drinking water of Pullalakkottai village, Virudhunagar District, Tamil Nadu: A case Study

Subbiah Thangadurai\*, Ganesan Saravana kumar<sup>#</sup>, and Sundaramoorthy Marimuthu

\*Post Graduate Studies and Research Department of Chemistry  
Raja Doraisingam Government Arts College, Sivagangai – 630 561

<sup>#</sup>Quality Control Lab, Zirconium complex, Tuticorin – 628 152

### Abstract

Drinking water quality is a universal health concern with global impact. Water analysis is an important part of the chemical analysis of environmental samples. Analysis of common inorganic anions and cations in water is mandatory. A case study of water pollution of the ground water in Pullalakkottai village, Virudhunagar District, Tamil Nadu is presented to highlight the need for the remedial measures. In general, groundwater is less vulnerable to pollution than surface waters. There are a number of possible sources of man-made contaminants, some of which are more important than others. We have collected bore water samples from the aforementioned study area, which are giving water supply to these residences. During the analysis we have encountered certain inorganic ions viz. sodium ( $\text{Na}^+$ ), potassium ( $\text{K}^+$ ), ammonium ( $\text{NH}_4^+$ ), chloride ( $\text{Cl}^-$ ), cyanate ion ( $\text{OCN}^-$ ), phosphate ( $\text{PO}_4^{3-}$ ), thiocyanate ( $\text{SCN}^-$ ), nitrate ( $\text{NO}_3^-$ ), sulphite ( $\text{SO}_3^{2-}$ ), sulphate ( $\text{SO}_4^{2-}$ ) and perchlorate ( $\text{ClO}_4^-$ ) by micro chemical and FTIR methods. Several transition elements have toxic effects. The presence of aluminium ions in water can have



significant implication for patients who require kidney dialysis. However, the situation regarding the analysis of cations in environmental samples is quite different to the case for anions. Many rapid and sensitive spectroscopic methods such as AAS (atomic absorption spectroscopy) and ICP-AES (inductively coupled plasma atomic emission spectroscopy) are available for cation analysis. Ion chromatography (IC) has almost replaced most of the wet chemical methods used in water analysis. The analysis showed that the concentrations and its anions and other parameters exceeded the permissible limit as per drinking water specification of World Health Organization (WHO). Therefore, it has attracted widespread attention to the environmental community over the last decade due to concerns that it poses a risk of public health. Hence, it is recommended that suitable water quality management is essential to avoid any further contamination.

**Keywords:** Bore water, aluminium, nitrate, perchlorate, AAS, ICP-AES, IC

### **PP 36** A Novel Synthesis of Zinc Oxide Incorporated into $\beta$ -Cyclodextrin Nanocomposite by using Hydrothermal Method: Biological Activities

**L.R. Sangavi, K. Bama, M. Sundrarajan\***

*Advanced Green Chemistry Lab, Department of Industrial Chemistry,  
School of Chemical Sciences, Alagappa University, Karaikudi - 600 003, Tamil Nadu, India.*

*\*Corresponding author: [drmsgreenchemistrylab@gmail.com](mailto:drmsgreenchemistrylab@gmail.com)*

#### **Abstract**

Novel and innovative method of hydrothermal mediated synthesis has been carried out for obtaining stable, cost effective biomaterials of ZnO nanoparticles and  $\beta$ -CD/ZnO nanocomposites were prepared using zinc sulphate precursor in a greener way. The synthesis nanocomposite was analyzed suitable characterization by XRD, FT-IR, UV-Vis and RAMAN and SEM microscope. The antibacterial tests were done against Gram-negative by agar well diffusion method.

**Keywords:**  $\beta$ -Cyclodextrin, Zinc Oxide, Hydrothermal Method

#### **Introduction**

Beta-cyclodextrin ( $\beta$ -CD) is the 7-membered sugar ring molecular form of cyclodextrin and it has various applications. In the pharmaceutical industry, it can be used as complexing agent for increasing the solubility of poorly soluble drug as well as increasing their bioavailability and stability [1]. Zinc oxide (ZnO) is non-toxic in human body. ZnO is widely used to treat a variety of skin conditions, including dermatitis etc [2]. The present investigation describes for the first time, synthesis and characterization of  $\beta$ -CD/ZnO nanocomposites via hydrothermal method as well as  $\beta$ -CD used as capping agent for synthesis of ZnO nanoparticles. The antibacterial activity of  $\beta$ -CD/ZnO nanocomposites were done and to study the improved antibacterial activity.

### Experimental details

The  $\beta$ -CD/ZnO composites were prepared by hydrothermal method about 0.1 M of zinc sulphate ( $\text{ZnSO}_4$ ) was dissolved 0.1 M of sodium hydroxide and 0.1 g of  $\beta$ -CD. The mixture was stirred for 30 min. After the mixture taken to the autoclave for 24 that oven temperature ( $120^\circ\text{C}$ ) and then evaporated by decompress at  $100^\circ\text{C}$  to remove the water. The resulting solid products were dried in an oven. The grinding sample was calcinations at  $200^\circ\text{C}$  for 3 h used muffle furnace. After the calcinations process,  $\beta$ -CD/ZnO composites were obtained via hydrothermal method. Schematic illustration of  $\beta$ -CD/ZnO nanocomposite by using hydrothermal method is shown in Figure 1.

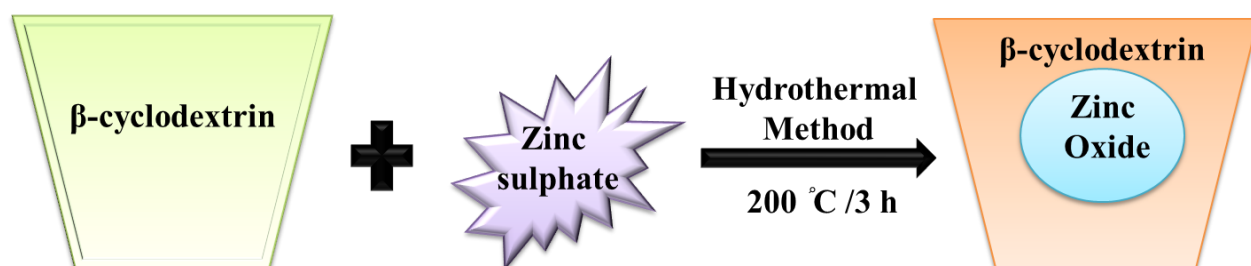


**Figure 1: Synthesis of  $\beta$ -CD/ ZnO nanocomposite by using simple hydrothermal method**

### Results and discussion

The composite cross-linking properties were confirmed by XRD, SEM, FT-IR, UV-Vis, and RAMAN Spectrum analysis. The coated nanocomposite is clearly shown in SEM image. The X-ray diffraction of  $\beta$ -CD/ZnO nanocomposites, X-ray diffraction pattern is used to confirm the phase, purity, average particle size and overall crystallinity of the synthesized nanoparticles and nanocomposites, from the peaks at  $2\theta = 31^\circ, 34^\circ, 36^\circ, 47^\circ, 56^\circ, 62^\circ, 67^\circ$  and  $68^\circ$  of ZnO nanoparticles are corresponding to (100), (002), (101), (102), (110), (103), (112) and (201) in the JCPDS data card 89-1397 [2]. The  $\beta$ -CD/ZnO nanocomposite has been successfully synthesized and the functional groups of the composite confirmed by FT-IR studies. The FT-IR spectra of bare ZnO nanoparticles exhibit peaks at  $3382\text{ cm}^{-1}, 2927\text{ cm}^{-1}, 1080\text{ cm}^{-1}, 866\text{ cm}^{-1}$  and  $400\text{ cm}^{-1}$  represent due to the multi hydroxyl group of  $\beta$ -CD, asymmetric  $-\text{CH}_3$ , C-O stretching vibration, and Zn-O, Zn-Zn bond stretching vibrations. The UV-Vis analysis of  $\beta$ -CD/ZnO nanocomposites, the absorption peak again damped and blue shifted from  $397\text{ nm}$  to  $382\text{ nm}$  for  $\beta$ -CD/ZnO nanocomposites when ZnO nanoparticles incorporated into  $\beta$ -CD nanocomposite. The SEM and RAMAN spectrum indicated the spherical shape ZnO nanoparticles calcined at  $200^\circ\text{C}$  for 3 h which were present in pure form of nanocomposite. The spectrum of ZnO nanoparticle reveals two Raman burly peaks at  $444\text{ cm}^{-1}$  and  $611\text{ cm}^{-1}$ . The antibacterial activity of  $\beta$ -CD/ZnO nanocomposites was examined against *E.coli* among Gram-negative bacterium [1].

## Conclusion

The  $\beta$ -CD/ZnO nanocomposites have been synthesized via hydrothermal method. The composites cross-linking properties were confirmed by XRD, SEM, FT-IR, UV-Vis, RAMAN spectrum analysis. The antibacterial activities were studied using bacteria *E. coli*. The composite were well performed and strong antibacterial activity against *E. coli* bacteria.

## References

- S. Selvam, R. Rajiv Gandhi, J. Suresh, S. Gowri, S. Ravikumar, M. Sundrarajan, Antibacterial effect of naval synthesized sulfated  $\beta$ -Cyclodextrin crosslinked cotton fabric and its improved antibacterial activities with ZnO, TiO<sub>2</sub> and Ag nanoparticles coating. International Journal of Pharmaceutics, 434 (2012) 366-374.
- Chunmeiwang, Jinxin He. Research on the multifunction fabric loaded with nano-ZnO and  $\beta$ -Cyclodextrin. Advanced Materials Research, 1439 (2013) 332-334.

## **PP-37** Ionic Liquid Assisted Green Synthesis of Rare Earth Lanthanum Oxide Nanoparticles: Antibacterial and Morphology Properties

V. Muthulakshmi<sup>1</sup>, M. Balaji<sup>1</sup>, P. Nithya<sup>1</sup>, A. Surya<sup>1</sup>, and M. Sundrarajan<sup>1\*</sup>

Advanced Green Chemistry Lab, Department of Industrial Chemistry,  
School of Chemical Sciences, Alagappa University, Karaikudi-3, Tamil Nadu, India

\*Corresponding author: Tel: + 91 94444 96151

E-mail: drmsgreenchemistrylab@gmail.com

## Abstract

An environmental friendly approach is introduced for the ionic liquid assisted synthesis of rare earth Lanthanum Oxide Nano Particles (La<sub>2</sub>O<sub>3</sub> NPs) using the *Andrographis paniculata* plant extract. The crystallinity temperature to produce La<sub>2</sub>O<sub>3</sub> NPs was determined by TG-DTA studies. The prepared La<sub>2</sub>O<sub>3</sub> NPs were characterized by XRD, FTIR, Laser-Raman, SEM with EDX and TEM to confirm the formation of nanosized particles. Optical properties of La<sub>2</sub>O<sub>3</sub> NPs were analyzed by UV-Vis and PL studies.

**Keywords:** La<sub>2</sub>O<sub>3</sub> NPs, *Andrographis paniculata*, Morphology, Antibacterial Activity.

## Introduction

Lanthanum oxide nanoparticles have been extensively studied owing to their exceptional luminescence, magnetic and electronic properties, which are significantly different from those of bulk materials. Its used to develop ferro electric materials, as a components of optical materials and is a feed stock for certain catalysts. *Andrographis paniculata* (*A.paniculata*) is an important medicinal plant which belongs to the family Acanthaceae and used as a traditional herbal medicine plant. *A. paniculata* has been reported to have a broadrange of pharmacological effects

including anti-cancer, anti-diarrheal and anti-inflammatory. Aqueous extract of *A. paniculata* was more potent than ethanolic extract in anti-oxidant activities.

### Experimental Details

For the synthesis of rare earth  $\text{La}_2\text{O}_3$  NPs (Figure:1) prepared by greener method of Lanthanum chloride hexa hydrate  $[\text{LaCl}_3 \cdot 6\text{H}_2\text{O}]$  used as a precursor with environment benign of *A. paniculata* plant extract and  $[\text{BMIM}]\text{PF}_6$  ILs is a capping agent. Lanthanum Chloride solution (0.1 N), and 1 mL  $[\text{BMIM}]\text{PF}_6$  (IL) were added to the ethanolic solution of *A. Paniculata* plant extract and stirred for 4 hours continuously at room temperature. Then the solution are transferred into a 60 mL Teflon-lined stainless steel autoclave, followed by heat treatment at  $120^\circ\text{C}$  for 6 hours. The resulted precipitate was centrifuged and finally dried at  $100^\circ\text{C}$  overnight to evaporate water. The powdered samples will finally grinded using mortar and pestle and calcinated in a muffle furnace 4 hours at  $600^\circ\text{C}$  to get  $\text{La}_2\text{O}_3$  NPs.

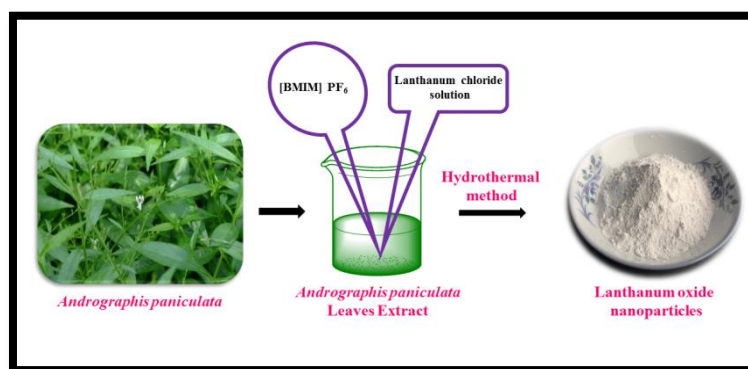


Figure: 1

### Results and Discussion

The prepared  $\text{La}_2\text{O}_3$  NPs characterized by various method such as, structural property was studied by Powder X-ray diffraction (XRD), the functional group studied by Fourier transform-infrared and Laser Raman spectroscopy, the optical property analyzed by Ultraviolet (UV-vis) and photoluminescence spectroscopy, the thermal behavior discussed by TG-DTA analysis, the surface morphology was discussed by SEM with EDX and TEM. In FT-IR analysis the peak at  $3453$  and  $3418\text{ cm}^{-1}$  indicate the presence of OH stretching vibration. The C=O asymmetric and symmetric stretching vibration peaks were observed at  $1504$  and  $1461\text{ cm}^{-1}$ .

In XRD the peak at  $25.2860$ ,  $26.7180$ ,  $30.8467$  and  $34.0527$  were conformed the crystalline nature and formation of a body-centered cubic structure of the  $\text{La}_2\text{O}_3$  NPs. The photoluminescence emission peak observed at violet region at  $419\text{ nm}$  with excitation wavelength at  $220\text{ nm}$ . The SEM image explores the formation of honeycomb structure as well as spheroid and cubic structure of  $\text{La}_2\text{O}_3$  NPs at higher magnification of the spheroid particles average diameter measured  $540.5\text{ nm}$  using by garden.inc digital micrograph software.

## Conclusion

Green synthesis of rare earth  $\text{La}_2\text{O}_3$  NPs have been successfully synthesized by ionic liquid assisted hydrothermal method using *A.Paniculata* plant extract. It was found that the reaction parameters determined such as crystal structure and morphology. The nanoparticles appeared to be honeycomb structure as well as spheroid in shape. The  $\text{La}_2\text{O}_3$  NPs confirmed by UV-visible spectrophotometer, PL, FTIR, XRD and EDX techniques.

## References

- I. Avinash, P. Mohendra, B. Manisha, J. Nano. Research, 11 (2009) 2079-2085.  
C. Chiappe, M. Malvadi, C.S. Pomelli, Pure Appl. Chem, 81 (2009) 767-776.  
S. K. Kannan and M. Sundrarajan, Journal of Nanoscience, 13[3] 2014, 1450018 – 1450025.  
P. Nithya, M. Balajia, S. Jegatheeswaran, S. Selvam and M. Sundrarajana, Journal of Photochemistry & Photobiology, B: Biology 178 2018, 481–488.

## **PP 38** Separation and Detection of Melamine in Milk-based products and Beverage products by TLC and HPTLC methods

S. Thangadurai<sup>1\*</sup>, K. Isabella Elavarasi<sup>1,2</sup>, G. Sivakavi<sup>1</sup>, C. Prabhakar<sup>1</sup>, A. Shankar<sup>1</sup> and M. Kaleeswari<sup>1</sup>

<sup>1</sup>Post Graduate Studies and Research Department of Chemistry  
Raja Doraisingam Government Arts College, Sivagangai – 630 561

<sup>2</sup>Department of Industrial Chemistry, Alagappa University, Karaikudi – 630 003

## Abstract

Melamine occurs as an environmental contaminant in foods and wastewater, and is considered to be released from melamine resin products into foods. Melamine containing large amount of nitrogen may be deliberately added to milk in order to increase the protein content for economic adulteration in food stuffs. The melamine contaminated milk powder contamination scandal occurred in China in 2008. Its main consequences so far have been urinary stone formation in children with associated renal damage and increased child mortality. Nine years have been passed, but food safety issues still remain of concern in the daily lives of millions of Chinese. Very little is known about the effects of excessive exposure to melamine contaminated milk powder in infants on growth, adolescent and adult health, although short-term effects have become apparent during the scandal. The adulteration of milk by melamine resulted in kidney illness, reproductive damage, bladder or kidney stone which can lead to bladder cancer. Nowadays, melamine was intentionally added to food and animal feed to boost the protein content in India. Applications of thin-layer chromatography (TLC) and high performance thin layer liquid chromatography (HPTLC) methods have been utilized for the separation and detection of melamine in milk based food products and beverage products. This study is able to accurately determine the melamine, fraudulently added, in protein supplements, commonly used from milk powder and beverage products. In this study, some milk-based dairy product samples and some

local brand beverages have been collected from the local market for the analysis of melamine by TLC and HPTLC. This paper describes a fast method for the sensitive and selective determination of melamine in a wide range of food matrices, including several milk-based products and certain beverages. The purpose of our study is to develop a fast and inexpensive method that will work reliably. That should be used for screening of melamine in milk-based products, beverage products and other food products.

**Keywords:** Melamine, adulteration, milk, beverage, TLC, HPTL

## **PP 39** Green Synthesis of Yttrium Oxide Nanoparticles and its Antibacterial Activity

**M. Alagumeenal<sup>a</sup>, P. Nithya<sup>a</sup>, M. Balaji<sup>a</sup>, S. Jegatheeswaran<sup>a</sup>, A. Surya<sup>a</sup>, S. Selvam<sup>b</sup>,  
K. Bharathi<sup>c</sup> and M. Sundrarajan<sup>a\*</sup>**

<sup>a</sup>Advanced Green Chemistry Lab, Department of Industrial Chemistry, School of Chemical Sciences, Alagappa University, Karaikudi - 630 003, Tamil Nadu, India.

<sup>b</sup>Laser and Sensor Application Laboratory, Engineering Building, Pusan National University, Busan - 609735, South Korea.

\*Corresponding author: Tel: + 91 94444 96151

E-mail: drmsgreenchemistrylab@gmail.com

<sup>c</sup>Department of Chemistry, Poompuhar college (Autonomous), Melaiyur 609107, Tamil Nadu.

### **Abstract**

In this study, the synthesized of Yttrium oxide ( $Y_2O_3$ ) nanoparticles was carried out from *Gloriosa superba* leaves extract. The synthesized were characterized by using XRD, FT-IR, UV-DRS, Raman Spectroscopy and SEM with EDX. The Yttrium oxide ( $Y_2O_3$ ) nanoparticles has excellent antibacterial activity.

**Keywords:** Green synthesis, *Gloriosa superba*, Yttrium oxide NPs, Antibacterial activity.

### **Introduction**

Nano sized metal oxides, in a variety of morphologies (such as particles, spheres, rods and sheets) have attracted a great deal of attention. Yttrium oxide ( $Y_2O_3$ ), as an important member among rare earth compounds, has been actively studied in the recent years. It is one of the most promising elements for the fabrication of optoelectronic devices and chemical catalysis.  $Y_2O_3$  is a well-known material for its characteristics of high dielectric constant and good thermal stability in a powder state.  $Y_2O_3$  can be used as high efficient additives and functional composite materials like yttria-stabilized zirconia films.  $Y_2O_3$  can be used as high efficient additives and functional composite materials like yttria-stabilized zirconia films. In addition to that, it is widely used as a host material for various rare earth dopants and is of interest for potential applications in biological imaging as well as photodynamic therapy.

## Experimental Details

Yttrium oxide (**Figure: 1**) prepared by hydrothermal method by using *Gloriosa superba* leaves extract. 0.1N Yttrium nitrate solution were added to ethanolic solution of *Gloriosa superba* plant extract and these solution transferred into autoclave heated at 120 °C for 12 hours. The resulting sample was filtered, washed with distilled water and dried at 100 °C. The powder sample was calcinated in a muffle furnace at 600 °C for 6 hours to get  $Y_2O_3$ .

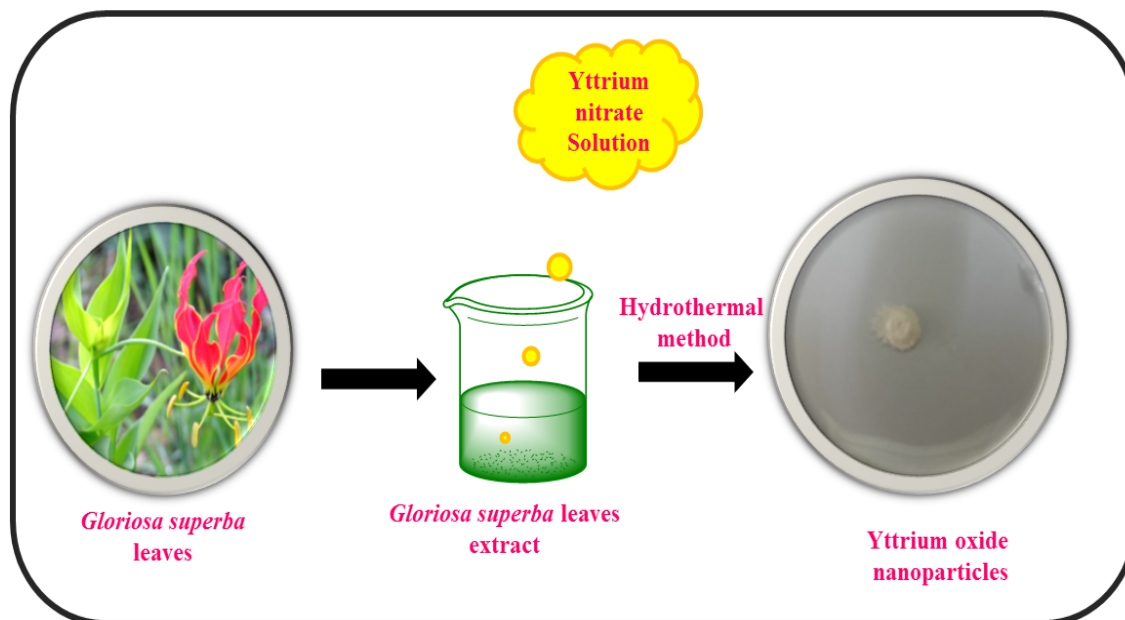


**Figure: 1**

## Results and Discussion

The synthesized  $Y_2O_3$  were characterized by XRD, FT-IR, Raman Spectroscopy, UV-DRS and SEM with EDX. The XRD patterns of  $Y_2O_3$  nanoparticles shows  $2\theta$  values at 27.38 °, 36.03 °, 46.75 ° and 64.42° arecorresponds to 110, 011, 020 and 211 planes, which are in good agreement with the International Center of Diffraction Data card (JCPDS: 89-5591) are confirming the formation of crystalline body centered cubic structure. In FT-IR spectrum of band peak is 3443  $cm^{-1}$ , 2923  $cm^{-1}$ , 1647  $cm^{-1}$  and 1384  $cm^{-1}$  indicates O-H stretching, C-H stretching, C=O stretching and N=O stretching vibration respectively. The band due to the stretching frequency of Y-O can be seen below at 487  $cm^{-1}$ , indicating the formation of  $Y_2O_3$ .

## Conclusion

$Y_2O_3$ nanoparticles were green synthesized using *Gloriosa superba* leaves extract. The synthesized nanoparticles retained the orthorhombic structure, which was confirmed by X-ray diffraction studies. The synthesized  $Y_2O_3$  nanoparticles exhibit good antibacterial activity. The achievement of such green synthesis of  $Y_2O_3$  nanoparticle, contributes the rise of synthetic procedures using environmentally benign natural resources.

## References

- M.Vivek, P.S.Kumar, S.Steffi and S.Sudha, Journal of MedBiotechno, 1.3 2011, 43-48.  
J.Y.Song and B.S.Kim, Journal of Bioprocess Biosyst.Eng 32 2009, 79-84.

## **PP 40** Ionic Liquid Assisted Green Synthesis of Magnesium Oxide Nanoparticles and its Antibacterial Activity

**S. Sathya<sup>a</sup>, P. Nithya, M. Balaji<sup>b</sup>, K. Bama<sup>b</sup>, K. Ramanujam<sup>b</sup>, S. Ambika<sup>c</sup>,  
K. Elangovan<sup>a\*</sup>, and M. Sundrarajan<sup>b\*</sup>**

<sup>a</sup>Alagappa Govt.Arts College, Karaikudi-630 003, Tamil Nadu, India.

E-mail: geethailangovan231@gmail.com

<sup>b</sup>Advanced Green Chemistry Lab, Department of Industrial Chemistry, School of Chemical Sciences, Alagappa University, Karaikudi - 630 003, Tamil Nadu, India.

E-mail: drmsgreenchemistrylab@gmail.com

<sup>c</sup>Central Electro Chemical Research Institute, Karaikudi.

## Abstract

Magnesium oxides nanoparticles were successfully synthesized from Mg (NO<sub>3</sub>)<sub>2</sub>.6H<sub>2</sub>O through a simple greener route using leaves extract (*Morinda citrifolia*). The synthesized samples were characterized by different techniques such as X-ray diffraction (XRD), Fourier transform infrared (FTIR) spectroscopy and Scanning electron microscopy (SEM) with Energy dispersive X-ray spectroscopy (EDX) analysis. Ionic liquid assisted green synthesis of MgO NPs exhibit excellent antibacterial activity.

**Keywords:** Ionic liquid, Hydrothermal method, Green synthesis, MgO NPs, Antibacterial activity.

## Introduction

Nano biotechnology is a growing, interdisciplinary field of research interlacing material science, bio nanoscience and technology. The advances made in the field of nano biotechnology to harness the benefit of life sciences, health care and industrial biotechnology are remarkable. Nanoparticles exhibit completely new or improved properties with larger particles of the bulk materials and these novel properties are derived due to the variation in specific characteristics such as size and morphology of the particles. Magnesium oxide (MgO) is an interesting basic metal oxide that has many applications. For example, MgO with ultrafine, nanoscale particles and high specific surface area have shown great promise as destructive adsorbent for toxic chemical agents. Nanoscale MgO exhibits unique optical, electronic, magnetic, thermal, mechanical and chemical properties due to its characteristic structures.

## Experimental Details

MgO oxide nanoparticles (**Figure 1**) prepared by greener method by Mg (NO<sub>3</sub>)<sub>2</sub>.6H<sub>2</sub>O used as a precursor with environment benign *Morinda citrifolia* leaves extract and [IMIM] BF<sub>4</sub>



(IL) is a capping agent. Magnesium nitrate (0.1 N) solution and 1 mL [IMIM]BF<sub>4</sub> (IL) were added to the ethanolic solution of *Morinda citrifolia* leaves extract and stirred for 6 hours continuously at room temperature. The resulting sample were filtered, washed with distilled water and dried at 100 °C. The powered sample was calcinated in a muffle furnace at 700°C to get MgO nanoparticles.

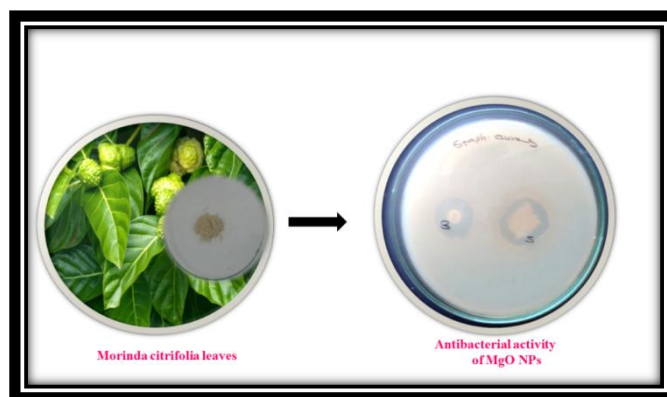


Figure: 1

## Results and Discussion

Magnesium oxide nanoparticles are synthesized by simple hydrothermal method in ionic liquid medium and characterized by XRD, FT-IR, UV-DRS, SEM with EDX and TEM analysis. The face centered cubic structure of prepared MgO nanoparticles was confirmed and the average particles size is 20-32 nm from XRD pattern. The MgO nanoparticles were confirmed by SEM with EDX. Antibacterial studies done against *S.aureus* than *E.coli* by agar diffusion test. It can be shown that zone of inhibition was found to be more in gram positive bacteria compared with gram negative bacteria. Since antibacterial character finds wide application in the health and hygiene of textile sector, this method of preparation of magnesium oxide will be useful in cost effective way [2, 3].

## Conclusion

In this present work, MgO nanoparticles were synthesized *Morinda citrifolia* leaves extract in ionic liquid medium. The study of precursor and leaf extract compositions play a major role in defining the molecular features the MgO nanoparticles. This work suggested that the bacterial susceptibility of nanoparticles not only rely on the cell wall structures of Gram-positive and Gram-negative bacteria but also dependent on the cellular enzymes and biochemical events.

## References

- K. Ramanujam and M. Sundrarajan, Word Journal of Pharmacy and Pharmaceutical sciences, 3[1] 2014, 1989-2004.
- K. Ramanujam and M. Sundrarajan, Journal of Photochemistry and Photobiology B: Biology, 141 2014, 296-300.
- S.B. Khan, M. Faisal, M.M. Rahman and Jamal, Journal of Sci. Total Environ, 409[15] 2011, 2987- 2922.

**PP 41** Electrodeposition of Cu-Zn-Sn alloy using sulphate based electrolyteN. Radha\*<sup>a</sup> and Indragandhi<sup>b</sup><sup>a</sup> *Asst. Professor of Chemistry, Alagappa Govt. Arts College, Karaikudi – 3  
Chemradha74@gmail.com*<sup>b</sup> *Student in chemistry, Alagappa Govt. Arts College, Karaikudi – 3***Abstract**

Cu-Zn-Sn alloys materials having variety of applications especially solar cell as absorber layer, corrosion resistance, bearing applications electronic applications etc., In this study, the electrodeposition of Cu-Zn-Sn alloy from sulphate based electrolyte using potentiostatic as well as galvanostatic method has been investigated. The cyclic voltametric studies provide the information about the reduction potentials of individual metals. The morphology and structural studies of these coatings were characterized by scanning electron microscopy and X-ray diffraction techniques. The X-Ray diffraction analysis confirms the Cu-Zn-Sn alloy formation in coatings. The composition analyses were carried out by X-Ray fluorescence technique. These studies confirm the possibilities of preparing Cu-Zn-Sn alloy system with high quality with various compositions using electrochemical methods.

**Keywords:** Cu-Sn-Zn, Thin film, Potentiostatic and galvanostatic method and cyclic voltametry.

**PP 42** Ionic liquid – Assisted tri doping of nitrogen, phosphorus, and fluorine into graphene instantaneously enhanced the morphology of ternary compositeA. Mayakrishnan<sup>a</sup>, M. Balaji<sup>a</sup>, S. Jegatheeswaran<sup>a</sup>, P. Nithya<sup>a</sup>, V. Muththulakshmi<sup>a</sup>,  
S. Selvam<sup>b</sup>, M. Rajan<sup>c</sup>, and Mahalingam Sundrarajan<sup>a\*</sup><sup>a</sup> *Advanced Green Chemistry Lab, Department of Industrial Chemistry, School of Chemical Sciences, Alagappa University, Karaikudi - 630 003, Tamil Nadu, India.*<sup>b</sup> *Laser and Sensor Application Laboratory, Engineering Building, Pusan National University, Busan - 609735, South Korea.*<sup>c</sup> *Department of Natural products chemistry, School of chemistry, Maduraikamaraj University, Madurai-625021, Tamilnadu, India*<sup>\*</sup> *Corresponding author: Dr. M. Sundrarajan,**Email: sundrarajan@yahoo.com; drmsgreenchemistrylab@gmail.com***Abstract**

In this work nitrogen, phosphorus, fluorine tri doped graphene (NPF-Graphene), was synthesized via rapid and effective functionalization with imidazolium ionic liquids (1-Butyl-3-methylimidazolium hexafluorophosphate) through thermal decomposition. It was found that thermal decomposition provides nitrogen, phosphorus, and fluorine sources for tri-doping with N, P, and F, and simultaneously facilitates act as template for formation of spherical shape phosphate

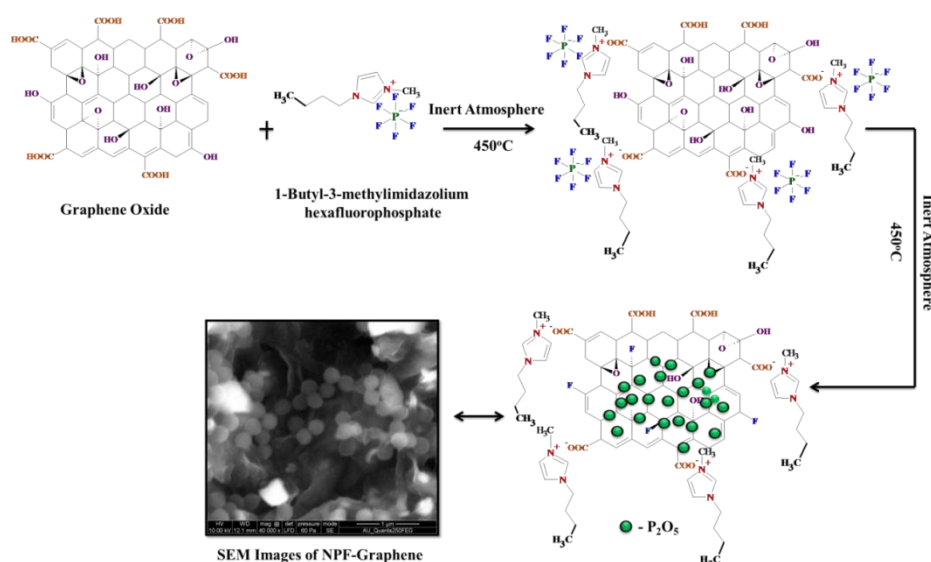
particles on graphene sheet. The resulting (NPF-Graphene) were characterized by X-ray diffraction (XRD), Fourier transform infrared spectroscopy (FTIR), X-ray photoelectron spectroscopy (XPS), Scanning electron microscopy (SEM). Furthermore, XPS show that the nitrogen and fluorine have been covalently attached to the graphene. SEM and TEM images demonstrate that after functionalization, phosphates are doped in spherical structure. Thus ionic liquid successfully made the dual role in this process.

**Keywords:** Graphene, Ionic Liquid, Functionalization, Ionic Interactions, 1-Butyl-3-methylimidazolium hexafluorophosphate

## Introduction

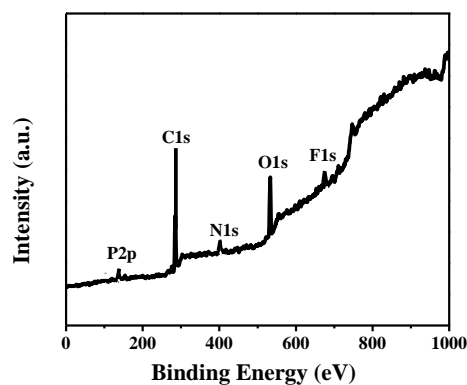
Graphene, 2-dimensional structure that consists of  $sp^2$ -hybridized carbons, has attracted enormous interest due to its large specific surface area, high electrical. However, improving the properties of graphene are the biggest challenges in the practical applications. Furthermore, modification of graphene with heteroatoms is an alternative to noble-metal based composite. Moreover, the tri doping process provides graphene with unique electronic property and further enhances the chemical reactivity due to the synergistic coupling effect of three kinds of heteroatoms [2-3]. Herein, we report a versatile routine to synthesize N, P, and F tri-doped graphene (named as NPF-Graphene) by introducing ionic liquid such as 1-Butyl-3-methylimidazolium hexafluorophosphate by simple one step reaction.

## Experimental Details



## Results and Discussion

XRD patterns of NPF-Graphene proves the presence of crystalline phosphate particle. In FTIR the peak at 1295 and 1240  $\text{cm}^{-1}$  were attributed to the C-N stretching modes of imidazolium ring. XPS survey



spectrum of NPF-Graphene shows peaks for C, N, P, F, and O indicating the tri-doping of carbon with N, P, and F. Raman spectra of NPF-Graphene clearly show the D- and G-bands indicating  $sp^2$ -hybridized carbon atoms in a graphene layer.

## Conclusion

In summary, we have demonstrated that thermal pyrolysis of graphene oxide in the presence of 1-Butyl-3-methylimidazolium hexafluorophosphate, generated graphene materials tri-doped with nitrogen, phosphorus, and fluorine.

## Reference

- J. Suntivich, K. J. May, H. A. Gasteiger, J. B. Goodenough, Y. Shao-Horn, *Science* 2011, 334, 1383 – 1385.
- P. G. Collins, K. Bradley, M. Ishigami, A. Zettl, *Science* 2000, 287, 1801 – 1804.
- N. Daems, X. Sheng, I. F. J. Vankelecom, P. P. Pescarmona, *J. Mater. Chem. A* 2014, 2, 4085 – 4110

## PP-43 Green Synthesis of RuO<sub>2</sub> Nanoparticles Using *Gloriosa Superba* Leaves Extract and its Antibacterial Activity

R. Jegatheeswari<sup>a</sup>, P. Nithya, M. Balaji<sup>a</sup>, S. Jegatheeswaran<sup>a</sup>, K. Ramanuja<sup>a</sup>, S. Selvam<sup>b</sup>, S. Ambika<sup>c</sup>, M. Abdul kadir<sup>d</sup>, S. Gowri<sup>e</sup>, G. Selvanathan, and M. Sundrarajan<sup>a\*</sup>

<sup>a</sup>Advanced Green Chemistry Lab, Department of Industrial Chemistry, School of Chemical Sciences, Alagappa University, Karaikudi - 630 003, Tamil Nadu, India.

\*Corresponding author: Tel: + 91 94444 96151

E-mail: [drmsgreenchemistrylab@gmail.com](mailto:drmsgreenchemistrylab@gmail.com)

<sup>b</sup>Laser and Sensor Application Laboratory, Engineering Building, Pusan National University, Busan - 609735, South Korea.

<sup>c</sup>Central Electro Chemical Research Institute, Karaikudi.

<sup>d</sup>Department of Chemistry, M.S.S. Wakf Board College, Madurai.

<sup>e</sup>Department of Nanoscience and Technology, Alagappa University, Karaikudi.

## Abstract

The plant extract using synthesis of nanomaterials can be cost effective and eco-friendly approach. In this work we report the green synthesis of Ruthenium oxide nanoparticles using *Gloriosa superba* extract by hydrothermal method. The synthesized nanoparticles retained the orthorhombic structure, which was confirmed by X-ray diffraction studies. The FT-ITR spectrum analysis to confirm Ru-O symmetric stretching of RuO<sub>2</sub> NPs. Further, these RuO<sub>2</sub> nanoparticles were found to exhibit higher antibacterial behavior with two different pathogens.

**Keywords:** Green synthesis, *Gloriosa superba*, Ruthenium oxide NPs, Antibacterial activity.

## Introduction

An important development of green processes for the synthesis of metal/metal oxide nanoparticles is evolving into an important branch of nanotechnology. Ruthenium (IV) oxide is the inorganic compound with the formula RuO<sub>2</sub>. This black solid is the most common oxide of

ruthenium. It is widely used as an electro catalyst for producing chlorine, chlorine oxides, and O<sub>2</sub> catalyst is ruthenium (IV) oxide [1].

### Experimental Details

Ruthenium oxide (**Figure: 1**) prepared by hydrothermal method by using *Gloriosa superba* leaves extract. 0.1N Ruthenium trichloride (RuCl<sub>3</sub>) solution were added to ethanolic solution of *Gloriosa superba* plant extract and these solution transferred into autoclave heated at 120 °C for 12 hours. The resulting sample was filtered, washed with distilled water and dried at 100 °C. The powder sample was calcinated in a muffle furnace at 600°C for 6 hours to get RuO<sub>2</sub>.

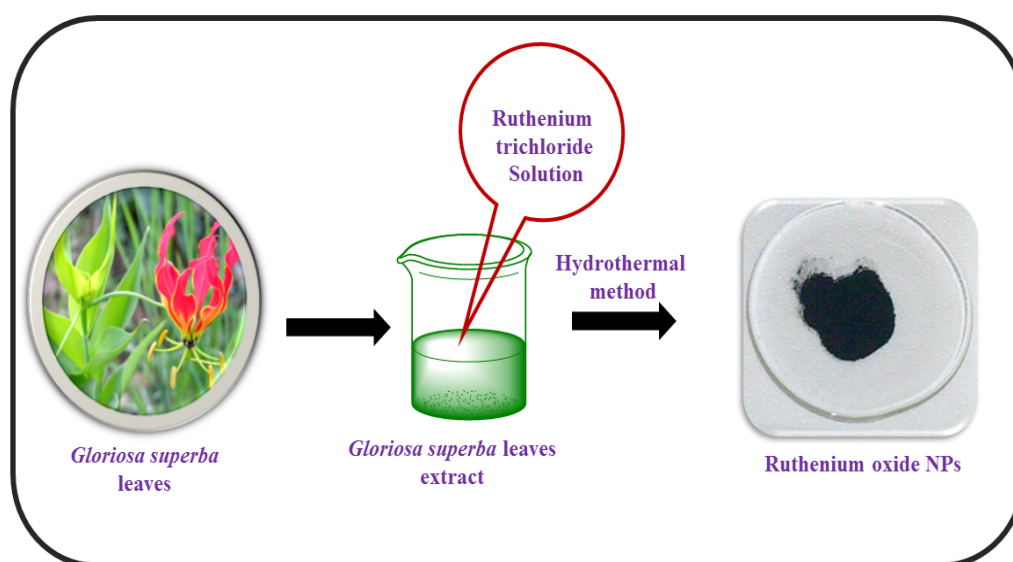


**Figure 1:**

### Results and Discussion

The synthesized RuO<sub>2</sub> were characterized by XRD, FT-IR, Raman Spectroscopy, UV-DRS and SEM with EDX. The XRD patterns of RuO<sub>2</sub> nanoparticles shows 2 $\theta$  values at 28.38 °, 35.33 °, 40.65 ° and 54.42° are corresponds to 110, 011, 020 and 211 planes, which are in good agreement with the International Center of Diffraction Data card (JCPDS: 88-0323) are confirming the formation of crystalline orthorhombic structure. In FT-IR spectrum of band peak is 3443 cm<sup>-1</sup>, 2923 cm<sup>-1</sup>, 1647 cm<sup>-1</sup> and 1384 cm<sup>-1</sup> indicates O-H stretching, C-H stretching, C=O stretching and N=O stretching vibration respectively. The band due to the stretching frequency of Ru-O can be seen below at 463 cm<sup>-1</sup>, indicating the formation of RuO<sub>2</sub>.

## Conclusion

RuO<sub>2</sub> nanoparticles were green synthesized using *Gloriosa superba* leaves extract. The synthesized nanoparticles retained the orthorhombic structure, which was confirmed by X-ray diffraction studies. The synthesized RuO<sub>2</sub> nanoparticles exhibit good antibacterial activity.

## References

- T.N.V.K.V. Prasad and E. Elumalai, Asian Pac. J. Trop. Biomed, 1[6] 2011, 439-442.  
Banerjee and R. Narendhirakannan, Journal of Nanomater. Biostructure, 6[4] 2011, 961-968.

## **PP 44** Electrodeposition of Cu-Sn alloy using potentiostatic and galvanostatic method

**M. Kavitha, C. Rani\***

*Master of Science Student in chemistry, Alagappa Govt. Arts College*

*\* Asst. Professor, Department of Chemistry, Alagappa Govt. Arts College, Karaikudi – 3  
viswanathanrani@gmail.com*

## Abstract

In this report, the Cu-Sn alloy were successfully coated on copper substrate from phenol sulphonic acid (PSA) electrolyte at room temperature by using galvanostatic and potentiostatic method. Cu-Sn alloy coatings have been widely used in industry for their unique properties, such as good conductivity, high corrosion resistance and excellent solderability. The cyclic voltametric studies provide the information about the reduction potentials of individual metals. To characterize the morphology and structure of the Cu-Sn alloy electrodeposition were characterized by scanning electron microscopy (SEM) and X-ray diffraction (XRD). The chemical composition of deposited sample was analyzed using X-ray fluorescence method. These alloys have found various new applications such as shape memory materials, lithium battery anodes and absorbers in solar cells.

**Keywords:** Cu-Sn alloy, Potentiostatic Galvanostatic, Thin film and Cyclic voltammetry

## PP 45 Characterization Andin Vitro Bioactivity of Strontium Substituted Hydroxyapatite /Graphene Oxide/ Polyacrylic Acid Nano Composite

Ayyappan Keerthana<sup>a</sup>, Murugesan Balaji<sup>a</sup>, Sonamuthu Jegatheewaran<sup>a</sup>, A. Rukmani<sup>b</sup>, V.Mahesh Kumar<sup>b</sup>, M. Sundrarajan<sup>a\*</sup>

<sup>a</sup>Advanced Green Chemistry Lab, Department of Industrial Chemistry, School Of Chemical science , Alagappa University, Karaikudi-630003, Tamil Nadu, India.

\*Corresponding author: drmsgreenchemistrylab@gmail.com

### Abstract

A novel green route for the synthesis of halfly and fully strontium substituted hydroxyapatite / Graphene oxide / PolyAcrylicAcidAcid (PAA) Nano composite by Freeze-Drying method. In the first step, the identification and morphology of chemically synthesized Sr-Hydroxyapatite particles were determined by EDX and SEM analyses. The chemical changes and cristanallity changes of the nano composite were evaluated by FT-IR and XRD studies. The synthesized GO's showed the characteristic band in UV-vis Spectroscopy and XRD peaks confirms its crystalline nature. The Composite improve their physical and mechanical properties.

**Keywords:** Strontium substitutedHydroxyapatite, Graphene oxide, PolyAcrylicAcid, Antibacterial Activity

### Introduction

Hydroxyapatite is the most suitable biocompatible material for bone implant coating. Many pathways to synthesis hydroxyapatite, namely dry process, sol-gel method, microwave assisted method, biomimetic method and others. A series of Sr-substituted hydroxyapatite ( $Sr_xCa_{1-x})_5(PO_4)_3OH$ , where X=1.00, 3.00, 5.00 were made by a standard sol gel route. Strontium and other divalent cations with similar physical and chemical properties to the calcium. So it can ready to substitute the calcium and replace the calcium in hydroxyapatite. Hydroxyapatites have low fracture toughness, poor tensile strength and weak wear resistance. One promising method to tackle with these problems is exploiting Graphene and its derivative.

### Experimental Details

Pure and strontium substituted hydroxyapatite is prepared by the sol-gel method. (Ca+Sr)/p molar ratio of 5/3. Graphene oxide is prepared by modified hummer method. PAA/GO/HAP Nano composite was synthesized by mixing three aqueous solutions. PAA powder is dissolved in acetic acid solution and then stirred to achieve a homogeneous suspension (solution 1). The as-synthesized GO powder was dispersed in 50 ml DI water by sonication for 30 minutes (solution2). The as-synthesized Sr-HAP powder was dispersed in 50 ml water by sonication for 30 minutes (solution 3) by mixing the solution 1, 2, 3 a gray suspension was

obtained which was stirred for 24 hours at room temperature. Schematic illustration of Graphene oxide/hydroxyapatite composition by sol-gel method.

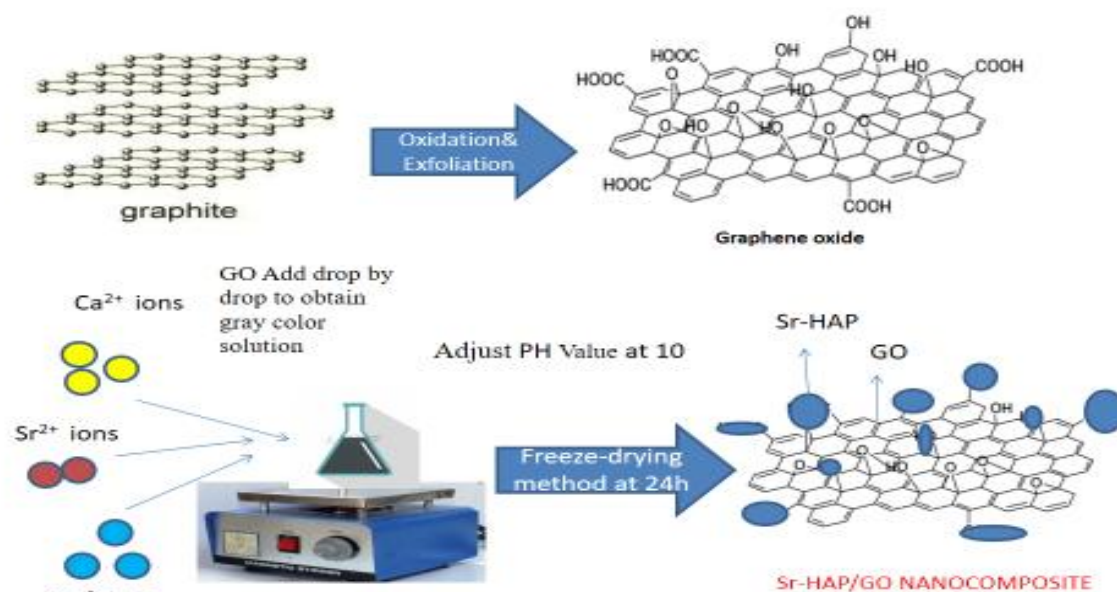


**Figure 1: Synthesis of Graphene oxide/hydroxyapatite composition by sol-gel method**

## Results and Discussion

Crystalline nature of the sample was analyzed by X-ray diffraction (XRD; JEOL IDX 8030). Strontium substituted Hydroxyapatite to decrease the noisy level and increase the crystallinity. Mean peaks of Hydroxyapatite at 25.8, 31.8, 32.3, and 32.9 (JCPDS 860740). Compatible with a Sr-HA solid solution, since the crystalline structure of Hydroxyapatite was maintained and no other phase containing strontium was formed after the calcium partial substitution by strontium. UV-DRS can be used for finding band gap of a material. Increase the ratio of strontium in hydroxyapatite to increase the band gap.

## Conclusion

A series of Sr-substituted hydroxyapatites were successfully synthesized by sol-gel method. Crystallite size decreased with up to 20% substitution of Strontium then increased with higher content. Graphene oxide, PolyAcrylicAcid, Hydroxyapatite nanoparticles were prepared by simple freeze-drying method and obtained results showed that the GO/PAA/HAP nano composites have a much higher bioactivity rather than that of pure HAP nanoparticles.

## References

Sanja Erokoic, Ana Jankovic, Djordje Veljovic, corrosion stability and bioactivity in simulated body fluid of silver/Hydroxyapatite and silver/Hydroxyapatite/Lignin Coatings on Titanium obtained by electrophoretic deposition



M.D.O'Donnell, Y.Fredholm, A.de Rouffignac R.G.Hill, structural analysis of a series of Strontium-substituted Apatite's

Ming li, pan xiong, Feng yan, sijie li, changong Ren, Zhichen yin, Ang li, Huafang Li, On Overview of Graphene –based Hydroxyapatite composites for Orthopedic Applications

## **PP 46** Study the *in-vitro* Antioxidant Activity of Alumina/PEO Electrospun nanofibrous Mats

**G. Archana, T. Stalin\***

*\*Department of Industrial Chemistry, School of Chemical Sciences  
Alagappa University, Karaikudi - 630 003, Tamilnadu.*

*E-mail: archganesgmla@gmail.com and drstalin76@gmail.com*

### **Abstract**

Nanofiber technology is an exciting area and attracting the attention of many researchers as a potential solution to the current challenges in the biomedical field. Here we demonstrated alumina/PEO nanofibrous mats by the electrospinning technique. The structural and thermal characteristics of Alumina/PEO were investigated by SEM, FTIR, XRD, DSC studies. The antioxidant activity of the alumina/PEO nanofibrous mat has been investigated using 1,1-diphenyl-2-picrylhydrazyl (DPPH) scavenging assay by employing UV-Vis spectroscopy.

### **Introduction**

Electrospinning is found to be a versatile and cost-effective technique for the fabrication of multi-functional nanofibers from various natural and synthetic polymers, polymer blends, ceramics, composites etc., Electrospun nanofibrous mats have numerous remarkable characteristics such as very high surface to volume ratio having highly porous structure in the nanoscale and they show distinctive physical and mechanical properties. Alumina powder is currently believed to be one the most promising known biological material. A wide range of polymers can be electrospun to suit different applications. Metal oxide nanofibrous mats have been widely used for futuristic applications in chemical catalysis, biosensing, storage devices and biomedical devices. The aim of this study is to demonstrate the *in vitro* antioxidant activity of the alumina/PEO nanofibrous mats.

### **Experimental part**

Aqueous solution of 5 wt % PEO were prepared by dissolving in DI water at room temperature with stirring for 4 h. On the other hand, alumina was synthesized by hydrothermal approach. The alumina was subsequently loaded into the solution. The mixture was stirred at room temperature for 12-24 h with a magnetic stirrer. The prepared solution was placed in a 10 ml syringe fitted with 23 gauge needle. The tip to collector distance was kept at 15 cm, and the solutions were pumped with a flow rate of 0.6 ml/h. When a voltage of 15 kV was applied to the

metal needle tip, the nanofibers were deposited on the collector. The collected nanofibers were dried at room temperature to remove the residual solvent.

### Results and discussion

The alumina containing electrospun PEO nanofibers were characterized by scanning electron microscopy (SEM) to determine the uniformity of the fibers. We confirmed the presence of alumina in PEO nanofibers by UV-Vis-NIR spectroscopy. Changes in the alumina crystallinity upon fiber processing were examined using DSC and XRD analysis. Finally we examined the *in vitro* antioxidant activity by DPPH assay method. Interestingly the addition of alumina enhances the antioxidant activity of PEO nanofibrous mats.

### Conclusion

The alumina and PEO polymeric materials have used to fabricate the carrier matrix by electrospinning technique. Alumina/PEO nanofibrous mats yielded bead-free fiber morphology. Moreover, the thermal stability of the nanofibers was altered due to the addition of alumina within the nanofibrous mat. The radical scavenging ability of the produced alumina/PEO nanofibers was determined by the DPPH assay. The enhanced antioxidant activity was concerned with increased surface area of nanofibers.

### References

- Chen, C.H.; Chen, S.H.; Shalumon, K.T.; Chen, J.P. Dual functional core–sheath electrospun hyaluronic acid/polycaprolactone nanofibrous membranes embedded with silver nanoparticles for prevention of peritendinous adhesion. *Acta biomaterialia*, **2015**, *26*, 225-235.
- Al-Kattan, A.; Nirwan, V.P.; Munnier, E.; Chourpa, I.; Fahmi, A.; Kabashin, A.V. Toward multifunctional hybrid platforms for tissue engineering based on chitosan (PEO) nanofibers functionalized by bare laser-synthesized Au and Si nanoparticles. *RSC Advances*, **2017**, *7*, 31759-31766.

## **PP 47** A facile and efficient synthesis of carbocycle-fused bis-1,2,3-selenadiazoles derivatives and their antimycobacterial activities

C. Nanthini, S. Siyama sundhari, A. Saranya, S. Chitra,<sup>a</sup>

<sup>a</sup>Department of Chemistry, Alagappa Govt. Arts College, Karaikudi-630 003  
E.mail: schitrachem@gmail.com

### Abstract

A series of bis-1,2,3-selenadiazole derivatives have been synthesized by the oxidative cyclization of bis semicarbazones of 2-(3-oxo-1,3-diarylpropyl)-1-cyclohexanones using selenium(IV) oxide. The synthesized compounds were evaluated for their *in vitro* antimicrobial activity against *Escherichiacoli* (ATCC 25922), *Staphylococcus aureus* (ATCC 11632) and

*Candida albicans* (ATCC 90028) and invitro antituberculosis activity against *Mycobacterium tuberculosis* H37Rv (MTB). )

**Keywords:** I,5-Diketones, Selenadiazoles, Antimicrobial, *Mycobacterium tuberculosis*.

## **PP 48** Design and performance of a bromelain-alginate hydrogel membrane and their antibacterial studies

**M. Jeyalakshmi, T. Stalin\***

*Department of Industrial Chemistry, School of Chemical Sciences*

*Alagappa University, Karaikudi - 630 003, Tamilnadu.*

*E-mail: jeyamurugesanjv1997@gmail.com and drstalin76@gmail.com*

### **Abstract**

In recent years there has been growing interest in the application of alginate hydrogels as support materials in numerous biomedical applications. A new approach for the synthesis of bromelain containing sodium alginate hydrogels was prepared via ionotropic gelatin technique. The obtained hydrogels were characterized by means of UV, FT-IR and SEM analysis. These bromelain alginate hydrogels have high swelling ratios, benefitting various applications such as drug delivery. Furthermore, bromelain loaded alginate hydrogel revealed the highest antibacterial activities against *S. aureus* pursued by *E. coli* in compared with the anionic polysaccharide hydrogel membrane. Together, our study indicates that the bromelain loaded hydrogel may serve as versatile platform for diverse applications in biomedical field. In this study, bromelain is introduced into alginate hydrogel to enhance the antibacterial efficacy.

### **Introduction**

Hydrogels are three dimensionally crosslinked network capable of swelling after absorbing large amount of water, have been widely used in tissue engineering and regenerative medicine. Owing to their biocompatibility and biodegradability, natural polymers are extensively studied for hydrogel fabrication. Alginate is a naturally occurring anionic polysaccharide derived

from marine algae. Hydrogels composed of alginate are capable of encapsulating a wide range of bioactive components such as vitamins, minerals, and nutraceuticals.

### Experimental details

A 3 wt % Sodium alginate powder was made by dissolving with DI water and stirred at 70°C for two hours. To this solution 10 % bromelain (w/w with respect to polymer) were added and stirred continuously to form a homogeneous solution. The prepared solution was then poured in a mold, were then covered with parafilm and left to cure at room temperature for 12 hrs. To this solution 5 % CaCl<sub>2</sub> aqueous solution was squeezed gently from a micropipette. The hydrogels were allowed to remain in the Ca<sup>2+</sup> solution over night to complete the cross-linking process. Thereafter, soft hydrogels were taken out of the ionic solution and washed in DI water several times to remove the unreacted Ca<sup>2+</sup> ions from the hydrogel surface. Finally the hydrogels were then allowed to freeze drying process. After drying, the hydrogel membranes were stored in dessicator till used.

### Results and Discussion

The chemical crosslinking process of sodium alginate with CaCl<sub>2</sub> is evidenced from FTIR spectra. The UV-Vis-NIR spectra were performed to characterize the encapsulation of bromelain in alginate hydrogel. The morphology of the alginate hydrogels were analysed using SEM analysis. The bromelain loaded hydrogel possess good antibacterial activity against *S. aureus* and *E. coli* bacteria.

### Conclusion

In summary, we report a facile approach to prepare bromelain/alginate hydrogels with excellent properties. Additionally, bromelain loaded hydrogel exhibited antibacterial activities against pathogenic Gram-negative and Gram-positive strains. These results showed that the bromelain loaded hydrogel membranes could be a promising material for biomedical studies.

### References

- Hao, T.; Li, J.; Yao, F.; Dong, D.; Wang, Y.; Yang, B.; Wang, C. Injectable fullerenol/alginate hydrogel for suppression of oxidative stress damage in brown adipose-derived stem cells and cardiac repair. *ACS nano*. **2017**, *11*, 5474-5488.
- Pérez-Madrigal, M.M.; Torras, J.; Casanovas, J.; Häring, M.; Alemán, C.; Díaz, D.D. Paradigm shift for preparing versatile M<sup>2+</sup> free gels from unmodified sodium alginate. *Biomacromolecules*, **2017**, *18*, 2967-2979.

**PP 49** Preparation and characterizations of ferrocene coated PVA/HEC nanofibrous webs for anti tumour studies

P. Muthuselvi, T. Stalin\*

*Department of Industrial Chemistry, School of Chemical Sciences  
Alagappa University, Karaikudi - 630 003, Tamilnadu.*

*E-mail: muthupps1996@gmail.com and drstalin76@gmail.com*

**Abstract**

Aims of the study to be design a method for creating a nanofibrous scaffolds by encapsulating ferrocene into the electrospun PVA/HEC fibers. The nanofibers were uniformly coated by a thin layer of ferrocene. SEM, FTIR, DSC and XRD analysis confirm the deposition of ferrocene on the PVA/HEC nanofibers. The porosity and swelling behaviours of the ferrocene nanofibrous web also measured.

**Introduction**

Electrospinning is a widely used technique to produce multifunctional nanofibers from remarkable range of organic and inorganic materials. The unique characteristics of electrospun nanofibers such as high surface area, controllable fiber diameter and morphologies can be obtained by changing the process parameter. Poly (vinyl alcohol) and hydroxyl ethyl cellulose nanofibers are extensively used in various fields such as pharmaceutical industries, paints, and emulsion polymerizations. In this work we discovered ferrocene coated PVA/HEC nanofibrous web to enhance porosity and swelling properties.

**Experimental details**

In order to prepare the ferrocene/PVA/HEC solution; PVA and HEC was dissolved in water and afterwards ferrocene was added. The amount ferrocene was as 5 wt % with respect to polymer solution. The resulting solutions were stirred at room temperature for overnight. Finally elctrospinning was performed and ferrocene/PVA/HEC webs were obtained. Electrospinning of pure PVA/HEC nanofibers were produced for comparative measurements.

**Results and discussion**

SEM-EDX was used to examine the morphology and elemental composition of thenanofibrous web. The chemical structure of Ferrocene loaded PVA/HEC nanofibers was also investigated by FTIR spectroscopy. Mechanical strength, tensile strength and elastic modulus of the nanofibrous web were also evaluated. In addition, the porosity and swelling measurements have also been studied for the stability of ferrocene coated PVA/HEC nanofibrous web.

**Conclusion**

In summary, we demonstrated ferrocene can be successfully incorporated into the prepared nanofibrous web. The prepared ferrocene nanofibers exhibited good swelling properties.

Further, the ferrocene coated nanofibrous web was characterized by FT-IR, XRD and SEM analysis. Furthermore, the prepared nanofibrous webs were extended its well established application in anti tumour studies.

## References

- Qu, F.; Zhang, Y.; Rassoly, A. Electrochemical biosensing platform using hydrogel prepared from ferrocene modified amino acid as highly efficient immobilization matrix. *Anal. Chem.* **2014**, *86*, 973-976.
- Chahal, S.; JahirHussain, F.; Kumar, A.; Electrospun hydroxyethyl cellulose nanofibers Functionalized with calcium phosphate coating for bone tissue engineering. *RSC. Adv.* **2015**, *5*, 29497-29504.

## **PP 50** A facile and efficient synthesis of carbocycle-fused mono-1,2,3-selenadiazoles derivatives and their antimycobacterial activities

S. Siyama sundhari, A.Saranya, C. Nanthini, S.Chitra,<sup>a</sup>

<sup>a</sup>Department of Chemistry, Alagappa Govt.Arts College, Karaikudi-630 003  
E.mail:schitrachem@gmail.com

## Abstract

A series of mono-1,2,3-selenadiazole derivatives have been synthesized by the oxidative cyclization of mono semicarbazones of 2-(3-oxo-1,3-diarylpropyl)-1-cyclohexanones using selenium(IV) oxide. The synthesized compounds were evaluated for their in vitro antimicrobial activity against Escherichiacoli (ATCC 25922), Staphylococcus aureus (ATCC 11632) and Candida albicans (ATCC 90028) and invitro antituberculosis activity against Mycobacterium tuberculosis H37Rv (MTB). )

**Keywords:** I, 5-Diketones, Selenadiazoles, Antimicrobial, Mycobacterium tuberculosis.

## **PP 51** Preparation of Chemically Crosslinked Chitosan-Curcumin Hydrogel and their Swelling behavior, Pore structure stability and biological activity

**P. Vasanthi, T. Stalin\***

*\*Department of Industrial Chemistry, School of Chemical Sciences  
Alagappa University, Karaikudi - 630 003, Tamilnadu.  
E-mail:vasanthilatha1996@gmail.com and drstalin76@gmail.com*

### **Abstract**

The aim of this study is to develop a curcumin loaded Chitosan hydrogel with excellent antibacterial activity. The production of chitosan hydrogels is however time consuming and they are widely used for biological applications. Various tests were carried out including FTIR, UV-Vis, XRD, Swelling and porosity measurements to evaluate the efficiency of the prepared hydrogel matrix. In addition, antibacterial activity of the examined hydrogels for *S. aureus* and *E. coli* bacterial strains was investigated employing disc agar diffusion method.

### **Introduction**

Various natural and synthetic polymers have been studied in hydrogel researches. Chitosan is the second abundant polysaccharide obtained from the deacetylation of the natural biopolymer chitin. Many polymers used in hydrogel membranes, like chitosan, exert their mucoadhesive characteristics via interaction between opposite charges. This specific feature can provide the ability of tissue binding for the aim of specific drug delivery. In this study, we used a facile, freeze-thaw approach for the fabrication of curcumin/chitosan composite hydrogel.

### **Experimental details**

Aqueous solution of Chitosan is obtained by dissolving 2 % (w/w) in 25 % acetic acid. The solution was mechanically stirred for 2 h in order to be homogenized. Then 10 % curcumin (with respect to polymer) was added into the chitosan solution under stirring for further 2 h. The mixture was then dropped into the glutaraldehyde solution (30 %), keeping for 1 h to form a hydrogel matrix. The formed hydrogels were soaked and washed with distilled water. Finally, the hydrogels are freeze thawed. The resulting hydrogels were kept in a desiccator prior to analysis.

### **Results and discussion**

The degree of crosslinking was identified by infrared spectroscopy. The morphology of the bromelain embedded chitosan hydrogels was observed by scanning electron microscopy (SEM) to evaluate their microstructures. The degree of crystallinity of the bromelain/chitosan hydrogels was characterized by XRD analysis. The swelling behavior and porosity measurement of the crosslinked hydrogels was also studied.

## Conclusion

The hydrogels were prepared via a simple chemical crosslinking process. The crosslinking reaction and mechanism of chitosan with addition of glutaraldehyde was deduced. With the encapsulation of curcumin, chitosan hydrogel show decreased swelling capacity but increased stability in pH 7.4. More importantly, curcumin loaded chitosan hydrogel possess high microbial activity compared to pure chitosan hydrogel.

## Reference

Benner, S.W.; Hall, C.K.; Effect of monomer sequence and degree of acetylation on the self-assembly and porosity of chitosan networks in solution. *Macromolecules*, **2016**, *49*, 5281-5290.

## **PP 52** Improve the stability and their performance of cesium lead bromide-iodide based photo-sensitizer for inorganic perovskite solar cell

**M. Manoj Kumar, K. Sakthi Velu, B. Suganya Bharathi, G. Vignesh Kumar and T. Stalin\***  
*Photochemistry Lab, Department of Industrial Chemistry, School of Chemical Sciences, Alagappa University, Karaikudi-03, Tamilnadu-India.*

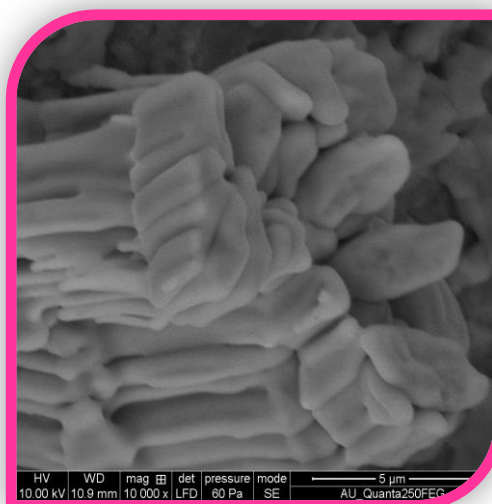
## Abstract

Cesium lead bromide-iodide based inorganic perovskite photo-sensitizer was prepared by the two step solution process method. As prepared CsPbBr<sub>3</sub>-I<sub>3</sub> Photo-sensitizer was characterized various technique such as XRD pattern, FT-IR and UV-Visible spectroscopy. Electrical conductivity of cesium lead bromide-iodide photo-sensitizer was determine that the Electrochemical impedance spectroscopy. The multicrystalline nature of the surface morphology of the CsPbBr<sub>3</sub>-I<sub>3</sub> Photo-sensitizer was observed in FE-SEM image. X-ray diffraction pattern was used to determine the cubic phase of the CsPbBr<sub>3</sub>-I<sub>3</sub> Photo-sensitizer. The functional group of CsPbBr<sub>3</sub>-I<sub>3</sub> photo-sensitizer was identified by the FT-IR spectroscopy. UV-Visible spectroscopy was show in the absorption maximum of CsPbBr<sub>3</sub>-I<sub>3</sub> photo-sensitizer. The electrical conductivity of CsPbBr<sub>3</sub>-I<sub>3</sub> photo-sensitizer used in the fabrication of perovskite solar cell device was achieved the higher. The surface morphology of mixed halide ions based CsPbBr<sub>3</sub>-I<sub>3</sub> photo-sensitizer FE-SEM images shown in polycrystalline nature.



Perovskite solar cell was prepared with bromide-iodide coated on the FTO/TiO<sub>2</sub> used as photo-anode, Spiro-OMeTAD used as hole transport materials and Gold used as back electrode. CsPbBr<sub>3</sub>-I<sub>3</sub> photo-sensitizer give the 8.2% of sunlight into electrical energy conversion efficiency.

**Keywords:** Cesium lead bromide-iodide, Photo-Sensitizer, Inorganic perovskite solar cell, Efficiency.



FE-SEM image of CsPbBr<sub>3</sub>-I<sub>3</sub> photo-sensitizer

### PP 53 A facile domino protocol for the regioselective synthesis of 1,3-diphenyl-3-(4,5,6,7-tetrahydrobenzo[c]thiophen-4-yl)propan-1-one derivatives

A. Saranya, C. Nanthini, S. Siyama sundhari, P. Muthuraja<sup>a</sup>, S. Chitra,<sup>a\*</sup>

<sup>a</sup>Department of Industrial Chemistry, Alagappa University Karaikudi-630 003

<sup>a\*</sup>Department of Chemistry, Alagappa Govt.Arts College, Karaikudi-630 003

E.mail:schitrachem@gmail.com

#### Abstract

A series of novel 1,3-diphenyl-3-(4,5,6,7-tetrahydrobenzo[c]thiophen-4-yl)propan-1-one has been synthesised regioselectively from the reaction of 2-(3-oxo-1,3-diarylpropyl)-1-cyclohexanones with ethyl cyanoacetate/malononitrile and sulphur powder in the presence of morpholine under thermal as well as microwave irradiation conditions . This transformation presumably occurs *via* domino Gewald reaction-dehydrogenation

synthesis of 1,3-diphenyl-3-(4,5,6,7-tetrahydrobenzo[c]thiophen-4-yl)propan-1-one

**Keywords:** 1,5-Diketones, thiophene, Gewald reaction, cycloaddition

**PP 54** Polyethylene glycol assisted synthesis of inorganic cesium lead iodide polycrystalline photo-sensitizer for planar perovskite solar cell

**P. Sathappan, K. Sakthi Velu, B. Suganya Bharathi, G. Vignesh Kumar and T. Stalin\***  
*Photo-chemistry Lab, Department of Industrial Chemistry, School of Chemical Sciences,  
Alagappa University, Karaikudi-03, Tamilnadu-India.*

**Abstract**

Development of newer photo-anode material of polyethylene glycol (PEG) assisted synthesis of cesium lead iodide ( $\text{CsPbI}_3$ ) photo-sensitizer for Inorganic perovskite solar cell. PEG assisted synthesis of cesium lead iodide (PEG- $\text{CsPbI}_3$ ) was prepared by simple two-step solution process method. PEG- $\text{CsPbI}_3$  photo-sensitizer in black color cubic crystalline phase at  $300^\circ\text{C}$  that result confirmed by XRD pattern. The formation of the PEG- $\text{CsPbI}_3$  photo-sensitizer functional groups were identified by the FT-IR spectra. UV-visible spectroscopy was used to determine that the absorption maximum of polyethylene glycol assisted synthesis of cesium lead iodide photo-sensitizer. Multicrystalline structure of PEG- $\text{CsPbI}_3$  photo-sensitizer surface was show in HR-TEM image. The planar structure perovskite solar cell were assembled with PEG stabilized  $\text{CsPbI}_3$  photo-sensitizer coated on the FTO/ $\text{TiO}_2$  photo-anode and 2, 2', 7, 7' Tetrakis (N, N'-di-p-methoxyphenyl-amine)-9, 9'-spirobiflouene (Spiro-OMeTAD) used as hole transport materials and thus gold used as back electrode (counter electrode).

Finally, Polyethylene glycol stabilized  $\text{CsPbI}_3$  photo-sensitizer coated on the FTO/ $\text{TiO}_2$  photo-anode was achieved 8.4% of power conversion efficiency compared with PEG untreated  $\text{CsPbI}_3$  photo-sensitizer coated on the FTO- $\text{TiO}_2$  photo-anode give the 7.6% of power conversion efficiency.

**Keywords:** Polyethylene glycol, Cesium lead iodide, Photo-sensitizer, Perovskite Solar Cell, Efficiency.

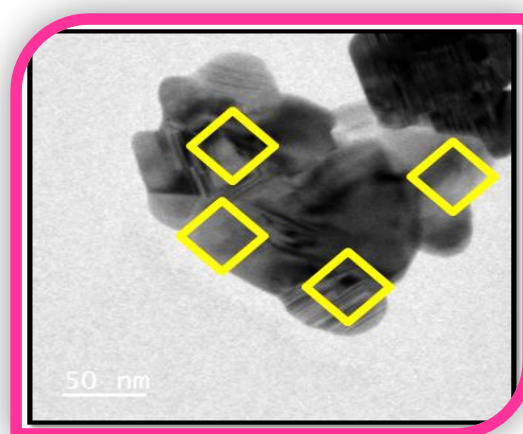


**Figure.**HR-TEM image of PEG assisted synthesis of  $\text{CsPbI}_3$  perovskite

## PP 55 Synthesis and characterizations of core-shell Ag@SiO<sub>2</sub> nanoparticles for enhanced antibacterial and cytotoxicity studies

B. Suganya bharathi, T. Stalin\*

\*Department of Industrial Chemistry, School of Chemical Sciences  
Alagappa University, Karaikudi - 630 003, Tamilnadu.  
E-mail: sbsuganyaa@gmail.com and drstalin76@gmail.com

### Abstract

Silver (Ag) based nanomaterials are one type of highly effective antimicrobial materials and it is widely used in medical devices, consumer products, and wound dressings. We have demonstrated a facile approach for the preparation of Ag@SiO<sub>2</sub> nanoparticles by *stober* process. The surface morphologies of the prepared core-shell materials were confirmed by SEM and TEM analysis. Our results showed that the Ag@SiO<sub>2</sub> nanoparticles exhibit well-defined antibacterial inhibition against *E. coli* bacteria. In addition, the materials have excellent cytotoxicity towards fibroblast cell line.

### Introduction

Core-shell nanostructure materials have recently been subject to extensive research for their unique functionalities from cores and shells and great application potentials in various fields. Among various metals, silver (Ag) NPs have attracted significant interest owing to their remarkable optical properties related with the localized surface plasmon resonance. Silica has long been used as a stable coating for metal nanoparticles, allowing the formation of stable nanostructures. For the fabrication of core-shell Ag@SiO<sub>2</sub> nanoparticles are prepared through a facile surfactant free strategy.

### Experimental details

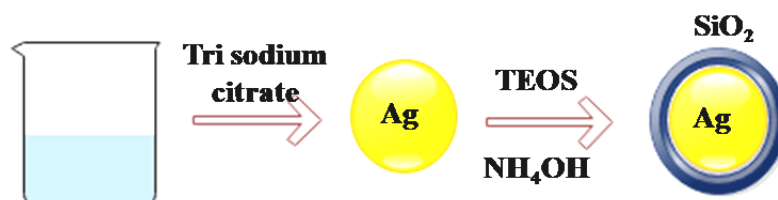


Figure 1. Schematic representation for the preparation of core-shell Ag@SiO<sub>2</sub> nanoparticles

### Results and discussion

The UV-Vis spectrum indicates that the SPR band is located at 431 nm. The SEM observation confirms that core-shell Ag@SiO<sub>2</sub> nanoparticles. The transmission electron microscopy images further confirmed the spherical shape and uniform particle size. The SiO<sub>2</sub>coated Ag nanoparticles surface was analysed by using XRD and EDS techniques. The

antibacterial test of Ag@SiO<sub>2</sub> against *E.coli* was performed by agar diffusion method. Moreover, the excellent biocompatibility was demonstrated by low cytotoxicity against fibroblast cell line even at higher concentration of 200 µg/ml.

### Conclusions

According to the above results, we propose a possible mechanism for the formation of the core-shell Ag@SiO<sub>2</sub> nanoparticles through the simple approach. The UV-Vis spectroscopy proves to be a convenient and fast way to optically detect SiO<sub>2</sub> shell on the surface of colloids. The convenient synthesis, uniform core-shell structure, and excellent antibacterial and cytotoxicity performance make our material highly promising for biomedical studies.

### References

- Tan, P.; Li, Y.H.; Liu, X.Q.; Jiang, Y.; Sun, L.B. Core-shell AgCl@ SiO<sub>2</sub> nanoparticles: Ag (I)-based antibacterial materials with enhanced stability. *ACS Sustainable Chemistry & Engineering*. **2016**, *4*, 3268-3275.
- Alimunnisa, J.; Ravichandran, K.; Meena, K.S. Synthesis and characterization of Ag@ SiO<sub>2</sub> core-shell nanoparticles for antibacterial and environmental applications. *Journal of Molecular Liquids*. **2017**, *231*, 281-287.

## **PP 56** Development of PANI-based coating to suppress copper corrosion

**M. Kowsalya<sup>1</sup>, M. Priyanga<sup>1</sup>, S Sathiyarayanan<sup>2</sup>, Aiswarya Bhaskar<sup>2,\*</sup>**

<sup>1</sup>Chemistry Department, Alagappa Govt. Arts and Science College, Karaikudi, Tamil Nadu 630002

<sup>2</sup>Corrosion and Material Protection Division, CSIR-Central Electrochemical Research Institute (CECRI), Karaikudi, Tamil Nadu, 630002, \*Email: aiswarya@cecri.res.in

### Abstract:

Copper is a metal widely used in various industries for different applications. Copper is subjected to corrosion, particularly to environmental assisted cracking [1, 2]. Selected coatings were investigated in this work to see their influence on suppression of corrosion by creating a protective layer on the surface. In this work, PANI-based materials were synthesized and coated on copper foils. The raw copper foils were purchased as it is from MTI Corporation and etched in low concentrated nitric acid. The obtained coated foils were characterized using various techniques such as Scanning electron microscopy (SEM), optical microscopy and FESEM. The elemental analysis on the coated and uncoated foils was performed using Energy-dispersive X-rayspectroscopy (EDX) analysis. The surface species were investigated using X-rayphotoelectron spectroscopy (XPS). The corrosion behaviour of the coated and uncoated foils was investigated and compared using electrochemical characterization in saline solution. More details regarding

the synthesis parameters, coating procedure and the influence on corrosion suppression will be described in the poster.

### Acknowledgement:

The CSIR-CECRI in house project (IHP 0105) is gratefully acknowledged by the corresponding author (Dr. Aiswarya Bhaskar) for the financial support.

### References

- S. Kim, T.-H. Le, C. S. Park, G. Park, K. H. Kim, S. Kim, O. S. Kwon, G. T. Lim, H. Yoon, *Scientific Reports* **7** (2017) 15184  
 S. Dai, J. Chen, Y. Ren, Z. Liu, J. Chen, C. Li, X. Zhang, X. Zhang, T. Zeng, *Int. J. Electrochem. Sci.*, **12** (2017) 10589 – 10598

## PP 57 Studies on Chemical and Radiation Stability of Some Ionic Liquids-Theoretical Approach

R. Josephine Punitha, S. Karthick and G. Gopu\*

Department of Industrial Chemistry, Alagappa University, Karaikudi – 630003

\*E-mail: nggopi79@gmail.com

### Abstract

Density functional theory was used to calculate the oxidation potentials and the reduction potentials of some ionic liquids by the backbone of highest occupied molecular orbital (HOMO) and lowest unoccupied molecular orbital (LUMO) energy values. For that purpose, the linear relationships between the HOMO energies and the oxidation potentials, and the linear relationships between the LUMO energies and the reduction potentials were obtained. The chemical and radiation stability were well-arranged and ordered for anions and cations of the ionic liquids by calculated oxidation potentials and reduction potentials. Also, we have calculated the various electronic properties such as Total energy, HOMO-LUMO Energy Gap, Ionization potential, Electron affinities, Chemical Hardness and Electronegativity. The anion stability is related to electronegativity and ion size, whereas the cation stability is related to the branching and length of alkyl chain. Stability has been induced by the branching of alkyl group in Imidazolium and pyridinium derivatives as shown in Table 1. Results expressed that the stability increased by the substitution (alkyl) in both derivatives. From the results obtained, Imidazolium derivatives have a more stability compare to pyridinium derivatives.

**Table 1: Conformation Energies and Reduction potential**

S. No	Cation Name	$E^{(+)}$	$E_{(Lumo)}$	Reduction Potential
1	1,3 BMP	-445.357841	-0.2382743	-1.29981
2	1,4 BMP	-445.356639	-0.2332659	-1.35944
3	1-ethyl 2,3 DMI	-384.109728	-0.0077733	-4.04589

4	1-ethyl 2 MP	-366.707274	-0.2399261	-1.28015
5	1-ethyl 3 MI	-344.636276	-0.1899806	-1.87512
6	1-ethyl 3 MP	-366.707738	-0.2420686	-1.25466
7	1-methyl 3 PI	-381.439593	-0.0742808	-3.25355
8	1-butyl P	-366.699943	-0.2469263	-1.19675

**Keywords:** Ionic Liquid, DFT, Electronic Properties, Chemical and Radiation Stability

### References:

Tian Guo-cai, et al, *Trans. Nonferrous Met. Soc. China*, 19 (2009) 1639–1644.

Niranjan V. Ilawe Shriram Ramanathan, Bryan M. Wong, Jianzhong Wu, and Jia Fu  
*J. Phys. Chem. C, Just Accepted Manuscript*, 2016.

## PP 58 An Efficient Synthesis of Dihydropyrimidine Derivatives Using Biginelli Multicomponent Reaction as Key Step

P. Siva, M. Krishnan, A. Meenal, R. Eswar and G. Gopu\*

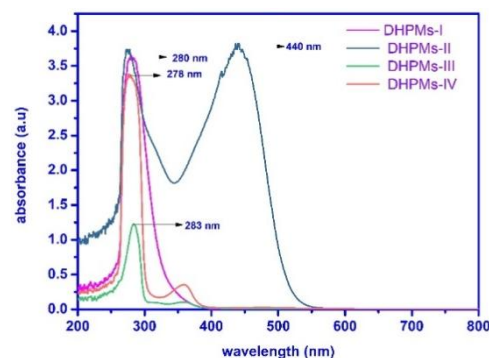
Department of Industrial Chemistry, Alagappa University, Karaikudi – 630003

E-mail: nggopi79@gmail.com

### Abstract

Among the various organic synthesis, Multicomponent reactions is the most significant route in organic industry for the application in the microbiology and pharmaceutical industry. Two component reactions are basically different from multicomponent reaction in the various aspects. In this work, Biginelli condensation treated as a one-pot multicomponent acid-catalyzed reaction. The synthesized Dihydropyrimidine (DHPMs) derivatives from using easily-accessible starting materials, aldehyde, ethyl acetoacetate, (thio)urea, ethanol, HCl. DHPMs have stimulated resurgence of interest in the past two years due to the wide ranging pharmacological activities, the compounds with a broad variety of biological activities and inhibitors of calcium channel, anti-inflammatory, antimicrobial activity. A convenient and efficient protocol for the one-pot synthesis of 3,4-dihydropyrimidin-2-(1H)-one/thione derivatives of aldehydes and ethyl acetoacetate compounds with HCl as the catalyst was described. We had the advantages of good performance, simplicity, and short time reaction. Identification of products using UV-Vis, FT-IR, <sup>1</sup>H NMR, <sup>13</sup>C NMR and Mass spectral data.

**Figure 1:** UV-Vis spectra of different Dihydropyrimidine (DHPMs) derivatives



**Keywords:** Biginelli reaction, Multicomponent synthesis, Dihydropyrimidine(DHPMs), Microbiological study and 3,4-dihydropyrimidin-2-(1H)-one/thione

## References

- Honnappa Nagarajaiah, Arindam Mukhopadhyay, Jarugu Narasimha Moorthy, 'Biginelli reaction', *Tetrahedron Letters*, 57 (2016) 5135–5149
- C. Oliver Kappe, 'Dihydropyrimidine Synthesis New Tricks from an Old Dog', *Acc. Chem. Res.*, 33, 2000, 879-888.

## **PP 59** Fe-containing oxides as conversion anode model systems for lithium-ion battery

M. Priyanga<sup>1</sup>, M. Kowsalya<sup>1</sup>, Aiswarya Bhaskar<sup>2\*</sup>

<sup>1</sup>*Chemistry Department, Alagappa Govt. Arts and Science College, Karaikudi, Tamil Nadu.*

<sup>2</sup>*Corrosion and Material Protection Division, CSIR-Central Electrochemical Research Institute (CECRI), Karaikudi, Tamil Nadu, 630002, \*Email: aiswarya@cecri.res.in*

Lithium-ion batteries are most promising power sources for portable electronic devices due to their high energy density. To exploit lithium-ion batteries to their maximum applications, innovative electrode materials should be developed and existing materials should be improved. In a lithium-ion battery, negative electrode materials are required in excess amount (with respect to the specific capacity) in comparison with the positive electrode materials. Hence, it is important to reduce the amount of negative electrode so as to reduce the cell size and further the production cost[1]. At present, the widely used negative electrode material is graphite. Graphite has a limited specific capacity of 372 mAh g<sup>-1</sup>. Moreover, it suffers from safety issues. Due to the lower working voltage of graphite, the lithium plating can occur on the electrode surface which could lead to a thermal runaway. Hence, intense research on alternative negative electrode materials are going on worldwide to hunt for alternate materials with higher specific capacity as well as better safety characteristics.

Conversion reaction-based transition metal oxides are promising candidates as anodes for lithium-ion batteries because of their high theoretical capacities. Among those, the Fe-containing oxide materials are particularly attractive due to their low cost and high abundance. In this work, Fe-containing oxide materials were synthesized or bought as it is from manufacturer. The phase purity, particle size as well as elemental analysis were conducted using X-ray diffraction, Scanning electron microscopy as well as Energy-dispersive X-ray spectroscopy (EDX) analysis, respectively. The electrochemical characterization was performed using cyclic voltammetry and galvanostatic cycling techniques and will be discussed in the poster.

## Acknowledgement

The CSIR-CECRI in house project (IHP 0105) is gratefully acknowledged by the corresponding author (Dr. Aiswarya Bhaskar) for the financial support.

## References

- N. Nitta and G. Yushin, Part. Part. Syst. Charact., 2014, 31, 317–336.  
N. Zhang, X. Han, Y. Liu, X. Hu, Q. Zhao, and J. Chen, Adv. Energy Mater., 2014, 1401123.

## **PP 60** Electrochemical Detection of Phenol on Copper Based Metal-Organic Framework

S. Vijayabose, T. Ponmuthuselvi and S. Viswanathan\*

*Department of Industrial Chemistry, Alagappa University, Karaikudi-630 003, Tamil Nadu.*

*\*Corresponding Author E-mail: [rviswa@gmail.com](mailto:rviswa@gmail.com)*

### Abstract:

Copper based metal-organic framework (Cu-MOF) was prepared by Solvothermal method. The morphology and structure of Cu-MOF were characterized via SEM, UV-DRS, FT-IR and XRD. The Cu-MOF was applied in the modification of a carbon paste to obtain a biomimetic sensor for the electrochemical determination of phenol. Electrochemical studies show that Cu-MOF/CPE is better electro catalytic activity for phenol oxidation as compared to bare CPE. Differential pulse voltammetric studies showed the phenol oxidation displayed high performance, offering a low detection limit range from 3  $\mu\text{M}$  to 60  $\mu\text{M}$  and a detection limit of 6  $\mu\text{M}$ . It is due to easy fabrication, adequate robustness, renewability, good reproducibility and high stability.

**Keywords:** Metal-organic framework, Carbon paste electrode, Differential pulse voltammetry, Phenol

### Introduction

Large amounts of industrial wastewater containing toxic and non-degradable organic compounds have recently been discharged into the aquatic environment. The electrochemical oxidation process is considered the most promising treatment method because of their high efficiency, wide applicability and environmental compatibility. In an electrochemical oxidation process various factors are available, the anode material is very important so the first time we have used metal-organic frameworks (MOFs). MOFs are a new class of hybrid inorganic-organic porous crystalline materials assembled using metal ions or clusters and organic linkers via coordination bonds, often resulting in fascinating structural topologies and offering unique chemical properties.

### Experimental Details

Cu-MOF was synthesized by Solvothermal method from the precursors of copper nitrate benzene tricarboxylic acid (BTC). Biomimetic sensors were constructed by a composition of 5:75:20wt% Cu-MOF: graphite powder: mineral oil in a mortar for 20 minutes to get a carbon



paste. The resulting modified carbon paste was placed in a plastic tube (1.0 mm internal diameter) and a copper wire was inserted to obtain the external electric contact.

## Results and Discussion

Morphological studies clearly show the synthesized Cu-MOF is highly porous in nature. The crystals of Cu-MOF are octahedral-shaped with smooth surfaces. The UV DRS technique was used to analyze solid samples of Cu-MOF. Metal organic framework of Cu-MOF exhibits two absorption bands around 303 nm and 700 nm. The first one is addressed in the aromatic ligand and the latter one broad peak is due to the d-d transition of  $\text{Cu}^{2+}$ . The infrared spectra also presented the expected bands for the complex, with the O-H stretching (from the water) at 3000-3500  $\text{cm}^{-1}$ , C-H stretching (from the rings) at around 1500  $\text{cm}^{-1}$  and C-H out-of-plane bending at 675  $\text{cm}^{-1}$ . The carboxylate bands were also visible at 1650  $\text{cm}^{-1}$ , with a wavenumber consistent with the formation of a complex.

To investigate the electro catalytic activity of phenol oxidation on Cu-MOF/CPE. The cyclic voltammetric behavior of phenol was carried out in a solution 100  $\mu\text{M}$  phenol in pH 6.0 0.1 M phosphate buffer, saturated with  $\text{N}_2$ . In these conditions, the Cu-MOF/CPE observed phenol undergoes oxidation a two pack at  $E_{p1a} = +0.854$  V,  $E_{p2a} = +0.386$  and one reduction peak at  $E_{p3c} = +0.59$  V, which is formed dihydric phenol from quinone. Cu-MOF/CPE shows the phenol oxidation peak was increasing its compared to bare CPE, indicating that this reaction is thermodynamically favored, which can be attributed to the catalytic ability of Cu-MOF.

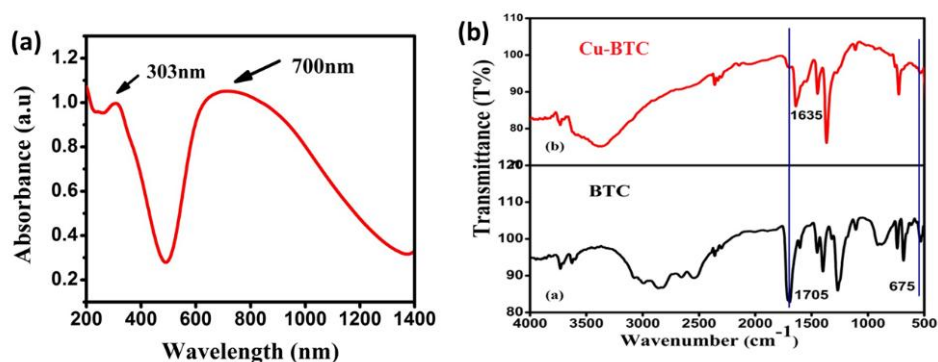


Fig: 1 (a) UV-DRS spectrum of Cu-MOF (b) FT-IR Spectra of (i) Benzene tricarboxylic acid (BTC) (ii) Cu-MOF

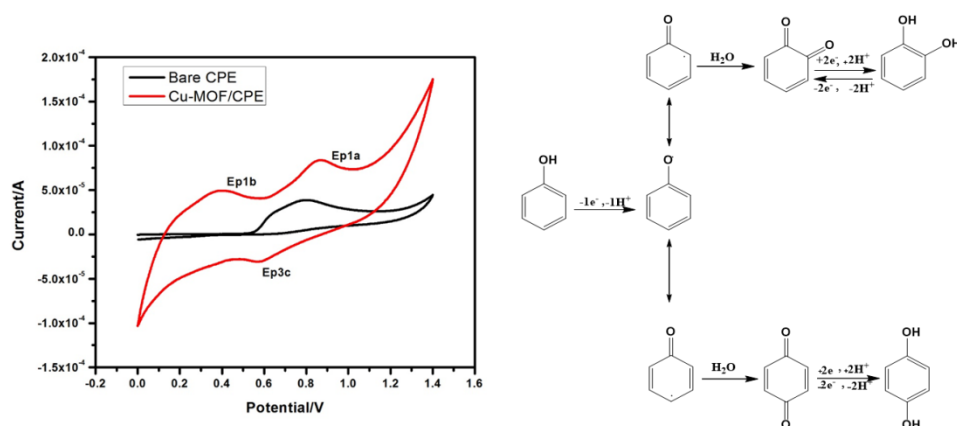


Fig. 2. (a) CV responses of the bare CPE and the Cu-MOF/CPE in 0.1M phosphate buffer (pH 6) solution containing 100 μM phenol. (b) Schematic diagram of oxidation mechanism

## Conclusion

A novel Cu-MOF material was synthesized and used to fabricate a sensitive and selective electrochemical biomimetic glucose sensor. The structural features of Cu-MOF were characterized by XRD, FT-IR, and SEM. In this study, a Cu-based MOF was successfully employed in the modification of a carbon paste to obtain a biomimetic sensor for the determination of phenol by DPV. The Cu-MOF sensor exhibited high selectivity, acceptable sensitivity, good repeatability, and adequate stability and lifetime.

## Reference

- H. Furukawa, K. E. Cordova, M. O'Keeffe, O. M. Yaghi, *Science* 2013, 341, 1230444.  
 A. A. Kumar, B. E. K. Swamy, P. S. Ganesh, T. S. Rani, G. V. Reddy, *J. Electroanal. Chem.* 2017, 799, 505–511.

## PP 61 Synthesis of new ionic liquid crystal bearing biphenyl core and Investigation of mesophase behaviour

M. Parimala, R. Mangaiyarkarasi and S. Umadevi\*

*Liquid Crystal Lab, Department of Industrial Chemistry, School of Chemical Sciences, Alagappa University, Karaikudi -3, Tamil Nadu, India.*

*Email: parimalamanickam80@gmail.com mangairajkumarchem@gmail.com and umadevilc@gmail.com*

## Abstract

This work describes the development of a new of ionic liquid crystal based on imidazolium salt with biphenyl core. Here in, we present the preparation of the compound, its chemical characterization and our preliminary results on mesophase behavior. New calamitic (rod-like) ionic liquid crystal was synthesized and chemically characterized using infrared and nuclear magnetic resonance spectroscopy. Mesomorphic behaviour was studied by employing polarizing optical microscope and differential scanning calorimetry. The synthesized ILC compound shows a highly ordered smectic A (SmA) phase.

**Keywords:** Ionic liquid crystal, biphenyl core, imidazolium cation, anisotropic fluid, organized structure, SmA phase.

## Introduction

Ionic liquid crystals (ILC) are a fascinating class of materials, both from fundamental and from application points of view. Up to date, several ILCs exhibiting interesting properties with a potential for wide applications have been reported [1]. For example, ILCs displaying a columnar hexagonal mesophase showing a very high ionic conductivity have been described [2]. Further, ILC exhibiting a cubic phase, which behaves as nano ion channel networks is reported [3]. ILCs include unique properties of ionic liquids such as ionic conductivity, high polarizability, low vapour pressure and the interesting features of LCs namely organized structure, anisotropic chemical and physical properties, response to electric and magnetic field etc. as promising materials for various applications. They find applications in areas namely energy storage devices, sensors, regioselective synthesis, anisotropic conductors, separation membranes, power sources, and so forth.

## Experimental details

Scheme 1: Schematic representation of synthesis of ionic liquid crystal 3

## Results and Discussion

Herein, we describe a simple two-step strategy for the synthesis of a new calamitic (rod-like) ILC with biphenyl moiety bearing an imidazolium cation. The new ILC is chemically characterized through infrared (IR), nuclear magnetic resonance spectroscopy (NMR) techniques and mesophase behaviour was studied using polarizing optical microscopy (POM), differential scanning calorimetry (DSC) and X-ray diffraction studies (XRD).

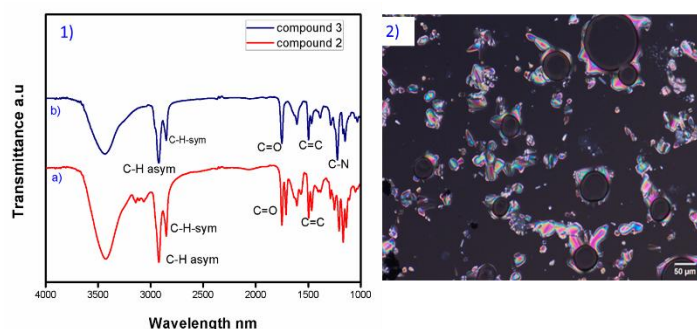


**Figure 1: FT-IR spectrum of compound 2 and 3: POM image of compound 3**

Fig 1a shows FT-IR spectrum of the synthesized compound **2**, the sharp peak observed at  $1735\text{ cm}^{-1}$  corresponds to the C=O stretching of ester group in compound **2** and the peak at  $2806\text{ cm}^{-1}$  is due to C-H symmetric stretching and the peak at  $2933\text{ cm}^{-1}$  is due to asymmetric C-H stretching. The broad peak at  $3451\text{ cm}^{-1}$  is due to O-H stretching from the moisture content. Fig 1b) display the IR spectrum of the synthesized ILC, **3** with imidazolium moiety which shows sharp peak at  $1736\text{ cm}^{-1}$  due to C=O stretching of the ester linkage and the peaks at  $1250\text{--}1020\text{ cm}^{-1}$  corresponds to C-N stretching, indicating the presence imidazolium ring. The textural observation of the mesophase exhibited by ILC compound, **3** was observed under POM. This compound displayed the textural features of SmA namely fan-shaped focal conic texture coupled with a homeotropic regions. Fig 1(2) shows a POM image of compound **3** sandwiched in a normal glassslide and a coverslip, obtained at  $126^\circ\text{C}$  on cooling from isotropic phase. This image clearly indicated the presence of SmA phase with a lamellar ordering.

## Conclusion

A new ILC based on imidazolium salt containing a biphenyl core was prepared successfully by a simple facile strategy. The synthesized ILC compound exhibited a highly ordered smectic A (SmA) phase with a lamellar ordering. Combination of the ionic liquid properties namely ionic conductivity, low vapour pressure and interesting properties of LC behaviour in such ILC can be exploited for the synthesis of nanomaterials as well as organic synthesis as a organized reaction medium.

## References

- K. Binnemans, *Chem. Rev.*, 2005, 105, 4148.
- M. Yoshio, T. Mukai, H. Ohno, T. Kato, *J. Am. Chem. Soc.*, 2004, 126, 995.
- T. Ichikawa, M. Yoshio, T. Mukai, H. Ohno, T. Kato, *J. Am. Chem. Soc.*, 2007, 129, 10663.

**PP 62** **Phytochemical and Biochemical Screening of Some Solvent Extracts of *Gracillaria Edulis* (Family: Gracilariaceae) Collected From Thondi Coast, India Tamilnadu, India**

**Chandraleaga.G<sup>1</sup> and Ramadas.V<sup>2</sup>**

<sup>1</sup> *Research Scholar, P.G & Research Department of Zoology, Raja Doraisingam Govt. Arts College, Sivagangai – 630561. (Email: sivachandra2020@gmail.com)*

<sup>2</sup> *Assistant Professor, P.G & Research Department of Zoology, Raja Doraisingam Govt. Arts College, Sivagangai – 630561. (Email: rammarine@yagoo.com)*

**Abstract**

**Objective:** Screening of phytochemicals and biochemical composition of some solvent extracts of marine seaweed *G.edulis*.

**Methods:** Extracts from seaweed was prepared using Soxhlet apparatus with various solvents such as, chloroform, methanol and distilled water. Phytochemical and biochemical analysis were carried out using standard methods.

**Result:** The phytochemical analysis revealed the presence of Tannins, Phytosterols, Glycosides, Alkaloids, Flavanoids, Protein, Diterpenes, Saponin, Resins, Reducing sugar and Non-Reducing sugar in the *G.edulis*. Out of the three solvents tested, Chloroform was identified as the best solvent for most of the phytochemical compounds from the algae chosen for the study followed by methanol and distilled water. The biochemical analysis of these seaweed was carried out using quantitative methods and the results indicated the presence of Carbohydrate, Lipid, Protein, Chlorophyll, Carotenoid, Phenol, Flavanoid, Mannitol and Water retention capacity.

**Keyword:** Macro algae – Red algae, Thondi Coast, Phytochemical and Biochemical Composition.

**Introduction**

Seaweeds are primitive non-flowering plants without true root stem and leaves. They include one of the commercially important marine renewable source. Seaweeds have been used as food stuff in the Asia diet for centuries as it contains carotenoids, dietary fibres, proteins, essential fatty acids, vitamins and minerals [1]. Seaweed extracts are considered to be a rich source of phenolic compounds. The large majority of these are terpenes, but fatty acids are also common with nitrogenous compounds [2]. Now a days, there is an increasing demand for biodiversity in screening programmes for selecting therapeutic drugs from natural products, the marine organisms; especially seaweeds are of immense interest since they have a broad range of biological activities such as antibacterial, antifungal, antiviral, antitumour, anti-inflammatory and antioxidants. Seaweeds have been recognized as potential sources of antibiotic substances. The production of antimicrobial activities was considered to be an indicator of the bioactive secondary metabolites [3, 4, 5]. Marine Seaweeds draws an extraordinary wealth of mineral elements from the sea that can account for up to 36% of its dry mass. The main elements being iodine and

calcium. The mineral macronutrients include sodium, calcium, magnesium, potassium, chlorine, sulfur and phosphorus and the micronutrients include iodine, iron, zinc, copper, selenium, molybdenum, fluoride, manganese, boron, nickel and cobalt. The chemical composition of seaweeds varies with seaweeds species, season, location and analytical methods [6].

## Methodology

### Collection samples:

The seaweed *Gracillaria edulis* has collected from Thondi coast of Tamil Nadu, India. The sample was placed inside sterile polythene bags underwater and transferred to the lab aseptically in ice boxes. The seaweed sample was washed with tap water several times and shade dried, powdered with a blender and stored in an air tight container and kept in a room temperature for further study.

### Extract preparation

The shade dried seaweed sample was ground to a coarse powder. Twenty grams of the powder were extracted with 200ml of different solvents such as, chloroform, methanol and water by soxhlation for 12 to 24hours. Seaweed extracts were subjected to various qualitative and quantity chemical tests to screen the phytochemical and biochemical constituents.

### Phytochemical screening

The phytochemicals of seaweeds, such as, Tannins (Gelatin test (Shaik, 2011) ), Phytosterols (Salkowski test (Srivastava *et al.*, 2010) ), Glycosides (Legal's test (Shaik, 2011) and Kellar Killani test (Srivastava *et al.*, 2010) ), Alkaloids (Wagner's test (Shaik, 2011) ), Carbohydrates (Test for reducing sugars ( Fehling's test (Sofowora, 1993) and Benedict's test (Srivastava *et al.*, 2010) ) (Test for non reducing sugars ( Molisch's test (Srivastava *et al.*, 2010)), Flavanoids (Alkaline reagent test (Shaik, 2011) ), Diterpenes (Copper acetate test ( Shaik, 2011) ), Protein (Xanthoproteic test (Shaik, 2011) )and (Biuret test ( Shaik, 2011) ), Resins (Acetone water test (Shaik, 2011) ) and Saponins ( Foam test ( Srivastava *et al.*, 2010) ) and (Froth test (Shaik, 2011) ) have been analysed.

### Biochemical analysis

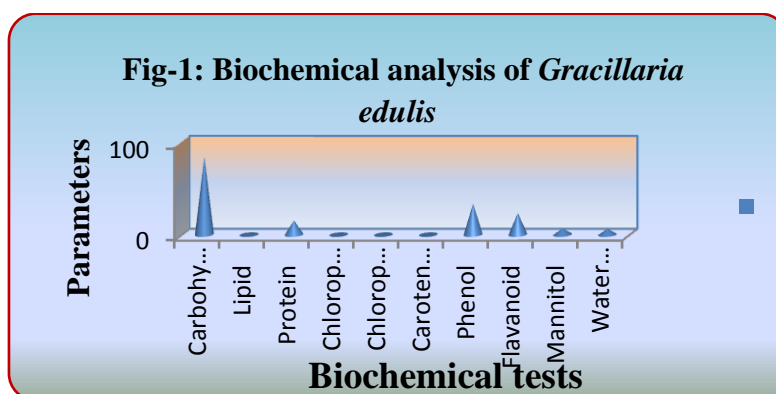
The biochemical constituents of seaweed, such as, Lipid (Bligh and Dyer, 1959), Carbohydrate (Hedge and Hofreiter, 1962), Protein (Lowry *et al.*, 1951), Phenol (Vijayabasker and Shiyamala, 2011), Flavanoids (Meenakshi *et al.*, 2009), Chlorophyll and caroteinoid (Kirk and Allen), Mannitol (Black *et al.*, 1951) and water retention capacity (Ruperez and Calixto, 2001) have been analysed.

### Results:

The phytochemical screening of the edible Rhodophycean seaweed *Gracillaria edulis* gave positive result for secondary metabolites namely Tannins, Phytosterols, Glycosides,

Alkaloids, Reducing and Non-reducing sugars, Flavanoids, Protein, Diterpenes, Saponins and Resins. The biochemical analysis of the Red Seaweed *Gracillaria edulis* have showed the presence of carbohydrate ( $84 \pm 0.072$  mg/g), the lipid ( $1.08 \pm 0.04$  mg/g), chlorophyll 'a' pigment ( $0.5589 \pm 0.062$  mg/g), Chlorophyll 'b' pigment ( $0.6852 \pm 0.017$  mg/g). Besides, *Gracillaria edulis* showed the presence of protein content ( $15.46 \pm 0.05$  mg/g), total phenolic content ( $33.66 \pm 1.10$  mg/g), total flavonoids ( $23.33 \pm 0.58$  mg/g), carotenoid ( $0.1606 \pm 0.052$  mg/g), mannitol ( $6.8 \pm 0.49$  mg/g) and water retention capacity ( $6.2 \pm 0.3$  mg/g). The quantitative result showed the (Figure – 1).

**Table-1: Biochemical analysis of *Gracillaria edulis***



## Discussions

The results of the Qualitative Phytochemical screening carried out on various extracts of chloroform, methanol and distilled water. The edible rhodophycean member *Gracillaria edulis* have positive result chloroform extract namely Phytosterols, Glycosides, Alkaloids and Non-reducing sugars, Flavanoids, Protein and Diterpenes. The methanol extract of seaweed contain Reducing sugar, Diterpenes, Protein and Saponins and the water extract of seaweeds contain the Tannins, Reducing sugar, Flavanoids, Protein, Resins and Saponins. Therefore, Chloroform extract was identified as the best solvent than other two extracts. Such preliminary phytochemical screening is helpful in prediction of the nature of drugs and also useful for detection of different constituents in different polarity solvent. The results were coincided with the reports of biochemical analysis of *Gracillaria edulis* showed highest quantity of carbohydrate and protein than the lipid and *Gracillaria edulis* also contain rich amount of chlorophyll a and b.

## Conclusion

Results revealed that, the marine sea weeds have several chemical constituents of high therapeutic efficacy. Further studies are required to investigate the extracts of for potential pharmacological properties. The present study suggests that, the seaweed extracts possessed phytochemical activity thus supporting their folkloric usage, promising a future scope for the use of these marine seaweeds against microbial populations.

## References

- Mohamed Fayaz KK, Namitha KN, Chidambara Murthy M, Mahadeva Swamy R, Sarada Salma Khanam PV, Subbarao, et al. Chemical composition, iron bioavailability and antioxidant activity of *Kappaphycus alvarezii* (Doty). *J Agri Food Chem*, 2005; 53: 792-797.
- Heo, S.J., E.J. Park, K.W. Lee and Y.J. Jeon, Antioxidant activities of enzymatic extracts from brown seaweeds. *Bioresour. Technol.*, 2005; 96: 1613-1623.
- Gonzalez Del Val, A., G. Platas, A. Basilio, J. Gorrochategui, I. Suay, F. Vicente, E. Portillo, M. Jimenez Del Rio, R.G. Garcia and F. Pelaez, Screening of antimicrobial activities in red, green and brown macroalgae from Gran Canaria (Canary Islands, Spain). *Int. Microbial.*, 2001; 4: 35-40.
- Chiheb, I., R. Hassane, Martinez- L. José, D.S.J. Francisco, G.V.J. Antonio, B. Hassan and K. Mohamed. Screening of antibacterial activity in marine green and brown macroalgae from the coast of Morocco. *Afr. J. Biotechnol.*, 2009; 8(7): 1258-1262.
- Srivastava, N., K. Saurav, V. Mohanasrinivasan, K. Kannabiran and M. Singh, Antibacterial Potential of Macroalgae Collected from the Mandapam Coast, India *British J. Pharmacol. And Toxicol*, 2010; 1(2): 72-76.
- K. Ito., K. Hori., "Seaweed: chemical composition and potential food uses". *Food Review International*, 1989; 5(1): 101-144.
- Obasi NL, Egbunu ACC, Ukoha PO, Ejikeme PM. Comparative phytochemical and antimicrobial screening of some solvent extracts of *Samanea saman* pods. *African journal of pure and applied chemistry* 2010; 4(9): 206-212.

## PP 63 Facile synthesis of reduced graphene oxide using microware reaction

N. Sowndharya, R. Mangaiyarkarasi and S. Umadevi\*

*Liquid Crystal Lab, Department of Industrial Chemistry, School of Chemical Sciences, Alagappa University, Karaikudi -3, Tamil Nadu, India.*

*Email: sowndharyanehru96@gmail.com, mangairajkumarchem@gmail.com and umadevilc@gmail.com*

### Abstract

In this current work, we present the facile and rapid synthesis of reduced graphene oxide with the help of microwave irradiation. Graphene oxide (GO) solution was prepared in bulk using Hummer's method, followed by microwave – ionic liquid crystal assisted in-situ reduction of GO in a short span of five minutes. The prepared GO and reduced GO (rGO) have been characterized using Fourier Transformer Infra Red Spectroscopy (FTIR), X-Ray Diffraction (XRD), Scanning Electron Microscopy (SEM) and Raman Spectroscopy.

**Keywords:** Ionic liquid crystal, organized structure, microwave heating, low vapour pressure, graphene oxide, high polarizability.

### Introduction

Graphene based materials are quite popular due to the interesting properties such as excellent optical transparency, flexibility and electrical conductivity and find interesting



applications namely energy storage, fuel cells, sensing materials etc [1]. Ionic liquid crystal (ILC) is a fascinating class of material which combine the intriguing properties of ionic liquids such as ionic conductivity, high polarizability, low vapour pressure and the interesting features of liquid crystals namely organized structure and anisotropic chemical and physical properties[2]. Microwave irradiation over conventional heating has obvious advantages such as uniform and volumetric heating, being quick, as the reaction time decreases many fold and high reaction temperature can be avoided [3]. By combining the advantages of both ILC and microwave heating, herein, we describe a facile and scalable route towards the production of reduced graphene oxide within 2 mins duration at 420 W power, without any additional solvent.

### Experimental Details

Graphene oxide (GO) was prepared in bulk using Hummer's method. A suitable amount of ILC was added to the graphene oxide (GO) powder (1:1 wt%), mixed gently in a mortar – pestle and the mixture was treated in a microwave oven at 420 W for 2 mins period.

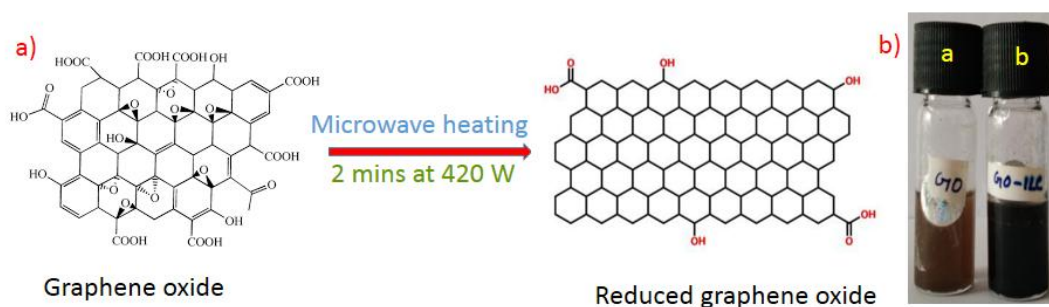


**Figure 1: Schematic representation of microwave reduction of graphene oxide  
Results and Discussion**

Upon microwave irradiation of an equal wt% of GO powder and ILC, the pale brown colour of GO/ILC (1/1,w/w) changed to black indicating the rapid reduction of GO to reduced GO(Fig. 1b). The total reaction time was set to be less than 5 minutes, which was sufficient for the reduction of GO. ILCs are efficient microwave absorbers and also offer an ordered reaction medium for the reduction. The microwave reduction of GO was completed within 2 minutes in the presence of the ILC, which is clearly visible as the colour change from yellow (GO solution) to completely black (rGO). The structure and morphology of both GO and rGO were analyzed using XRD, SEM, FTIR and Raman spectroscopy. A photograph of graphene oxide dispersed in ethanol (Fig1b-a) and the microwave-reduced GO dispersed in ethanol (Fig1b-b) are provided in Fig.1b. Herein, we provided the characterization details obtained for the graphene oxide. Fig.2a and b display an IR spectrum and a Raman spectrum obtained for GO.

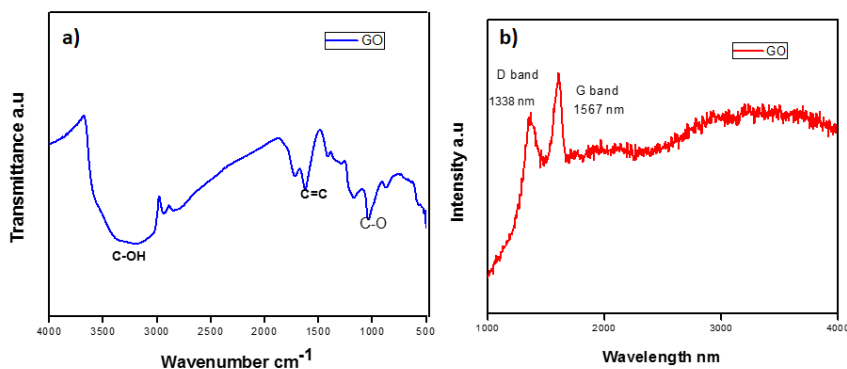


**Figure 2: a) FT-IR spectrum of synthesized GO b) Raman spectrum of GO**

IR spectrum shows that, synthesized GO has a peak at  $1081\text{ cm}^{-1}$  which is attributed to the C-O stretching vibration, confirming the presence of an oxide functional groups resulting from the oxidation process (Hummer's method). The peaks at  $1630\text{ cm}^{-1}$  to  $1650\text{ cm}^{-1}$  show the presence of C=C bond which remained after the oxidation process. The absorbed water in GO is shown by a broad peak extending from  $2885\text{ cm}^{-1}$  to  $3715\text{ cm}^{-1}$ , which is due to the O-H stretching of  $\text{H}_2\text{O}$  molecules. This supports the fact that GO is a highly absorptive material, as verified by its ability to become a gel-like solution. Fig.2b shows the Raman spectrum of GO, where the in-phase vibration (G band) of GO is at  $1567.04\text{ nm}$  and the disorder band (D band) of GO is at  $1338.22\text{ nm}$ .

## Conclusion

In summary, we have described a simple and effective approach for the reduction of graphene oxide in an ILC medium, using microwave irradiation for 2 mins at 420 W. The efficient and uniform microwave dielectric heating afforded by the ILC led to the rapid reduction of graphene oxide producing reduced graphene oxide embedded within the ILC template. We trust that such a facile and scalable process for the reduction of graphene oxide can offer great promise in energy storage device applications.

## References

- H. J. Han, Y. N. Chen and Z. J. Wang, *RSC Adv.*, 2015, **5**, 92940
- K. Goossens, C.W. Bielawski and Koen Binnemans, *Chem. Rev.*, 2016, **116**, 4643
- T. Kim, H. Chang Kang and T. Thanh Tung, *RSC Advances*, 2012, **2**, 8808.

## PP64 Lyotropic liquid crystal mediated synthesis of copper nanoparticles

N. Santhiya<sup>a</sup>, PR. Meyyathala<sup>b</sup> and Dr. S. Umadevia\*

<sup>a</sup>Department of Industrial Chemistry, Alagappa University, Karaikudi-630 003,  
Tamil Nadu, India

<sup>b</sup>District Institute of Education Training (DIET), Kalayorkovil, Sivagangai-630 551, Tamil Nadu.  
E-mail: santhiyachem94@gmail.com, meyyathal.riem@gmail.com and umadevilc@gmail.com

### Abstract

Synthesis of copper nanoparticles in a lyotropic liquid crystalline template formed by a mixture of non-ionic surfactant triton-X 100 and water in the ratio 42:58 wt% is described. Triton X-100 and water at this composition exhibits a hexagonal liquid crystal phase at room temperature. Copper nanoparticles were prepared in this medium by reducing cupric chloride using hydrazine hydrate as a reducing agent. For comparison, synthesis of copper nanoparticles was carried out in an aqueous template containing a cationic surfactant, cetyl trimethylammonium bromide (CTAB) using the same reducing agent under similar conditions. Synthesized particles were characterized using UV-Vis spectroscopy. Between two methods reported here, LC template was found to produce stable copper nanoparticles whereas copper nanoparticles synthesized in CTAB template aggregated upon formation.

**Keywords:** Lyotropic liquid crystal, template, hexagonal phase, surfactant, nanoparticles, UV-Vis

### Introduction

Lyotropic liquid crystals exhibit different phases like lamellar, cubic and hexagonal. These phases are thermodynamically stable, easily reproducible and offer an organized reaction media for the nanoparticles synthesis. Lyotropic liquid crystals (LLC) have been exploited for the synthesis of various metal and semiconducting materials[1]. Braun and co-workers had demonstrated that CdSe and CdS super lattices can be synthesized in a LLC phase formed by a nonionic organic amphiphile, water and semiconductor precursor[2]. Very recently, we reported the synthesis of silver nanoparticles in a hexagonal LLC phase [3]. Fascinating silver microparticles with anisotropic morphology were obtained by a simple method of reducing an appropriate amount of silver nitrate using a mild reducing agent ascorbic acid in LLC phase formed by water/triton X-100 mixture (58:42 wt%). Extending our work, herein we report the synthesis of copper nanoparticles in hexagonal LLC medium of water/triton X-100 mixture by reducing copper chloride using hydrazine hydrate at room temperature.

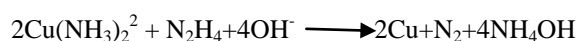
### Experimental Details

Synthesis of copper nanoparticles was carried out in a lyotropic liquid crystalline template formed by a mixture of non-ionic surfactant triton-X 100 and water in the ratio 42: 58 wt%. Triton X-100 and water at this composition exhibits a hexagonal liquid crystal phase at room

temperature. Copper nanoparticles were prepared in this medium at room temperature by reducing cupric chloride ( $\text{CuCl}_2$ ) using hydrazine hydrate ( $\text{N}_2\text{H}_4$ ) as a reducing agent in the basic medium. For comparison, synthesis of copper nanoparticles was carried out in an aqueous template containing a cationic surfactant, cetyl trimethylammonium bromide (CTAB) using the same reducing agent under similar conditions.

## Results and Discussion

A simple approach for synthesis of copper nanoparticles by employing two different templates has been described. Experimental conditions were maintained the same for both method. In the first method, Cu NPs were synthesized in presence of CTAB template by treating  $\text{CuCl}_2$  with  $\text{N}_2\text{H}_4$ , whereas in the second method, Cu NPs were synthesized in presence of a LLC template by treating  $\text{CuCl}_2$  with  $\text{N}_2\text{H}_4$ . The reduction reaction could be expressed as,



The formation of Cu nanoparticles was completed after about 2h, which was indicated by the formation of a deep wine red colour. Synthesized particles were characterized using UV-Vis spectroscopy. Between two methods reported here, LC template was found to produce stable copper nanoparticles whereas copper nanoparticles synthesized in CTAB template aggregated soon upon formation.

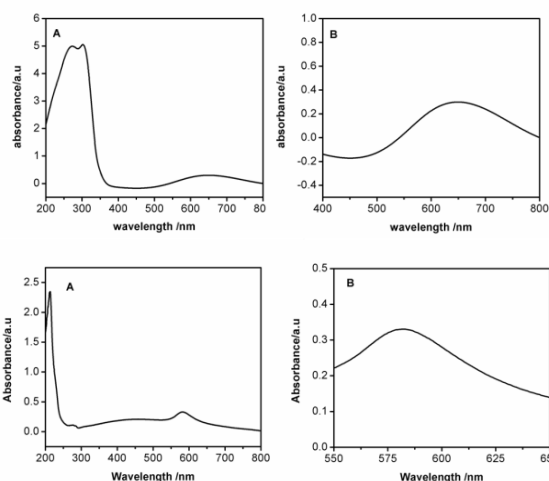


**Figure 1.** UV- Vis absorption spectra of Cu nanoparticles in triton X-100 template. A. Absorption due to triton X-100 and nanoparticles. B. Expanded version showing only the absorption due to copper nanoparticles.

**Figure 2.** UV- Vis absorption spectra of Cu nanoparticles in micellar template. A. Absorption due to CTAB and nanoparticles. B. Expanded version showing only the absorption due to copper nanoparticles.

## Conclusion

Copper nanoparticles were synthesized using  $\text{CuCl}_2$  and a reducing agent hydrazine hydrate in two different methods by employing a cationic surfactant CTAB (micellar) and a non-ionic surfactant triton X-100 in a LLC template at room temperature. UV-Vis spectroscopic studies of copper nanoparticles synthesized in LLC template showed absorption at around 648nm whereas the copper nanoparticles dispersion in micellar (CTAB) solution showed absorption at around 584nm. The copper nanoparticles formed in LLC template were stable for several months whereas the particles formed in CTAB medium aggregated within a week of formation.

## References

- J. H. Ding and D. L. Gin, Chem, Mater. **2000**, 12, 22-24.  
P. V. Braun, P. Osenar and S.I.Stupp.Nature,**1996**,380, 325-328  
S. Umadevi, R. Umamaheswari and V. Ganesh, Liq. Cryst. **2017**, 44, 1409

## PP 65 Synthesis and Characterization of Spinal Layered Cathode Materials for Lithium Ion Batteries

N. Vimalasruthi,<sup>a</sup> P. Periasamy<sup>b</sup> and S. Umadevi<sup>a</sup>

<sup>a</sup>Liquid Crystal Lab, Department of Industrial Chemistry, School of Chemical Science, Alagappa University, Karaikudi-3, Tamil nadu, India

<sup>b</sup>Electrochemical power sources division, CSIR-CECRI, Karaikudi-,3 Tamil nadu, India  
Email: [annamsruthi2015@gmail.com](mailto:annamsruthi2015@gmail.com), [periasamylibatt@gmail.com](mailto:periasamylibatt@gmail.com) and [umadevilc@gmail.com](mailto:umadevilc@gmail.com)

## Abstract

High energy-density lithium ion batteries are in demand for portable electronic devices and electrical vehicles. Since the energy density of the batteries relies heavily on the cathode material used, major research efforts have been made to develop alternative cathode materials with a higher degree of lithium utilization and specific energy density. In particular, layered lithium transition metal oxides can deliver high capacity at lower cost than the conventional (LiCoO<sub>2</sub>). In this work, the preparation condition of layered LiNi<sub>0.3</sub>Mn<sub>0.3</sub>Co<sub>0.3</sub>O<sub>2</sub> - LiNi<sub>0.5</sub>Mn<sub>1.5</sub>O<sub>4</sub> composite cathode materials by solid state method. These materials showed excellent capacity retention 76.1%, 81.4% and 82.6 % (80:20, 70:30 and 60:40) between 2.8-4.8V at 15 cycles. It was found that the composite cathode materials exhibited better reversibility and higher discharge capacities than that of the bare LiNi<sub>0.5</sub>Mn<sub>1.5</sub>O<sub>4</sub> cathode materials.

**Keywords:** layered cathode materials, lithium ion batteries, capacity retention, charge discharge capacities.

## Introduction

In general, the commercial lithium-ion batteries use graphite-lithium composite (Li<sub>x</sub>C<sub>6</sub>) as anode, lithium cobalt oxide (LiCoO<sub>2</sub>) as cathode and a lithium-ion conducting electrolyte. When the cell is charged, lithium is extracted from the cathode and inserted at the anode. On discharge, the lithium ions are released by the anode and taken up again by the cathode. Numerous materials have been studied as cathodes in lithium ion battery including metal oxides, metal sulfides, conducting polymers and poly (sulfides). Among them, transition metal oxides are the most successful materials because of their chemical and structural stability, high lithium ion capacity and favorable electrical properties such as high conductivity of lithium ions and electrons. In addition, recently the use of layered LiCoO<sub>2</sub> as an intercalation cathode [1], the use of layered transition metal oxides including two dimensional layered oxides LiCoO<sub>2</sub>, LiNiO<sub>2</sub>, LiMnO<sub>2</sub> and LiV<sub>2</sub>O<sub>5</sub> and the three dimensional spinel LiMn<sub>2</sub>O<sub>4</sub> has well established and several groups have

focused their research on the maximization of electro-chemical properties of these existing materials [2-4].

### Experimental details

The first stage of this work included synthesis of composite cathode materials of  $\text{LiNi}_{0.3}\text{Mn}_{0.3}\text{Co}_{0.3}\text{O}_4$  (LNMC) and  $\text{LiNi}_{0.5}\text{Mn}_{1.5}\text{O}_4$  (LNM) by different ratio. It has been synthesized through a solid state method at  $1000^\circ\text{C}$  under air atmosphere. The second part of this work involved investigations of the electrochemical properties of the as-synthesized cathode materials for lithium ion batteries using cyclic voltametry and electrochemical impedance spectroscopy techniques.

### Result and discussion:

The synthesized materials were characterized by a combination of scanning electron microscopy (SEM), transmission electron microscopy (TEM) and X-ray diffraction (XRD). The efficiency of the prepared material, charge-discharge (CD) characteristics were carried out. The cells were charged & discharged at 0.051 mA in the voltage range between 2.8 and 4.8V. The discharge profile of bare  $\text{LiNi}_{0.5}\text{Mn}_{1.5}\text{O}_4$  cathode is  $108\text{ mAh}\cdot\text{g}^{-1}$  after 15 cycles and its related capacity retention 56%. The LNMC-LNM (wt. % 80:20, 70:20 & 60:40) composite cathode materials with capacity retention of 76.1%, 81.4% and 82.6%. It was found that the composite cathode materials exhibited better reversibility and higher discharge capacities than that of the bare  $\text{LiNi}_{0.5}\text{Mn}_{1.5}\text{O}_4$  cathode materials.

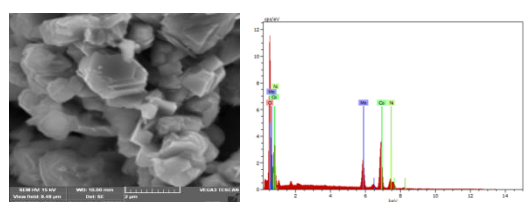


FIG 1 a. SEM and EDAX Image of LNMC

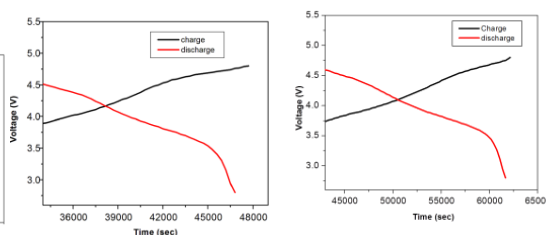
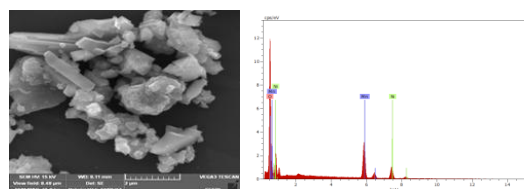
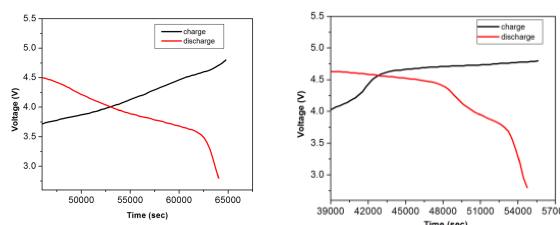


FIG 2 a. CD in LNMC: LNM (60:40) and (80:20)



1 b. SEM and EDAX image of LNM



2 b. CD in LNMC: LNM (70:30) and bare LNM

### Conclusion

Considering the important safety aspect of the lithium ion batteries for application, spinal layered cathode materials have been obtained through mixing of well characterized LNMC and LNM, synthesized using solid state method. The cyclic voltammetric results indicated that Ni and Mn were present as  $\text{Ni}^{2+}$  and  $\text{Mn}^{4+}$  respectively. The electrochemical performance indicated that

these compound have a high capacity and cycliability. These compounds can be used as cathode materials for future lithium-ion battery application.

## Reference

- Mizushima. K, Jones. P.C, Wiseman.P.J, Goodenough.J.B.; MRS Bull.1980, 15,783.  
Liu. H, Wu.Y.P, Rahm. E, Holze. R, Wu. H. Q, J. Solid State Electrochem. 2004, 8, 450.  
Whittingham. M.S, Chem. Rev. 2004, 104, 4271.  
Makhoniana. E.V, Pervov.V., Dubasova.V.S, Russ. Chem Rev. 2004, 73, 991.

## **PP 66** Photo switchable mono layer on Indium Tin Oxide substrate for alignment of liquid crystal

S. Esakkimuthu<sup>a</sup>, K. Mohana<sup>a</sup>, B. Sivaranjini<sup>a</sup>, and S. Umadevi<sup>a,\*</sup>

<sup>a</sup>Department of Industrial Chemistry, Alagappa University, Karaikudi-630 002

E-mail:asmuthu92@gmail.com,mohanakarupiah16@gmail.com, sivaranjini93alu@gmail.com  
and [umadevilc@gmail.com](mailto:umadevilc@gmail.com)

## Abstract

In this present work, we describe the synthesis of a photo-switchable azosilane compound and a simple methodology to covalently anchor this compound over an indium tin oxide (ITO) substrate. The synthesized compound was characterized by infrared spectroscopy (IR), nuclear magnetic resonance spectroscopy (NMR) and UV-Visible spectroscopy. Azosilane monolayer on ITO substrate was characterized by atomic force microscopy (AFM), contact angle (CA) and IR techniques. In the visible light, azosilane monolayers on ITO induced a vertical alignment of bulk liquid crystal (LC) sample whereas upon irradiation with a UV light, a planar orientation of the LC sample was obtained.

**Keywords:** self-assemble monolayer, azo compound, ITO substrate, liquid crystals, photo-switchable, alignment

## Introduction

Liquid Crystals (LCs) are self-assembled soft material with a huge potential for application in a wide variety of fields such as sensing, biomedical, photonics, optoelectronics, electronic conductors, photovoltaics etc. apart from their significant use in display technology. For majority of these LC applications, a pre-oriented well aligned sample of LC on a suitable substrate is highly crucial. In this regard, we perform self-assembled monolayers (SAMs) of tailor-made LC molecules on various substrates and investigate the alignment abilities of these films to orient the bulk LC sample [3,4]. Herein, we describe a SAM of azo-compound on the ITO substrate as an efficient alignment layers for the effective orientation of bulk LC sample. The orientation of the LCs can be easily altered between homeotropic and planar simply by irradiating the sample with visible or UV light respectively. The synthesis of the azo compound, surface modification of the ITO substrate with this compound and the characterization are described.

## Experimental details

An azosilane monomer used to form photo-switchable SAMs on ITO substrate was synthesized following a scheme shown in Figure 1a.

Figure 1: (a) Synthetic scheme followed to obtain the chlorosilane terminated compound **B** and (b) Graphical representation of photo-switchable SAM on chemically etched ITO.

The synthesis involved the O-alkylation reaction of 4-phenyl azophenol with 11-bromo undecene to obtain compound **A**. The vinyl moiety in compound **A** was converted to a dimethylchlorosilane via hydrosilylation reaction. A schematic representation depicting the formation of SAM of compound **B** over ITO substrate is shown in Figure 1b.

## Results and discussion

The present work describes the synthetic route to obtain an azo-based compound containing a terminal silane group and a facile strategy for anchoring this molecule on ITO. All the synthesized compounds were characterized by using UV, IR and NMR spectroscopy. UV-Vis spectra and IR spectra obtained for compounds **A** and **B** are provided in Figure 2 (a) and (b) respectively. UV spectrum of compound **B** showed a characteristic absorption at 346 nm due to the presence of azo moiety. The FT-IR spectrum of synthesized compounds **A** and **B** displayed peaks at  $2919\text{ cm}^{-1}$  and  $2850\text{ cm}^{-1}$  which correspond to the asymmetric and symmetric stretching frequencies of the C-H functional group. The peak at  $1253\text{ cm}^{-1}$  in compound **B** is due to the stretching vibration of Si-C functional group which confirms the incorporation of silane into azoalkene. The SAM formation was confirmed through CA, AFM and IR studies. The LC alignment studies were carried using 4'-pentylbiphenyl-4-carbonitrile, commonly known as 5CB, which exhibits a room temperature nematic (5CB; Cr 24 N 35.5 I) phase.

## Conclusion

In the present work, we described the synthesis and characterization of an azo compound containing a terminal chlorosilane moiety. This compound was successfully anchored onto a pre-treated ITO substrate, the modified ITO substrates were characterized using UV-Vis, IR, AFM and CA studies. The azo-modified ITO substrate induced a vertical alignment of the bulk LC sample under visible light, which changed to a planar alignment upon irradiating the UV light.

## References

- M. Bremer, P. Kirsch, M. Klasen-Memmer, K. Tarumi, *Angew. Chem. Int. Ed.*, 2013, **52**, 8880, and references therein



A. M. Lowe, N. L. Abbott, *Chem. Mater.*, 2012, **24**, 746; *Liq. Cryst.*, 2013, **1**, 29.  
S. Umadevi, V. Ganesh, Sheela Berchmans, *RSC Adv.*, 2014, **4**, 16409.

## **PP 67** Synthesis and Characterization of N-Rich Imine Functionalized Covalent Organic Polymers towards Carbon Dioxide Capture

**C. Saravanan, P. Kousalya, A. Pavithra and P. Muthu Mareeswaran\***

*\*Department of Industrial Chemistry, Alagappa University, Karaikudi.  
saravanangri92@gmail.com*

### **Abstract:**

Carbon dioxide (CO<sub>2</sub>) is chemically stable and also acts as a greenhouse gas leads to global warming. Minimizing of atmospheric CO<sub>2</sub> level by capture, storage and converting CO<sub>2</sub> to usable materials. Capture by functionalized porous materials having basic sites are the promising method for the acidic CO<sub>2</sub> molecules. Here we report synthesis of a new imine functionalized covalent organic polymers (COPs) by Schiff base condensation method. By treating 4,4'-diaminodiphenylamine with 2,4,6-Tris(p-formylphenoxy)-1,3,5-triazine (TRIPOD) and terephthalaldehyde (TPT) to get an imine polymer. The synthesized polymer was characterized using FT-IR, <sup>13</sup>C NMR, XRD, TGA, FT-RAMAN, SEM and BET analyses. The CO<sub>2</sub> capture experiment will be carry out using these synthesized polymeric networks.

**Keywords:** schiff base chemistry, covalent organic polymer, high surface area, large pore volume, CO<sub>2</sub> adsorption.

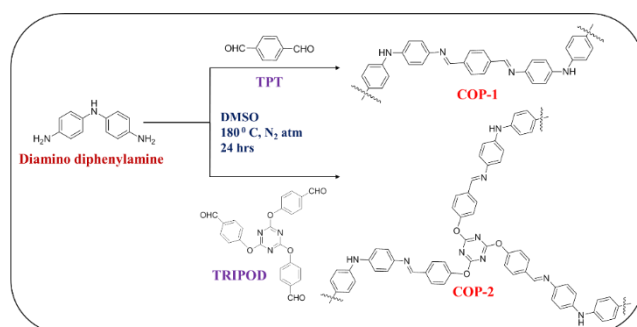
### **Introduction**

Carbon dioxide (CO<sub>2</sub>) is the major anthropogenic greenhouse gas mainly evolved from combustion of fossil fuels. The atmospheric CO<sub>2</sub> level is rising enormously due to the fast industrialization, lead to the drastic impact on climate change, such as rising of sea levels, alteration in ecosystems, loss of biodiversity and diminution in crop yields by global warming. The global temperature can be reduced by minimizing of CO<sub>2</sub> concentration through capture, storage and subsequent utilization of CO<sub>2</sub> to fuels, chemicals, and materials.<sup>1</sup> Capture of CO<sub>2</sub> molecules by porous solid sorbents is recognized as one of the promising and sustainable technologies. Various porous materials such as porous carbons, porous silica, porous CaO, metal-organic frameworks (MOFs), porous organic polymers, Covalent Organic Frameworks (COFs), Porous Aromatic Frameworks (PAFs) Covalent Organic Polymers (COPs), Zeolitic Imidazolate Frameworks (ZIFs) and nitrogen doped carboneous sorbents offer a much better balance between permeability and selectivity due to their well-defined porosities, high specific surface areas and rigid framework structures. Functionalized porous materials have attracted much attention because they have many desirable advantages of variable morphologies, low cost,

adjustable porosity, lightweight, easy processability, fast adsorption kinetics, high chemical and thermal stability, and controllable heteroatom doping exhibits better CO<sub>2</sub> selectivity towards N<sub>2</sub> and methane. To enhance sorbent-CO<sub>2</sub> interactions or selectivity by incorporating CO<sub>2</sub>-philic moieties or pore functionalization using polar groups such as hydroxy, nitro, amine, sulfonate, azo, imidazole, triazine, imine, etc.<sup>2</sup>

## Experimental Details

The imine-linked polymer was synthesized by the Schiff base condensations in DMSO under inert atmosphere, catalyst-free conditions with only water as a side product. The polymerization pathway is shown in scheme 1.



Scheme 1: synthetic route to COPs.

## Results and Discussion

The synthesized COPs are characterized using FT-IR, <sup>13</sup>C NMR, XRD, TGA, FT-RAMAN, SEM and BET analyses. Here we briefly described about the FT-IR spectrum of the synthesized polymers given in Figure 1.

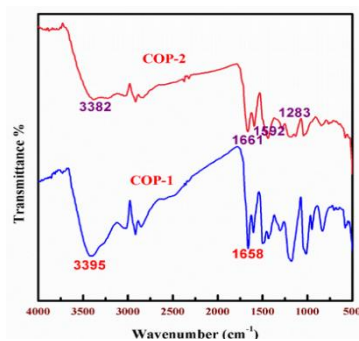


Figure 1. FT-IR spectra of COPs.

An evident imine stretch (C=N) is found at around 1660 cm<sup>-1</sup> (Fig. 1) in both the COPs, revealing the presence of the imine bands. Although bands at 1592, 1438 cm<sup>-1</sup> corresponds to triazine ring and 1283 cm<sup>-1</sup> for C-O-C linkage.

## Conclusion

We have synthesized new imine functionalized covalent organic polymers by Schiff base condensation of 4,4'-diamino diphenylamine with 2,4,6-Tris(p-formylphenoxy)-1,3,5-triazine (TRIPOD) and terephthalaldehyde (TPT). The synthesized polymers are characterized using FT-IR,  $^{13}\text{C}$  NMR, XRD, TGA, FT-RAMAN, SEM and BET analyses. The attempt towards  $\text{CO}_2$  capture will be made using these polymeric networks.

## References

- A. Itadani, A. Oda, H. Torigoe, T. Ohkubo, M. Sato, H. Kobayashi, Y. Kuroda, *ACS Applied Materials and Interfaces*, 8, 2016, 8821.
- T. Islamoglu, T. Kim, Z. Kahveci, O. M. El-Kadri, H. M. El-Kaderi, *Journal of Physical Chemistry C*, 120, 2016, 2592;
- S.-H. Jia, X. Ding, H.-T. Yu, B.-H. Han, *RSC Advances*, 5, 2015, 71095.

## PP 68 Synthesis of Schiff-Base Network (SBN) Polymer Membrane on Silica Support

M. Senthilkumaran, L. Eswaran, Dr. P. Muthu Mareeswaran\*

Department of Industrial Chemistry, Alagappa University, Karaikudi – 630 003, India

E.mail, [senthilkumaransbk@gmail.com](mailto:senthilkumaransbk@gmail.com), [eshwar1806@gmail.com](mailto:eshwar1806@gmail.com).

**Abstract:** Schiff-base network (SBN) polymers synthesized from the polycondensation reaction between various type of amines and terephthalaldehyde. Synthesised polymers are confirmed by FT-IR and Solid-state  $^{13}\text{C}$  MAS-NMR spectroscopy. The crystallinity nature of synthesised polymers are analysed using XRD. The polymers will be further analysed using SEM, TEM and BET analysis.

**Keywords:** Schiff-base networks, Solid state  $^{13}\text{C}$  MAS-NMR spectroscopy, Microporous structure.

## Introduction

Porous organic materials have attracted considerable attention due to their potential applications in the fields of gas storage, separation, biotechnology and catalysis. These porous materials possess many interesting properties such as the high thermal/chemical stability, large porosity and specific surface area, as well as low mass densities. Schiff-base network (SBN) polymers can be synthesized by one step chemical reaction and these polymers have several unique characteristics. The materials made by these polymers are promising candidates for potential applications in material science such as high BET surface areas and tailorable microporosity. These materials are cheap due to the low price starting compounds and the ease of synthesis, no catalyst necessity for the formation of the polymeric networks (1,2,3). Here, we describe in detail, the synthesis of the three type polymers and chemical conformation.

## Experimental Details

APTES modified activated silica is synthesised using APTES. Synthesis of all Schiff-base network (SBN) polymers was carried out in a single condensation step between APTES modified activated silica, amines (1,4-diaminobenzene, 1,3-diaminobenzene and 1,6-diaminopyridine) and terephthalaldehyde. The powder product was filtered by Büchner funnel and washed with excess acetone, tetrahydrofurane and dichloromethane. The solvent was removed under vacuum at room temperature to afford the materials denoted as Si-T-PPD, Si-T-DAP, Si-T-DPA.

## Results and Discussion

The synthesised polymers contains imine linkages are confirmed by FT-IR and Solid-state  $^{13}\text{C}$  MAS-NMR. From XRD (Figure. 1), Si-T-PPD polymer is crystalline nature. Another two polymers are amorphous nature, this indicates the presence of random frameworks. The morphology of the materials will be studied SEM and TEM. The porous nature (surface area, pore size and pore volume) of the synthesised materials will be explored by BET analysis (Nitrogen sorption isotherm).

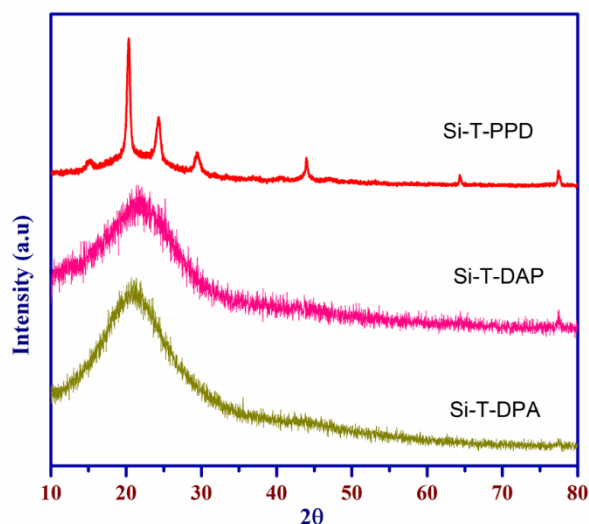


**Figure. 1** XRD patterns of Si-T-PPD, Si-T-DAP, Si-T-DPA

## Conclusion

Successfully synthesised all Schiff-base network (SBN) polymers using single step condensation reaction. The imine linkage and silica functionalization is confirmed using FT IR spectral techniques. The functionalizations are further confirmed using Solid-state  $^{13}\text{C}$  MAS-NMR spectroscopy. They have revealed the imine functionalization. The amorphous nature of the polymers are confirmed using XRD technique.

## References

- X. Feng, X.S. Ding, D.L. Jiang, *Chemical Society Reviews*, vol.4,2012, 6010-6022.  
N. Stock, S. Biswas, *Chemical Reviews*, vol.112 [2] 2012, 933–969.  
Z. Chang, D.S. Zhang, Q. Chen, X.H. Bu, *Physical Chemistry Chemical Physics*, vol.15, 2013, 5430-5442.

## **PP 69** Symmetric Oxamidato-Bridged Binuclear Cobalt (II) Complexes: Synthesis, Spectral, Electrochemical and its DNA Binding Studies

M. Sethupathi, R. Indumathi, T. Valarmathi, V. Vinoth Kumar, A. R. Maheswari,  
N. Sengottuvelan\*

*Department of Industrial Chemistry, Alagappa University, Karaikudi.*

*Email : nsvelan@gmail.com*

## Abstract

Transition metal complexes play an important role in nucleic acids chemistry for their diverse applications such as footprinting agents, sequence specific binding, structural probes, and therapeutic agents[1]. There is growing interest in investigating cobalt and other transition metal complexes for their interaction with DNA [2]. Here we have synthesized  $\text{Co}_2(\text{oxpn})(\text{Br-sal})_2$  and  $\text{Co}_2(\text{oxpn})(\text{m-sal})_2$  and characterized using various spectroscopic techniques. The  $\text{Co}_2(\text{oxpn})(\text{Br-sal})_2$  and  $\text{Co}_2(\text{oxpn})(\text{m-sal})_2$  complexes show intense band in the region 400 and 405 nm respectively which could be attributed to ligand to metal charge transfer transitions. In the visible region, 530 and 582 nm for the  $\text{Co}_2(\text{oxpn})(\text{Br-sal})_2$  and absorptions near 529 and 564 nm  $\text{Co}_2(\text{oxpn})(\text{m-sal})_2$  respectively are assigned as  ${}^4\text{T}_{1g}(\text{F}) \rightarrow {}^4\text{T}_{2g}(\text{F})$  and  ${}^4\text{T}_{1g}(\text{F}) \rightarrow {}^4\text{A}_{2g}$ , for d-d transitions, consistent with Co in an square planar environment[3]. The FTIR spectra of cobalt(II) complexes  $\text{Co}_2(\text{oxpn})(\text{Br-sal})_2$  and  $\text{Co}_2(\text{oxpn})(\text{m-sal})_2$  show sharp bands resulting from the C=N stretching vibration at 1633 and 1647  $\text{cm}^{-1}$  suggesting in the presence of azomethine functional group in complexes. The oximidato C=O stretching vibration bands were observed for complexes  $\text{Co}_2(\text{oxpn})(\text{Br-sal})_2$  and  $\text{Co}_2(\text{oxpn})(\text{m-sal})_2$  at 1515 and 1527  $\text{cm}^{-1}$  respectively. The coordination of the nitrogen and oxygen atoms is confirmed with the presence of new bands for complexes  $\text{Co}_2(\text{oxpn})(\text{Br-sal})_2$  and  $\text{Co}_2(\text{oxpn})(\text{m-sal})_2$  at 526 and 477  $\text{cm}^{-1}$  and 645 and 528  $\text{cm}^{-1}$  assignable to  $\nu(\text{Co-N})$  and  $\nu(\text{Co-O})$  respectively. The cyclic voltammetric studies show first reduction potential at -0.76 and -0.82 V and the second reduction potential lies at -1.13 and -1.23 V for  $\text{Co}_2(\text{oxpn})(\text{Br-sal})_2$  and  $\text{Co}_2(\text{oxpn})(\text{m-sal})_2$  complexes respectively. Moreover, the electron-withdrawing bromide ion that is present at the para position to the phenolic group decreases the electron density at the metal centre leading to easy reduction, and shifts the reduction potential to less negative potential. The complex showed metal centered quasi reversible cyclic voltammetric response. The DNA-binding properties of these complexes were examined by absorption spectral

studies and the results indicate that the complexes were bound to CT-DNA via groove mode. The binding strength of the complexes with CT DNA calculated with UV spectroscopic titration experiment has shown that  $\text{Co}_2(\text{oxpn})(\text{Br-sal})_2$  and  $\text{Co}_2(\text{oxpn})(\text{m-sal})_2$  exhibits the highest  $K_b$  values. The observed  $K_b$  value of  $\text{Co}_2(\text{oxpn})(\text{Br-sal})_2$  and  $\text{Co}_2(\text{oxpn})(\text{m-sal})_2$  are  $8.17 \times 10^3 \text{ M}^{-1}$  and  $1.35 \times 10^4 \text{ M}^{-1}$  respectively. The lower binding constants for bromo based cobalt complexes may be due to the less number of  $\pi$ - $\pi$  or hydrogen bonding interactions or combination of functional moiety. This is expected as the incorporation of substituent groups on aromatic ligand would hinder the insertion of the aromatic ring in between the DNA base pairs. The results are of importance towards further designing and developing Co(II) based complexes and systematic assessment of DNA binding for their potential applications as therapeutic agents.

## Reference

- Metcalf, C.; Thomas, J. A. Chem. Soc. Rev. 32, (2003), 215–224.  
M. Murrie, S. J. Teat, H. Stoeckli-Evans, H. U. Gudel, Angew. Chem. Int. Ed. 42 (2003) 4653–4656.  
Z. N. Chen, J. Qiu, W. X. Tang, K. B. Yu, Inorg. Chim. Acta 1994, 224, 171–176.

## **PP 70** *Diplocyclos palmatus* source for red luminescent carbon quantum dots to intercellular bioimaging in *Artemia salina*: A Green approach

**A. Hercularunbaby<sup>a</sup>, P. Nithya<sup>a</sup>, V. Muththulakshmi<sup>a</sup>, A. Keerthana<sup>a</sup>, C. Pragathiswaran<sup>b</sup>  
H. Gurumallesh Prabu<sup>c</sup> and M. Sundrarajan<sup>a\*</sup>**

<sup>a</sup>Advanced Green Chemistry Lab, Department of Industrial Chemistry, School of Chemical Sciences, Alagappa University, Karaikudi - 630 003, Tamil Nadu, India

<sup>b</sup>Department of Chemistry Periyar E.V.R college Tiruchirapalli- 620 023, Tamil Nadu, India

<sup>c</sup>Department of Industrial Chemistry, School of Chemical Sciences, Alagappa University, Karaikudi - 630 003, India

\*Corresponding author: Dr. M. Sundrarajan,

Email: [sundrarajan@yahoo.com](mailto:sundrarajan@yahoo.com); [drmsgreenchemistrylab@gmail.com](mailto:drmsgreenchemistrylab@gmail.com)

## Abstract

In this work, red luminescent carbon quantum dots (RCQDs) were synthesized from *Diplocyclos palmatus* using a facile and cost effective hydrothermal process. As synthesized RCQDs were 2 - 8 nm in size with spherical morphology and oxygen rich surface functionalities. These RCQDs apparent excellent photoluminescent (PL) properties and exhibited fluorescence emission in between 650 and 750 nm. The RCQDs showed defects in their structure and were highly crystalline in nature as confirmed by Raman spectroscopy and powdered X-ray diffraction analysis, respectively. These RCQDs showed excellent biocompatibility on *Artemia salina* even at high concentration (0.1 mg/mL) 24 h post-treatment. Furthermore, the RCQDs were demonstrated as fluorescent bioimaging probes, self-localizing themselves selectively in digestive part of *Artemia salina*.

**Keywords:** *Diplocyclos palmatus*, Carbon quantum dots, Bioimaging, *Artemia salina*

## Introduction

Carbon quantum dots (CQDs) are zero-dimensional carbonnanomaterials. They possess unique and exciting properties such asexcitation-dependent/independent fluorescence, multicolor emission, excellent dispersibility and solubility in aqueous and organic solvents, resistant to photo bleaching, competitive quantum yields and long fluorescence lifetimes. The CQDs are eco-friendly, relatively nontoxic, and photo stableas compared to semiconductor QDs and organicdyes.The CQDs fabricated fromgreen synthesis reduce use of acid/alkali treatments, high temperature, toxicorganic solvents, and complicated purification methods.

## Experimental Details

*Diplocyclos palmatus* leaves were cut down into tiny pieces (1–2 cm) anddipped in absolute ethanol. The mixture was kept under constantstirring for 4 h, and the resultant extract was centrifuged at 8000 rpmfor 10 min to achieve a clear supernatant. The extract was concentrated by evaporating the ethanol in a rotaryevaporator until residual slurry was obtained. The slurry was heated at 100°Cand the residue dispersed inabsolute ethanol for proper dispersion of RCQDs. The dispersion wasfurther filtered to obtain pure RCQDs then allowed to dry at 65 °C for 24 h toobtain dried powder.

## Result and Discussion

The synthesized RCQDs showed an absorption peak at 280 nm corresponding to the  $n-\pi^*$  electronic transitions within thecarbon structure in UV Visible stereoscopy. The C 1s and O 1s XPS spectral analysis of RCQDs showing significant peaks of C=O and C–O,indicative of oxidation during carbonization thereby givingred-emission [2].RCQDs were found to be sized in the range of2–8 nm (fig-1a) which is in agreement with results obtained by the DLS, calculated to be the average size of 4–7nm.Cellular internalization of RCQDs was confirmedby confocal microscopic images shown in Figure 1b.

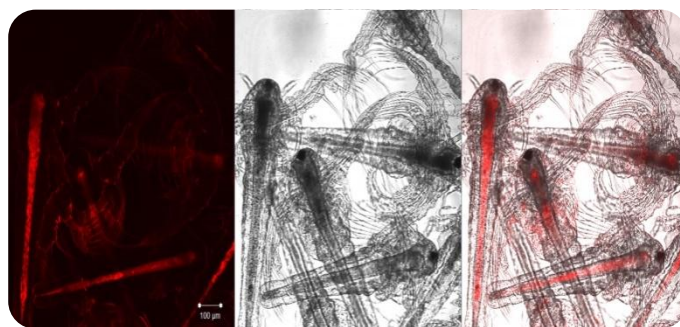


**Figure-1 (a) TEM images of RCQDs, (b) Bright field and fluorescent images of intercellular bioimaging in *Artemia salina***

## Conclusion

We demonstrate scalable, rapid, and economically viable green synthesis of RCQDs using *Diplocyclos palmatus* as a carbon source that showed bright red fluorescence. The RCQDs were highly biocompatible and photo stable, established excellent cellular uptake, and showed selective emission longer UV region. We, therefore, showed the intracellular bioimaging capability of RCQDs under live cellular conditions. This will pave the way in devising novel green-synthesis-based probes such as RCQDs with multifunctional in biomedical nanotechnology in future.

## Reference

- X. J. Mao, H. Z. Zheng, Y. J. Long, J. Du, J. Y. Hao, L. L. Wang, D. B. Zhou, Study on the fluorescence characteristics of carbon dots. *Spectrochim. Acta, Part A* 2010, 75, 553–557.
- X. Xu, R. Ray, Y. Gu, H. J. Ploehn, L. Gearheart, K. Raker, W. A. Scrivens, *J. Am. Chem. Soc.* 2004, 126, 12736–12737.

## PP 71 Imidazolium Based Ionic Liquid Template for Structurally Upgraded Cerium Oxide Nanorods

A. Surya<sup>a</sup>, M. Balaji<sup>a</sup>, M. Rajan<sup>b</sup> and M. Sundrarajan<sup>a\*</sup>

<sup>a</sup>Advanced Green Chemistry Lab, Department of Industrial Chemistry, School of Chemical Sciences, Alagappa University, Karaikudi - 630 003, Tamil Nadu, India.

<sup>b</sup>Natural Products Chemistry Lab, School of Chemistry, Madurai Kamaraj University, Madurai – 625 021, Tamil Nadu, India.

\*Corresponding author: Dr. M. Sundrarajan,  
Email: [sundrarajan@yahoo.com](mailto:sundrarajan@yahoo.com); [drmsgreenchemistrylab@gmail.com](mailto:drmsgreenchemistrylab@gmail.com)

## Abstract

Cerium Oxide (CeO<sub>2</sub>) nanorods are synthesized by using hydrothermal treatment method in the presence of imidazolium based ionic liquids such as 1-Butyl-3-methylimidazolium hexafluorophosphate. Ceria nanorods have been consisted with average size of 40 to 60 nm in diameter. The morphology, crystallinity, and chemical composition of the obtained materials were characterized by scanning electron microscopy (SEM), X-ray diffraction (XRD) and FTIR analysis. The catalytic properties of the as-prepared CeO<sub>2</sub> nanorods were explored by condensation reaction between 1, 3-indanedione and cinnamaldehyde. CeO<sub>2</sub> nanorods exhibit the best performance for condensation reaction to production of ninhydrin and its derivatives. The superior catalytic performance of this material can be related to its nanorod like structure, small particle size, large surface area, and high number of surface oxygen vacancy sites.

**Keywords:** Cerium Oxide nanorods, Ionic liquids, 1-Butyl-3-methylimidazolium hexa fluoro phosphate, condensation reaction, Ninhydrin

## Introduction

Rare earth metal oxides, especially cerium oxide (CeO<sub>2</sub>) have been a topic of interest to researchers in different fields owing to wide band gap semiconducting material (~3.2 eV) can



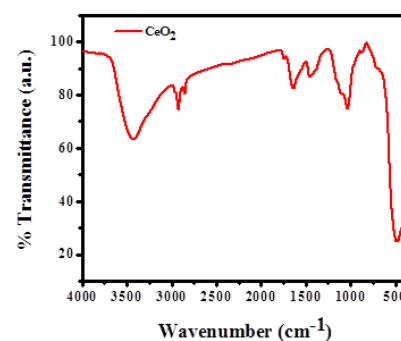
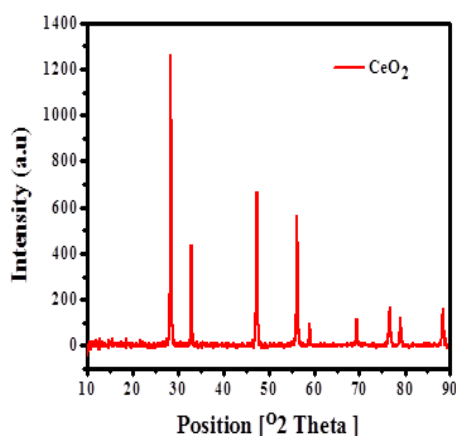
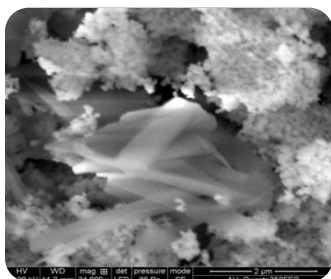
absorb light in the near UV region and slightly in the visible region. The high catalytic ability of cerium oxide is closely related to its energy of oxygen vacancies formation on its surfaces which closely linked to how easily the cerium atom can change its oxidation states between  $Ce^{3+}$  and  $Ce^{4+}$  without disruption of the fluorite lattice structure. The high oxygen storage capacity largely depends on exposed crystalline planes and surface-to-volume ratio of  $CeO_2$ . These unique abilities of  $CeO_2$  have made it suitable for many catalytic oxidation processes. Therefore, morphology-controlled synthesis of well-developed shapes and sizes inorganic materials is an important goal of modern materials chemistry. The objective of this study is to synthesize  $CeO_2$  nanorods by using hydrothermal treatment method in the presence of 1-butyl-3-methylimidazolium ionic liquids. The catalytic activities were tested by synthesis of ninhydrin by condensation reaction between 1, 3-indanedione and cinnamaldehyde.

## Experimental Details

### Ionic liquid assisted preparation of cerium oxide nanorods

$CeO_2$  nanorods were prepared from  $CeCl_3$  and ionic liquid such as 1-Butyl-3-methylimidazolium hexafluorophosphate as a templating agent. A minimum amount of 1-butyl-3-methyl imidazolium hexafluorophosphate is completely dissolved in 100ml of water. To this solution 2.46g of  $CeCl_3$  (0.1N) dissolved in 100ml ethanol and 10% NaOH solution with constant stirring at room temperature. Then the solution will be kept under constant stirring using magnetic stirrer for 5 hours and settle for 24 hours. The supernatant liquid will be discarded carefully and the remaining solution will be centrifuged. The nanoparticles of cerium oxide placed in muffle furnace at  $450^\circ C$  for 4 hours to get expected products.

## Result and Discussion Conclusion



In summary,  $CeO_2$  nanorods were successfully synthesized by one-step hydrothermal with 1-Butyl-3-methylimidazolium hexafluorophosphate ionic liquids directly without subsequent thermal treatment. This method is simple, one-step, and reproducible, and there is no need to use templates or surfactant because the ionic liquid acts as solvent and template.  $CeO_2$  nanorods have

higher catalytic ability in the condensation reaction as compared to commercial ceria nanoparticles.

## **PP 72** Development of Low Cost Carbon based material as counter electrode for dye-sensitized solar cells

**M. R. Samantaray<sup>a</sup>, K. Ramachandran<sup>a</sup>, G. Murugadoss<sup>b</sup>, R. Thangamuthu<sup>b</sup> and S. Karuppuchamy<sup>a\*</sup>**

<sup>a</sup>Department of Energy Science, Alagappa University, Karaikudi, Tamil Nadu-630 003, India

<sup>b</sup>Electrochemical Materials Science Division, CSIR-Central Electrochemical Research Institute, Karaikudi, Tamil Nadu-630 003, India

E-mail: skchamy@gmail.com and skchamy@alagappauniversity.ac.in

### **Abstract**

Owing to our inevitable energy necessity, alternative energy resources have to be utilized for our energy needs to enervate the energy demand as well as healthy suitable environment to living species. On the consideration of above statement, solar cell development strategies raises rapidly in this era. Among the 1<sup>st</sup>, 2<sup>nd</sup>, 3<sup>rd</sup> generation of solar cells, nanoporous semiconductor based dye sensitized solar cell (DSSCs) have gained much interest in recent years because of their low production costs and ease of fabrication. The performance of this type of solar cells depends on semiconductor materials, morphology, structure of sensitizing molecules, counter electrode and redox mediator used. Our work deals with the synthesis of new porous carbon material and their application as counter electrode (CE) in DSSC. Activated carbon materials have an impressive electrocatalytic activity due to more active sites from three dimension mesoporous honeycomb like structure. In the present work, Carbon/Graphite composite electrode has been prepared and utilized for DSSC application. The Photoelectrochemical characterization was carried out to investigate the catalytic performance of carbon based composite counter electrode. The photoelectrochemical parameters of the DSSC will be reported and discussed in detail.

## **PP 73** Fabrication of Efficient Perovskite Solar Cell

**K. Ramachandran<sup>a</sup>, G. Murugadoss<sup>b</sup>, Vibha Saxena<sup>c</sup>, R. Thangamuthu<sup>b</sup> and S. Karuppuchamy<sup>a\*</sup>**

<sup>a</sup>Department of Energy Science, Alagappa University, Karaikudi-630 003, Tamil Nadu, India.

<sup>b</sup>Electrochemical Materials Science Division, CSIR-Central Electrochemical Research Institute, Karaikudi-630 003, Tamil Nadu, India.

<sup>c</sup>Technical Physics Division, Bhabha Atomic Research Centre, Trombay, Mumbai-400085, India.

### **Abstract**

Considerable interest in photovoltaic technologies has become an unavoidable choice for the clean energy source due to the global warming issues. The current photovoltaic market is

dominated by crystalline silicon based technologies despite their high cost. Hence, creating new technologies for the production of low cost solar cells is essential. The most recent interesting innovation is the discovery of solar cells based on hybrid perovskite materials. In recent years, organic-inorganic perovskite solar cells (PSCs) have received much attention among the photovoltaic research community due to their remarkable high efficiency, low cost, and simple fabrication process. As a result, power conversion efficiency of PSCs has reached up to 22%, approaching a closer efficiency value of the commercial silicon solar cells. Such a high PCE is attributed to the relatively large open-circuit voltage ( $V_{OC}$ ) of PSCs, generally over 1.0 V, which is outstanding compared to other photovoltaic technologies such as organic- or silicon based solar cells. The best efficiencies that have been achieved by perovskite materials use a general formula such as  $AMX_3$ , where A is the organic component cation as methylammonium (MA), M is the metal cation (Pb) and X corresponds to the halide (I) or a mixture of halides (Cl, Br, I) anions. One of the key variables in the fabrication of such devices is the thickness of the light harvesting perovskite layer. Herein, we introduced a thin  $PbI_2$  interlayer for control over all perovskite thickness before depositing the mixed perovskite layer by one step method. The thickness of the  $PbI_2$  layer was optimized by device performance and compared the efficiency for  $MAPbI_3$  and  $MAPbICl$  perovskites.

## **PP 74**    **Synthesis and Characterization of Nickel Manganese Oxide Composite materials for Supercapacitor Applications**

**K. Uma Maheswari, I. Karuppusamy, A. Senthamarai Selvam and S. Karuppuchamy\***  
*Department of Energy Science, Alagappa University, Karaikudi-630 003, Tamilnadu, India*  
*Email: skchamy@alagappauniversity.ac.in*

### **Abstract:**

Development of high-performance and environmentally friendly energy storage devices becoming an attracting field of research among the materials scientists. Among the energy storage devices, lithium ion batteries and supercapacitors (SCs) have attracted worldwide attention. In general, Li-ion batteries have high energy densities, low power densities and good cycle life. In contrary, with the features of higher power density than batteries and higher energy density than conventional dielectric capacitors, supercapacitors have attracted widespread attention for next-generation power devices. SCs have been used in many applications, such as, power Back-up, pacemakers, aerospace, hybrid electric vehicle system and emergency lighting. The electrode material is a backbone that determines the SC's functional performance. Supercapacitors are classified into two types such as electric double layer capacitors and pseudocapacitors on the basis of their charge storage mechanisms. The promising electrode material for pseudocapacitors is  $RuOx$ , however due to its expensive nature it can't be utilized for commercial applications.

Therefore, inexpensive alternative materials with superior pseudocapacitance containing transitional metal oxides, such as ZnO,  $\text{Co}_3\text{O}_4$ ,  $\text{MnO}_2$ , NiO, and  $\text{SnO}_2$ , have been studied as the electrode material for pseudocapacitors. In the present work, we synthesized the nanostructured Nickel Manganese Oxide Composite materials by using microwave method and subsequently the physicochemical characterization has also been carried out. The electrochemical performance of the synthesized materials will be reported.

## **PP 75**    **Synthesis of Sn Anchored $\text{Co}_3(\text{PO}_4)_2$ for the Reduction of Formaldehyde**

**R. Banupriya, R. Karkuzhali and G. Gopu\***

*Department of Industrial Chemistry, Alagappa University, Karaikudi – 630003*

*\*E-mail: nggopi79@gmail.com*

### **Abstract:**

A simple, low cost and high performance of advanced electrocatalyst of key significance for the improvement of environmentally-pleasant energy technologies. Herein, we report the facile synthesis of Sn doped cobalt phosphate ( $\text{Co}_3(\text{PO}_4)_2$ ) nanoparticles were ultra sonicated and made by a microwave-assisted process and utilized as an electrocatalyst for the reduction of formaldehyde. The phase formation, morphological surface structure, elemental composition, and textural properties of the synthesized Sn doped ( $\text{Co}_3(\text{PO}_4)_2$ ) have been examined by powder X-ray diffraction (XRD), Fourier Transform-Infrared Spectroscopy (FT-IR), Field Emission-Scanning Electron Microscopy (FE-SEM). The performance of an electrocatalytic reduction of formaldehyde over Sn doped ( $\text{Co}_3(\text{PO}_4)_2$ ) nanoparticles modified electrode was evaluated in an alkaline solution using Cyclic Voltammetry (CV) techniques. Studies were made for the formaldehyde reduction by varying the experimental parameters, such as loading the catalyst, concentration of formaldehyde and long-term stability. The good electrocatalytic performances of Sn doped  $\text{Co}_3(\text{PO}_4)_2$  nanoparticles should be related to its good surface morphological structure and high number of active surface sites. The present investigation illustrates the promising application of Sn doped  $\text{Co}_3(\text{PO}_4)_2$  nanoparticles as a low-cost and more abundant electrocatalyst for the reduction of formaldehyde.

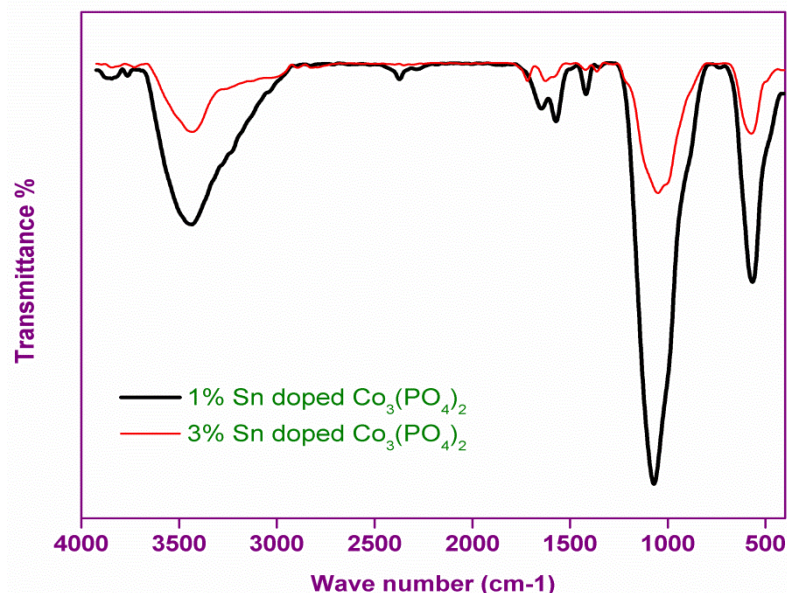


**Figure:** The FT-IR spectrum for Sn doped Co<sub>3</sub>(PO<sub>4</sub>)<sub>2</sub> nanoparticles at different weight percentages.

**Keywords:** Sn doped Cobalt Phosphate, Electrocatalysts, Microwave assisted synthesis, Reduction.

**References:**

- Arunachalam, P.; Ghanem, M.A.; Al-Mayouf, A.M.; Al-shalwi, M. Enhanced electrocatalytic performance of mesoporous nickel-cobalt oxide electrode for methanol oxidation in alkaline solution. *Mater. Lett.* **2017**, 196,365–368.
- Tong, Y.Y.; Gu, C.D.; Zhang, J.L.; Tang, H.; Li, Y.; Wang, X.L.; Tu, J.P. Urchin-like Ni-Co-P-O nanocomposite as novel methanol electro-oxidation materials in alkaline environment. *Electrochim. Acta* **2016**, 187, 11–19.
- J. Chen, Y. Zhang, M. Zhang, B. W. Yao, Y. R. Li, L. Huang, C. Li and G. Q. Shi, *Chem. Sci.*, 2016, 7, 1874–1881.

## **PP 76** Robust Method of Synthesis of Metal Chalcogenides Doped GCN

**R. Vennila, R. Karkuzhali and G. Gopu\***

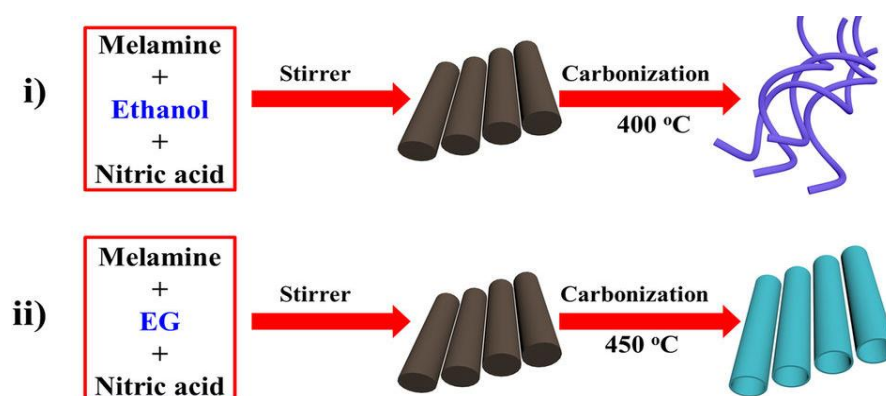
*Department of Industrial Chemistry, Alagappa University, Karaikudi – 630003*

*\*E-mail: nggopi79@gmail.com*

**Abstract:**

The development of stable, active and low-cost electrocatalyst as an electrode material for energy storage devices has been an emerging trend. A large number of electrochemical energy technologies have been developed in the past. These systems continue to be optimized in terms of cost, lifetime and performance, leading to their continued expansion into existing and emerging market sectors. In this work, different types of Chalcogens metal have been synthesized and made to embedded with Graphitic Carbon Nitride (GCN) to form as an electrocatalyst. As prepared

electrocatalyst must optimize and taken for further studies. The phase formation, morphological surface structure, elemental composition, and textural properties of the synthesized electrocatalyst have been examined by powder X-ray diffraction (XRD), Fourier Transform-Infrared Spectroscopy (FT-IR), Field Emission-Scanning Electron Microscopy (FE-SEM). Generally, chalcogens are very reactive with metals and hence GCN has unexpected properties such as tunable band gaps, high catalytic activities. Nowadays, GCN based sensor and energy storage application has attracted due to the novel properties such as high photostability, biocompatibility, low toxicity. Further, chemical doping is the introduction of a hetero atom such as Nitrogen, Boron, Sulphur and Phosphorus into the GCN which enhances the chemical and physical properties. This becoming eminent in fuel cell applications.



**Keywords:** Graphitic Carbon Nitride, Chalcogens, tunable band gaps, fuel cell.

### References:

- Wei, H.; Zhang, Q.; Zhang, Y.; Yang, Z.; Zhu, A.; Dionysiou, D. D. Enhancement of the Cr(VI) Adsorption and Photocatalytic Reduction Activity of g-C<sub>3</sub>N<sub>4</sub> by Hydrothermal Treatment in HNO<sub>3</sub> Aqueous Solution. *Appl. Catal., A* 2016
- Zhang, J.; Hu, Y.; Jiang, X.; Chen, S.; Meng, S.; Fu, X. Design of a Direct Z-Scheme Photocatalyst: Preparation and Characterization of Bi<sub>2</sub>O<sub>3</sub>/g-C<sub>3</sub>N<sub>4</sub> with High Visible Light Activity. *J. Hazard. Mater.* 2014, 280, 713–722
- Yue, X.; Yi, S.; Wang, R.; Zhang, Z.; Qiu, S. Cadmium Sulfide and Nickel Synergetic Co-Catalysts Supported on Graphitic carbon nitride for Visible-Light-Driven Photocatalytic Hydrogen Evolution. *Sci. Rep.* 2016, 6, 22268.

## PP 77 Electrochemical Determination of Guanine: using a Boron Doped Carbon Quantum Dot/Mn<sub>3</sub>O<sub>4</sub> Composite Modified Screen-Printed Carbon Electrode

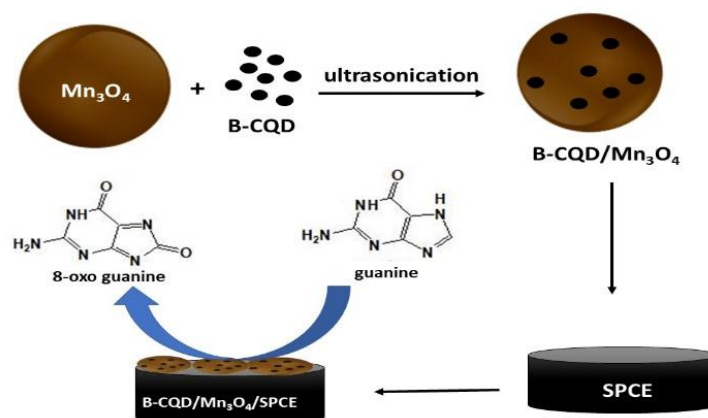
Ganesan Muthusankar<sup>1</sup>, Shen-Ming Chen<sup>2,\*</sup> and Gopalakrishnan Gopu<sup>1,\*</sup>

<sup>1</sup>Department of Industrial Chemistry, Alagappa University, Karaikudi – 630003, Tamilnadu, India. nggopi79@gmail.com (Gopalakrishnan Gopu)

<sup>2</sup>Department of Chemical Engineering and Biotechnology, National Taipei University of Technology, No. 1, Section 3, Chung-Hsiao East Road, Taipei 106, Taiwan, ROC. smchen78@ms15.hinet.net (Shen-Ming Chen)

### Abstract

Herein, we report the synthesis of boron doped carbon quantum dots (B-CQD) modified Mn<sub>3</sub>O<sub>4</sub> using the ultrasonic method. The as-synthesized B-CQD/Mn<sub>3</sub>O<sub>4</sub> composite was characterized by X-ray diffraction (XRD), Fourier-transform infrared spectroscopy (FT-IR), transmission electron microscopy (TEM), energy-dispersive X-ray analysis (EDS) and elemental mapping. The composite modified screen-printed carbon electrode (B-CQD/Mn<sub>3</sub>O<sub>4</sub>/SPCE) was employed for the simple and sensitive electro-chemical determination of guanine (G). The electrochemical sensor shows an effective and tenacious electro-oxidation performance towards the oxidation of G. Electrochemical behavior interrelated to the electro-oxidation of G at the B-CQD/Mn<sub>3</sub>O<sub>4</sub>/SPCE was examined, displaying that their oxidation peak currents were highly improved owing to the catalytic effect of B-CQD/Mn<sub>3</sub>O<sub>4</sub>. The proposed sensor is highly sensitive and selective for the G oxidation over adenine (A). Remarkably, B-CQD/Mn<sub>3</sub>O<sub>4</sub>/SPCE has exhibited 8.95  $\mu\text{A } \mu\text{M}^{-1} \text{ cm}^{-2}$  sensitivity and a linear range of 0.009–329  $\mu\text{M}$  with a detection



limit of 0.73  $\mu\text{M}$  (at an S/N ratio of 3). Further, the sensor was applied for the detection of G in biological samples such as human urine and blood serum.

**Keywords:** Boron doped carbon quantum dot Guanine Electrocatalysis, Cyclic Voltammetry · Differential Pulse Voltammetry

**PP 78**    **An Efficient and Eco-Friendly Synthesis of *N,N'*-Disubstituted Thiourea Derivatives**

P. Shanmugavelan<sup>1\*,2</sup>, . A. Ponnuswamy<sup>2</sup> and S. Dhinakaran<sup>1</sup>

<sup>1</sup>*Department of Chemistry, School of Sciences, Tamil Nadu Open University, Saidapet, Chennai - 600 015.*

<sup>2</sup>*Department of Organic Chemistry, School of Chemistry, Madurai Kamaraj University, Madurai.*

*E.Mail: shanchemmku@gmail.com.*

**Abstract:** In the present investigation, an efficient and environmentally benign method for the synthesis of *N,N'*-disubstituted thiourea derivatives under solvent-free condition in excellent yields (80-88%) has been reported. This protocol has advantages such as (a) no use of hazardous reagents and volatile organic solvents, (b) rapid reaction rate, (c) excellent yield, and (d) simple work-up procedure.

**Keywords:** Efficient, Eco-friendly, Excellent yields, Disubstituted thioureas

**Introduction**

Thioureas are of potential importance in medicinal chemistry due to their biological activities like anti-HIV,<sup>1</sup> anti-tuberculosis,<sup>2</sup> anti-arrhythmic activities,<sup>3</sup> and in connection with biomimetic models.<sup>4</sup> Moreover, thioureas are valuable building blocks for the synthesis of five- and six-membered heterocycles.<sup>5</sup> Among them, *N,N'*-disubstituted thiourea functionality is a key structural element of many biologically active compounds and serve as intermediates for the preparation of pharmaceutical and agricultural chemicals.<sup>6-8</sup> Therefore, synthesis of *N,N'*-disubstituted thiourea has attained importance and various synthetic strategies have been attempted by the researchers.

As the synthesis of thiourea has been a topic of research interest for over a century, still more emphasis is being given to search for similar and better green protocols due to today's eco-friendly conscious attitude.

**Results and Discussion**

In our preliminary study, for the purpose of optimization, synthesis of thiourea was attempted (Scheme 1) under different conditions *viz.* (i) Solution phase protocol under reflux and (ii) Solvent-free protocol. Initially, a mixture of allylbromide (**1**, 1 eq), and potassium thiocyanate (2 eq) was ground for 20 minutes at room temperature to afford isothiocyanate (**3**) in excellent yield (98 %). Isothiocyanate (**3**, 1 eq) was then refluxed with aniline (**3a**) in 1,4-dioxane. The reaction was completed in 4 hours to afford thiourea (**4a**) in 86% yield. To eradicate the limitations associated with solution phase, we conducted the same under solvent-free condition which resulted in comparable yield of thiourea (**4a**, 84 %) in just 10 minutes under conventional heating (80°C). The reaction does not occur at room temperature. But in the case of aliphatic



amine (methylamine), the reaction was completed in just 2 minutes at room temperature with 86% yield. Thus, the solvent-free protocol was found to be remarkable compared to solution-phase protocol.

Having optimized, the broad scope of the above said protocol was established via the synthesis of a library of thiourea derivatives (**4a-o**, Scheme 2) in good to excellent yields (80-88%). The sensitivity of the reaction towards the steric effect is evidenced from the trace of the thiourea formed from the meta-bromoaniline (entry 7) and inertness of the ortho-chloroaniline (entry 8) towards the isothiocyanates.

### Structural assignment

The synthesized thioureas (**4a-o**) were completely characterized by mass, IR and NMR (1D & 2D) spectral techniques. The  $^1\text{H}$  NMR spectrum of a representative compound, **4f** shows a broad singlet at 7.61 ppm for one proton (NH), multiplet around 7.26-7.43 ppm for five aromatic protons (ArH), doublet at 6.96 ppm with  $J=8.1$  Hz for two protons (ArH), doublet at 6.46 ppm with  $J=8.1$  Hz for two protons (ArH), doublet at 6.20 ppm with  $J=3.9$  Hz for one olefinic proton (C=CH), doublet at 5.74 ppm with  $J=8.1$  Hz for one proton (NH), broad singlet at 5.56 ppm for one methine proton (CH), singlet at 2.27 ppm for three methyl protons (ArCH<sub>3</sub>) and multiplet around 1.50-2.18 ppm for six alicyclic methylene protons [(CH<sub>2</sub>)<sub>3</sub>]. In  $^{13}\text{C}$  NMR spectrum of **4f**, the signal due to C=S appeared at 179.59 ppm, one olefinic carbon at 130.43 ppm, one methine carbon at 51.41 ppm, three alicyclic methylene carbons appeared at 18.84, 25.80 and 29.30 ppm, one aromatic methyl carbon appeared at 20.82 ppm, four tertiary carbons appeared at 139.54, 137.04, 136.74 ppm and 133.22 ppm, five aromatic carbons appeared at 129.82, 128.45, 127.24, 126.01 and 124.71 ppm. The IR spectrum of **4f** showed the band due to C=S at  $1536\text{ cm}^{-1}$  and NH at  $3232\text{ cm}^{-1}$ . The mass spectrum of **4f** shows peak at  $m/e = 323.42$  [M+1].

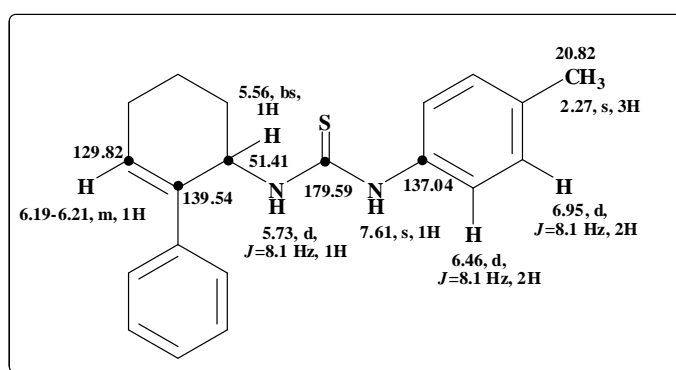


**Figure 1:** Selected  $^1\text{H}$ ,  $^{13}\text{C}$  NMR chemical shift values of compound **4f**.

### Conclusion

An efficient and environmentally benign synthesis of N,N'-disubstituted thiourea derivatives under solvent-free condition in excellent yields has been reported in the present investigation. Advantages of our protocol are (a) no use of hazardous reagents and volatile organic solvents, (b) rapid reaction rate, (c) excellent yield, and (d) simple work-up procedure.

## References

- T.K. Venkatachalam, E. A. Sudbeck, C. Mao, Uckun, F. M. Bioorganic & Medicinal Chemistry Letters, vol.11, 2001, 523-529.
- S. Karakus, S. Rollas, Farmaco, vol. 57, 2002, 577-586.
- E. G. Chalina, L. Chakarova, European Journal of Medicinal Chemistry, vol. 33, 1998,975-982.
- (a) Y. Tobe, S. Sasaki, K. Hirose, K. Naemura, Tetrahedron Letters, 38, 1997, 4791-4798.
- b) J. Smith, J. L. Liras, S. E. Schneider, E. V. Anslyn, Journal of Organic Chemistry, vol. 61, 1996, 8811-8822.
- U. Heinelt, D. Schultheis, S. Jager, M. Lindenmaier, A. Pollex, H. S. Beckmann, Tetrahedron, vol. 60, 2004, 9883-9892.
- A. Ricci, A. Carra, A. Torelli, C. A. Maggiali, G. Morini, C. Branca, Cytokin, Plant Science 2001, vol. 160, 1055–1065.
- P. Boden, J. M. Eden, J. Hodgson, D. C. Horwell, M. C. Pritchard, J. Raphy, N. Suman-Chauhan, Bioorganic & Medicinal Chemistry Letters, vol. 5, 1995, 1773–1778.
- H. A. Wieland, W. Engel, W. Eberlein, K. Rudolf, H. Doods, Journal of Pharmacology, vol. 125, 1998, 549–555.

## **PP 79** Synthesis of Pd nanoparticles by bio-reduction process using natural plant of *Aerva lanata* extract

**R<sup>a</sup>. Jayamani and M. Sundrarajan\***

<sup>a</sup> Assistant professor, PG department of chemistry, Ananda college, Devakottai

<sup>b</sup> Advanced Green Chemistry Lab, Department of Industrial Chemistry, School of Chemical Sciences, Alagappa University, Karaikudi - 630 003, Tamil Nadu, India

### Abstract

Synthesis of palladium nanoparticles were achieved by simple green chemistry method, using an *Aerva Lanata* (AL) plant extract. The aqueous AL extract used and it is act as a reducing and stabilizing agents make the reduction of Pd<sup>2+</sup> ions from palladium chloride(PdCl<sub>2</sub>) to palladium nanoparticles(Pd<sup>0</sup>).Synthesis of palladium nanoparticles using AL extracts is a value effective method can be used as an economical and biocompatible can be described as simple green direction does not need for the organic solvents and expensive chemicals for the developing palladium nanoparticles. The effect of the heat of palladium nanoparticles were approved out at 80°C. The formation of synthesized palladium nanoparticles using AL extract were characterized through UV-Visible spectroscopy andFourier transform infrared spectroscopy (FTIR).

**Keywords:** Palladium chloride, AL plant extract, green synthesis, UV-visible, FTIR studies.

## PP 80 Highly potential membranes based on poly (aryl hexafluoro sulfone benzimidazole) for high-temperature PEM fuel cell

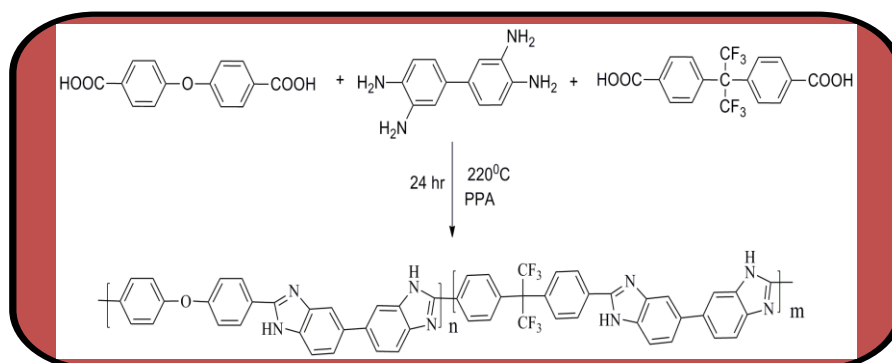
A. Susaimanickam<sup>a1</sup>, P. Muthuraja<sup>a1</sup>, S. Prakash<sup>a</sup>, P. Manisankar<sup>a\*</sup>

<sup>a</sup>Address of corresponding author: Former Syndicate Member, Former Dean, Faculty of Science Professor & Head (Rtd.), Department of Industrial Chemistry, Alagappa University, Karaikudi 630003, Tamil Nadu, INDIA \*Tel: +91 4565 228836, Fax: +91 4565 225202,  
<sup>b</sup>Department of Chemistry, Arumugam Pillai Seethai Ammal College, Tiruppattur, Tamil Nadu,  
 Prof. P. Manisankar ([manisankarp@alagappauniversity.ac.in](mailto:manisankarp@alagappauniversity.ac.in))

<sup>a1</sup> equally contributed

### Abstract

Poly (aryl hexafluoro sulfone benzimidazole), termed as PArF<sub>6</sub>SO<sub>2</sub>BI, were synthesized and characterized systematically. PArF<sub>6</sub>SO<sub>2</sub>BI membranes showed good chemical stability in terms of oxidative weight loss due to the electron-withdrawing sulfone functional group. Synthesized membranes showed good conductivity. Higher conductivity of 3.26 x 10<sup>-2</sup> S cm<sup>-1</sup> at 160°C with acid doped level of 286.8 wt % for 3:1 PArF<sub>6</sub>SO<sub>2</sub>BI is observed. The as-synthesized PArF<sub>6</sub>SO<sub>2</sub>BI membranes exhibit improved proton conductivity. Thus it is concluded that the PArF<sub>6</sub>SO<sub>2</sub>BI membranes possess better characteristics to be used as polymer electrolyte membrane in the fabrication of high-temperature PEM fuel cell.



**Keywords:** poly (aryl hexafluoro sulfone benzimidazole); fuel cells; proton conductivity; stability

## PP 81 A Facile Green Synthesis of Zinc oxide Nanoparticles Using *Justicia gendarussa* leaves extract for its enhanced antibacterial activities

R. Rajeswari, and H. GurumallesPrabhu \*

Department of Industrial Chemistry, School of Chemical Sciences  
 Alagappa University, Karaikudi-03, Tamilnadu, India  
 E-mail: [rajiraji756@gmail.com](mailto:rajiraji756@gmail.com)

### Abstract

A facile novel green route synthesis is adopted to prepare Zinc oxide nanoparticles. This is the first report on biosynthesis of Zinc oxide nanoparticles by employing the extract of the

leaves of *Justicia gendarussa*. The precursor used to synthesis zinc oxide nanorod is Zinc nitrate hexahydrate  $Zn(NO_3)_2 \cdot 6H_2O$ . The synthesized Zinc oxide nanoparticles (ZnO NPs) was confirmed by standard characterization studies. The prepared ZnO NPs possessed a broad spectrum were antimicrobial activity against both gram-negative and gram positive organisms like *Staphylococcus mutans* (MTCC 497), *Bacillus subtilis* (MTCC 441), gram negative organisms, *Proteus vulgaris* (MTCC 426), *Klebsiella pneumoniae* (MTCC 109), and with a zone of inhibition from 7-12 mm.

**Key words:** Novel strategy, Green synthesis, Zinc oxide, nanoparticles, *Justicia gendarussa*, Antibacterial activity.

## Introduction

A facile green route strategic approach is the alternative route of synthesizing biocompatible nanoparticles. It is the ecofriendly method compared to other biological methods and the other chemical methods [1]. Synthetic strategies using plant extracts [2] play a major role in the formation of nanoparticles. This environmental green route synthesis method doesn't include any toxic chemicals in the preparation methods.

Zinc oxide (ZnO) nanoparticles are synthesized by various chemical methods including homogeneous precipitation, organometallic synthesis, thermalevaporation, sol-gel processing [3]. As prepared nanosized ZnO possess high surface area to volume ratio, and it is a safe material. The plant mediated ZnO nanoparticles synthesis is preferred because of its environmentally friendly, cost effective and safe nature for human therapeutic use.

The leaves of *J. gendarussa* contains phytoconstituents such as, flavonoids, alkaloids, amino acids saturated steroidal saponins, and rich in potassium salts (Ratnasooriya *et al.*, 2007). [4] Plant extract mediated drugs are known to be good for combination therapy which as multidrug resistance modifiers [5]. In the present study, the antibacterial activity of ZnO nanoparticles using leaves extracts of *Justicia gendarussa* were studied.

## Materials and methods:

### Materials

Many plant leaves were collected, after screening the leaf samples of *J. gendarussa* were selected. These leaf samples were collected from Kolli hills, Tamil Nadu South India. Zinc nitrate [ $Zn(NO_3)_2 \cdot 6H_2O$ ], and ethanol were purchased from Merck chemicals Ltd, India and used as received without any further purification.

### Preparation of ZnO nanoparticles

Collected leaf samples of *J. gendarussa* were washed thoroughly with running water and cut into small pieces. Boiled with ethanol and double distilled water in a round bottom flask. The extract was filtered and used for the preparation of ZnO nanoparticles. 0.1M of  $Zn(NO_3)_2 \cdot 6H_2O$

was mixed with distilled water, along with that 15mL of *J. gendarussa* leaf extract was slowly added under stirring, then the contents were transferred to autoclave and kept it under 120 °C in a furnace. After that the precipitate was washed centrifuged and collected and labeled as ZnO nanoparticles.

## Results and discussion

The synthesized nanoparticles were characterized by XRD SEM and TEM. The structure and size was analysed and given in the XRD pattern. The size was calculated by debye Scherrer's formula. The morphology was analyzed by scanning electron microscope small nanorods of ZnO nanoparticles were observed. The TEM image of the ZnO nanoparticles is shown in fig.1. The antibacterial activity of ZnONPs was tested against gram positive and gram negative bacteria.

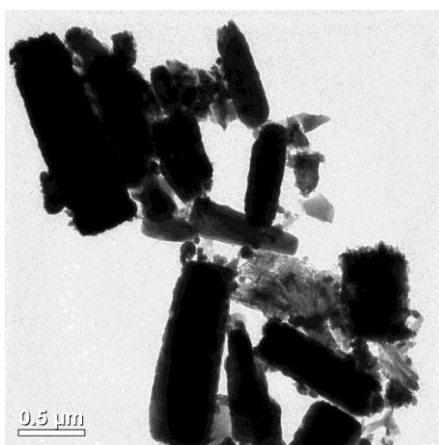


Fig:1 TEM image of ZnO nanoparticle

## Antibacterial activity

The antibacterial activity of ZnO nanoparticles showed good antibacterial activity against gram negative bacteria, the zone of inhibition for ZnO NPs was larger than that for the control. The nanoparticles easily get through the cellular membranes, and binds to the enzymes and proteins, causing breakage of DNA bonds. ZnO nanoparticles produce reactive oxygen species (ROS), which cause cell death. [6]

## Conclusion

ZnO nanoparticles were successfully synthesized by hydrothermal method using *J. gendarussa* leaf extract, the morphology and crystalline structure was further confirmed with the characterization of XRD, SEM, and TEM results. The antibacterial activity of ZnO nanoparticles were examined for gram positive, and gram negative bacteria, the larger the zone of inhibition was exhibited in gram negative bacteria. ZnO nanoparticles distort bacterial cell membrane and cause cell death. These examined results demonstrate that ZnO nanoparticles could be considered as an excellent antibacterial agent.

**References**

- S. Iravani, Green synthesis of metal nanoparticles using plants, *Green Chemistry*.vol.13 2011, 2638-2650.
- S.P. Chandran, M. Chaudhary, R. Pasricha, A. Ahmad, M. Sastry, Synthesis of gold nanotriangles and silver nanoparticles using Aloe vera plant extract, *Biotechnology Progress*.vol. 22 2006, 577-583.
- M.S. Tokumoto, V. Briois, C.V. Santilli, Preparation of ZnO Nanoparticles: Structural Study of the Molecular Precursor. *Journal of Sol–Gel Science and Technology*, vol. 26 [3] 2003, 547-551.
- W.D. Ratnasooriya, S.A. Deraniyagala and D.C. Dehigaspitiya,. Antinociceptive activity and toxicological study of aqueous leaf extract of *Justicia gendarussa* Burm. F.in rats.*Pharmacognosy. Magazine*. Vol 3 [11] 2007, 145-155.
- S. Hemaiswarya, A.K. Kruthiventi and M. Doble, Synergism between natural products and antibiotics against infectious diseases. *Phytomedicine*, vol [15] 2008. 639-652.
- K. Markowska, A M. Grudnia, and K.I.Wolska, Silver nanoparticles as an alternative strategy against bacterial biofilms.*Acta Biochimica Polonica*.vol60 [4] 2013. 523-30.